SCUOLA NORMALE SUPERIORE DI PISA

TESI DI PERFEZIONAMENTO

IN CHIMICA

Novel titanium precursors for homo- and co-polymerization of α-olefins: catalytic activity and materials characterization

Candidato

Dott. Mohammad Hayatifar

Relatore

Prof.ssa Anna Maria Raspolli Galletti

Presidente del Corso di Perfezionamento

Prof. Vincenzo Barone

Pisa, Aprile 2011

Ciclo di Perfezionamento 01/01/2008 – 31/12/2010

Abstract

Billions of pounds of commodity plastics, based on polyolefin resins, are produced annually and are used in wide variety of sectors in our daily lives. Despite its long history, the polyolefin industry is continuing to grow steadily and remains technologically driven because of continuous discoveries of new catalyst and applications. As a consequence polymerization of α-olefins has been one of the focus areas for catalyst research both in industry and academia. Enormous efforts have been dedicated to fine tune of the processes and to obtain better control of the polymerization and to produce tailored polymer structures.

The literature review of the thesis is focused on the use of Group 4 metal complexes as precursors for α-olefin homo- and copolymerizations. More precisely, the review concentrates on the use of complexes bearing [*O*,*O*] and [*O*,*N*] type ligands which have gained considerable interest. Furthermore, the chemistry of group 4 metals complexes bearing homoleptic *N*,*N*-dialkylcarbamato ligands as potential precursors for olefin polymerization are discussed.

The experimental part consists mainly of synthesis of new Group 4 metal complexes bearing *N*,*N*-dialkylcarbamato ligands and their use as catalytic precursors in α-olefin homo- and copolymerization. Part of the experimental work deals with utilizing three different titanium complexes based on *N*,*N*-dialkylcarbamato chelate ligands with the general formula of [$Ti(O_2CNR_2)_4$, R = Et (**I**), Me (**II**)] and [$Ti(O_2CNR_2)_2Cl_2$, R = Me (**III**)] as precatalysts for the ethylene polymerization. These precursors exhibited high activity for polymerization of ethylene when activated with MAO, affording high-density polyethylenes with broad molecular weight distribution. However, polymerization of propylene resulted in atactic polypropylene materials in which activation with TMA-depleted MAO increased the polymerization activity considerably compared to that when MAO used as cocatalyst.

The precursors **I**-**III** were also employed for the copolymerization of ethylene with 1-hexene in the presence of appropriate cocatalyst. They exhibited moderate activity for E/H copolymerization featured broad molecular distribution and high comonomer incorporation. In all cases the main reaction parameters such as Al/Ti molar ratio, solvent, pressure and temperature were investigated.

Thermal behavior and structural characterization of E/H copolymers were studied in detail by means of DSC, FTIR-M and ^{13}C NMR spectroscopy as well.

The natural aminoacid derivatives of *N*,*N*-dialkylcarbamato complexes of Group 4 metals, **2a**–**2f** and **3a**–**3d**, were prepared by the reaction of homoleptic carbamato complexes of titanium and zirconium with the chiral natural aminoacids such as L-leucine and L-phenylalanine. Interestingly these products showed good solubility in common low-polarity solvents, in spite of the presence of [NH_2] amino groups and characterized by NMR and IR spectroscopy.

For my Dad, Mom, Wife and all my family.
I would give everything away but their love.

Acknowledgments

I am most grateful to my supervisor, Professor Raspolli Galletti, for providing me the opportunity to work in her research group and for her professional guidance and continuous support.

Besides my supervisor, I owe my deepest gratitude to Prof. Guido Pampaloni, Dr. Fabio Marchetti, Prof. Claudia Forte and Prof. Bernazzani for professional guidance and insightful conversations throughout the course of this work.

I am indebted to the Scuola Normale Superiore di Pisa for funding my research unless this thesis would not have been possible. In this I would also like to include my appreciation to Prof. Vincenzo Barone, head of the PhD course in chemistry, whose kind supports regarding administration process was incredible.

I owe to thank Marco Martinelli who has made available his support in a number of ways. Furthermore I thank to my all friends and colleagues. You all know who you are and I wish all the best for each of you in the future.

Last but not the least, I want to thank my family: my parents and sisters. I am a lucky person to have such a great family. You all have supported me, throughout the many obstacles in my life to date. I am truly indebted to you all. I would like to express my deepest gratitude to Mina for her love, patience and endless understanding.

Pisa, April 2011

Mohammad Hayatifar

Table of Contents:

Abbreviations

acac	Acetylacetonate
CB	Chlorobenzene
^{13}C CP-MAS NMR	^{13}Carbon cross polarization-magic angel spinning NMR
CGC	Constrained geometry complex
^{13}CNMR	^{13}Carbon nuclear magnetic resonance
Cp	Cyclopentadienyl
dbm	Dibenzoylmethanate
DEAC	Diethylaluminiumchloride
DMAO	TMA-depleted methylaluminoxane
DSC	Differential scanning calorimetric
EASC	Ethylaluminiumsesquichloride
E/H	Ethylene/1-hexene
Et	Ethyl
FTIR	Fourier transformer infrared
GPC	Gel permeation chromatography
ΔH_c	Enthalpy of crystallization
HCL	Hydrochloricacid
HDPE	High-density polyethylene
ΔH_m	Enthalpy of melting
HNMR	Proton nuclear magnetic resonance
Hz	Hertz
IR	Infrared
LLDPE	Linear low-density polyethylene
MAO	Methylaluminoxane
MMA	Methyl methacryalte
MMAO	Modified methylaluminoxane
Me	Methyl
M_n	Number average molecular weight
M_v	Viscosity average molecular weight
M_w	Weight average molecular weight
MWD	Molecular weight distribution

$\overline{n}_E$	Average sequence length of ethylene
$\overline{n}_H$	Average sequence length of 1-hexene
NMR	Nuclear magnetic resonance
PE	Polyethylene
Ph	Phenyl
PP	Polypropylene
PS	Polystyrene
ROMP	Ring opening metathesis polymerization
SCB	Short-chain branch
SCBD	Short-chain branch distribution
SEC	Size exclusion chromatography
T_c	Crystallization temperature
T_g	Glass transition temperature
THF	Tetrahydrofuran
TIBAL	Triisobutylaluminium
TMA	Trimethylaluminium
T_m	Melting temperature
T_m°	Equilibrium melting temperature
TREF	Temperature rising elution fractionation

1 Introduction

1.1 Background

Synthetic polymers are vital to our society, affecting practically every aspect of modern life. For example, they are used in food packaging, water- and gas pipes, cables and cars and in medical applications like joint and bone replacements.[1-4] The ubiquitous nature of these materials is a tremendous research effort, especially in the novel polymer design, as well as in the development of polymerization technologies with enhanced economic and environmental efficiencies. The most common polymers are polyolefins, especially PE (polyethylene) and PP (polypropylene), which have become a significant focal point of such research. These polymers are often considered first for use in any application because of their excellent cost/performance value such as low density, easy recyclability and processability. PE and PP are today's highest volume commodity plastics and they are the most widely utilized thermoplastic polymers. Figure 1 shows the world plastics production in 2004, PE and PP taken 32 and 20 %, respectively.

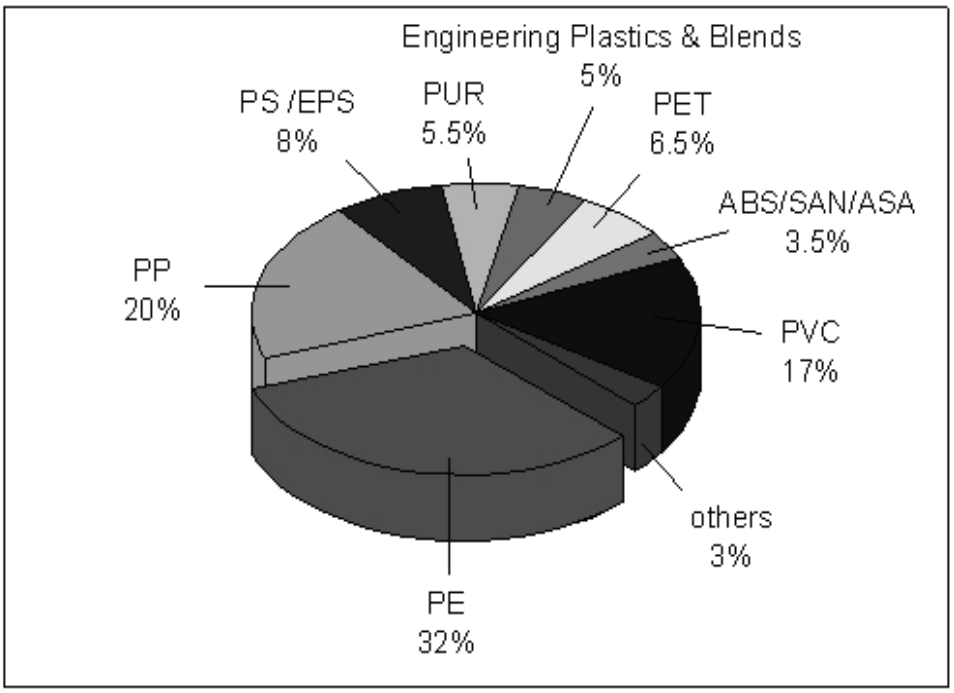

Figure 1. World Plastics Production, breakdown by types of plastic 2004 (tonnage in percent), Source: PlasticsEurope Deutschland, WG Statistics and Market Research.

New applications and growing markets in the developing world, combined with the mature growth in the developed markets, are expected to fuel continuing strong growth for polyolefins. According to Nexant ChemSystems Co. analysis, in 2005 the market for polyolefins was 65 million tons with a 6% growth rate for PE and 40 million tons with an 8% growth rate for PP.[5] Figures 2 and 3 present ChemSystems forecasts on demand, capacity and capacity utilization trends for PE and PP from 1997 to 2010 (latter years estimated).

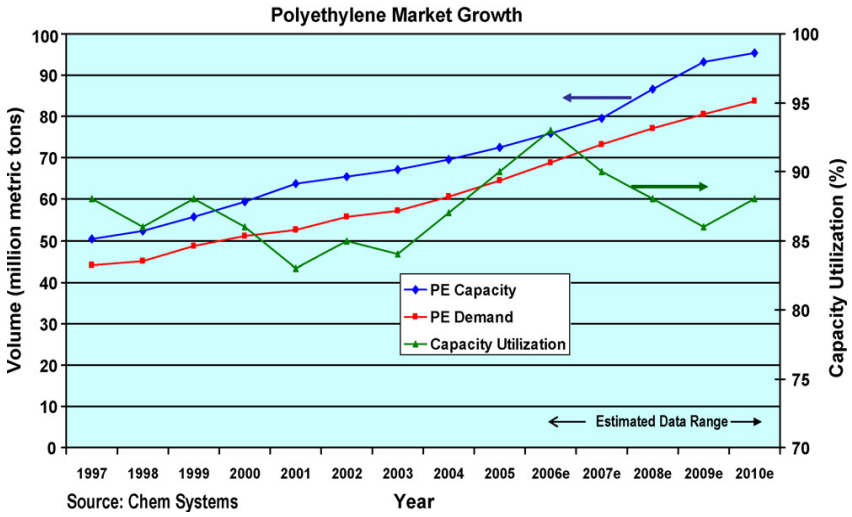

Figure 2. Market growth of polyethylene from 1997.

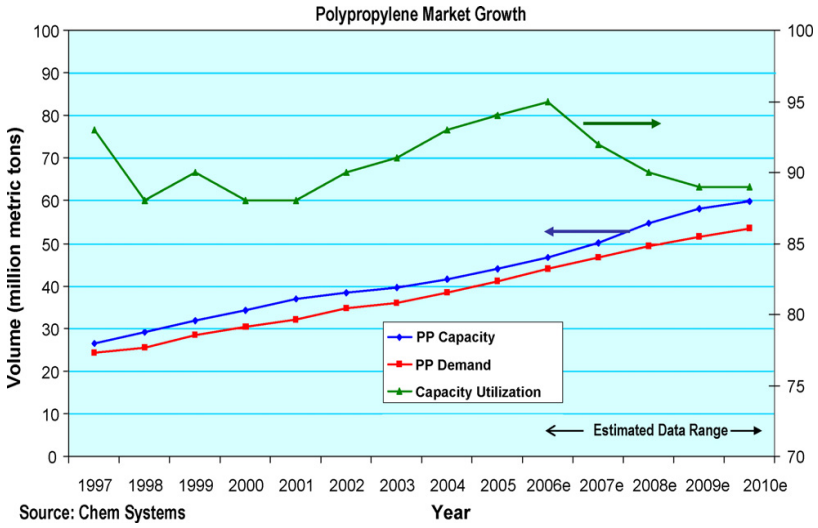

Figure 3. Market growth of polypropylene from 1997.

Until 1953, processes for olefin polymerization were based on a radical process carried out at high temperatures and high pressures. polymerization of ethylene under these conditions (2000-3000 bar; 120-230 $^{\circ}$C) yields low-density PE, a low melting, highly branched PE, containing both long- and short branches.[6] In addition, high molecular weight polypropylene cannot be made via free radical polymerization because of hydrogen transfer to monomer and formation of the highly favored and resonanced-stabilized allylic radicals[7] which results in polypropylene oligomers. The free radical polymerization of olefins has therefore some disadvantages.

Such shortcomings naturally drove research efforts from traditional free radical methods towards novel and more efficient means of obtaining polyolefins. The discovery in the late 1950's of Ziegler/Natta coordination polymerization has revolutionized ethylene and high molecular weight propylene polymerization and allowed access to new stereoregular polymeric materials, such as isotactic polypropylene.[8] In 1963 both Karl Ziegler and Giulio Natta were awarded with the Nobel Prize for their discovery.

After the original work, Ziegler-Natta catalysts have been developed to achieve higher productivities and better stereoselectivity. The current state-of-the-art Ziegler-Natta catalyst comprises of $MgCl_2$ support, $TiCl_4$, aluminium alkyl(s) and internal- and/or external-donor(s).[9-13] Even though the performance of Ziegler-Natta catalysts have been greatly improved in terms of obtaining higher activities and high molecular weight polymers,[14] they have an inherent characteristic of being "multi-site" catalysts, i.e. the environment around the active sites varies, thus resulting in broad molecular weight distributions as well as variations in stereoselectivity.

On the contrary, well-defined homogeneous "single-site" catalysts provide a solution for this drawback of the heterogeneous Ziegler-Natta catalysts. The development of these homogeneous catalysts began via the use of aluminium alkyl activated titanocene derivates in ethylene polymerization,[15-19] but unfortunately these catalysts showed low activity for ethylene and were inactive for propylene polymerization. This situation changed dramatically in the early 1980s when Kaminsky and Sinn discovered that TMA (trimethylaluminium) and a substantial amount of water along with titanocene dichloride complexes were highly active catalysts for the polymerization of ethylene.[20,21] The rise in activity was explained by the formation of MAO (methylaluminoxane) through hydrolysis of TMA. This was later confirmed with the activation of titanocenes and zirconocenes by using a preformed MAO.[22,23] This discovery stimulated a renaissance in Ziegler/Natta catalysis, both in industry and academy and a vast number of patents and

academic papers concerning metallocene catalyzed olefin polymerization have been published. Today metallocene catalysts are well-studied and they can be fine-tuned to produce a number of different poly(α-olefin) structures.[24-29]

Following the success of metallocene mediated polymerization, a number of different homogeneous catalysts (non-metallocences) have been developed. Using these novel catalysts new polymer types, which have not been accessible through Ziegler-Natta and metallocene catalysis, have been obtained.[30,31] This area has gained such rapid momentum, with many new catalyst systems being reported across and also beyond the transition series. To have an idea of the proportion of this growth, figure 4a shows the increase in the number of publications by year over the past decade, while Figure 4b gives the number of publications by Group for the 4 year periods 1994-1997 and 1998-2001. Notable are the increased number of publications for the Group 8 and Group 10 metals over the past 4 years, with the number of publications on the Group 10 metals for the period 1998-2001 substantially surpassing those for the Group 4 metals over the previous 4-year period. Meanwhile, a quick search of the Web[33c] on the topic of "non-metallocene" precursors demonstrates +140% growth in the literature production during the last decade (2001-2010) compared with the number of publications between 1991 and 2000. The new non-metallocene catalyst systems have used a wide range of different organic ligand frameworks.[32,33] The multitude of different ligand options allows one to modify electronic, geometric and steric characteristics of the active site and through this influence the performance of the catalyst. In addition to Group 4 metal complexes which have been at the forefront of these developments, notable achievements have also been established among Ni, Pd, Fe and Co complexes with diimine, diimine-pyridine and salicylaldiminate ligands.[34-38] Late transition metal complexes have opened doors for new types of polyolefins including hyperbranched polyethylene and copolymers of ethylene with polar monomers.[34,39] The development of new catalysts for olefin polymerization continues to be an active area of research in both academic and industrial research groups.[40-46]

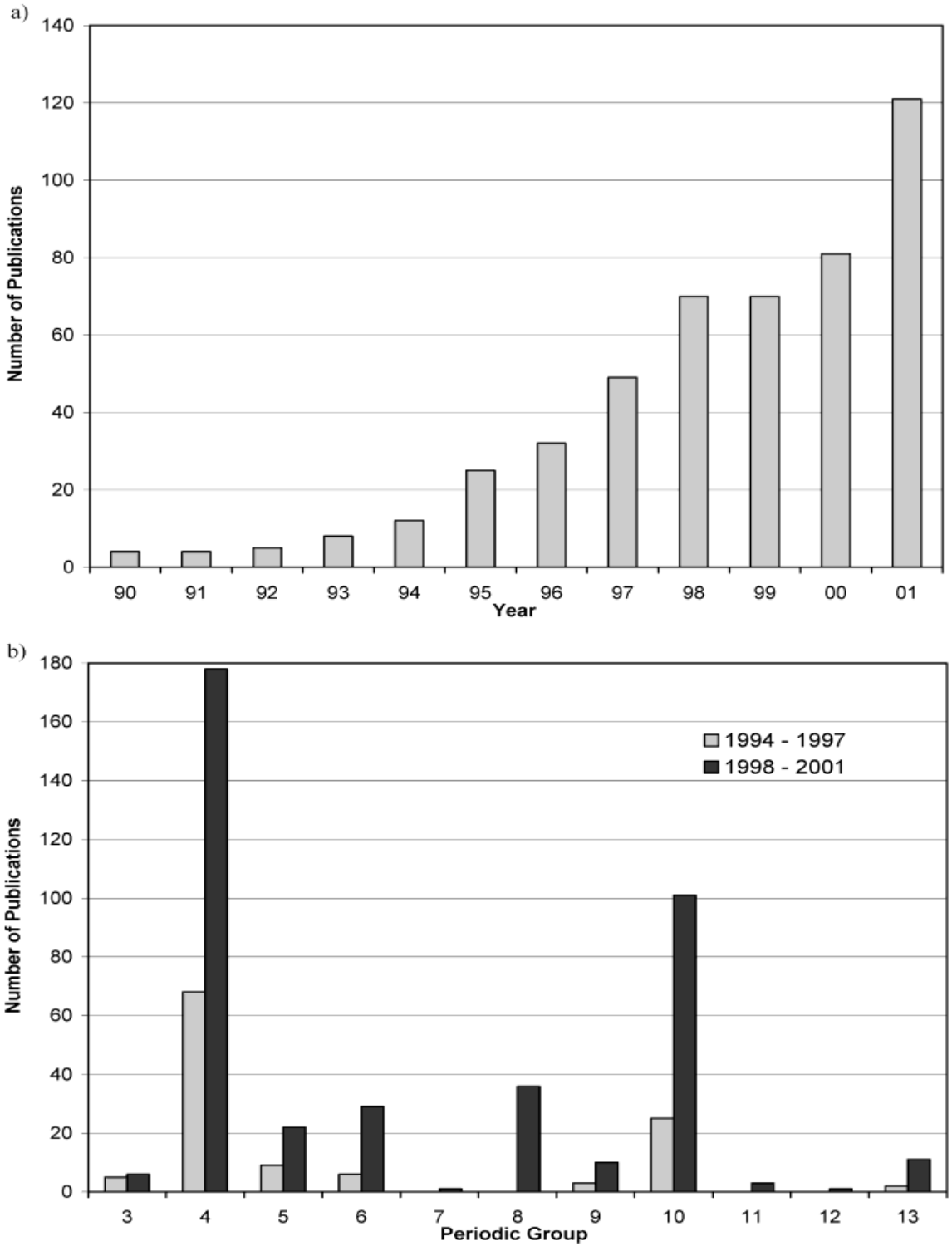

Figure 1.4. Numbers of publications on non-metallocene olefin polymerization catalyst systems appearing in the academic literature: (a) by year between 1990 and 2001, and (b) by periodic group for the 4-year periods 1994-1997 and 1998-2001.

1.2 The scope of the thesis

The work done within this thesis can be divided into two parts. The first and major part of the thesis is devoted to the homopolymerization of ethylene and propylene and copolymerization of ethylene/1-hexene by using Ti(IV) complexes bearing *N*,*N*-dialkylcarbamato ligands. Detailed thermal and structural characterization of obtained copolymers is investigated in this part. The second part includes the synthesis of new chiral aminoacid-containing Group 4 tetracarbamato complexes to be employed as catalytic precursors.

The work done earlier, for example with the complexes supported by phenoxy-imine ligand systems has shown that by changing the ligand structure around the metal center it is possible to tailor the performance of the polymerization catalysts.[47-49] To the best of our knowledge, in the field of olefin polymerization catalysis, the behaviour of carbamato metal complexes, especially early transition metal ones, is almost unknown. For this reason the major part of the thesis was devoted to investigate the olefin polymerization behavior of Group 4 metal complexes bearing *N*,*N*-dialkylcarbamato ligands. These rather cheap, easy to synthesize metal complexes appear good candidates as catalytic precursors for the polymerization.

Ti(IV) complexes bearing *N*,*N*-dialkylcarbamato ligands were synthesized and used in ethylene and propylene homopolymerization as well as ethylene/1-hexene copolymerization. The effect of main reaction parameters such as cocatalyst, solvent and temperature on the productivity was discussed in order to modulate the characteristics of the resulting polymer samples. Various techniques such as NMR, DSC, FTIR and SEC were used for the characterization of the polymeric materials.

Structural characterization and crystallization behavior of the copolymers were studied in depth. The purpose was to achieve better understanding about the structure and the isothermal crystallization behavior of E/H copolymers with high comonomer incorporation.

In the last part of the thesis, new Group 4 metal complexes were synthesized by reaction of *N*,*N*-dialkylcarbamato complexes of titanium and zirconium by some chiral natural aminoacids with the aime of imparting characteristics of stereo-selective catalysts. The new compound were investigated by means of FTIR and NMR and employed preliminarly in ethylene polymerization as catalytic precursors.

1.3 Literature review

1.3.1 Group 4 metallocens

As early as 1957, metallocene catalysts for ethylene polymerization were reported by Natta et al.[17] and by Breslow and Newburg[15]. They found that dichlorobis(cyclopentadienyl)titanium when activated with triethylaluminium or diethylaluminium chloride was effective in polymerizing ethylene. However, these catalysts were of no commercial importance as their catalytic activities were much lower than of classical Ziegler-Natta catalysts and they were inactive towards polymerization of other α-olefins. In 1975, Meyer et al.[50] observed that addition of small amounts of water, usually known as severe catalyst poison, to dichlorobis(cyclopentadienyl)titanium-dimethylaluminium chloride system led to a significant increase in ethylene polymerization rate. Reichert and Meyer also reported a similar increase in activity upon addition of water to titanocene/diethylaluminium chloride system. Soon after, Kaminsky and Sinn[20] reported that ethylene polymerization activity increased to about 104 g PE $mmol^{-1}Ti\ h^{-1}$ when trimethylaluminium (TMA) pretreated with water ($Al:H_2O$ = 2:1 to 5:1) was added to bis(cyclopentadienyl)dimethyltitanium. They attributed this increase in activity to the formation of an aluminoxane *via* partial hydrolysis of TMA. This was further evidenced by Kaminsky and Sinn[21,51] from the observation that bis(cyclopentadienyl)dimethylzirconium when activated with a preformed methylaluminoxane (MAO) resulted in an ethylene polymerization activity of about 104 g PE $mmol^{-1}.Zr\ h^{-1}$. However, these early catalytic systems were unsuitable for commercial production of poly(ethylene)s and resulted in atactic polypropylene, due to no chiral induction from the ligand framework,[23] under the temperature conditions (in the range 30–100 °C) usually applied for propylene polymerization with heterogeneous Ziegler-Natta catalysts. Note that polymers obtained with achiral zironocenes appeared to be very pure atactic propylenes, in contrast to atactic polymers containing isotactic and syndiotactic sequences, usually formed in the presence of heterogeneous Ziegler-Natta catalysts.[52]

Significant increase in catalyst activity and molecular weights were reported by Ewen[53] by modification of the structure of Kaminsky catalyst. He also reported the first stereoselective polymerization of propylene using a $TiCp_2Ph_2$/MAO system. This catalyst

was shown to produce isotactic poly(propylene)s with a novel stereoblock structure by a chain-end stereocontrol mechanism, wherein the chirality of the last inserted monomer unit determines the stereocontrol during the polymerization. Brintzinger et al.[54] found that racemic isomer of *ansa*-metallocenes of C_2 symmetry, such as, dichloroethylenebis(indenyl)zirconium and dichloroethylenebis(tetrahydroindenyl)-zirconium in conjunction with MAO produced poly(propylene)s with very high activities and isotacticities of more than 95%. Ewen also reported the analogous hafnium catalysts which produced high molecular weight, highly isotactic poly(propylene)s.[55] In these cases, stereocontrol is by enantiomorphic or catalytic site control mechanism, where the chirality of the catalyst determines the stereochemistry of the polymerization. Syndiospecific propylene polymerization was first reported by Ewen et al.[56] using a Cs-symmetric catalyst, namely, dichloroisopropylidene(cyclopentadienyl)(9-fluorenyl)zirconium [$Me_2C(Cp)(Flu)ZrCl_2$]. These important results led to phenomenal growth of interest in stereospecific polymerization with homogeneous catalysts. During the last decade, a variety of new catalysts have been presented for the stereospecific polymerization of α-olefins, based on non-bridged metallocene or stereo-rigid *ansa*-metallocene as the procatalysts. Apart from isotactic[57-61] and syndiotactic[57,59,62-63] polypropylenes and other (α-olefin)s,[64] hemiisotactic,[59,64,65] isoblock,[60,61,66] syndioisoblock (stereocopolymer),[67] stereoblock isotactic[68] and stereoblock isotactic-atactic[69-71] polypropylenes have been obtained using these new catalysts.

Cyclic olefins such as cylopentene and norbornene were also polymerized by metallocene catalysts.[72-88] While classical Ziegler-Natta catalysts produce ring-opened products, metallocene catalysts promote vinyl polymerization. Further developments led to catalysts which are capable of polymerizing styrene to syndiotactic poly(styrene)s.[89-92]

In general, metallocene catalysts are capable of polymerizing almost all vinyl monomers with very high activity to give polymers with narrow molecular weight and composition distributions. A number of reviews are available on metallocene catalyzed olefin polymerization.[93-119]

Recently a new family of metallacyclic metallocene catalysts (**1**) was reported by Alt.[120] These species exhibit higher activity than metallocenes and are self immobilizing in solution.

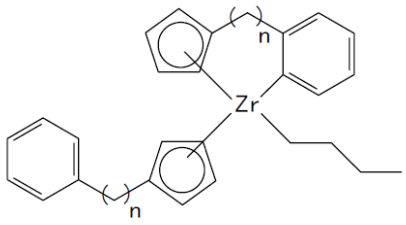

1

Figure 5. Representation of metallacycle metallocene precursor.

When the metallacycles are activated with MAO, the ring expands through repeated insertion of ethylene into the metal carbon sigma bond of the metallacycle, finally resulting in an insoluble polymer that is directly attached to one π-ligand of the active catalyst cation. Poly(ethylene)s produced by metallacycles possess lower molecular weights than those obtained with metallocene dichlorides, presumably due to more facile chain transfer reaction.

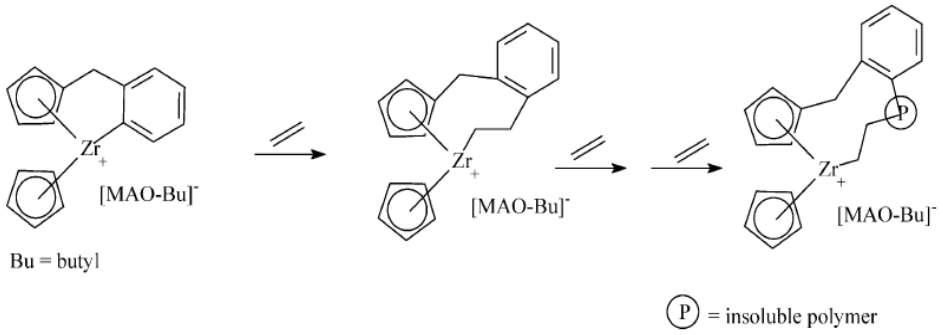

Scheme 1. Schematic representation of ethylene polymerization process activated by metallacylce complex/MAO catalytic system.

1.3.2 The role of cocatalyst

The key to extremely high activity of single-site catalysts in polymerization is the cocatalyst. Methylaluminoxanes (MAOs) are very important activators for catalyst precursors. MAO is obtained by controlled hydrolysis of TMA. The exact structure of MAO still remains obscure. However, several studies have shown that MAO is composed of oligomers of [-Al(CH_3)-O-] units with linear or cage structures and a molecular weight

of roughly 800-1200, and still the structure of MAO is under intensive study.[121] Generally, TMA (either unreacted or formed by disproportionation reactions between the oligomeric components) is present along with MAO. The role of MAO is to alkylate the metallocene dichloride and then abstract a methide ion to generate an electron deficient species which is responsible for the polymerization activity. TMA present in MAO acts as a scavenger of impurities as well as a chain transfer agent.[122]

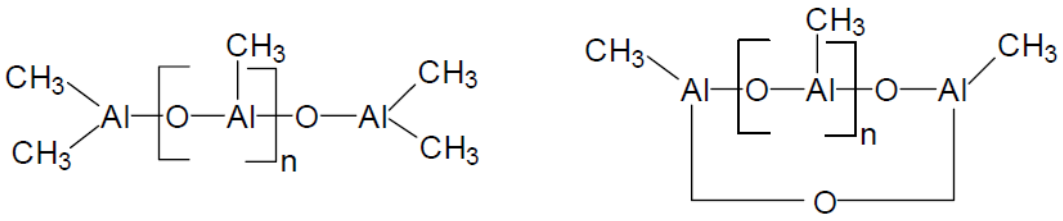

Figure 6. Different structures of MAO.

MMAO is a modified methylaluminoxane in which 25 % of the methyl groups are replaced by isobutyl groups. MMAO is more soluble and has got a longer shelf life than MAO.[123] It must be emphasized that alternative, potentially cheaper alkylaluminoxanes, such as ethyl or *i*-butyl derivatives, which are more soluble in aliphatic hydrocarbons than methylaluminoxane, or other alkylaluminium compounds used as activators for metallocene procatalysts, show inferior activity. Cryoscopic, ^{1}H, ^{17}O and ^{27}Al NMR studies have shown that ethylaluminoxane has a trimeric structure, while a dimeric structure has been proposed for isobutylalumioxane.[124]

One of the disadvantages of metallocene/MAO systems is the large amount of expensive MAO that is often needed for appreciable polymerization activity. Several organoboron compounds such as $B(C_6F_5)_3$, $[Me_2PhNH][B(C_6F_5)_3]$, $[Ph_3C][B(C_6F_5)_4]$ were also found to be efficient activators for metallocene-catalyzed polymerization of olefins. Reaction of these compounds with metallocene dialkyls such as $ZrCp_2(CH_3)_2$ and $ZrEt(Ind)_2(CH_3)_2$ results in the formation of a 14 electron species, $[ZrCp_2(CH_3)]^+$ which is the true active species in polymerization.[125-126] It was observed by Bochmann and Lancaster[127] that zirconium dibenzyl complexes react with boron activators to give cationic Zr-benzyl complexes which are thermally more stable than analogous cationic methyl complexes.This may be attributed to Zr-phenyl interaction that reduces electron deficiency of the metal center. Several modifications of boron cocatalysts have been

reported recently. It is generally observed that more weakly coordinating anions result in higher polymerization activity. Certain carboranes were also found to be effective activators for metallocene-catalyzed olefin polymerizations.[128-129]

Several types of cocatalysts, their role as activators in olefin polymerization and their activation mechanism were recently reviewed by Chen and Marks.[130]

To understand the nearly unlimited versatility of metallocene complexes, it is necessary to take a closer look at the catalyst precursor and its activation process with the cocatalyst (Scheme 2). In most cases the catalyst precursor is a metallocene dichloride complex consisting of two aromatic five-membered ring systems, which can be tethered in addition by a bridging unit (*ansa*-metallocene complexes). The introduction of substituents at certain positions of the two aromatic ligands and/or the bridge modifies not only the steric and electronic conditions in the molecule but also the symmetry of such a metallocene dichloride complex. Another variable parameter is the metal: M = *e.g.* Ti, Zr, Hf.[111]

Neutral metallocene compound (ML_2Cl_2) is inactive without an activator and requires a strong Lewis acid (i.e. methylaluminoxane) to form a cationic metal center, which is active in α-olefin polymerization.

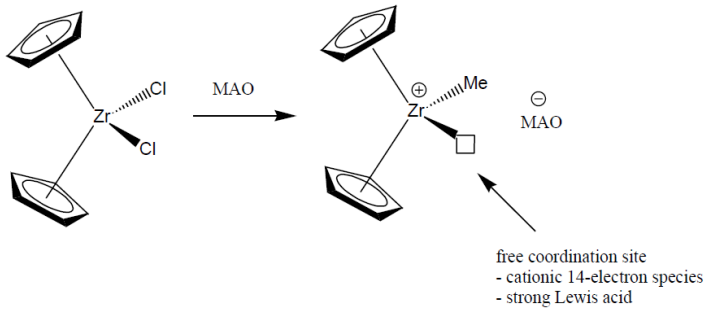

Scheme 2. Activation scheme of metallocene complex by MAO.

1.3.3 Group 4 non-metallocene catalysts for α-olefin polymerization

As mentioned earlier, in particular, non-metallocene olefin polymerization catalysts have been intensively studied in recent years owing to the merits of the increased opportunities for observing new polymerization behavior and the increased patentability of the observation. In this part Group 4 non-metallocene polymerization catalysts will be

reviewed, with more emphasizes on the development of complexes bearing [*O,O*] and [*O,N*] ligands which have obtained a considerable interest especially since the mid-1990s. This interest is due to the fact that metallocene catalysts are well patented and these non-metallocene catalysts with single-site properties offer an attractive alternative. Most complexes are dichloride derivatives and as such need a suitable activator before they can be used as catalysts in a polymerization reaction.[130-131]

1.3.3.1 Mechanism of polymerization

As already discussed, MAO is often chosen as the cocatalyst for Group 4 metal complexes. As depicted in Scheme 3, MAO has two roles in activation step: firstly, it alkylates the metal complex and secondly, it abstracts one of the alkyl groups to form the active species.[22,23] The rate of alkylation and the abstraction process is affected by the nature of the metal, the ligand structure around it and by the chemical nature of the labile leaving groups. According to this mechanism potential ligand structures should be designed so that they do not donate too much electron density to the metal center and consequently diminish the high positive charge of the catalytic site as this can lead to a slower alkylation rate. Halides and alkyl groups are generally preferred as leaving groups.

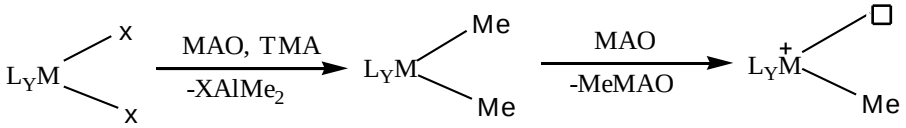

Scheme 3. Activation of Group 4 complexes with MAO.

The catalytically active sites, which are formed through alkyl abstraction, are strong Lewis acids that can coordinate the olefin monomer to vacant site (Scheme 4). The coordinated monomer is then inserted by migration into the metal-carbon bond to form a longer alkyl-group. Then the chain growth takes place via multiple *cis*-insertions of monomer into the metal-carbon bond. This polymerization mechanism was proposed by Cossee and Arlman and is generally accepted for homogeneous catalysts.[132] This mechanism requires that the catalyst candidates are designed to have two labile leaving groups in *cis*-positions toward each other to enable fast propagation rates. Complexes

bearing leaving groups in *trans*-position towards each other often lead to moderate activities (less than 30 kg PE $mol_{Ti}^{-1} \cdot h^{-1} \cdot bar^{-1}$).[133] It should be noted, however, that the configuration of complexes is usually determined for dichloride or other non-activated catalysts and it is possible that activated species may adopt a different configuration.

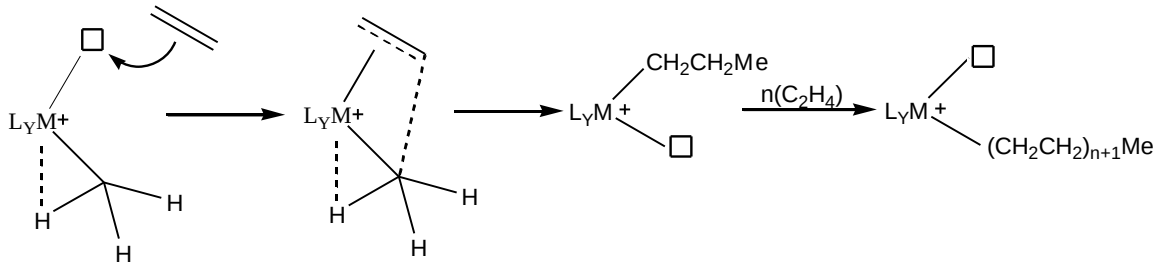

Scheme 4. Propagation step in olefin polymerization.

The polymerization reaction is terminated by hydrogen transfer to monomer, by chain transfer to aluminium or by β-H elimination as depicted in Scheme 5. The dominant termination mechanism is depended on the catalyst structure, reaction conditions and the type and amount of used cocatalyst.

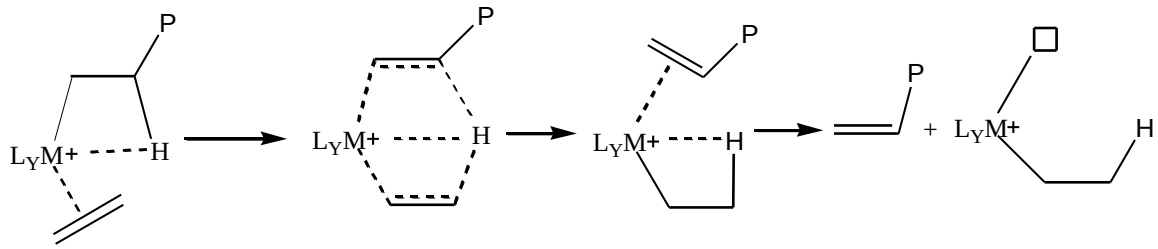

Hydrogen transfer to monomer

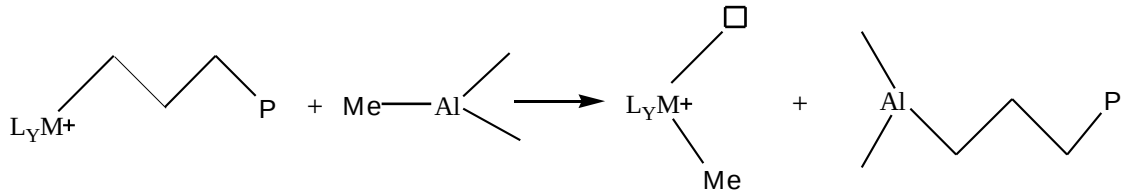

Chain transfer to aluminium

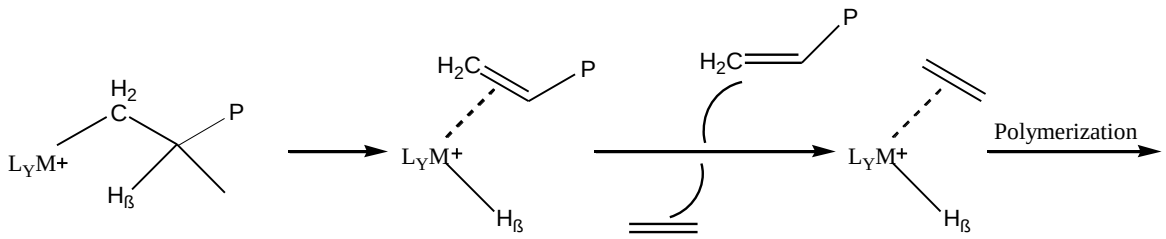

β-H elimination

Scheme 5. Termination mechanisms for polymer chain growth.

Propylene and other α-olefins can coordinate to the vacant site of the active metal center in four different modes, as depicted in Figure 7. Both primary (1,2) and secondary (2,1) insertions are possible but for α-olefins 1,2-insertions are electronically favored. It has been shown that the ligand structure around the active metal site determines the position of the growing chain and by doing so also determines the orientation of the coordinating monomer. The single-site catalysts can be designed to give the desired stereoregularity for the polymer product. The isotactic polymers consist of chiral centers of the same configuration whereas syndiotactic polymers comprise of alternative chiral centers. In atactic polymers no order of configuration is present. A schematic representation of the stereoregularity, as it was proposed by Giulio Natta, is depicted in Figure 8.[8f] In addition to the basic structures given in Figure 8, the use of single-site catalysts has also opened doors for synthesis of hemi-isotactic and stereo-blockcopolymers.[134-137] Moreover, it is also possible to design a dual-side metallocene catalyst to introduce controlled errors into the polypropylene chain and so tailor the polymer properties.[138]

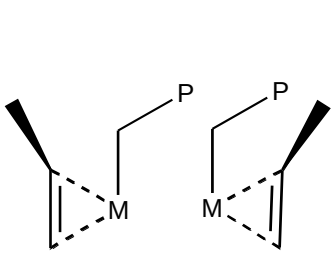

(1,2) propylene insertion

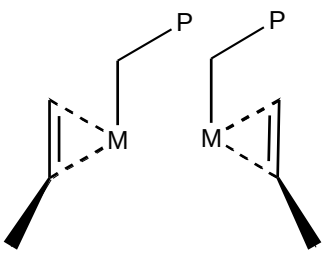

(2,1) propylene insertion

Figure 7. Possible insertion modes of propylene.

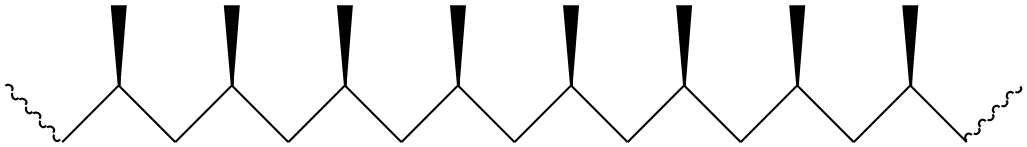

Isotactic PP

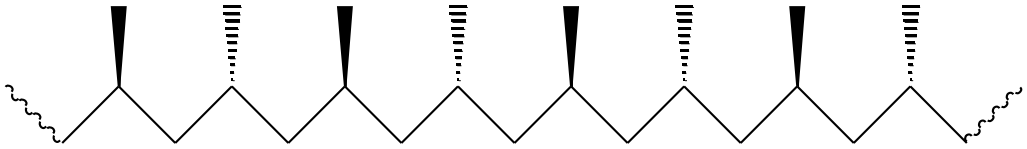

Syndiotactic PP

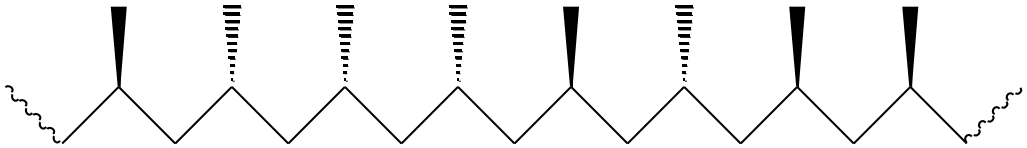

Atactic PP

Figure 8. Possible stereostructures of polypropylene.

1.3.3.2 Constrained geometry catalysts (CGC)

Researchers at Dow[139,140] and Exxon[141-143] contributed to the development of metallocene analogous with mono-cyclopentadienyl amido complexes (**2**) which are known as "constrained geometry catalysts, CGC". CGCs originated by exchanging one of the cyclopentadienyl donors of *ansa*-metallocene with a pendant amido donor group. This substitution vastly changes the electronics of the ligand, which remains dianionic in nature. The smaller bite angle of these ligands to a metal center is the origin of the term "constrained geometry". However, because of the more open coordination sphere, they are superior to bridged metallocenes in ethylene copolymerizations incorporating higher α-olefins, cyclic olefins, and styrene.[144]

Furthermore, because CGCs retain their activity and ability at high temperatures (140-180 °C), thus they are especially suitable for solution polymerization processes to produce high-molar mass polyethylenes.

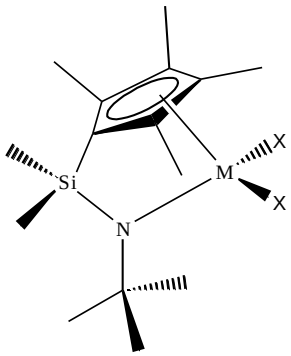

2

Figure 9. Example of constrained geometry catalyst (CGC).

Constrained geometry catalysts produce polyolefins with narrow molecular weight and comonomer distributions. As shown in Figure 10, the comonomer distribution, measured by the Temperature Rising Elution Fraction (TREF) technique, for the homogeneous ethylene/octane copolymer prepared by the CGC catalyst is more uniform or "narrower" than that of conventional LLDPE, which is mixture of all different kinds of polymer molecules that have different levels of α-olefin comonomer incorporated in the polymer backbone.[5a]

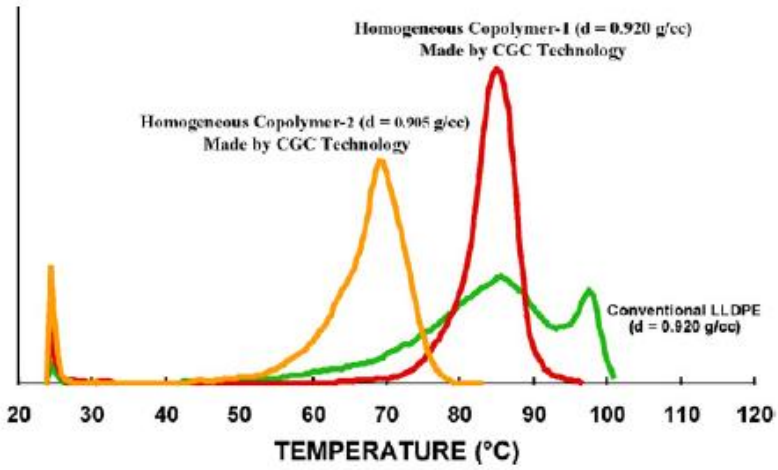

Figure 10. Comonomer distribution of ethylene-octene copolymers measured by TREF.

Generally, narrow molecular weight and comonomer distributions were found to improve physical properties at the expense of processability. Dow has developed a new technology called "INSITE" which produces polymers with good physical properties without sacrificing processability.[145] Improved processability could be due to the presence of small amounts of long chain branching resulting from reincorporation of α-olefins produced as a result of β-H transfer at higher temperatures. Evidence for this mechanism was reported by Soga and coworkers[146,147] who polymerized ethylene with oligoethylene and polypropylene macromonomer.

Dow INSITE technology is capable of producing polyolefin elastomers (POE) and polyolefin plastomers (POP) by copolymerization of ethylene with α-olefins such as 1-hexene, 1-octene and 1-decene. Stevens studied the effect of Cp substituents, bridging group and metal in the copolymerization of ethylene with 1-octene using the constrained geometry catalyst, $Ti[Me_2Si(Me_4Cp)N^tBu]Cl_2$/MAO.[148] Ultra-low density elastomers with as high as 56 mol% 1-octene content were obtained under appropriate polymerization conditions.

Conventional Ziegler-Natta catalysts incorporate only very small amounts of styrene (<1 mol %) into polyethylene chains.[149,150] In most cases, mixtures of homopolymers were produced and polymer molecular weights were also very low.[151,152] Metallocenes exhibit very low activities and poor regiospecificity in such copolymerizations. Constrained geometry catalysts are capable of copolymerizing ethylene and styrene with very high activities, high styrene contents and no contamination with polystyrene impurities.[153-158] The reactivity ratios (r_1 and r_2) calculated from copolymer composition and monomer feed by using the Fineman-Ross eqution as follows:

$$F(f-1)/f = (r_1.F^2/f) - r_2 \qquad (F = [M_1]/[M_2];\ f = d[M_1]/d[M_2])$$

and found to be 23.4 for ethylene and 0.015 for styrene, clearly indicating that the styrene does not prefer multiple insertion whereas ethylene does. Sernetz et al. studied the effect of ligands on ethylene/styrene copolymerization using constrained geometry catalysts observing that sterically hindered catalysts show higher activity due to high electron density at the metal.[159] Xu obtained a perfectly alternating ethylene-styrene copolymer with well defined isotactic structure using the catalyst system $[Me_2Si(Flu)(N^tBu)TiMe][B(C_6F_5)_4]$.[160] In another study, Chung and Lu reported

copolymerization of ethylene with a reactive monomer such as *p*-methylstyrene that the resulting copolymers are useful intermediates in the preparation of functional polyolefins.[161] A broad range of polyolefin elastomers based on terpolymers of ethylene with p-methyl styrene and a third olefin such as propylene and 1-octene was also produced using constrained geometry catalysts.

Copolymerization of ethylene with cyclic olefins such as norbornene using various constrained geometry catalysts has been reported.[162-164] In all cases, unexpectedly low norbornene incorporations (<50 mol %) were observed. Microstructure of the copolymers depends on catalyst structure, yielding copolymers with mainly isolated norbornene units, alternating monomer sequences or short norbornene microblocks.

Several modifications of constrained geometry catalysts have been reported in the literature.[165] Figure 12 shows a short list of complexes that have already been synthesized.

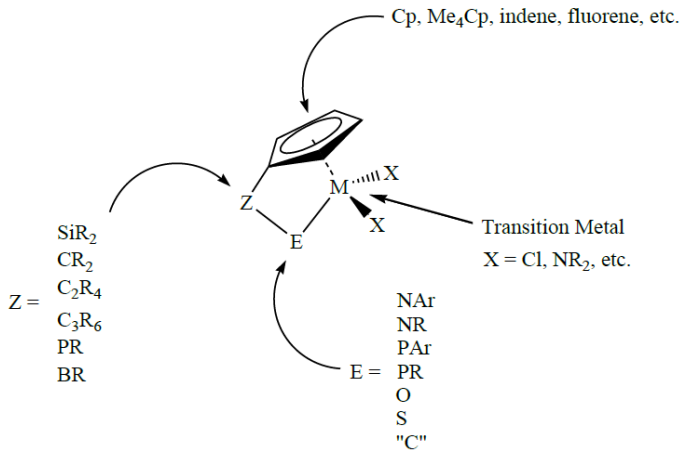

Figure 11. Typical constrained geometry complexes.

Teuben and coworkers[166] reported ethylene-bridged titanium complexes (**3**) which showed higher activities for homopolymerization of ethylene and its copolymerization with 1–octene than the corresponding $-SiMe_2$ bridged complexes. A phosphorus-bridged cyclopentadienyl amide titanium complex (**4**) was reported by Kotov et al.[167] which produced linear high molecular weight polyethylenes with an activity of 100 g PE $mmol^{-1}Ti \cdot h^{-1} \cdot bar^{-1}$. Park and coworkers reported bridged cyclopentadienyl hydrazido titanium complexes which exhibit lower activities for polymerization of ethylene but produce high molecular weight polymers.[168]

Several indenyl and fluorenyl constrained geometry derivatives that exhibit higher activities for the polymerization of ethylene have also been reported.[169-173] Klosin et al. reported heteroatom susbstituted constrained geometry complexes which when activated with $B(C_6F_5)_3$ show dramatic increase in activity for ethylene/1-octene copolymerizations.[174]

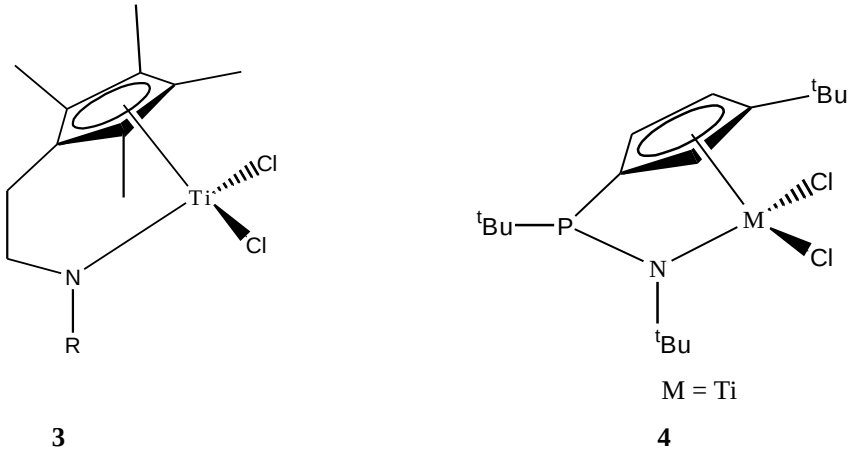

3 **4**

Figure 12. Structures of ethylene- and phosphorus-bridged CGC derivatives for ethylene polymerization.

Bazan and coworkers reported the use of a combination of a constrained geometry catalyst and a boratabenzene zirconium catalyst for obtaining long chain branched poly(ethylene)s without addition of another olefin.[175] The boratabenzene complex oligomerizes ethylene to α-olefins which get incorporated into polyethylene chains produced from constrained geometry catalysts. This is termed as "tandem catalysis" wherein two independent catalysts work cooperatively to produce a single product.[176a]

A series of *ansa*-cyclopentadienyl-phenoxy titanium complexes (PHENICS) were prepared by Imai et al.[176b]. These complexes exhibited good catalytic activities for copolymerization of ethylene and 1-hexene upon activation with TIBA/borate. Particularly, the PHENICS complexes with a bulky substituent at the *ortho* position of the phenoxy moiety showed excellent catalytic behavior (27,700 $kg \cdot mol^{-1} \cdot h^{-1}$ at 80 °C, 6000 $kg \cdot mol^{-1} \cdot h^{-1}$ at 180 °C).

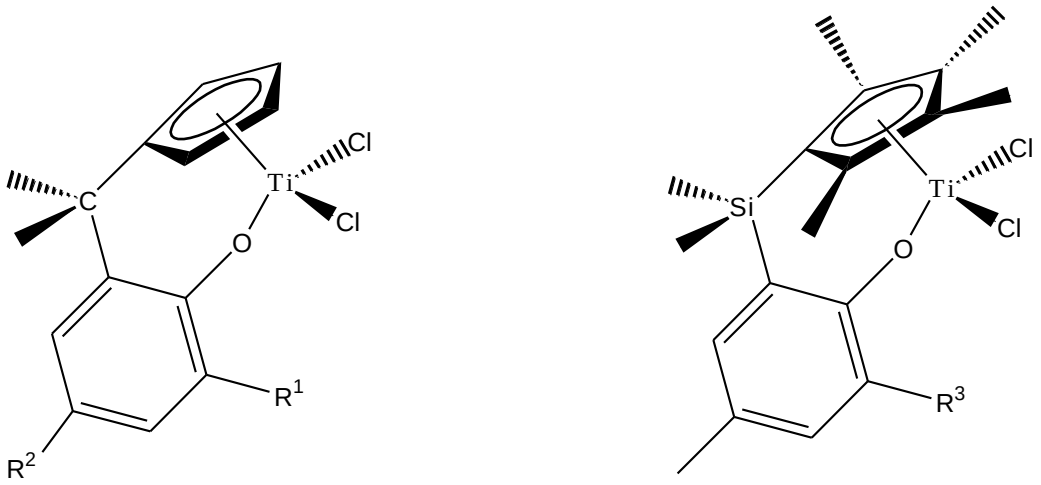

R^1 = H, R^2 = H
R^1 = ^{t}Bu, R^2 = Me

R^3 = ^{i}Pr, ^{t}Bu, A

Figure 13. PHENICS complexes.

1.3.3.3 Chelating amides and related ligands

1.3.3.3.1 Diamide ligands

Dianionic diamide chelate ligands in which two amide functionalities are linked by a spacer represent the class of amide ligands and have been frequently used as ancillary ligands in deriving new non-metallocene catalysts. In 1996, McConville and coworkers reported chelating diamide complexes of titanium (**5**) bearing bulky substituents which are capable of polymerizing higher α-olefins with very high activities.[177,178]For example, 1-hexene is polymerized with an activity of 3.5×10^5 g polyhexene·$mmol_{Ti}^{-1}$·h^{-1}. Activities of these catalysts decrease in toluene which may be attributed to the possible coordination of toluene to titanium that decreases the rate of insertion of 1-hexene. It was observed that chain transfer to aluminum is the only chain termination mechanism for these catalysts when MAO was used as cocatalyst.[179] However, when boron activators such as $B(C_6F_5)_3$ are used, no chain transfer occurs, resulting in a living polymerization system. Thus the catalyst system $Ti[ArN(CH_2)_3NAr]Me_2/B(C_6F_5)_3$ polymerizes 1-hexene, 1-octene and 1-decene with high molecular weights and narrow polydispersities (1.05-1.11). Catalyst activities and polymer molecular weights increase when polymerizations

are run in dichloromethane which may be due to greater charge separation between the ions in presence of this polar solvent.

Uozumi and coworkers obtained isotactic polypropylenes using chelating diamide complexes with various $AlR_3/Ph_3CB(C_6F_5)_4$ co-catalysts and found that higher isotacticities were observed when bulky aluminum alkyls such as trihexyl or trioctyl aluminum were used.[180,181] Isotacticities were also found to increase in presence of cyclohexene at low propylene concentrations. Several modifications of these catalysts such as using various kinds of bridging units were employed as can be seen in figure 15.[182-200]

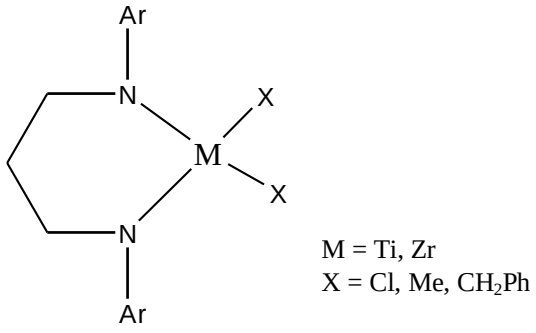

5

Figure 14. Schematic representation of titanium complexes bearing diamide chelate ligands.

A set of McConville's analogues such as the compounds **6** and **7** where the spacer length is similar to McConville's propylene bridge but the flexibility of the spacer is reduced due to the introduction of a aromatic ring has been reported.[185-191] The effect of such a tuning on the polymerization behavior is not straightforward. For example, the titanium and zirconium analogues of **6** activated by cocatalyst MAO show as low activities for ethylene polymerization as several hundreds kg $PE{\cdot}mol_{cat}^{-1}{\cdot}h^{-1}{\cdot}bar^{-1}$ while the titanium analogue of **6** could be highly activated by $Ph_3CB(C_6F_5)_4/Al^iBu_3$ for ethylene/1-butene copolymerization with 12,400 kg of $polymer{\times}mol^{-1}{\cdot}h^{-1}$ activity at 6 (kg/cm^2) of ethylene pressure.[185-188] The use of longer spacer as in **8** also gives rise to high activity of 5200 kg $PE{\cdot}mol^{-1}{\cdot}h^{-1}$ for ethylene polymerization. Boron and indium atoms play interesting role as spacers since the compounds **9** and **10** are very active for ethylene/1-octene copoymerization.[193,194]

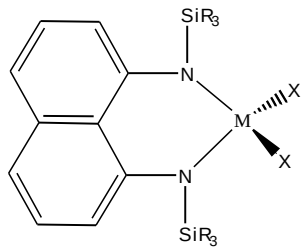

M = Ti, Zr
R = Me, ^{i}Pr
X = Cl

6

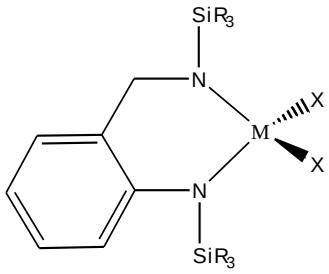

M = Ti; R = Me; X = Me, CH_2Ph, Cl
M = Zr; R = Me; X = Cl

7

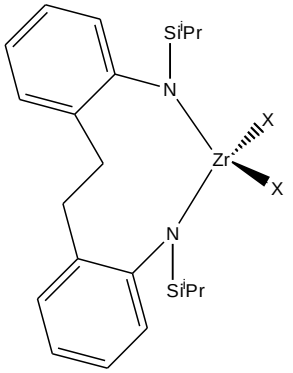

X = Me, Cl

8

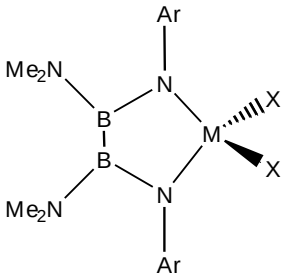

M = Ti; X = Me, Cl
M = Zr; X = CH_2Ph
Ar = 2,6-diisopropylphenyl

9

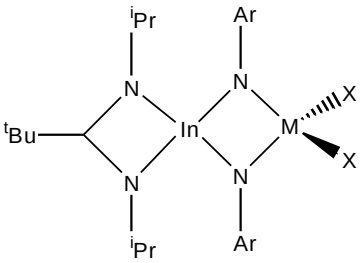

M = Ti
X = NMe_2
Ar = 2,6-diisopropylphenyl

10

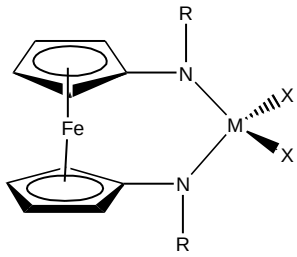

M = Zr
X = CH_2Ph
R = Me

11

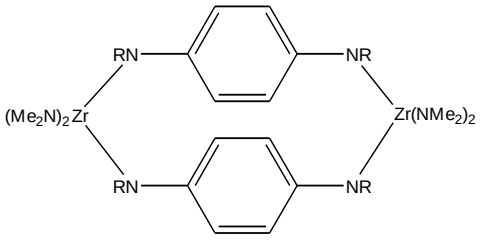

12

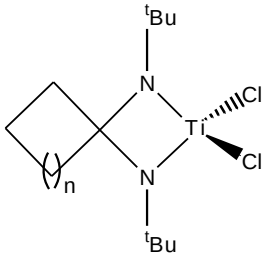

13

Figure 15. Examples of Group 4 complexes supported by diamide ligands.

1.3.3.3.2 β-Diketiminate and related six-membered chelate ligands

Recently several early transition metal complexes bearing β-diketiminate or "nacnac" ligands have been reported. However, their polymerization activities were generally

moderate to low. Jin and Novak reported a series of mono(β-diketiminate)zirconium(IV) complexes (**14**) which exhibit activity of 45 kg PE·mol^{-1}·h^{-1}·bar^{-1}.[201] These catalysts were stable for longer reaction periods up to 16 h. A β-diketiminate Ti(III) complex (**15**) was reported by Theopold and it exhibited a very low activity.[202]

Collins and coworkers reported bis(β-diketiminate)zirconium complexes which are slightly more active than the mono(β-diketiminate) ones and yield poly(ethylene)s with narrow molecular weight distributions.[203] Zirconium complexes in which the β-diketiminate ligand is in the η^5 coordination mode (6 electron donor) exhibit activities as high as 2200 kg·mol^{-1}·h^{-1}·bar^{-1} when electron withdrawing *p*-$CF_3C_6H_3$ substituents are present on the nitrogen.[204]

Active catalysts for the living polymerization of ethylene at room temperature are obtained with titanium complexes of the type **16**, based on 7-arylimino-indole ligands, which also form six-membered chelates.[205] The highest activity (1140 kg·mol^{-1}·h^{-1}·bar^{-1}) is observed with the electron-withdrawing pentafluorophenyl group attached to the imino nitrogen atoms.[206]

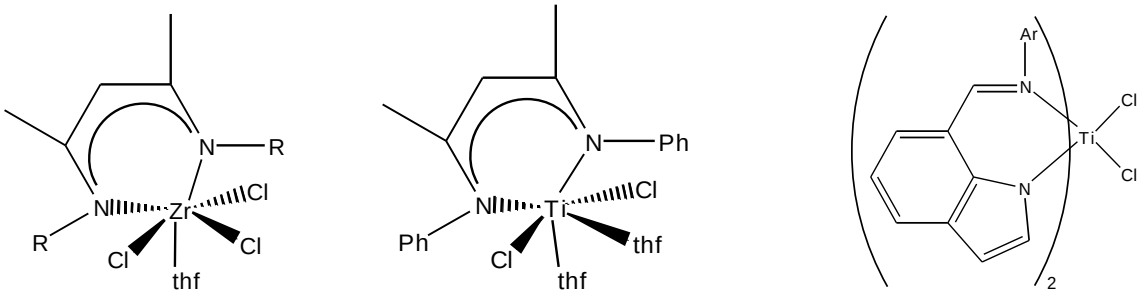

14 **15** **16**

Figure 16 Examples of Group 4 complexes bearing β-Diketiminate (**14**,**15**) and arylimino-indole (**16**) ligands.

1.3.3.3.3 Pyrrolide-imines and related five-membered chelate ligands

Pyrrolide-imine ligand has been actively employed in developing various metal complexes[207-213] such as **17**. When the complexes **17** were activated by MAO for ethylene polymerization, the activity range of several tens to thousands kg PE·mol^{-1}·h^{-1}·bar^{-1} was observed for zirconium[211], hafnium[210] complexes while the high activity of 14,100 kg

PE·mol^{-1}·h^{-1}·bar^{-1} was seen only for the titanium complex.[207,208] The titanium complex of **17** is also highly active for the living copolymerization of ethylene and norbornene, producing high-molecular-weight polymer with a molecular weight distribution of 1.16 and approximately 50:50 comonomer content.[207]

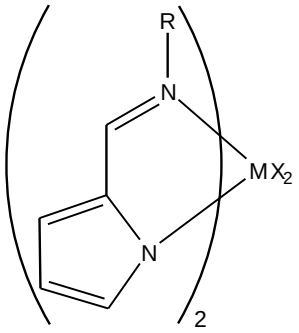

M = Ti, Zr and Hf
X = Cl

17

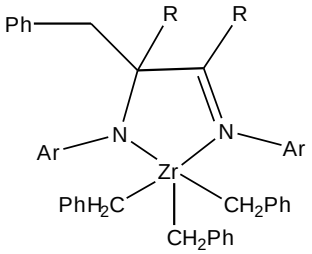

18

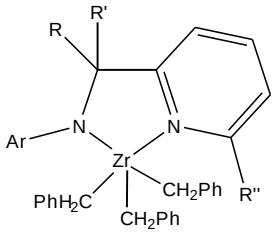

19

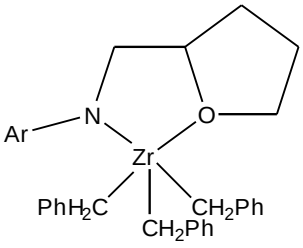

20

Figure 17. Schematic representation of Group 4 metal complexes of pyrrolide-imine and related five-membered chelate ligands.

Murray reported related five-membered Zr amido systems for the polymerization of ethylene (**18**).[214] Upon activation of **18** with MMAO, activities up to 6100 kg·mol^{-1}·h^{-1}·bar^{-1} were reached for ethylene polymerization. Higher activities were achieved for the copolymerization of ethylene with 1-hexene using complexes **19** and **20**.[215,216] The activity is strongly dependent on the size of the aryl substituent. The highest activity was observed for Ar = 2,6-^{i}Pr-C_6H_3, whereas more bulky or less bulky substituents (Ar = 2,4,6-^{t}Bu$_3$C$_6$H$_2$ or Ph) result in greatly reduced activities.

1.3.3.3.4 Amidinates and related four-membered chelate ligands

Amidinate ligands are monoanionic bidentate N-C-N chelates that tend to form 6-coordinate complexes with Group 4 metals and a limited number of examples of 5-coordinated amidinate metal complexes is known as illustrated in figure 18. Complexes such as **21** and **22** have had a long-standing presence in olefin polymerization catalysis.[217] More recently, Eisen and co-workers reported the formation of isotactic PP using tris-(amidinate) Zr complexes bearing chiral N-substituents,[218] or with bis(amidinate) complexes **21** bearing achiral substituents R at higher propylene pressures.[219] At lower propylene pressure, epimerization becomes faster than the stereoregular insertion of propylene, and atactic polymer is thus formed.[220,221]

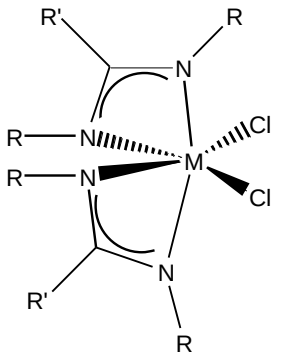

M = Ti, Zr
R = ^{i}Pr, Cy, TMS
R′ = Ph

21

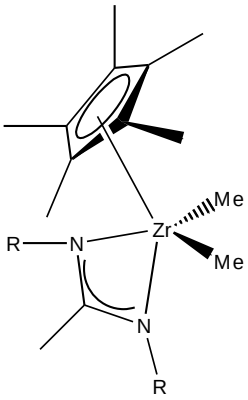

R = ^{t}Bu
R′ = cyclohexyl
R′ = 2,6-diisopropylphenyl

22

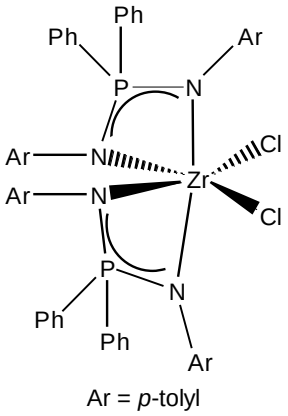

Ar = *p*-tolyl

23

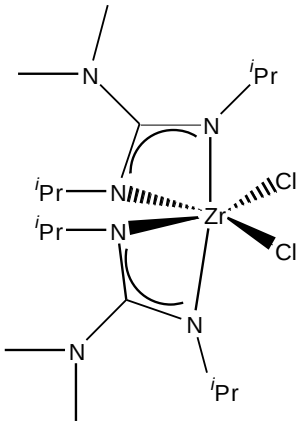

24

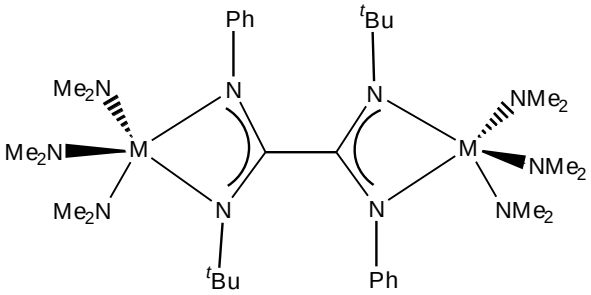

M = Ti, Zr

25

Figure 18. Examples of Group 4 complexes bearing amidinate ligands.

Unsymmetrically substituted amidinate complexes of the type **22** (R ≠ R´), reported by Jayaratne and Sita,[222] are moderately active for the polymerization of 1-hexene after activation with $[NHMe_2Ph][B(C_6F_5)_4]$, but at low temperature the polymerization proceeds in a living manner with good stereocontrol to form isotactic (>95%) poly(1-hexene). The related bis(iminophosphonamide) complex **23**, developed by Collins and coworkers, showed an ethylene polymerization activity of 1400 kg mol^{-1} h^{-1} bar^{-1}, substantially higher than obtained for bis-amidinate complexes of the type **21**.[223] Binuclear oxalic amidinate complexes of titanium and zirconium (**25**) have been reported by Green and coworkers showed moderate activities for the polymerization of ethylene; the activity can be increased by prealkylation of the dimethylamide complexes with TMA or Al^iBu_3.[224]

Sterically related to the amidinate ligand is the guanidine ligand, as shown in complex **24**, but this ligand offers the possibility for an enhanced resonance stabilization of a cationic metal center. Precatalyst **24** exhibits a higher ethylene polymerization activity (340 $kg{\cdot}mol^{-1}{\cdot}h^{-1}{\cdot}bar^{-1}$) compared to its amidinate relatives.[225] Activities of up to 800 $kg{\cdot}mol^{-1}{\cdot}h^{-1}{\cdot}bar^{-1}$ have been disclosed in the patent literature for titanium and zirconium complexes bearing heterocyclic guanidinate-type ligands.[226]

1.3.3.3.5 Group 4 complexes bearing [*O,O*]-type ligands as catalysts for olefin polymerization

Monoanionic alkoxide ligands are considered to be isonumeral and isolobal with Cp (cyclopentadienyl) ligands, i.e. they can both bind to a metal using one *s* and two *p* orbitals.[227] In this way, alkoxide ligands can donate up to six electrons to the metal center[228] with two labile halogen or alkyl group this would result in a 16-electron complex and, when activated, forms a cationic 14-electron species. However, due to the higher electronegativity of oxygen, the alkoxides are more often regarded as four-electron donor ligands.[229] Applying this concept means that by using [*O,O*] and [*N,O*] chelating ligands it is possible to generate cationic 14-electron species.

Complexes with an acetylacetonato (acac) type backbone are known for most transition metals (Figure 19).[230] Group 4 complexes with bis(*β*-diketonato) ligands have been shown to adopt the *cis*-configuration, which is suitable for *α*-olefin polymerizations although steric effects can favor the *trans*-isomer.[231,232] Some of these types of complexes

have been utilized as catalysts for ethylene polymerization.[233-235] Janiak et al. reported the synthesis of zirconium complexes with acetylacetonate and dibenzoylmethanate (dbm) ligands.[233] These catalysts were studied by varying the number of chelating ligands and it was found that after MAO activation all the complexes were active in ethylene polymerizations, the maximum activity of 1130 kg mol^{-1} h^{-1} bar^{-1} was achieved with $Zr(dbm)Cl_2$ complex. The fact that even $Zr(acac)_4$ was active in ethylene polymerization implies that the TMA present in MAO is able to remove one or more chelating ligands to generate the active species. All the diketonato-catalysts were able to produce high M_w polyethylene with a reasonably narrow molecular weight distribution (PDI close to 3).

The dibenzoylmethane ligand has also been used with a titanium complex.[234] MAO activated $Ti(dbm)_2Cl_2$ was found to be less active than the zirconium analogue, exhibiting ethylene polymerization activity up to 530 $kg \cdot mol^{-1} \cdot h^{-1} \cdot bar^{-1}$. Also, this catalyst system produces polymers with a much broader molecular weight distribution.

The role of the cocatalyst for activation of *β*-diketonato-complexes was demonstrated by Mitani et al.[235] Zirconium complexes with various acetylacetonato-type ligands were synthesized and activated with different Al-compounds. The use of MAO and TMA as activators leads to the formation of polyethylene while the use of chlorinated aluminium alkyls, like dimethylaluminium chloride, resulted in the formation of oligomeric products. Both the oligomerization activity as well as the distribution of oligomers was dependent on the nature of the substituents in the acetylacetonate backbone.

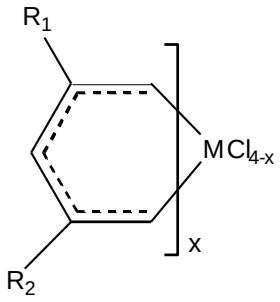

M = Group 4 metal
X = 1-4
R_1 = Ph or alkyl group
R_2 = Ph or alkyl group

Figure 19. General representation of studied acac-type Group 4 metal complexes.

β-diketonato complexes have also been used as polymerization catalysts for number of other monomers. For example, zirconium acetylacetonato precursors were able to produce elastic polypropylene and the use of titanium diketonato complexes in the polymerization of styrene resulted in formation of syndiotactic polymer.[236,237]

The dinuclear titanium complex with ethoxide ligands (**26**) was found to react with MAO to give mainly a heterobimetallic cationic monomethyl species with ethoxide bridges as the main active species for the polymerization of propylene and ethylene.[238] The lifetime of this complex is sufficiently long to allow an effective polymerization. The obtained polymers display intermediate tacticities and high molecular weight. The presence of the chlorine atoms in the complex has proven crucial for the formation and stabilization of an octahedral single site active species.

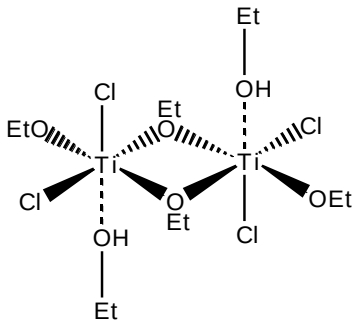

26

Figure 20. Structure of dinuclear titanium complex bearing ethoxide ligands.

A number of complexes bearing one alkoxide group with an additional oxygen donor have been prepared and used in ethylene polymerizations.[239-243] Sobota et al. have investigated such titanium complexes with 3-hydroxy-2-methyl-4-pyrone and 2-methoxyphenol ligand structures as displayed in Figure 21.[239] Despite the differences between these ligands only a small effect on catalytic activity was observed. However, in the case of complexes bearing only one ligand the activity difference is more profound favoring the 3-hydroxy-2-methyl-4-pyrone-based catalysts. Also, an effect of the leaving group was observed: the replacement of chloride by an ethoxide group leads to a decreased activity. Basso et. al. have also studied similar catalysts to Sobota ones.[240-242] The zirconium analogue of Sobota's 3-hydroxy-2-methyl-4-pyrone complex proved to be more active than the titanium one.

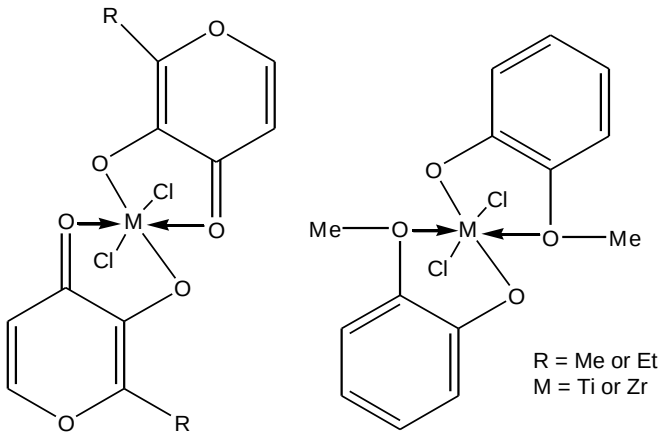

Figure 21. General description of Group 4 metal complexes bearing pyrone and methoxophenol ligands.

The activity of both the zirconium and titanium catalysts was dependent on polymerization temperature as well as Al/M ratio. However, the zirconium complex was more thermally stable then titanium analogue and the activity was enhanced at higher polymerization temperatures. Also the increase in Al/M ratio lead to increased activity. The opposite behavior was observed for titanium catalysts. It was also noted that unlike the titanium-complex, the zirconium analogue has two stereoisomers when in solution. The MAO activated methyl substituted pyrone-complex was nearly inactive in ethylene polymerization. Replacing the methyl group in the pyrone ring with an ethyl one leads to enhanced activity.[242] According to electrochemical studies the length of the alkyl chain does not affect the electronic density on the metal center. This implies that the improved activity is probably related to better stability of the complex.

Probably the most notable example of the catalysts with one aryloxide group together with an additional oxygen donor is the one reported by Fujita et al. (Figure 22).[243] By changing the carbonyl moiety into an ether one, researchers at Mitsui Chemicals were able to prepare highly active phenoxy-ether catalysts. These catalysts display activities up to 34700 $kg \cdot mol^{-1} \cdot h^{-1}$ with TIBA/ $Ph_3CB(C_6F_5)_4$ activation. Both the activity of the catalyst and the Mw of the resulting polymer were found to be dependent on the substituent on the *ortho*-position to phenoxy oxygen.

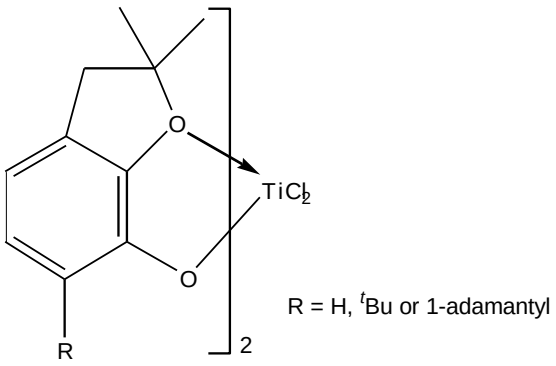

Figure 22. Highly active phenoxy-ether catalytic precursor developed at Mitsui Chemicals.

In addition to the above mentioned monoanionic-ligands also number of complexes bearing dianionic [*O,O*] ligands have been synthesized and tested in ethylene polymerizations.[244-246] Bisphenolato ligands with varying bridges have been shown to be active catalysts for different polymerization reactions. However, it has also been shown, both theoretically and experimentally, that these types of catalysts exhibit better activity when the bridging unit includes additional donor-atom.[245,246]

Recently, Waymouth et al. used Group 4 bis(phenolate) ether complexes in propylene polymerization. They could generate high molecular weight, highly isotactic polypropylenes at elevated temperatures (50-80 °C) upon activating with MAO.[247] Despite similar coordination geometries in the solid state, the hafnium complexes are more stereo- and regioselective than the zirconium congeners. Bercaw reported that titanium complexes supported by bis(phenolate) ligands with benzene-diyl linker in the presence of MAO as cocatalyst produce polypropylene with the activity up to 72 kg PP·mol^{-1}·h^{-1}.[248] They speculated that the benzene-diyl linked pre-catalyst can access only a C_s symmetric cationic catalyst species.

The titanium complex based on the calix[4]arene backbone (Figure 23) [249] represents another interesting example of this class of compounds. Activation with MAO leads to only moderately active catalyst producing ultrahigh-molecular-weight polyethylene. However the catalyst has a good thermal stability and polymerizes ethylene at 120 °C producing a polymer with narrow (1.3) polydispersity.

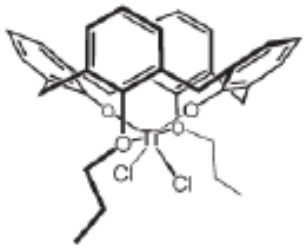

Figure 23. Structure of the thermally stable calyx[4]arene titanium catalyst.

1.3.3.3.6 Group 4 metal complexes bearing [*O,N*]-type ligands as catalysts for olefin polymerization

[*O,N*]-type complexes have received considerable interest during the recent years in developing novel highly active polymerization catalysts. Catalyst with salicylaldiminato ligands have especially been in the center of attention. Salicylaldimines were utilized initially by Grubbs and co-workers as ligand precursors for nickel catalysts used in ethylene polymerisation.[250] Since then the group 4 metal analogues, named FI-catalysts (Figure 24), have been well-studied by many research groups and numerous reports and reviews concerning these complexes have been published.[251-282]

Figure 24. Structure of an Ordinary FI Catalyst.

As mentioned before, FI catalysts are heteroatom [*O,N*] coordinated early transition metal complexes, which makes FI catalysts different from Group 4 metallocence catalysts that possess cyclopentadienyl (Cp) carbanion-based ligands. Because of the coordination of heteroatom-based [*O,N*] ligands that are more electron withdrawing than Cp carbanion-based ligands, the catalytically active species originating from FI catalysts possess a highly electrophilic nature with respect to the active species derived from

Group 4 metallocene catalysts (Table 1). High electrophilicity is normally advantageous for exhibiting high catalyst efficiency in olefin polymerization.[251,252]

Table 1. Mulliken Charges on the Central Metals of Cationic Active titanium Species.

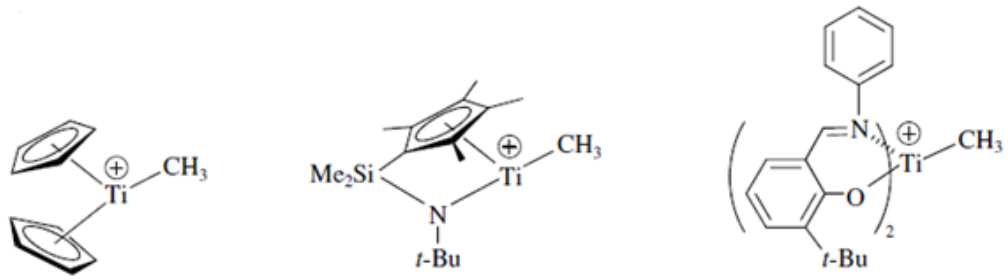

1.417 | 1.599 | 1.741 (au)

Additionally, such character is advantageous for the incorporation of olefins with a high nucleophilic nature such as bridged-cyclic-olefins (*e.g.*, norbornene).[252-254] Additionally, [*O,N*] ligation renders the metal-ligand bonding properties of FI catalysts more ionic and polarized compared to the bonding properties of classical Group 4 metallocene catalysts.[255]

Due to this ionic and polarized nature, FI catalysts are more strongly adsorbed on the surfaces of inorganic compounds (*e.g.*, $MgCl_2$, hetero-poly compounds, clays) than Group 4 metallocene catalysts are, and moreover, they undergo chemical interactions to the degree that an inorganic compound can function as an activator. Indeed, FI catalysts can form highly active supported catalysts in combination with $MgCl_2/AlR'_n(OR)_{3-n}$, hetero-poly compounds/AlR_3, and clays/AlR_3, establishing MAO- and borate-free supported olefin polymerization catalysts.[256-262] In the case of the FI catalyst/$MgCl_2/AlR'_n(OR)_{3-n}$ system, $AlR'_n(OR)_{3-n}$ works as an alkylating agent for the FI catalyst and $MgCl_2$ functions as an activator and, simultaneously, as a support for the FI catalyst (activator/support).[257] Supported catalysts possess the technological advantages of good morphology control, high polymer bulk density and little reactor fouling.

The heteroatom ligation gives another interesting character to FI catalysts. Namely, the coordination of [*O,N*] ligands makes FI catalysts "already poisoned." Therefore, the catalytically active species stemming from FI catalysts exhibit higher functional group tolerance, resulting in the achievement of ethylene/polar monomer copolymerization

without reaction modifications such as masking the functionality as an innocuous species, which is a major untapped area for early transition metal catalysts.[263]

The structural features of FI catalysts such as the effects of the metal center and the effects of the substituents in the imino-nitrogen and the *ortho*-phenoxy position have been studied. For the complexes with a *t*-Bu group in the *ortho*-phenoxy position and aniline as the imino moiety, the activity was increased in the order: Zr>Hf>Ti.[264,265] Increase of the steric bulk in the substituent of the *ortho*-position to the phenoxy leads to improved activity. The complex displayed in Figure 25 with a very bulky cumyl substituent in the *ortho*-position is the most active catalysts know for polymerization of ethylene, exhibiting activity up to 6,552,000 $kg \cdot mol^{-1} \cdot h^{-1} \cdot bar^{-1}$.[46,265] This exceptionally high activity can be explained by two factors: cation-anion separation is enhanced and the bulkier substituent also improves the protection of the phenoxy oxygen which is susceptible to attack by the free TMA present in MAO.

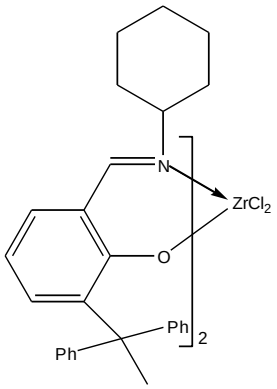

Figure 25. Schematic structure of the most active ethylene polymerization FI-catalyst.

As stated also the variations of imino-substituents have a pronounced effect on the activity of FI-catalysts. Addition of an alkyl substituent in the 2-position of the imino-phenyl lead to significant decrease in activity[266] and, on the other hand, the use of fluorine substituent(s) can increase the catalytic activity.[252] From the studies carried out with alkylphenyl substituents it is evident that not only electronic effects are responsible for gaining good activity; replacing the benzyl-group with an ethylphenyl or propylphenyl one, significantly increases the activity of titanium salicylaldiminato catalysts.[127] Even more interestingly, these modifications in the imine-group of FI-catalysts can open the door to variations on the resulting polymer structure. FI-catalysts with a fluorinated-

phenyl substituent in the imino-position are able to polymerize ethylene in a living manner at reasonably high temperatures.[213,267]

Due to structural and electronic features, FI catalysts exhibit unique and versatile catalytic properties that cannot be replicated by conventional olefin polymerization catalysts.[256,268,271] (1) They allow for a wide variety of catalyst design possibilities because of ligand accessibility and amenability to modification (enormous structural diversity)[268], (2) they can exist as mixtures of isomers that are capable of mutually transforming (multimodal behavior[270,271], highly syndiospecific PP with an extremely high T_m[47,272,273]), (3) they allow the ligand structure to change from phenoxy-imine to phenoxy-amine (formation of ultra-high molecular weight polymers[266,274] and isotactic polymers[47]), (4) they generate highly electrophilic active species that are highly ionic and polarized (high incorporation capability for strained cyclic olefins[275], versatility vis-à-vis activator selection resulting in MAO- and borate-free supported catalysts[257]), (5) they display high functional group tolerance (ethylene/polar monomer copolymerization[263]) and (6) due to the highly controlled living nature of *ortho*-fluorinated Ti-FI catalysts for both ethylene and propylene polymerizations, they allow to synthesize both ethylene- and propylene-based diblock and multi-block copolymers comprised of crystalline and amorphous segments and/or two different kinds of crystalline segments.[212,267,276-278]

Bis(phenoxy-ketimine)-catalysts (Figure 26), closely related to the FI-catalysts discussed above, have also been studied in ethylene polymerizations.[283-285] Chen et al. have studied the effect of substituents at the ketimine carbon in ethylene polymerizations (Figure 26).[283] The ketimine-catalysts were found to be more active then the aldimine-analogue and the introduction of electron-withdrawing group onto the ketimine carbon atom led to a considerable increase in the activity of these catalysts., an increase in the Mw of the produced PE was also observed. Recently Coates et al. have reported the effect of the ketimine substituent on both the activity and selectivity in propylene polymerizations.[284]

Coates et al. have also reported the bis(phenoxy-ketimine)-titanium catalyst which is able to polymerize ethylene in a living manner even though the imino-phenyl is not *ortho*-fluorinated.[285] Group 4 complexes with bis(phenoxy-ketimine) ligands have also been used as catalysts for example in living polymerization of propylene and copolymerization of ethylene with polar monomers.[284,386,287]

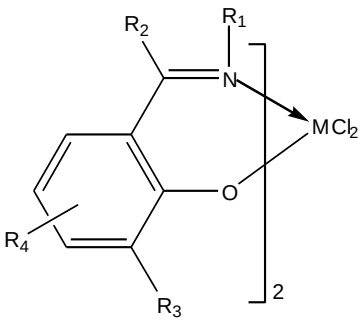

Figure 26. General description of bis(phenoxyketimine) Group 4 metal complexes.

In addition to ligands based on phenoxides with nitrogen donors, [*O*,*N*] complexes based on an acac-backbone have been studied in ethylene polymerizations (Figure 27).[288-292] Li et al. have published several reports describing the use of this type of catalysts in the copolymerization of ethylene with various other olefins.[283-287] With MMAO activation these types of complexes exhibit high activities and are able to polymerize ethylene in a *quasi*-living manner.[290,291] The highest activity of 7350 $kg \cdot mol^{-1} \cdot h^{-1} \cdot bar^{-1}$ is obtained with these catalysts when *t*-Bu and CF_3 substituents are used in the acac-backbone and phenyl group with one fluorine in the imino-position.[292] However, a decrease in activity was observed if a phenyl group with more fluorine atoms was used. Very recently, closely related imino alkoxide complexes (Figure 27) have been reported, however the stability of these catalysts was extremely poor and as a result also the activity remained low.[293]

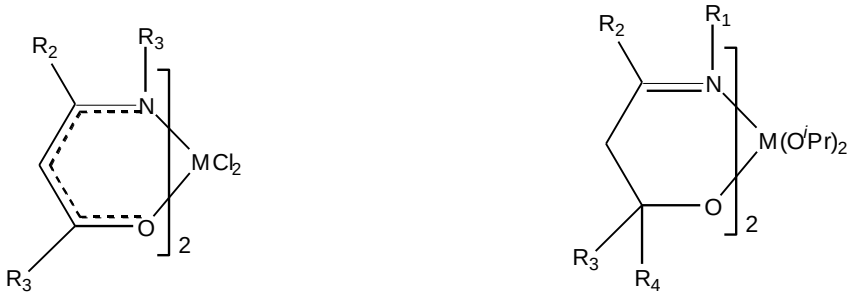

Figure 27. General description of enaminoketonato and imino alkoxide complexes based on acac-type backbone.

1.4 References

[1] Sadiku, E. *Woodhead Publishing in Textiles* **2009**, 81.

[2] Kirwan, M. J.; Strawbridge, J. W. in *Food Packaging Technology* edited by Coles, R.; McDowell, D.; Kirwan, M. J. **2003**, 174.

[3] Jadhav, K.; Patel, S.; Mhaske, S. T. *Popular Plastics and Packaging* **2007**, *52*, 87.

[4] The Compelling Facts about Plastics in: *WWW.PLASTICSEUROPE.ORG*, Oct. 2008.

[5] (a) Chum, P. S.; Swogger, K. W. *Prog. Polym. Sci.* **2008**, *33*, 797. (b) Hustad, P. D. *Science* **2009**, *325*, 704.

[6] (a) Doak, K. W. *Encyclopedia of Polymer Science and Engineering*; Wiely-Interscience: New York, **1986**; Vol. 6, pp 386-429. (b) Smedberg, A.; Hjertberg, T.; Gustafsson, B. *J. Polym. Sci. Part A: Polym. Chem.* **2003**, *41*, 2974-2984.

[7] (a) Stevens, M. P. *Polymer Chemistry: An Introduction*; 3rd ed.; Oxford University Press Inc.: New York, **1999**, p 181. (b) Mülhaupt, R. *Macromol. Chem. Phys.* **2003**, *204*, 289.

[8] (a) Ziegler, K.; Holzkamp, E.; Breil, H.; Martin, H. *Angew. Chem.* **1955**, *67*, 541. (b) Ziegler, K. *Angew. Chem.* **1964**, *76*, 545. (c) Natta, G. *J. Polym. Sci* **1955**, *16*, 143. (d) Natta, G.; Pino, P.; Corradini, P.; Danusso, F.; Mantica, E.; Moraglio, G. *J. Am. Chem. Soc.* **1955**, *77*, 1708. (e) Natta, G. *Angew. Chem.* **1956**, *68*, 393. (f) Huggins, M. L.; Natta, G.; Desreux, V.; Mark, H. *J. Polym. Sci.* **1962**, *56*, 153. (g) Natta, G. *Angew. Chem.* **1964**, *76*, 553.

[9] Vestberg, T.; Denifl. P.; Wilen, C-E. *J. Appl. Polym. Sci.* **2008**, 11, 2021.

[10] Mohammed, A.; Denifl, P.; Reichert, K-H. *Macromol. Mat. Eng.* **2005**, *290*, 1220.

[11] Chadwick, J. C.; Thomas G.; Severn, J. R.; in *Tailor-Made Polymers – via immobilization of Alpha-Olefin Polymerization Catalyst* edited by Severn J. R. and Chadwick J. C. Wiley VCH, **2008**, 43.

[12] Kashiwa, N. *J. Pol. Sci. Part A: Polym. Chem.* **2004**, *42*, 1.

[13] Ferraro, A.; Camurati, I.; Dall'Occo, T.; Piemontesi, F.; Cecchin, G. *Kinetics and Catalysis*, **2006**, *47*, 176.

[14] Odian, G. G. *Principles of Polymerization*; 4th ed.; Wiley-Interscience: Hoboken, NJ; 2004, p 641.

[15] Breslow, D. S.; Newburg, N. R. *J. Am. Chem. Soc.* **1957**, *79*, 5072.

[16] Breslow, D. S.; Newburg N. R. *J. Am. Chem. Soc.* **1959**, *81*, 81.

[17] Natta, G.; Pino, P.; Mazzanti, G.; Giannini, U. *J. Am. Chem. Soc.* **1957**, *79*, 2997.

[18] Natta, G.; Pino P.; Mazzanti, G.; Giannini, U.; Mantica E.; Peraldo, M. *Chim. Ind. (Milan)* **1957**, *39*, 19.

[19] Natta, G.; Pino P.; Mazzanti, G.; Lanzo R. *Chim. Ind. (Milan)* **1957**, *39*, 1032.

[20] Andersen, A.; Cordes, H. G.; Herwig, J.; Kaminsky, W.; Merck, A.; Mottweiler, R.; Pein J.; Sinn, H.; Vollmer, H. J. *Angew. Chem.* **1976**, *88*, 689.

[21] Sinn, H.; Kaminisky, W. *Adv. Organomet. Chem.* **1980**, *18*, 99.

[22] Sinn, H.; Kaminsky, W.; Vollmer, H. J.; Woldt, R. *Angew. Chem.* **1980**, *92*, 346.

[23] Kaminsky, W.; Miri, M.; Sinn, H.; Woldt, R. *Macromol. Chem. Rapid Commun.* **1983**, *4*, 417.

[24] Resconi, L; Cavallo, L.; Fait, A.; Piemontesi, F. *Chem. Rev.* **2000**, *100*, 1253.

[25] Resconi, L.; Fritze, C. in *Polypropylene Handbook*, edited by Nello Pasquini, Carl Hanser Verlag, Munchen, **2005,** 107.

[26] Wang, B. *Coord. Chem. Rev.* **2006**, *250*, 242.

[27] Moehring, P. C.; Coville, Neil J. *Coord. Chem. Rev.* **2006**, *250*, 18.

[28] Kaminsky, W. *J. Polym. Sci., Part A: Polym. Chem.* **2004**, *42*, 3911.

[29] Brintzinger, H. H.; Fischer, D.; Mülhaupt, R.; Rieger, B.; Waymouth, R. M. *Angew. Chem. Int. Ed. Engl.* **1995**, *34*, 1143.

[30] Mason, A. F.; Coates, G. W. *Macrom. Eng.* **2007**, *1*, 217.

[31] Coates, G. W.; Hustad, P. D.; Reinartz, S. *Angew. Chem. Int. Ed.*, **2002**, *41*, 2236.

[32] Britovsek, G. J. P.; Gibson, V. C.; *Angew. Chem. Int. Ed.* **1999**, *28*, 428.

[33] (a) Gibson, V. C.; Spitzmesser, S. K. *Chem. Rev.* **2003**, *103*, 283. (b) Takeuchi, D. *Dalton Trans.* **2010**, *39*, 311. (c) http://apps.isiknowledge.com/.

[34] Ittel, S. D.; Johnson, L. K.; Brookhart, M. *Chem. Rev*. **2000**, *100*, 1169.

[35] Britovsek, G. J. P.; Bruce, M.; Gibson, V. C.; Kimberley, B. S.; Maddox, P. J.; Mastroianni, S.; McTavish, S. J.; Redshaw, C.; Solan, G. A.; Stromberg, S.; White, A. J. P.; Williams, D. J. *J. Am. Chem. Soc.* **1999**, *121*, 8728.

[36] Britovsek, G. J. P.; Gibson, V. C.; Spitzmesser, S. K.; Tellmann, K. P.; White, A. J. P.; Williams, D. J. *J. Chem. Soc., Dalton Trans.* **2002**, 1159.

[37] Johnsob, L. K.; Killian, C. M.; Brookhart, M. *J. Am. Chem. Soc.* **1995**, *117*, 6414.

[38] (a) Wang, C.; Friedrich, S.; Younkim, T. R.; Li, R. T.; Grubbs, R. H.; Bansleben, D. A.; Day, M. W. *Organometallics* **1998**, *17*, 3149. (b) Younkim, T. R.; Conner, E. F.; Henderson, J. I.; Friedrich, S.; Grubbs, R. H.; Bansleben, D. A. *Science* **2000**, *287*, 460.

[39] Johnson, L. K.; Mecking, S.; Brookhart, M. *J. Am. Chem. Soc.* **1996**, *118*, 267.

[40] Moore, E. P. Jr. *Polypropylene Handbook: Polymerization, Characterization, Properties, Applications*, Hanser, Munich **1996**.

[41] Moore, E. P. Jr *The Rebirth of Polypropylene: Supported Catalysts*, Hanser, Munich **1998**.

[42] V. Scheirs; W. Kaminsky, editors, *Metallocene-Based Polyolefins*, Wiley, Chichester, UK), Vols 1 and 2 **1999**.

[43] Busico, V. in *Stereoselective Polymerization with Single-Site Catalysts*, editors Baugh, Lisa S; Canich Jo Ann M. **2008**, CRC Press LLC, 203.

[44] Nomura, K.; Liu, J.; Sudhakar, P.; Boonyarach, K. *J. Mol. Catal. A: Chem.* **2008**, *267*, 1.

[45] Aharonovich, S.; Volkis, S.; Eisen, M. S. *Macromol. Symp.* **2007**, *260*, 165.

[46] Severn, J. R.; Chadwick, J. C. *Chem. Rev.* **2005**, *105*, 4073.

[47] Makio, H.; Fujita, T. *Bull. Chem. Soc. Jpn.* **2005**, *78*, 52.

[48] Furuyama, R.; Saito, J.; Ishii, S.; Mitani, M.; Matsui, S.; Tohi, Y.; Makio, H.; Matsukawa, N.; Tanaka, H.; Fujita, T. *J. Mol. Catal. A: Chem.* **2003**, *200*, 31.

[49] Furuyama, R.; Fujita, T.; Funaki, S. F.; Nobori, T.; Nagata, T.; Fujiwara, K. *Catal. Surveys from Asia* **2004**, *8*, 61.

[50] Reichert, K. H.; Meyer, K. R.; *Makromol. Chem.* **1973**, *169*, 163.

[51] Sinn, H.; Kaminsky, W.; Vollmer, H. J.; Woldt, R. *Angew. Chem. Int. Ed. Eng.* **1980**, *19*, 390.

[52] Kaminsky, W. 'Polyolefins' in *Handbook of Polymer Synthesis*, M. Dekker, New York, **1992**, Part A, pp. 1-76.

[53] Ewen, J. A. *J. Am. Chem. Soc.* **1984**, *106*, 6355.

[54] Wild, F. R. W. P.; Zsolnai, L.; Huttner, G.; Brintzinger, H. H. J. *Organomet. Chem.* **1982**, *232*, 233.

[55] Ewen, J. A.; Haspeslagh, L.; Atwood, J. L.; Zhang, H. *J. Am. Chem. Soc.* **1987**, *109*, 6544.

[56] Ewen, J. A.; Jones, R. L., Razavi, A.; Ferrara, J. P. *J. Am. Chem. Soc.* **1988**, *110*, 6255.

[57] Antberg, M.; Dolle, V.; Haftka, S.; Rohrmann, J.; Spaleck, W.; Winter, A.; Zimmermann, H. J. *Makromol. Chem. Macromol. Symp.* **1991**, *48/49*, 333.

[58] Erker, G.; Nolte, R.; Aul, R.; Wilker, S.; Krüger, C.; Nor, R. *J. Am. Chem. Soc.* **1991**, *113*, 7594.

[59] Ewen, J. A. *Macromol. Symp.* **1995**, *89*, 181.

[60] Hermann, W. A.; Rohrmann, J.; Herdtweck, E.; Spaleck, W.; Winter, A. *Angew. Chem. Int. Ed. Engl.* **1989**, *28*, 1511.

[61] Mise, T.; Miya, S.; Yamazaki, H. *Chem. Lett.* **1989**, 1853.

[62] Cheng, H. N.; Ewen, J. A. *Makromol. Chem.* **1989**, *190*, 1931.

[63] De Rosa, C.; Auriemma, F. *Prog. Polym. Sci.* **2006**, *31*, 145.

[64] Herfert, N.; Fink, G. *Makromol. Chem. Macromol. Symp.* **1993**, *66*, 157.

[65] Ewen, J. A.; Elder, M. J.; Jones, R. L.; Haspeslagh, L.; Atwood, J. L.; Bott, S. G.; Robinson, K. *Makromol. Chem. Macromol. Symp.* **1991**, *48/49*, 253.

[66] Spaleck, W.; Antberg, M.; Dolle, V.; Klein, R.; Rohrmann, J.; Winter, A. *New J. Chem.* **1990**, *14*, 499.

[67] Razavi, A.; Peters, L.; Nafpliotis, L.; Vereecke, D.; Den Dauw, K.; Atwood, J. L.; Thewald, U. *Macromol. Symp.* **1995**, *89*, 345.

[68] Kaminsky, W.; Buschermöhle, M. in *Recent Advances in Mechanistic and Synthetic Aspects of Polymerization*, D. Reidel, Dordrecht, **1987**, p. 503.

[69] Mallin, D. T.; Rausch, M. D.; Liu, Y. –G.; Dong, S.; Chien, J. C. W. *J. Am. Chem. Soc.* **1990**, *112*, 2030.

[70] Coates, G. W.; Waymouth, R. M. *Science* **1995**, *267*, 217.

[71] Hauptman, E.; Waymouth, R. M.; Ziller, J. W. *J. Am. Chem. Soc.* **1995**, *117*, 11586.

[72] Arndt-Rosenau, M.; Beulich, I. *Macromolecules* **1999**, *32*, 7335.

[73] Tritto, I.; Boggioni, L.; Sacchi, M. C.; Locatelli, P.; Ferro, D. R.; Provasoli, A. *Macromol. Rapid Commun*. **1999**, *20*, 279.

[74] Bergstrom, C. H.; Ruotoistenmaki, J.; Aitola, E. T.; Seppala, J. V. *J. Appl. Polym. Sci*. **2000**, *77*, 1108.

[75] Lasarov, H.; Pakkanen, T. T. *Macromol. Chem. Phys*. **2000**, *201*, 1780. 38.

[76] Lee, D. -H.; Jung, H. -K.; Kim, W. -S.; Min, K. -E.; Park, L.- S.; Seo, K. -H.; Kang, I. -K.; Noh, S. -K. *Polymer* **2000**, *24*, 445.

[77] Lee, D. -H.; Jung, H. -K.; Choi, Y. -Y.; Kim, H. -J.; Kim, W. -S.; Min, K. -E.; Park, L. -S.; Kang, I. -K. *Polymer* **2000**, *24*, 751.

[78] Kaminsky, W.; Beulich, I.; Arndt-Rosenau, M. *Macromol. Symp*. **2001**, *173*, 211.

[79] Tritto, I.; Marestin, G.; Boggioni, L.; Sacchi, M. C.; Brintzinger, H. -H.; Ferro, D. R. *Macromolecules* **2001**, *34*, 5770.

[80] Lee, D. -H.; Lee, J. -H.; Kim, H. -J.; Kim, W. -S.; Min, K. -E.; Park, L. -S.; Seo, K. -H.; Kang, I. -K. *Polymer* **2001**, *25*, 468.

[81] Tritto, I.; Boggioni, L.; Jansen, J. C.; Thorshaug, K.; Sacchi, M. C.; Ferro, D. *Macromolecules* **2002**, *35*, 616.

[82] Naga, N.; Imanishi, Y. *Macromol. Chem . Phys.* **2002**, *203*, 159.

[83] Wendt, R. A.; Mynott, R.; Fink, G. *Macromol. Chem. Phys*. **2002**, *203*, 2531.

[84] Wendt, R. A.; Fink, G. *J. Mol. Catal. A. Chem*. **2003**, *203*, 101.

[85] Kaminsky, W.; Tran, P. -D.; Werner, R. *Macromol. Symp*. **2004**, *213*, 101.

[86] Lee, S. -G.; Hong, S. -D.; Park, Y. -W.; Jeong, B. -G.; Nam, D. -W.; Jung, H.Y.; Lee, H.; Song, K. H. *J. Organomet. Chem*. **2004**, *689*, 2586.

[87] Donner, M.; Fernandez, M.; Kaminsky, W. *Macromol. Symp*. **2006**, *236*, 193.

[88] Li, X.; Hou, Z. *Coord. Chem. Rev*. **2008**, *252*, 1842.

[89] Po, R.; Cardi, N. *Prog. Polym. Sci.* **1996**, *21*, 47.

[90] Tomotsu, N.; Ishihara, N.; Newman, T. H.; Malanga, M. T. *J. Mol. Catal. A. Chem.* **1998**, *128*, 167.

[91] Kaminsky, W.; Lenk, S. *Macromol. Symp*. **1997**, *118*, 45.

[92] Schellenberg, J.; Tomotsu, N. *Prog. Polym. Sci. (Oxford)* **2002**, *27*, 1925.

[93] Montagna, A. A.; Dekmezian, A. H.; Burkhart, R. M. *Chemtech* **1997**, *27*, 26.

[94] Hackmann, M.; Rieger, B. *Cattech* **1997**, *1*, 79.

[95] Brintzinger, H. H.; Fischer, D.; Mülhaupt, R.; Rieger, B.; Waymouth, R. M. *Angew. Chem. Int. Ed. Engl.* **1995**, *34*, 1143.

[96] Reddy, S. S.; Sivaram, S.; *Prog. Polym. Sci.* **1995**, *20*, 309.

[97] Horton, A. D. *TRIP* **1994**, *2*, 158.

[98] Kaminsky, W.; Arndt, M. *Adv. Polym. Sci.* **1997**, *127*, 143.

[99] Soga, K.; Shiono, T. *Prog. Polym. Sci.* **1997**, *22*, 1503.

[100] Gupta, V. K.; Satish, S.; Bhardwaj, I. S. *JMS Rev. Macromol. Chem. Phys.* **1994**, *C34*, 439.

[101] Huang, J.; Reuspel, G. L. *Prog. Polym. Sci.* **1995**, *20*, 459.

[102] Kaminsky, W. *Macromol. Chem . Phys.* **1996**, *197*, 3907.

[103] Bochmann, M. *J. Chem. Soc. Dalton Trans.* **1996**, 255.

[104] Fink, G.; Mülhaupt, R.; Brintzinger, H. H.*"Ziegler Catalysts"*; Springer: Berlin, **1995.**

[105] Hamielec, A. E.; Soares, J. B. P. *Prog. Polym. Sci.* **1996**, *21*, 651.

[106] Mashima, K.; Nakayama, Y.; Nakamura, A. *Adv. Polym. Sci.* **1997**, *133*, 1.

[107] Kaminsky, W. *J. Chem. Soc. Dalton. Trans.* **1998**, 1413.

[108] Jordan, R. F. *Adv. Organomet. Chem.* **1991**, *32*, 325.

[109] Kaminsky, W.; Scheirs, J. *Metallocene based polyolefins, Wiley*, **2000**, Vol. I and II.

[110] Coates, G.W. *Chem. Rev*. **2000**, *100*, 1223.

[111] Alt, H. G.; Köppl, A. *Chem. Rev*. **2000**, *100*, 1205.

[112] Resconi, L.; Cavallo, L.; Fait, A.; Poiemontesi, F. *Chem. Rev.* **2000**, *100*, 1253.

[113] Hlatky, G. G. *Chem. Rev.* **2000**, *100*, 1347.

[114] Fink, G.; Steinmetz, B.; Zechlin, J.; Przybyla, C.; Tesche, B. *Chem. Rev.* **2000**, *100*, 1377.

[115] Pedeutour, J.; Radhakrishnan, K.; Cramail, H.; Deffieux, A. *Macromol. Rapid Commun.* **2001**, *22*, 1095.

[116] Kaminsky, W. Ed. Special Issue: Olefin Polymerization, *Macromol. Symp.* **2006**, *236*, 1-258.

[117] Razavi, A.; Thewalt, V. *Coord. Chem. Rev.* **2006**, *250*, 155.

[118] Möhring, P. C.; Coville, N. J. *Coord. Chem. Rev.* **2006**, *250*, 18.

[119] Busico, V. *Dalton Trans.* **2009**, 8794.

[120] Alt, H. G.; Licht, E. H.; Licht, A. I.; Schneider, K. J. *Coord. Chem. Rev*. **2006**, *250*, 2.

[121] Linnolahti, M.; Severn, J. R.; Pakkanen, T. A. *Angew. Chem. Int. Ed.* **2008**, *47*, 9279.

[122] Giannetti, E.; Nicoletti, G.; Mazzochi, R. *J. Polym. Sci. , Polym. Chem. Ed.* **1985**, *23*, 2117.

[123] Small, B. L.; Brookhart, M. *J. Am. Chem. Soc.* **1998**, *120*, 7143.

[124] Sugano, T.; Matsubara, T.; Fujita, T.; Takahashi, T. *J. Mol. Catal.* **1993**, *82*, 93.

[125] Taube, R.; Krukowa, L. J. *J. Organomet. Chem.* **1988**, *347*, C 9.

[126] Chien, J. C. W.; Tsai, W. M.; Rausch, M. D. *J. Am. Chem. Soc.* **1991**, *113*, 8570.

[127] Bochmann, M.; Lancaster, S. J. *Organometallics* **1993**, *12*, 633.

[128] Crowther, D. J.; Borkowsky, S. L.; Swenson, D.; Meyer, T. Y.; Jordan, R. F. *Organometallics* **1993**, *12*, 2897.

[129] Hlatky, G. G.; Eckman, R. R.; Turner, H. W. *Organometallics* **1992**, *11*, 1413.

[130] Chen, E.Y.; Marks T.J. *Chem. Rev.* **2000**, *100*, 1391.

[131] Bochmann, M. *Organometallics* **2010**, *29*, 4711.

[132] Arlman, E. J.; Cossee P. *J. Catal.* **1964**, *3*, 99.

[133] Pärssinen, A.; Luhtanen, T.; Klinga, M.; Pakkanen, T.; Leskelä, M.; Repo, T. *Organometallics* **2007**, *26*, 3690

[134] Guerra, G.; Cavallo, L.; Moscardi, G.; Vacatello, M.; Corradini, P. *Macromolecules* **1996**, *29*, 4834.

[135] Yano, A.; Kaneko, T.; Sato, M.; Akimoto, A. *Macromol. Chem. Phys*. **1999**, *200*, 2127.

[136] Ewen, J. A.; Jones, R. L.; Elder, M. J.; Camurati, I.; Pritzkow, H. *Macromol. Chem. Phys.*, **2004**, *205*, 302.

[137] Bochmann, M. *J. Chem. Soc., Dalton Trans.* **1996**, *3*, 255.

[138] Dietrich, U.; Hackmann, M.; Rieger, B.; Klinga, M.; Leskelä, M. *J. Am. Chem. Soc*. **1999**, *121*, 4348.

[139] Stevens, J. C.; Timmers, F. J.; Wilson, D. R.; Schmidt, G. F.; Nickias, P. N.; Rosen, R. K.; Knight, G. W.; Lai, S. -Y. *EP 0416815*, Dow Chem. Co. **1991**.

[140] Stevens, J. C.; Neithamer, D. R. *EP 0418044*, Dow, **1991**.

[141] Canich, J. A. M. *US 5026798*, Exxon, **1991**.

[142] Canich, J. A. M.; Licciardi, G.F. *US 5057475*, Exxon, **1991**.

[143] Canich, J. A. M. *EP 0420436*, Exxon, **1991**.

[144] McKnight, A. L.; Waymouth, R. M. *Chem. Rev*. **1998**, *98*, 2587.

[145] Chum, P. S.; Kao, C. I.; Knight, G. W. *Plastics Engineering* **1995**, *June*, 21.

[146] Shiono, T.; Moriki, Y.; Soga, K. *Macromol. Symp.* **1995**, *97*, 161.

[147] Soga, K.; Uozumi, T.; Nakamura, S.; Toneri, T.; Teranishi, T.; Sano, T.; Arai, T.; Shiono, T. *Macromol. Chem. Phys.* **1996**, *197*, 4237.

[148] Stevens, J. C. *Stud. Surf. Sci. Catal*. **1994**, *89*, 277.

[149] Mani, R.; Burns, C. M. *Macromolecules* **1991**, *24*, 5476.

[150] Soga, K.; Lee, D.; Yangihara, H. *Polym. Bull.* **1988**, *20*, 237..

[151] Kakugo, M.; Miyatake, T.; Mizunuma, K. *Stud. Surf. Sci. Catal***. 1990**, *56*, 517.

[152] Miyatake, K.; Mizunuma, M.; Kakugo, M. *Makromol. Chem. Macromol. Symp*. **1993**, *66*, 203.

[153] Sernetz, F. G.; Mülhaupt, R.; Waymouth, R. M. *Macromol. Chem. Phys*. **1996**, *197*, 1071.

[154] Nomura, K.; Okumara, H.; Komatsu, T.; Naga, N.; Imanishi, Y. *J. Mol. Catal. A. Chem*. **2002**, *190*, 225.

[155] Noh, S. -K.; Lee, J.; Lee, D. -H. *J. Organomet. Chem*. **2003**, *667*, 53.

[156] Noh, S. K.; Lee, M.; Kum, D. H.; Kim, K.; Lyoo, W. S.; Lee, D. -H. *J. Polym. Sci. Part A. Polym. Chem*.**2004**, *42*, 1712.

[157] Skeril, R.; Sindelar, P.; Salajka, Z.; Varga, V.; Cisarova, I.; Pinkas, J.; Horacek, M.; Mach, K. *J. Mol. Catal. A. Chem*. **2004**, *224*, 97.

[158] Martinez, S.; Exposito, M. T.; Ramos, J.; Cruz, V.; Martinez, M. C.; Lopez, M.; Munoz-Escalona, A.; Martinez-Salazar,J. *J. Polym. Sci. Part A. Polym. Chem*. **2005**, *43*, 711.

[159] Sernetz, F. G.; Mülhaupt, R.; Amor, F. J. *J. Polym. Sci., Part A. Polym. Chem*. **1997**, *35*, 1571.

[160] Xu, G. *Macromolecules* **1998**, *31*, 2395.

[161] Chung, T. C.; Lu, H. L. *J. Polym. Sci. A. Polym. Chem*. **1997**, *35*, 575.

[162] Ruchatz, D.; Fink, G. *Macromolecules* **1998**, *31*, 4674.

[163] Ni, J.; Lü, C.; Zhang, Y.; Liu, Z.; Mu, Y. *Polymer* **2008**, *49*, 211.

[164] Naga, N. *J. Polym. Sci. Part A: Polym. Chem.* **2005**, *43*, 1285.

[165] Cano, J.; Kunz, K. *J. Organomet. Chem.* **2007**, *692*, 4411.

[166] van Leusen, D.; Beetstra, D. J.; Hessen, B.; Teuben, J. H. *Organometallics* **2000**, *19*, 4084.

[167] Kotov, V. V.; Avtomonov, E. V.; Sundermeyer, J.; Harms, K.; Lemenovskii, D. *Eur. J. Inorg. Chem.* **2002**, 678.

[168] Park, J. T.; Yoon, S. C.; Bae, B .J.; Seo, W. S.; Suh, I. H.; Han, T. K.; Park, J. R. *Organometallics* **2000**, *19*, 1269.

[169] Reb, A.; Alt, H. G. *J. Mol. Catal. A. Chem*. **2001**, *174*, 35.

[170] Alt, H. G.; Fottinger, K.; Milius, W. J. *J. Organomet. Chem*. **1999**, *572*, 21..

[171] Alt, H. G.; Reb, A. *J. Mol. Catal. A. Chem*. **2001**, *175*, 43.

[172] Alt, H. G.; Reb, A.; Milius, W. J. *J. Organomet. Chem***. 2001**, *628*, 169.

[173] Alt, H. G.; Reb, A.; Kundu, K. *J. Organomet. Chem*. **2001**, *628*, 211.

[174] Klosin, J.; Kruper Jr, W. J.; Nickias, P. N.; Roof, G. R.; De Waele, P. *Organometallic*s **2001**, *20*, 2663.

[175] Barnhart, R. W.; Bazan, G. C.; Mourey, T. *J. Am. Chem. Soc.* **1998**, *120*, 1082.

[176] (a) Wasilke, J. -C.; Obrey, S. J.; Tom Baker, R.; Bazan, G. C. *Chem. Rev*. **2005**, *105*, 1001. (b) Nobika, M.; Katayama, H.; Watanabe, T.; Kawamura-Kuribayashi, H.; Yanagi, K.; Imai, A. *Organometallics* **2009**, *28*, 3785.

[177] Scollard, J. D.; McConville, D. H.; Payne, N. C.; Vittal, J. J. *Macromolecules* **1996**, *29*, 5241.

[178] Scollard, J. D.; McConville, D. H. *J. Am. Chem. Soc*. **1996**, *118*, 10008.

[179] Scollard, J. D.; McConville, D. H.; Vittal, J. J.; Payne, N. C. *J. Mol. Catal. A. Chem*. **1998**, *128*, 201.

[180] Uozumi, T.; Tsubaki, S.; Jin, J. Z.; Ahn, C. H.; Sano, T.; Soga, K. *Macromol. Chem. Phys*. **2001**, *202*, 3279.

[181] Tsubaki, S.; Jin, J. Z.; Sano, T.; Uozumi, T.; Soga, K. *Macromol. Chem. Phys*. **2001**, *202*,482.

[182] Hagimoto, H.; Shiono, T.; Ikeda, T. *Macromol. Rapid Commun.* **2002**, *23*, 73.

[183] Ziniuk, Z.; Goldberg, I.; Kol, M. *Inorg. Chem. Commun.* **1999**, *2*, 549.

[184] Lorber, C.; Donnadieu, B.; Choukroun, R. *Organometallics* **2000**, *19*, 1963.

[185] Lee, C. H.; La, Y.-H.; Park, J. W. *Organometallics* **2000**, *19*, 344.

[186] Nomura, K.; Naga, N.; Takaoki, K. *Macromolecules* **1998**, *31*, 8009.

[187] Lee, C. H.; La, Y.-H.; Park, S. J.; Park, J. W. *Organometallics* **1998**, *17*, 3648.

[188] Nomura, K.; Naga, N.; Takaoki, K.; Imai, A. *J. Mol. Catal. A: Chem.* **1998**, *130*, 209.

[189] Nomura, K.; Oya, K.; Imanishi, Y. *Polymer* **2000**, *41*, 2755.

[190] Jeon, Y.-M.; Heo, J.; Lee, W. M.; Chang, T.; Kim, K. *Organometallics* **1999**, *18*, 4107.

[191] Gauvin, R. M.; Lorber, C.; Choukroun, R.; Donnadieu, B.; Kress, J. *Eur. J. Inorg. Chem.* **2001**, 2337.

[192] Jeon, Y.-M.; Park, S. J.; Heo, J.; Kim, K. *Organometallics* **1998**, *17*, 3161.

[193] Patton, J. T.; Feng, S. G.; Abboud, K. A. *Organometallics* **2001**, *20*, 3399.

[194] Patton, J. T.; Bokota, M. M. *Organometallics* **2002**, *21*, 2145.

[195] Daniele, S.; Hitchcock, P. B.; Lappert, M. F. *Chem. Commun.* **1999**, 1909.

[196] Daniele, S.; Hitchcock, P. B.; Lappert, M. F.; Merle, P. G. *J. Chem. Soc., Dalton Trans.* **2001**, 13.

[197] Kim, S.-J.; Jung, I. N.; Yoo, B. R.; Kim, S. H.; Ko, J.; Byun, D.; Kang, S. O. *Organometallics* **2001**, *20*, 2136.

[198] Horton, A. D.; v. Hebel, K. L.; With, J. D. *Macromol. Symp.* **2001**, *173*, 123.

[199] Shafir, A.; Arnold, J. *Organometallics* **2003**, *22*, 567.

[200] Wei, P.; Stephan, D. W. *Organometallics* **2002**, *21*, 1308.

[201] Jin, X.; Novak, B.M. *Macromolecules* **2000**, *22*, 6205.

[202] Kim, W. K.; Fevola, M. J.; Liable-Sands, L. M.; Rheingold, A. L.; Theopold, K. H. *Organometallics* **1998**, *17*, 4541.

[203] Vollmerhaus, R.; Rahim, M.; Tomaszewski, R.; Xin, S. K.; Taylor, N. J.; Collins, S. *Organometallics* **2000**, *19*, 2161.

[204] Rahim, M.; Taylor, N. J.; Xin, S. K.; Collins, S. *Organometallics* **1998**, *17*, 1315.

[205] Masugi, T.; Matsui, S.; Kojoh, S.; Takagi, Y.; Inoue, Y.; Fujita, T.; Kashiwa, N. *Chem. Lett.* **2001**, 566.

[206] Masugi, T.; Matsui, S.; Kojoh, S.; Takagi, Y.; Inoue, Y.; Nakano, T.; Fujita, T.; Kashiwa, N. *Macromolecules* **2002**, *35*, 4880.

[207] Yoshida, Y.; Saito, J.; Mitani, M.; Takagi, Y.; Matsui, S.; Ishii, S.-I.; Nakano, T.; Kashiwa, N.; Fujita, T. *Chem. Commun.* **2002**, 1298.

[208] Yoshida, Y. Matsui, S.; Takagi, Y.; Mitani, M.; Nakano, T.; Tanaka, H.; Kashiwa, N.; Fujita, T. *Organometallics* **2001**, *20*, 4793.

[209] Matsui, S.; Spaniol, T. P.; Takagi, Y.; Yoshida, Y.; Okuda, J. *J. Chem. Soc., Dalton Trans.* **2002**, 4529.

[210] Huang, J.-H.; Chi, L.-S.; Yu, R.-C.; Jiang, G. J.; Yang, W.-T.; Lee, G.-H.; Peng, S.-M. *Organometallics* **2001**, *20*, 5788.

[211] Matsugi, T.; Matsui, S.; Kojoh, S.-I.; Takagi, Y.; Inoue, Y.; Nakano, T.; Fujita, T.; Kashiwa, N. *Macromolecules* **2002**, *35*, 4880.

[212] Sakuma, A.; Weiser, M.-S.; Fujita, T. *Polym. J.* **2007**, *39*, 193.

[213] (a) Matsugi, T.; Fujita, T. *Chem. Soc. Rev.* **2008**, *37*, 1264. (b) Annunziata, L.; Pappalardo, D.; Tedesco, C.; Pellecchia, C. *Organometallics* **2009**, *28*, 688.

[214] Murray, R. E. (Union Carbide Chemicals & Plastics Technology Corp., USA). PCT Int. Appl. WO9901481, **1999**.

[215] Murray, R. E. (Union Carbide Chemicals & Plastics Technology Corp., USA). PCT Int. Appl. WO9901460, **1999**.

[216] Murray, R. E.; George, V. M.; Nowlin, D. L.; Schultz, C. C.; Petersen, J. L.; Poly-Preprints, 223rd ACS National Meeting, Orlando, FL, April 7-11, 2002; American Chemical Society: Washington, DC, 2002; Vol. 43, p 294.

[217] Richter, J.; Edelmann, F. T.; Noltemeyer, M.; Schmidt, H. G.; Shmulinson, M.; Eisen, M. S. *J. Mol. Catal. A: Chem.* **1998**, *130*, 149.

[218] Averbuj, C.; Tish, E.; Eisen, M. S. *J. Am. Chem. Soc.* **1998**, *120*, 8640.

[219] Volkis, V.; Shmulinson, M.; Averbuj, C.; Lisovskii, A.; Edelmann, F. T.; Eisen, M. S. *Organometallics* **1998**, *17*, 3155-3157.

[220] Volkis, V.; Schmulinson, M.; Shaviv, E.; Lisovskii, A.; Plat, D.; Kuehl, O.; Koch, T.; Hey-Hawkins, E.; Eisen, M. S. *PMSEPreprints*, 223rd ACS National Meeting,

Orlando, FL, April 7-11, 2002; American Chemical Soceity: Washington, DC, 2002; Vol. 86, pp 301-303.

[221] Busico, V.; Cipullo, R.; Caporaso, L.; Angelini, G.; Segre, A. L. *J. Mol. Catal. A: Chem.* **1998**, *128*, 53.

[222] Jayaratne, K. C.; Sita, L. R. *J. Am. Chem. Soc.* **2000**, *122*, 958.

[223] Vollmerhaus, R.; Shao, P. C.; Taylor, N. J.; Collins, S. *Organometallics* **1999**, *18*, 2731-2733.

[224] Chen, C. T.; Rees, L. H.; Cowley, A. R.; Green, M. L. H. *J. Chem. Soc., Dalton Trans.* **2001**, 1761-1767.

[225] Duncan, A. P.; Mullins, S. M.; Arnold, J.; Bergman, R. G. *Organometallics* **2001**, *20*, 1808.

[226] Andell, O.; Maaranen, J. (Borealis A/S, Denmark). PCT Int. Appl. WO9910353, **1999**.

[227] Zhang, J.; Tang, G.; Guoxin, J.; *Chin. Sci. Bull.*, **2006**, *51*, 2964

[228] Chrisholm, M. H. *Chemtracts-Inorg Chem. 4* **1992**, 273.

[229] Gibson V. C. *J. Chem. Soc. Dalton Trans.* **1994**, *11* 1607

[230] Collman, J. P.; Hegedus, L. S.; Norton J. R.; Finke R. G. *Principles and Applications of Organotransition Metal Chemistry*, University Science Books **1987**, 60

[231] Fay, R. C.; Lindmark, A. F. *J. Am. Chem. Soc. 105*, **1983,** 2118.

[232] Serpone, N.; Fay R. C. *Inorg. Chem.* **1967**,1835.

[233] Janiak C.; Scharmann T.G.; Lange K.C.H. *Macromol. Rapid Commun.* **1994**, *15*, 655.

[234] Matilainen, L.; Klinga, M.; Leskelä, M.; *J. Chem. Soc. Dalton Trans.* **1996**, 219.

[235] Oouchi, K.; Mitani, M.; Hayakawa, M.; Yamada T. *Macromol. Chem. Phys.* **1996**, *197*, 1545.

[236] Shmulinson S.; Galan-Fereres M.; Lisovskii A.; Nelkenbaum E.; Semiat R.; Eisen M.S. *Organometallics* **2000,** *19*, 1208.

[237] Wang J.; Liu Z.; Wang D.; Guo D. *Polym. Int.* **2000,** *49*, 1665. 53

[238] Gueta-Neyroud, T.; Tumanskii, B.; Kapon, M.; Eisen, M. S. *Macromolecules* **2007**, *40*, 5261.

[239] Sobota, P.; Przybylak, K.; Utko, J.; Jerzykiewicz, L. B.; Pombeiro, A. J. L.; da Silva, M.; Szczegot, K. *Chem. Eur. J.* **2001**, *7*, 951.

[240] de S. Basso, N. R.; Greco, P. P.; Carone C. L. P.; Livotto, P. R.; Simplıcio, L. M. T.; da Rocha Z. N.; Galland, G. B.; dos Santos, J. H. Z. *J. Mol. Catal. A: Chem.* **2007**, *267*, 129

[241] Carone, C.; de Lima, V.; Albuquerque F.; Nunes, P.; de Lemos, C.; dos Santos J. H. Z.; Galland, G. B.; Stedile, F. C.; Einloft, S.; de S. Basso, N. S. *J. Mol. Catal. A: Chem.* **2004**, *208*, 285.

[242] Fim, F.; Machado, T.; Santos de Sa, D.; Livotto, P. R.; da Rocha, Z.; de S. Basso, N. S.; Galland, B. G. *J. Polym. Sci. Part A Polym. Chem.* **2008**, *46*, 3830.

[243] Suzuki, Y.; Inoue, Y.; Tanaka, H.; Fujita T. *Macromol. Rapid Commun.* **2004**, *25*, 493.

[244] van der Linden, A.; Schaverien, C. J.; Meijboom, N.; Ganter, C.; Orpen, A. G. *J. Am. Chem. Soc.* **1995**, *117*, 3008.

[245] Froese, R. D. J.; Musaev, D. G.; Matsubara, T.; Morokuma K. *J. Am. Chem. Soc.* **1997**, *119*, 7190.

[246] Nakayama, Y.; Watanabe, K.; Ueyama, N.; Nakamura, A.; Harada, A.; Okuda J.; *Organometallics* **2000**, *19*, 2498.

[247] Kiesewetter, E. T.; Randoll, S.; Radlauer, M.; Waymouth, R. M. *J. Am. Chem. Soc.* **2010**, *132*, 5566.

[248]. Golisz, S. R.; Bercaw, J. E. *Macromolecules* **2009**, *42*, 8751.

[249] Frediani, M.; Semeril, D.; Comucci, A.; Bettucci, L.; Frediani, P.; Rosi, L.; Matt, D.; Toupet, L.; Kaminsky, W. *Macromol. Chem. Phys.* **2007**, *208*, 938.

[250] Bansleben, D. A.; Day, M. W.; Friedrich, S.; Li, R. T.; Wang, C.; Younkin, T. R.; Grubbs,R. H. *Organometallics* **1998**, *17*, 3149.

[251] Ishii, S.; Saito, J.; Mitani, M.; Mohri, J.; Matsukawa, N.; Tohi, Y.; Matsui, S.; Kashiwa, N.; Fujita, T. *J. Mol. Catal. A: Chem.* **2002**, *179*, 11.

[252] Ishii, S.; Furuyama, R.; Matsukawa, N.; Saito, J.; Mitani, M.; Tanaka, H., Fujita, T. *Macromol. Rapid Commun.*, **2003**, *24*, 452.

[253] Yoshida, Y., Mohri, J., Ishii, S., Mitani, M., Saito, J., Matsui, S., Makio, H., Nakano, T.; Tanaka, H.; Onda, M.; Yamamoto, Y.; Mizuno, A.; Fujita, T. *J. Am. Chem. Soc.*, **2004**, *126*, 12023.

[254] Yoshida, Y.; Matsui, S.; Fujita, T. *J. Organomet. Chem.* **2005**, *690*, 4382.

[255] Makio, H.; Fujita, T. *Chem. Lett.* **2005**, *34*, 1382.

[256] Mitani, M.; Saito, J.; Ishii, S., Nakayama, Y.; Makio, H., Matsukawa, N.; Matsui, S.; Mohri, J.; Furuyama, R.; Terao, H.; Bando, H.; Tanaka, H.; Fujita, T. *Chem. Rec.* **2004**, *4*, 137.

[257] (a) Nakayama, Y.; Saito, J.; Bando, H.; Fujita, T. *Chem. Eur. J.* **2006**, *12*, 7546. (b) Nakayama, Y.; Saito, J.; Bando, H.; Fujita, T. *Macromol Chem. Phys.* **2005**, *206*, 1847.

[258] Nakayama, Y.; Bando, H.; Sonobe, Y.; Fujita, T. *Bull. Chem. Soc. Jpn.* **2004**, *77*, 617.

[259] Nakayama, Y.; Bando, H.; Sonobe, Y.; Fujita, T. *J. Mol. Catal. A: Chem.* **2004**, *213*, 141.

[260] Nakayama, Y.; Bando, H.; Sonobe, Y.; Kaneko, H.; Kashiwa, N.; Fujita, T. *J. Catal.* **2003**, *215*, 171.

[261] Nakayama, Y.; Bando, H.; Sonobe, Y.; Suzuki, Y.; Fujita, T. *Chem. Lett.* **2003**, *32*, 766.

[262] Bando, H.; Nakaama, Y.; Sonobe, Y.; Fujita, T. *Macromol. Rapid Commun.* **2003**, *24*, 732.

[263] Terao, H.; Ishii, S.; Mitani, M.; Tanaka, H.; Fujita, T. *J. Am. Chem. Soc.* **2008**, *130*, 17636.

[264] Matsui, S.; Fujita T.; *Catal. Today* **2001**, *66*, 63.

[265] Matsui, S.; Inoue, Y.; Fujita T.; J. *Synth. Org. Chem. Jpn.* **2001**, *59*, 232. 54

[266] Matsui, S.; Mitani, M.; Saito, J.; Tohi, Y.; Makio, H.; Matsukawa, N.; Takagi, Y.; Tsuru, K.; Nitabaru, M.; Nakano, T.; Tanaka, H.; Kashiwa, N.; Fujita, T. *J. Am. Chem. Soc.* **2001**, *123*, 6847.

[267] Mitani, M.; Mohri, J-I.; Yoshida, Y.; Saito, J.; Ishii, S.; Tsuru, K.; Matsui, S.; Furuyama, R.; Nakano, T; Tanaka, H.; Kojoh, S-I.; Matsugi, T.; Kashiwa, N.; Fujita, T.; *J. Am. Chem. Soc.* **2002**, *124*, 3327.

[268] (a) Makio, H.; Kashiwa, N.; Fujita, T. *Adv. Synth. Catal.* **2002**, *344*, 477. (b) Weiser, M.-S.; Wesolek, M.; Mülhaupt, R. *J. Organomet. Chem.* **2006**, *691*, 2945.

[269] Makio, H., Fujita, T., *Acc. Chem. Res.* **2009**, *42*, 1532.

[270] Tohi, Y.; Makio, H.; Matsui, S.; Onda, M., Fujita, T. *Macromolecules* **2003**, *36*, 523.

[271] Tohi, Y.; Nakano, T.; Makio, H.; Matsui, S.; Fujita, T.; Yamaguchi, T. *Macromol. Chem. Phys.* **2004**, *205*, 1179.

[272] Mitani, M., Furuyama, R.; Mohri, J.; Saito, J.; Ishii, S.; Terao, H.; Kashiwa, N.; Fujita, T. *J. Am. Chem. Soc.* **2002**, *124*, 7888.

[273] Mitani, M.; Furuyama, R.; Mohri, J.; Saito, J.; Ishii, S.; Terao, H.; Nakano, T.; Tanaka, H.; Fujita, T. *J. Am. Chem. Soc.* **2003**, *125*, 4293.

[274] Saito, J.; Mitani, M.; Matsui, S.; Tohi, Y.; Makio, H.; Nakano, T.; Tanaka, H., Kashiwa, N.; Fujita, T. *Macromol. Chem. Phys.* **2002**, *203*, 59.

[275] Terao, H.; Iwashita, A.; Ishii, S.; Tanaka, H.; Yoshida, Y.; Mitani, M.; Fujita, T. *Macromolecules* **2009**, *42*, 4359.

[276] Mitani, M.; Nakano, T., Fujita, T. *Chem. Eur. J.* **2003**, *9*, 2396.

[277] Furuyama, R.; Saito, J.; Ishii, S.; Makio, H.; Mitani, M.; Tanaka, H.; Fujita, T. *J. Organomet. Chem.* **2005**, *690*, 4398.

[278] (a) Kojoh, S.; Matsugi, T.; Saito, J.; Mitani, M.; Fujita, T.; Kashiwa, N. *Chem. Lett.* **2001**, *30*, 822. (b) Hustad, P. D.; Coates, G. W. *J. Am. Chem. Soc.*, **2002**, *124*, 11578. (c) Fujita, M.; Coates, G. W. *Macromolecules* **2002**, *35*, 9640. (d) Weiser, M.-S.; Mülhaupt, R. *Macromol. Rapid Commun.* **2006**, *27*, 1009. (e) Yoon, J.; Mathers, R. T.; Coates, G. W. Thomas, E. L.; *Macromolecules* **2006**, *39*, 1913.

[279] Jia, A.-Q.; Jin, G.-X. *Dalton Trans.* **2009**, 8838.

[280] Suzuki, Y.; Terao, H.; Fujita, T. *Bull. Chem. Soc. Jpn.* **2003**, *76*, 1493.

[281] Lamberti, M.; Mazzeo, M.; Pappalardo, D.; Pellecchia, C. *Coord. Chem. Rev.* **2009**, *253*, 2082.

[282] (a) Nakayama, Y.; Kawai, K.; Fujita, T. *J. Jpn. Petrol. Inst.* **2010**, *53*, 111. (b) Makio, H.; Terao, H.; Iwashita, A.; Fujita, T. *Chem. Rev.* **2011** (published online).

[283] Chen, S.; Zhang, X.; Ma, M.; Lu, Y.; Zhang, Z.; Li, H.; Lu, Z.; Cui, N.; Hu, J.; *J. Organomet. Chem.* **2005**, *690*, 4184.

[284] Edson, J. B.; Wang, Z.; Kramer, E. J.; Coates, G. W. *J. Am. Chem. Soc.*, **2008**, *130* 4968.

[285] Reinartz, S.; Mason, A. F.; Lobkovsky, E. B.; Coates, G. W. *Organometallics* **2003,** *22*, 2542.

[286] Mason, A. F.; Coates G. W. *J. Am. Chem. Soc.*, **2004**, *126*, 6326.

[287] Zhang, X.; S.; Li, H.; Zhang, Z.; Lu, Y.; Wu, C.; Hu, Y. *J. Polym. Sci., Part A: Polym. Chem.* **2007**, *45*, 59.

[288] Tang, L-M.; Hu T.; Pan, L.; Li, Y-S. *J. Pol. Sci. Part A: Polym. Chem.* **2005**, *43*, 6323.

[289] Tang, L. M.; Duan, Y. Q.; Li, Y-S. J. *Polym. Sci. Part A: Polym. Chem.* **2005**, *43*, 1681.

[290] Li, X-F.; Dai, K.; Ye, W.P.; Pan L.; Li Y-S. *Organometallics* **2004,** *23*, 1223.

[291] Tang, L-M.; Hu, T.; Bo, Y-J.; Li, Y-S., Hu, N-H.; *J. Organom. Chem.* **2005**, 690 3125.

[292] Ye, W-P.; Zhan, J.; Pan, L; Hu, N-H.; Li Y-S. *Organometallics* **2008,** *27*, 3642.

[293] Marquet, N.; Kirillov, E.; Roisnel, T.; Razavi, A.; Carpentier, J-F. *Organometallics* **2009,** *28,* 606.

2 Transition Metal Complexes Based on *N*,*N*-Dialkylcarbamato Ligands

2.1 General aspects

The chemistry of transition metal complexes bearing *N*,*N*-dialkylcarbamato ligand, of formula $^{-}O_2CNR_2$, R being H, an alkyl or an aryl group. is relatively recent in the scientific literature, its development dating back to the 1970s.[1] The $^{-}O_2CNR_2$ ligand is monoanionic and contributes by one unit to the oxidation state in metal-containing covalent combinations.

Compounds containing this ligand are called "carbamates", and they are formulated as $[M(O_2CNR_2)_n]_m$, *n* and *m* corresponding to the oxidation number of the central atom M and the nuclearity of the system, respectively. These compounds are formally considered as derivatives of dialkylcarbamic acid R_2NCO_2H which are elusive species due to their tendency to decarboxylate, thus giving back CO_2 and the amine. Their isolation has been accomplished only recently using either dibenzylamine (Bz_2NH) or the cobalt aminophosphane complex $CoCl(NO)_2[PhP(OCH_2CH_2)_2NH]$.[2] In both cases, X-ray characterization has shown that the relevant carbamic acid molecules are not in the zwitterionic form, but rather are organized in a H-bonded dimeric structure.[2,3]

The first homoleptic derivative of this class, tetrakis(*N*,*N*-dimethylcarbamato)titanium(IV), of formula $Ti(O_2CNMe_2)_4$, was reported in 1965[4,5] and was synthesized by exhaustive carbonation of the dimethylamido precursor $Ti(NMe_2)_4$. The metal-amido/CO_2 route to *N*,*N*-dialkylcarbamato complexes was further pursued in 1974, for early transition metals,[6] which are known to form stable dialkylamido complexes. Shortly thereafter, the first dialkylcarbamato complexes of metal cations of groups 5 and 6[6] and of uranium(IV), $[U(O_2CNR_2)_4]_n$,[7] were prepared by carbonation of the corresponding dialkylamido precursors

$$M(NR_2) + n\ CO_2 \longrightarrow M(O_2CNR_2)_n \qquad (1)$$

However, a more general preparative method was necessary in order to overcome the initial restriction that N,N-dialkylamido metal complexes with aryl- or simple alkyl groups are sometimes difficult to prepare or are not reported in the literature.

An alternative synthetic route to *N*,*N*-dialkylcarbamato metal complexes from metal chloride in the presence of the secondary amine and carbon dioxide was also found to be

viable. This route was first adopted for the synthesis of *N,N*-dialkylcarbamato derivatives of uranium(IV)[8] and later extended to several halides of transition d and f metals, whose amido complexes are not easily available. The reaction is essentially a ligand substitution reaction whereby the anionic chloride ligand of the starting material is substituted by the carbamato group, formed in situ by the R_2NH/CO_2 system. Due to the elevated solubility of N,N-dialkylcarbamato derivatives and to the negligible solubility of the appropriate dialkylammonium chloride in the reaction solvent (toluene or an aliphatic hydrocarbon), product separation is generally easily achieved.

$$MCl_n + n\,CO_2 + 2nR_2NH \longrightarrow M(O_2CNR_2)_n + n[R_2NH_2]Cl \qquad (2)$$

The $TaCl_5/Et_2NH/CO_2$ route gives the homoleptic compound of tantalum(V), $Ta(O_2CNEt_2)_5$, which is mononuclear with the central metal atom surrounded by three bidentate and two monodentate diethylcarbamato groups,[9] while using the $Ta(NMe_2)_5/CO_2$ route[10] affords the product of partial substitution $Ta(NMe_2)_2(O_2CNMe_2)_3$.

N,N-Di-*iso*-propylcarbamato derivatives of group 4 (Ti, Hf) have been synthesized starting from the anhydrous metal chloride.[11] The mononuclear compounds in the IV oxidation state, of formula $M(O_2CN^iPr_2)_4$ (M = Ti and Hf)[11,12] containing the octacoordinated central metal atom have been reported and shown to be isostructural.

Incomplete removal of the anionic ligands by $R_2NCO_2^-$ in reactions using a metal-containing precursor or partial carbonation of the amido precursor by carbon dioxide leads to nonhomoleptic compounds, i.e., containing anionic ligands of a different nature. As mentioned before, reacting an amido precursor with carbon dioxide actually consists of setting up the conditions for an amido/carbamato exchange. Normally, a chloride/carbamato exchange, beside being more facile from a synthetic viewpoint is more effective due to the low solubility of the ammonium (or substituted ammonium) halide in the reaction mixture, thus leading the reaction to normally proceed to completion. For example, with the amido complexes of titanium(IV) and tantalum(V), only the use of carbon dioxide in substoichiometric amounts allows the isolation of partly carbonated compounds, such as $Ti(O_2CNMe_2)_2(NMe_2)_2$, $Ti(O_2CNMe_2)_3(NMe_2)$,[6c] and $Ta(O_2CNMe_2)_3(NMe_2)_2$.[6f]

The X-ray studies on these compounds[6d,6f] confirm the coordination flexibility of the carbamato ligand. The former compound, which is mononuclear, contains

hexacoordinated titanium(IV) with bidentate carbamato ligands, while the tantalum(V) compound is heptacoordinated with one mono and two bidentate $^{-}O_2CNMe_2$ ligands. Although the crystal structure of $Ti(O_2CNMe_2)_3(NMe_2)$ is unknown, on the basis of the IR spectra (strong absorption at 1576 cm^{-1}),[6d] all the carbamato ligands should be bidentate in this mixed amido-carbamato complex of titanium(IV).

The metal-chloride/NHR_2/CO_2 route to *N,N*-dialkylcarbamato metal complexes sometimes leads to incomplete halide removal, thus forming mixed chloro-carbamato derivatives. This is exemplified by the reaction of anhydrous $TaCl_5$[13] with the corresponding NHR_2/CO_2 system.[14]

$$TaCl_5 + 3CO_2 + 6R_2NH \longrightarrow Ta(O_2CNEt_2)_3Cl_2 + 3[NH_2Et_2]Cl \quad (3)$$

In this case, the room temperature reaction of $TaCl_5$ with $NHEt_2$ at atmospheric pressure of carbon dioxide gives the product of partial substitution $Ta(O_2CNEt_2)_3Cl_2$. By using a high $NHEt_2/TaCl_5$ molar ratio and by forcing the reaction conditions (50 °C, 6 atm of CO_2), it was possible to remove the all two chlorides and to form the homoleptic pentakis(*N,N*-diethylcarbamato)tantalum(V).[14]

Although organometallic derivatives containing carbamato ligands are relatively uncommon, but some cyclopentadienyl compounds have been obtained via metal-chloride or metal-amido routes(see Scheme 1 and the following eqs 4-9)[15,16,17,18,19,20]

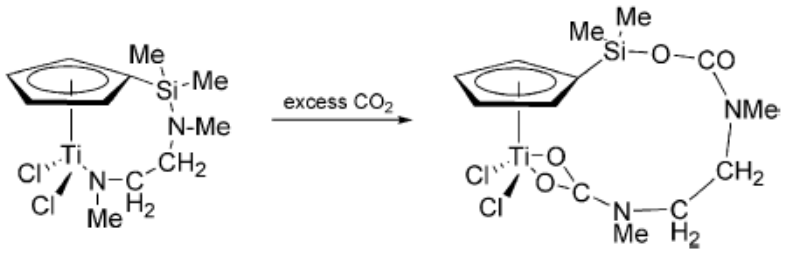

Scheme 1

$$[TiCp_2Cl_2]_2 + 2CO_2 + 2NHR_2 \longrightarrow 2Ti(O_2CNR_2)Cp_2 + 2[NH_2R_2]Cl \quad (R = Et, {}^{i}Pr) \quad (4)$$

$$TiCp^*(NR_2)_3 + 3CO_2 \longrightarrow Ti(O_2CNR_2)_3Cp^* \quad (5)$$

$$2M(O_2CNEt_2)_4 + MgCp_2 \longrightarrow 2M(O_2CNEt_2)_3Cp + Mg(O_2CNEt_2)_2 \quad (M = Zr, Hf) \quad (6)$$

$$2MCp_4 + 3Fe(O_2CNEt_2)_2 \longrightarrow 2M(O_2CNEt_2)_3Cp + 3FeCp_2 \quad (M = Zr, Hf) \quad (7)$$

$$2VCp_2Cl + 4CO_2 + 6NHEt_2 \longrightarrow V_2(O_2CNEt_2)_4Cp_2 + 2[NH_2Et_2]Cl + 2CpH \quad (8)$$

$$TaCp^*(N^tBu)(O_2CX)Y + CO_2 \longrightarrow Ta(O_2CX)Cp^*(N^tBu)Y \quad (9)$$
(X = NMe_2, Y = Me; X = NH^tBu, Y = Me)

The niobium and tantalum dicarbollide dimethylamido complexes $M(NMe_2)_3(C_2B_9H_{11})$, with a d^0 electronic configuration of the central metal atom, react with CO_2 affording the tris(*N,N*-dimethylcarbamato) complexes $M(O_2CNMe_2)_3(C_2B_9H_{11})$ of niobium(V) and tantalum(V).[21]

$$M(C_2B_9H_{11})(NMe_2)_3 + 3CO_2 \longrightarrow M(O_2CNMe_2)_3(C_2B_9H_{11}) \quad (M = Nb, Ta) \quad (10)$$

Carbamato complexes having alkyl groups as additional ligands are exemplified by: $Hf[O_2CN(Si\text{-}Me_3)_2]_2R_2$, R = Me, Et, CH_2SiMe_3,[22] and $Ta(O_2CNMe_2)_4R$, R = ^{t}Bu, ^{i}Pr, Et, CH_2SiMe_3.[23] X-ray diffraction studies show that the compound has an approximate pentagonal bipyramidal structure, two monodentate carbamato groups occupying the axial positions and defining an O-Ta-O angle of 171.5°. The other two carbamato groups in the basal pentagonal plane are bidentate.

2.2 Reactivity of transition metal complexes bearing *N,N*-dialkylcarbamato ligands

Despite being relatively new compounds, reactivity of metal carbamato complexes has been well studied in the recent years. While they are readily active with electrophilic compounds, such as water, proton-containing substances, alkyl and aryl halides, metal carbamates do not generally react with nucleophiles, as exemplified by the *N,N*-dialkylcarbamato derivatives of manganese(II) which are inert toward organic (as in LiMe and MgBrPh) or organometallic [as in $NaMn(CO)_5$ and $NaFeCp(CO)_2$] nucleophiles.[16] This is in agreement with valence-bond arguments suggesting that the oxygen atoms of the CO_2 moiety in dialkylcarbamato metal derivatives acquire a partial negative charge, the coordinated ligand thus being the potential site of attack by electrophiles, see Scheme 2. Attack by electrophiles at the nitrogen atom induces

elimination of CO_2, while attack at the oxygen atom may allow the CO_2 moiety to be retained in the products.

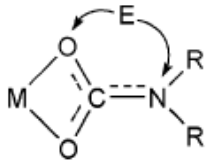

Scheme 2

2.2.1 Hydrolysis: Formation of μ_n-oxo derivatives

The reaction of water with metal-carbamato complexes leads to the formation of hydroxo-, oxo- or carbonato groups. If the process is conducted with an excess of water the complete hydrolysis of the carbamato group can occur. When, however, the amount of water is adequately controlled (stoichiometric amount), typically the formation of μ-oxo-carbamato complexes is observed.

The partial hydrolysis of the complexes $[M(O_2CNR_2)_n]_m$ is thermodynamically favored due to the release of CO_2 from the system which explains why the nature of the products is normally well defined and related to the metal/H_2O molar ratio which has been used.

Hydrolysis of $M(O_2CNR_2)_n$, see Scheme 3, produces μ-oxo complexes and accompanied by the formation of the appropriate secondary amine. The M-OH bond presumably formed in the first step is of sufficient Brønsted acidity to bring about the further attack, generally intermolecular, leading to μ-oxo derivatives:

$$L_nM(O_2CNR_2) \xrightarrow[-\,CO_2,\,-\,NHR_2]{H_2O} L_nM{-}OH \longrightarrow L_nM{-}O{-}ML_n$$

Scheme 3

The first example of this class of compounds, $U_4(\mu_3\text{-}O)_2(O_2CNEt_2)_{12}$, was initially detected[24] as a side product in the preparation of $[U(O_2CNEt_2)_4]_n$, the μ-oxo derivative being produced through a hydrolytic process with adventitious water present in the system.

$$4/n[U(O_2CNEt_2)_4]_n + 2H_2O \longrightarrow U_4(\mu_3\text{-}O)_2(O_2CNEt_2)_{12} + 4NHEt_2 + 4CO_2 \quad (11)$$

More complex structures arise from the controlled hydrolysis of copper(II)[25] and iron(II) *N,N*-dialkylcarbamates.[26] The iron(II) derivative of formula $Fe_8(\mu_4\text{-}O)_2(O_2CN^iPr_2)_{12}$ was synthesized by controlled hydrolysis of $[Fe(O_2CN^iPr_2)_2]_n$, under rigorous exclusion of dioxygen (the nuclearity of the starting iron(II) product is unknown). The octanuclear compound[14] of copper(II) of the same chemical composition as that of iron(II), namely, $Cu_8(\mu_4\text{-}O)_2(O_2CN^iPr_2)_{12}$, was similarly obtained by hydrolysis of the homoleptic copper(II) precursor with the stoichiometric amount of water.

$$8/n[M(O_2CN^iPr_2)_2]_n + 2H_2O \longrightarrow M_8(\mu_4\text{-}O)_2(O_2CN^iPr_2)_{12} + 4NH^iPr_2 + 4CO_2 \quad (12)$$

(M = Fe, Cu)

New μ_4-oxo octanuclear derivatives of cobalt(II) and nickel(II) have been prepared, of general formula $M_8(\mu_4\text{-}O)_2(O_2CN^iPr_2)_{12}$.[27] Beside the hydrolytic processes of the iron(II) carbamato complexes mentioned above, derivatives of iron(III) have also been studied in connection with their behavior with water.[28] For example, by reaction of the homoleptic compound $Fe(O_2CNEt_2)_3$ with the stoichiometric amount of water in toluene solution, a product of analytical composition $[Fe_2O(O_2CNEt_2)_4]_n$ was isolated as a red-brown substance, which is soluble even in aliphatic hydrocarbons. This is suggestive of low nuclearity, which was not established, however.

$$2Fe(O_2CNEt_2)_3 + H_2O \longrightarrow 1/n[Fe_2O(O_2CNEt_2)_4]_n + CO_2 + 2NHEt_2 \quad (13)$$

More recently, Belli Dell' Amico *et. al.* reported that controlled hydrolysis of the homoleptic titanium precursor, $Ti(O_2CNEt_2)_4$, leads to the formation of an octanuclear μ-oxo-titanium(IV) derivative in a high yield of 87% (Figure 2).[29]

$$8Ti(O_2CNEt_2)_4 + 8H_2O \longrightarrow [Ti_8(\mu\text{-}O)_8(O_2CNEt_2)_{16}].[NH_2Et_2][O_2CNEt_2] + 14NHEt_2 + 15CO_2 \quad (14)$$

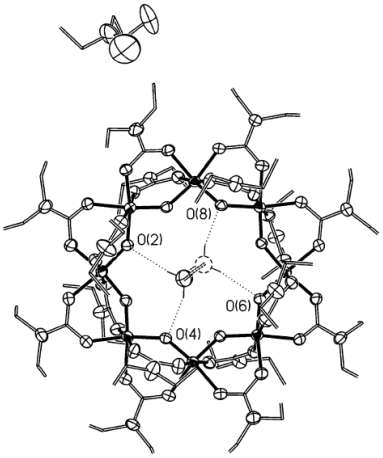

Figure 3. View of the $Ti_8O_8(O_2CNEt_2)_{16}$ ring with the disordered clathrated diethylammonium cation and the external carbamato anions.

2.2.2 Reaction with protic reagents

The addition of H^+ to a dialkylcarbamato group can occur at the oxygen atom or at the nitrogen atom, leading, respectively, to carbamic acids R_2NCO_2H, or to $R_2NH + CO_2$.

$$M(O_2CNR_2)_n + nH^+ \longrightarrow M^{n+} + nR_2NCO_2H \qquad (15)$$

The reactivity of metal carbamato complexes has been examined by a series of proton-active substances such as carboxylic acids, acetylacetone, hydrogen halides, hydrogen sulfide and water. The reactions usually proceed to completion under mild conditions and they may also be of preparative value in certain cases. For example, with acetylacetone, acacH, the *N*,*N*-dialkylcarbamato derivative of chromium(II) $Cr_2(O_2CNEt_2)_4(NHEt_2)_2$[30] gives $Cr(acac)_2$, further oxidation to Cr(III) by the third equivalent of acacH giving $Cr(acac)_3$. Displacement reactions of the carbamato ligands by acetylacetone have also been reported with titanium(III),[31] vanadium(III),[31] and nickel(II),[32] giving the corresponding *β*-diketonato complexes.

$$xM(O_2CNR_2) + nx\ \text{acacH} \longrightarrow M_x(acac)_{nx} + nx\ CO_2 + nx\ NHR_2 \qquad (16)$$

M = Ti; n = 3; R = ^{i}Pr; x = 1

M = Fe; n = 3; R = Et; ^{i}Pr; x = 1

M = Ni; n = 2; R = Et; x = 3

$$Cr_2(O_2CNR_2)_4(NHEt_2)_2 + 4acacH \longrightarrow 2Cr(acac)_2 + 4CO_2 + 6NHEt_2 \quad (17)$$

$$Cr(acac)_2 + acacH \longrightarrow Cr(acac)_3 + 1/2H_2 \quad (18)$$

The reactions of *N*,*N*-dialkylcarbamato complexes with hydrogen halides usually lead to halo-metalates[11,31] is carried out in anhydrous media, to minimize hydrolytic processes. This is particularly useful for heavier halides (Br, I) and for metal cations in a relatively high oxidation state.

$$M(O_2CNEt_2)_3 + 6HX \longrightarrow (NH_2Et_2)_3[MX_6] + 3CO_2 \quad (19)$$

M = Ti, V; X = Cl; M = Yb; X = I

$$M(O_2CNEt_2)_4 + 6HX \longrightarrow (NH_2Et_2)_2[MX_6] + 4CO_2 + 2NHEt_2 \quad (20)$$

M = Zr, Hf; X = Cl, Br, I

$$Ni(O_2CNR_2)_2 + 4HI \longrightarrow (NH_2R_2)_2[NiI_4] + 2CO_2 \quad (21)$$

R = Et, ^{i}Pr

2.2.3 Reaction with alkyl halides

There are two possible paths for reaction of a metal carbamate with an alkylating agent which are summarized in Scheme 4.

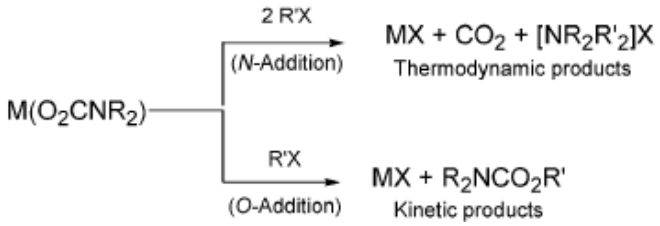

Scheme 4

Evolution of CO_2 and formation of the ammonium cation $[NR_2R'_2]+$ was observed by treating a transition metal carbamate with an alkyl halide: $M_6(O_2CNEt_2)_{12}$, M = Mn,[16] Co,[33] $Ni(O_2CNEt_2)_2$,[32] $Cu_2(O_2CNEt_2)_4(NHEt_2)_2$,[34] and $Pd(O_2CNEt_2)_2(NHEt_2)_2$ behave

accordingly.[35] The manganese derivative does not react with methyl iodide in a hydrocarbon solvent, but does so in THF, the observed product of the reaction being $[NR_2Me_2]_2[MnI_4]$.

$$1/6M_6(O_2CNEt_2)_{12} + 4\ MeI \longrightarrow 2CO_2 + [NMe_2R_2]_2[MI_4] \quad (22)$$

(M = Mn, R = Et, ^{i}Pr; M = Co, R = Et)

$$Pd(O_2CNEt_2)_2(NHEt_2) + 4MeI \longrightarrow 2CO_2 + 2[NMe_2Et_2]I + PdI_2(NHEt_2)_2 \quad (23)$$

2.2.4 Reaction with acyl halides

When a metal *N,N*-dialkylcarbamato is treated at room temperature with an acyl chloride, a fast reaction occurs [36] with formation of highly functionalized[37] carbamic-carboxylic anhydrides. For R = ^{i}Pr and R´ = Ph, the mixed anhydride can be isolated and characterized.[38,39,40]

$$M(O_2CNR_2)_n + nR´COCl \longrightarrow MCl_n + nR_2NC(O)OC(O)R´ \quad (24)$$

For several *N,N*-dialkylcarbamato complexes, the attack of the acyl electrophile occurs at the carbamato oxygen atom, independent of the nature of the metal [Na, Cu(II), Mn(II), Co(II), Ti(III), V(III), Fe(III)]. The resulting carbamic-carboxylic anhydride, incorporating carbon dioxide, sometimes undergoes decarboxylation to the appropriate amide.[36,41] This phenomenon has been observed for the complexes of Cu(II) and Fe(III) upon treatment with acyl chloride, leading to evolution of CO_2 and formation of the amide $Et_2NC(O)R´$, presumably due to the cleavage of the intermediate anhydride in the presence of metallic halides.

Formation of the mixed anhydride was observed also in the reaction of $Pd(O_2CNEt_2)_2(NHEt_2)_2$[35,42] or $Ni(O_2CNEt_2)_2$[32] with acetic anhydride, the transient mixed anhydride being spectroscopically detected.

$$Ni(O_2CNEt_2)_2 + 2(CH_3CO)_2O \longrightarrow Ni(O_2CCH_3)_2 + 2Et_2NC(O)OC(O)CH_3 \downarrow CO_2 + Et_2NC(O)CH_3$$

Scheme 5

2.2.5 Anionic ligand-transfer reactions

Some cases of transfer reactions of the carbamato ligand have been reported in scientific literature. Such reactions have been used for the synthesis of transition metal derivatives such as $Ti(O_2CNR_2)Cp_2$,[16] magnesium and phosphorus carbamates, $Mg(O_2CNR_2)_2$, R = Et,[19] ^{i}Pr.[43] The anionic ligands are redistributed in the products and no change of oxidation state takes place.

$$Mn_6(O_2CNEt_2)_{12} + 6(TiCp_2Cl)_2 \longrightarrow 12Ti(O_2CNEt_2)Cp_2 + 6MnCl_2 \quad (25)$$

$$MgCp_2 + 2M(O_2CN^iPr_2)_4 \longrightarrow Mg(O_2CN^iPr_2)_2 + 2M(O_2CN^iPr_2)_3Cp \quad (M = Zr, Hf) \quad (26)$$

$$MgCp_2 + Ti(O_2CN^iPr_2) \longrightarrow Mg(O_2CN^iPr_2)_2 + Ti(O_2CN^iPr_2)Cp_2 \quad (27)$$

2.2.6 Reactions with inorganic surfaces

It has been reported that *N,N*-dialkylcarbamato metal complexes are able to react with hydroxyl groups located on the surface of inorganic oxides. As an example, pre-dehydrated commercial silica of known surface area has been used extensively for this purpose. This leads to a grafting reaction completely shifted toward the product due to the formation of carbon dioxide. Equation 28 represents such a grafting reaction for a *N,N*-dialkylcarbamato derivative of nuclearity *m*, whereby a ≡Si-O-M bond is formed on the silica surface.[1]

$$[M(O_2CNR_2)_n]_m + \equiv Si(OH) \longrightarrow \equiv SiO[M_m(O_2CNR_2)_{nm-1}] + CO_2 + NHR_2 \quad (28)$$

This method of functionalizing the silica surface has been used extensively, with the *N,N*-dialkylcarbamato derivatives of tin(IV),[44] palladium(II),[45] platinum(II),[46] and gold(I).[47] It has been conclusively shown that the carbamato function is used for grafting the metal on the silica surface; thus, the remaining carbamato groups being still present on the grafted metal may be used for further reactions.

N,N-dialkylcarbamato complexes of copper (II) grafted on commercial silica or ZrO_2-SiO_2 matrix were prepared by treatment of suspension of the silica and silica–

zirconia matrices in a solution of the copper dialkylcarbamate leading to the functionalization of the respective substrates.[48] The results showed that the Cu/Si ratio is increased by increasing the grafting time and the ZrO_2–SiO_2 matrix is more reactive to attack by the carbamato complexes than either prepared or commercial SiO_2.

More recently, Pampaloni et al.[49] reported the grafting process of the Group 4 metal polycyclopentadienyls MCp_n (M = Ti, n = 3, 4; M = Zr, Hf, n = 4) and homoleptic *N*,*N*-dialkylcarbamates $M(O_2CNR_2)_n$ (M = Ti, n = 3, 4; M = Zr, Hf, n = 4) on amorphous silica. They observed that $M(O_2CNR_2)_4$ derivatives evolve more than one mol of carbon dioxide per mol of metal when the metal is quantitatively grafted on the silica surface, suggesting that both mono- and bis-grafted complexes are present, as sketched in Fig. 4. The results also showed carbamato groups were more reactive than cyclopentadienyl ones that may be ascribed to the evolution of carbon dioxide.

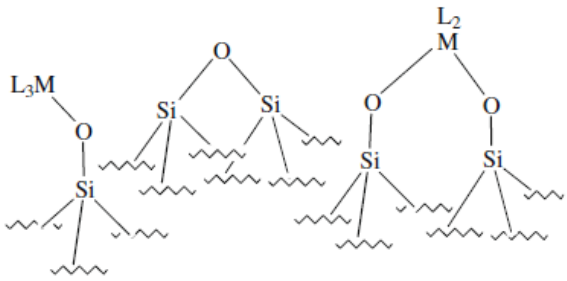

Figure 4. Hypothesized species present on the silica surface after reaction with $M(O_2CNR_2)_4$.

2.3 References.

[1] Belli Dell'Amico, D.; Calderazzo, F.; Labella, L.; Marchetti, F.; Pampaloni, G. *Chem. Rev.* **2003**, *103*, 3857.

[2] Aresta, M.; Ballivet-Tkatchenko, D.; Belli Dell'Amico, D.; Bonnet, M. C.; Boschi, D.; Calderazzo, F.; Faure, R.; Labella, L.; Marchetti, F. *Chem. Commun.* **2000**, 1099.

[3] Jamroz, M. H.; Dobrowolski, J. Cz.; Rodes, J. E.; Borowaik, M. *J. Mol. Struct.* **2002**, *618*, 101.

[4] Chandra, G.; Lappert, M. F. *Inorg. Nucl. Chem. Lett.* **1965**, *1*, 83.

[5] Chandra, G.; Jenkins, A. D.; Lappert, M. F.; Srivastava, R. C. *J. Chem. Soc. A* **1970**, 2550.

[6] (a) Chisholm, M. H.; Extine, M. *J. Am. Chem. Soc*. **1974**, *96*, 6214. (b) Chisholm, M. H.; Extine, M. *J. Am. Chem. Soc*. **1975**, *97*, 1623. (c) Chisholm, M. H.; Extine, M. W. *J. Am. Chem. Soc*. **1977**, *99*, 782. (d) Chisholm, M. H.; Extine, M. W. *J. Am. Chem. Soc*. **1977**, *99*, 792. (e) Chisholm, M. H.; Cotton, F. A.; Extine, M. W.; Stults, B. R. *Inorg. Chem.* **1977**, *16*, 603. (f) Chisholm, M. H.; Cotton, F. A.; Extine, M. W. *Inorg. Chem.* **1978**, *17*, 2000. (g) Chisholm, M. H.; Haitko, D. A.; Murillo, C. A. *J. Am. Chem. Soc*. **1978**, *100*, 6262.

[7] Bagnall, K. W.; Yanir, E. *J. Inorg. Nucl. Chem*. **1974**, *36*, 777.

[8] Calderazzo, F.; Dell'Amico, G.; Netti, R.; Pasquali, M. *Inorg. Chem*. **1978**, *17*, 471.

[9] Arimondo, P. B.; Calderazzo, F.; Englert, U.; Maichle-Mössmer, C.; Pampaloni, G.; Strähle, J. *J. Chem. Soc., Dalton Trans.* **1996**, 311.

[10] Chisholm, M. H.; Cotton, F. A.; Extine, M. W. *Inorg. Chem.* **1978**, *17*, 2000.

[11] Calderazzo, F.; Ianelli, S.; Pampaloni, G.; Pelizzi, G.; Sperrle, M. *J. Chem. Soc., Dalton Trans*. **1991**, 693.

[12] Belli Dell'Amico, D.; Calderazzo, F.; Ianelli, S.; Labella, L.; Marchetti, F.; Pelizzi, G. *J. Chem. Soc., Dalton Trans*. **2000**, 4339.

[13] *Handbook of Preparative Inorganic Chemistry*, 2nd ed.; Brauer, G., Ed.; Academic Press: New York, 1965; Vol. 2, p 1301.

[14] Agostinelli, E.; Belli Dell'Amico, D.; Calderazzo, F.; Fiorani, D.; Pelizzi, G. *Gazz. Chim. Ital*. **1988**, *118*, 729.

[15] Calderazzo, F.; Pampaloni, G.; Sperrle, M.; Englert, U. *Z. Naturforsch.* **1992**, *47b*, 389.

[16] Belforte, A.; Calderazzo, F.; Zanazzi, P. F. *J. Chem. Soc., Dalton Trans*. **1988**, 2921.

[17] Jime´nez, G.; Rodrı´guez, E.; Go´mez-Sal, P.; Royo, P.; Cuenca, T.; Galakhov, M. *Organometallics* **2001**, *20*, 2459.

[18] Gómez-Sal, P.; Irigoyen, A. M.; Martin, A.; Mena, M.; Monge, M.; Yelamos, C. *J. Organomet. Chem.* **1995**, *494*, C19.

[19] Abis, L.; Calderazzo, F.; Maichle-Mössmer, C.; Pampaloni, G.; Strähle, J.; Tripepi, G. *J. Chem. Soc. Dalton Trans.* **1998**, 841.

[20] Sánchez-Nieves, J.; Royo, P. *J. Organomet. Chem.* **2001**, *621*, 299.

[21] Batsanov, A. S.; Churakov, A. V.; Howard J. A. K.; Hughes, A. K.; Johnson, A. L.; Kingsley, A. J.; Neretin, I. S.; Wade, K. *J. Chem. Soc., Dalton Trans.* **1999**, 3867.

[22] Andersen, R. A. *Inorg. Chem.* **1979**, *18*, 2928.

[23] Chisholm, M. H.; Tan, L.-S.; Huffman, J. C. *J. Am. Chem. Soc.* **1982**, *104*, 4879.

[24] Calderazzo, F.; Dell'Amico, G.; Pasquali, M.; Perego, G. *Inorg. Chem.* **1978**, *17*, 474.

[25] Belli Dell'Amico, D.; Calderazzo, F.; Gingl, F.; Labella, L.; Strähle, J. *Gazz. Chim. Ital*. **1994**, *124*, 375.

[26] Belli Dell'Amico D.; Calderazzo, F.; Labella, L.; Maichle-Mössmer, C.; Strähle, J. *J. Chem. Soc., Chem. Commun.* **1994**, 1555.

[27] Belli Dell'Amico, D.; Bradicich, C.; Calderazzo, F.; Guarini, A.; Labella, L.; Marchetti, F.; Tomei, A. *Inorg. Chem.* **2002**, *41*, 2814.

[28] Belli Dell'Amico, D.; Boschi, D.; Calderazzo, F.; Ianelli, S.; Labella, L.; Marchetti, F.; Pelizzi, G.; Quadrelli, E. G. F. *Inorg. Chim. Acta* **2000**, *300*, 882.

[29] Belli Dell'Amico, D.; Calderazzo, F.; Costa, L.; Franchi, EE.; Gini, L.; Labella, L.; Marchetti, F. *J. Mol. Struct.* **2008**, *890*, 295.

[30] Belforte, A.; Belli Dell'Amico, D.; Calderazzo, F.; Devillers, M.; Englert, U. *Inorg. Chem.* **1993**, *32*, 2282.

[31] Belli Dell'Amico, D.; Calderazzo, F.; Giurlani, U.; Pelizzi, G. *Chem. Ber.* **1987**, *120*, 955.

[32] Bacchi, A.; Belli Dell'Amico, D.; Calderazzo, F.; Giurlani, U.; Pelizzi, G.; Rocchi, L. *Gazz. Chim. Ital.* **1992**, *122*, 429.

[33] Belli Dell'Amico, D.; Calderazzo, F.; Giovannitti, B.; Pelizzi, G. *J. Chem. Soc., Dalton Trans*. **1984**, 647.

[34] Belli Dell'Amico, D.; Dell'Innocenti, M.; Calderazzo, F. Unpublished results.

[35] Rocchi, L., Tesi di laurea, Universita` di Pisa, Pisa, Italy, 1988.

[36] (a) Belli Dell'Amico, D.; Calderazzo, F.; Giurlani, U. *Chem. Commun.* **1986**, 1000. (b) Belforte, A.; Belli Dell'Amico, D.; Calderazzo, F.; Giurlani, U.; Labella, L. *Gazz. Chim. Ital.* **1993**, *123*, 119.

[37] Petersen, U. *Kohlensäure-monoester, -diester bzw. -ester-Carbonsäure-Anhydride*. In Houben-Weil, *Methoden der Organischen Chemie*; Thieme, G. Verlag: Stuttgart, 1983, Vol. E4, p 64.

[38] Lawson, J. K.; Croom, J. A. T. *J. Org. Chem.* **1963**, *28*, 232.

[39] (a) Gross, H.; Bilk, L. *Angew. Chem.* **1967**, *79*, 532. (b) Shepard, K. L. *J. Chem. Soc., Chem. Commun.* **1971**, 928.

[40] Shepard, K. L.; Halczenko, W. *J. Heterocycl. Chem.* **1979**, *16*, 321.

[41] (a) Belforte, A.; Calderazzo, F. *J. Chem. Soc. Dalton Trans.* **1989**, 1007. (b) Belforte, A.; Belli Dell'Amico, D.; Calderazzo, F. *Chem. Ber*. **1988**, *121*, 1891.

[42] Anillo, A.; Belli Dell'Amico, D.; Calderazzo, F.; Nardelli, M.; Pelizzi, G.; Rocchi, L. *J. Chem. Soc., Dalton Trans.* **1991**, 2845.

[43] Calderazzo, F.; Pampaloni, G.; Sperrle, M.; Englert, U. *Z. Naturforsch.* **1992**, *47b*, 389.

[44] Abis, L.; Belli Dell'Amico, D.; Calderazzo, F.; Caminiti, R.; Garbassi, F.; Ianelli, S.; Pelizzi, G.; Robino, P.; Tomei, A. *J. Mol. Catal. A: Chem.* **1996**, *L113*, 108.

[45] Abis, L.; Belli Dell'Amico, D.; Busetto, C.; Calderazzo, F.; Caminiti, R.; Garbassi, F.; Tomei, A. *J. Mater. Chem.* **1998**, *8*, 2855.

[46] (a) Abis, L.; Belli Dell'Amico, D.; Busetto, C.; Calderazzo, F.; Caminiti, R.; Ciofi, C.; Garbassi, F.; Masciarelli, G. *J. Mater. Chem*. **1998**, *8*, 751.

[47] Abis, L.; Armelao, L.; Belli Dell'Amico, D.; Calderazzo, F.; Garbassi, F.; Merigo, A.; Quadrelli, E. A. *J. Chem. Soc., Dalton Trans.* **2001**, 2704.

[48] Belli Dell'Amico, D.; Bertagnolli, H.; Calderazzo, F.; D'Arienzo, M.; Gross, S.; Labella, L.; Rancan, M.; Scotti, R.; Smarsly, B. M.; Supplit, R.; Tondello, E.; Wendel, E. *Chem. Eur. J.* **2009**, *15*, 4931.

[49] Calucci, L.; Forte, C.; Pampaloni, G.; Pinzino, C.; Renili, F. *Inorg. Chim. Acta* **2010**, *363*, 33.

3 Homopolymerization of Ethylene

3.1 Introduction

In the research for more active new olefin polymerization catalysts, Group 4 transition metal complexes have been developed dramatically over the past decades. In this era, there is a continuing interest in the development of new Group 4 complexes based on non-cyclopentadienyl (non-Cp) ligands for α-olefin polymerization, which is supported by the search for new ligand frameworks that improve the understanding of structure-property relationships. A number of titanium and zirconium complexes based on different ligand types have been designed for ethylene/olefin polymerization.[1,2,3,4,5,6,7] Among these catalytic precursors, the titanium complexes bearing [*N,O*]- and/or [*O,O*]-type ligands have attracted considerable attention due to the their unique characteristics for olefin polymerization.[8,9,10] Some complexes based on bidentate [*O,O*] ligands have been shown to be active in ethylene polymerization. Flisak and Szczegot[11] studied the strength of co-ordinate bonds in titanium(IV) complexes with three different bidentate ligands of the type [*O,O*]: tetrahyrofurfurol, tetrahydrofurfuroxo anion, and ethylene glycol dimethylether and a complex with the monodentate ligand tetrahydrofuran. Moreover, these complexes present the highest catalytic activity in the ethylene polymerization, with a higher activity than those of the catalysts with bidentate ligands with chemically identical donor atoms.

In 1995, Schaverien and coworkers[12] published a study about a number of titanium and zirconium complexes with sterically hindered chelating phenoxide ligands as catalysts for the olefin polymerization.

Eisen and coworkers[13] also prepared various complexes of Group 4 metals with the ligand acetyl acetonate with different substituents **18-21** and tested for the polymerization of propylene in the presence of MAO. All the complexes were active and produced elastomeric polypropylene.

Titanium complexes based on maltolato and guaicolato ligands with an octahedral coordination **22-24** were synthesized by Sobota et al. and tested for ethylene polymerization.[14]In all complexes the titanium atoms were surrounded by four oxygen atoms from the chelating maltolato or guaicolato ligands and by two mutual *cis* chlorine or ethoxide groups.

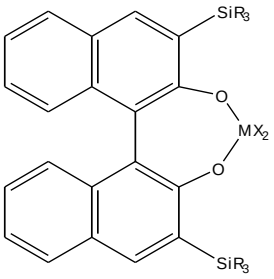

	SiR_3	MX_2
1	$SiMe_3$	$ZrCl_2$
2	$SiMe_2Ph$	$ZrCl_2$
3	$SiPh_3$	$ZrCl_2$
4	$SiMe_3$	$Ti(CH_2Ph)_2$
5	$SiMe_2Ph$	$Zr(CH_2Ph)_2$
6	$SiPh_3$	$ZrMe_2$
7	$SiPh_3$	$Ti(CH_2Ph)_2$
8	$SiPh_3$	$Zr(CH_2Ph)_2$
9	$SiPh_3$	$Zr(CH_2SiMe_3)_2$

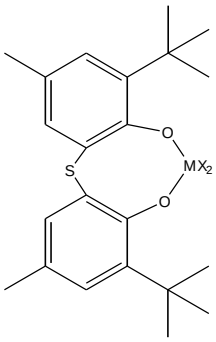

10: $TiCl_2$

11: $ZrCl_2$

12: $Ti(CH_2Ph)_2$

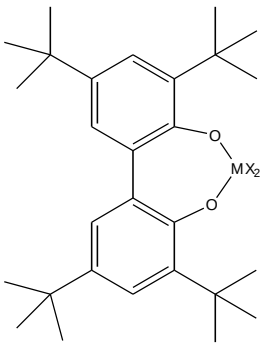

13: $Ti(CH_2Ph)_2$

14: $ZrCl_2(THF)_2$

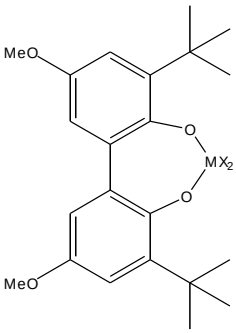

15: $Ti(CH_2Ph)_2$

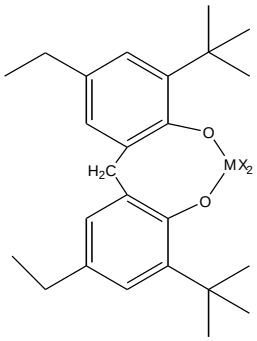

16: $Ti(CH_2Ph)_2$

17: $TiCl_2$

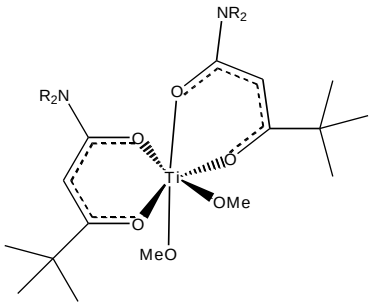

18: R = Et

19: R = Me

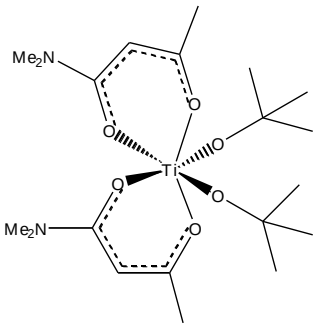

20

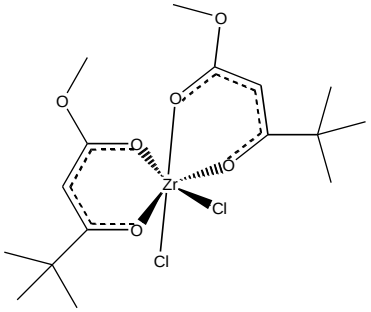

21

Galland[15] studied the behavior of bidentate zirconium complexes of maltol and naphtoquinone **26-27**. Both complexes were shown to be active in the ethylene polymerization producing high molecular weight polyethylene. In another study they synthesized $ZrCl_2(ethylpyrone)_2$ **28** and $ZrCl_2(methylpyrone)_2$ complexes[16] and investigated the catalytic activity of these complexes in ethylene polymerization in the presence of MAO, giving the best catalytic activities up to 310 $kg_{polymer}\ mol_{Zr}^{-1}\cdot h^{-1}\cdot atm^{-1}$

at 70 °C, Al/Zr = 2500. $ZrCl_2$(ethylpyrone)$_2$ showed a better performance in ethylene polymerization that the complex with a methyl group.

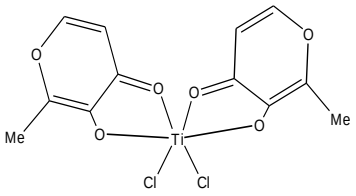

22

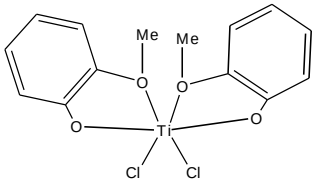

23

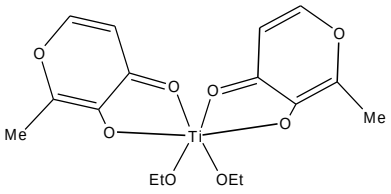

24

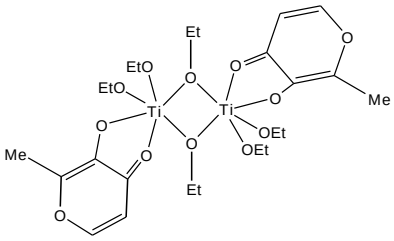

25

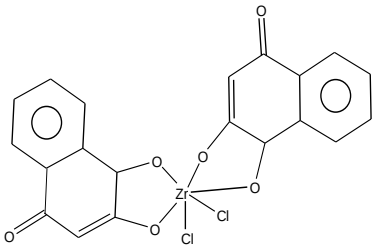

26

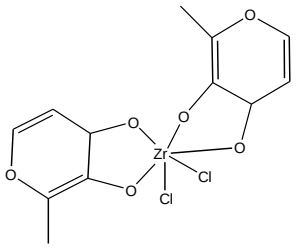

27

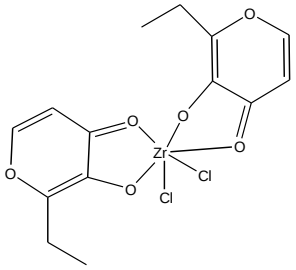

28

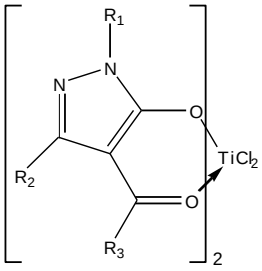

30: $R_1 = R_2 = Ph$, $R_3 = Me$
31: $R_1 = R_2 = R_3 = Ph$

Complexes of titanium(IV) bearing β-diketonato ligands containing pyrazolonate moiety **30**-**31** were synthesized by Repo and coworkers[17] and exhibited low activities for ethylene polymerizations, resulting in unimodal polyethylene with broad molecular weight distribution.

Development of metal complexes bearing *N*,*N*-dialkylcarbamate ligands is relatively recent in the scientific literature and some data on physical and chemical behaviour of them have been reported in the academic literature in the recent years, as mentioned in the previous chapter.[18] *N*,*N*-dialkylcarbamato complexes of titanium are an interesting group of catalyst precursors for a number of reasons: **1**) They are rather cheap catalytic precursors. **2**) They are easy to be synthesized. **3**) These precursors are scarcely toxic. **4**)

To the best of our knowledge, in the field of olefin polymerization catalysis, the behaviour of *N*,*N*-dialkylcarbamato metal complexes are almost unknown.

Recently, we described highly active norbornene ring-opening metathesis polymerization (ROMP) catalysts supported by *N*,*N*-dialkylcarbamato complexes of niobium.[19] These novel catalytic precursors, in the presence of methylaluminoxane (MAO) as a cocatalyst, catalyzed the ROMP of norbornene with the highest activity (29000 $kg_{polymer}\ mol_{Nb}^{-1} \cdot h^{-1}$) never reported up to now for niobium catalysts.

Our aim was to study the behavior of *N*,*N*-dialkylcarbamato complexes of titanium in α-olefin polymerization, and I will discuss the results on the ethylene homopolymerization in the present chapter. The aim is to find a correlation between the structure of the catalytic precursor and activity and to establish the main parameters affecting the activity of polymerization. The research started by utilizing three different titanium complexes based on *N*,*N*-dialkylcarbamato chelate ligands with the general formula of [$Ti(O_2CNR_2)_4$, R = Et (**I**), Me (**II**)] and [$Ti(O_2CNR_2)_2Cl_2$, R = Me (**III**)] (Chart 1) as pre-catalysts for the ethylene polymerization.

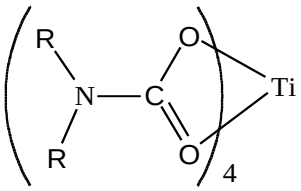

R= Et (**I**) & Me (**II**)

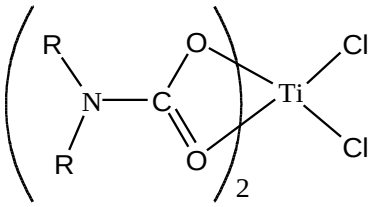

R= Me (**III**)

Chart 1.

3.2 Results and discussion

3.2.1 Synthesis of $TiCl_2(O_2CNMe_2)_2$

In order to compare the catalytic activity of homoleptic *N*,*N*-dialkylcarbamato titanium pre-catalysts with the corresponding partial chlorinated ones, we performed the synthesis of $TiCl_2(O_2CNMe_2)_2$. A first attempt to the synthesis of $TiCl_2(O_2CNMe_2)_2$, **III** starting from titanium(IV) chloride and $[NH_2Me_2][O_2CNMe_2]$, a commercial available ammonium salt, failed due to the almost complete insolubility of the product in the

reaction medium, which precludes its separation from the by-product (*i.e.* $[NH_2Me_2]Cl$) of the reaction.

$$TiCl_4 + [NH_2Me_2][O_2CNMe_2] \longrightarrow TiCl_2(O_2CNMe_2)_2 + 2[NH_2Me_2]Cl$$

Thus, the synthesis was performed with the metathetical reaction between 1 equivalent of $TiCl_4$ and 1 equivalent of $Ti(O_2CNMe_2)_4$.

$$TiCl_4 + Ti(O_2CNMe_2)_4 \longrightarrow 2TiCl_2(O_2CNMe_2)_2$$

An oily substance formed on mixing the reagents, which slowly converted into a bright yellow product after one day stirring at room temperature. Elemental analyses showed the presence of Ti, Cl, and CO_2 in the following ratio: 1.00/1.98/2.00, in agreement with the formula $TiCl_2(O_2CNMe_2)_2$. This latter was studied by IR spectroscopy in the solid state, and the spectrum showed the bands due to the C–H bonds at about 2900 cm^{-1}, and the characteristic bands of the carbamato group in the range 1572–1398 cm^{-1}. In particular, the absorptions at 1572 and 1479 cm^{-1} are typical of a bidentate carbamato ligand (asym ν_{CO2} and sym ν_{CO2} respectively).

Due to the scarce solubility of the complex $TiCl_2(O_2CNMe_2)_2$ in non coordinating common organic solvents (*i.e.* $CHCl_3$, CH_2Cl_2, toluene, CH_3CN), and the fact that such compound reacts with non-protic, polar solvents (*e.g. N,N*-dimethylformamide and dimethylsulphoxide) the NMR characterization has been obtained by CP/MAS ^{13}C NMR analysis: the spectrum exhibits the resonances of the methyl groups at $\delta = 36.1$ and 38.3 ppm and of the carbamic carbon at $\delta = 161.1$ ppm respectively.

Generally, two signals for the two alkyl *N*-substituents of the carbamato ligand are observed in the NMR spectrum of the *N,N*-dialkylcarbamato complexes in solution at low temperature (213 K), due to the diasterotopic character of the R groups. In the case of $TiCl_2(O_2CNMe_2)_2$ we might infer the same behavior for the two resonances at 36.1 and 38.3 ppm.

In consideration of the good effect of increasing the length of the alkyl chain on the solubility of metal carbamates[20], which might have an effect in the catalytic activity of the compound as well, an attempt was done to generate the mixed chlorocarbamato of titanium(IV), $TiCl_2(O_2CNEt_2)_2$. Unfortunately, the treatment of $TiCl_4$ with two

equivalents of $[NH_2Et_2][O_2CNEt_2]$ – generated *in situ* from CO_2 and $NHEt_2$ – failed due to the formation of mixtures of $TiCl_{4-n}(O_2CNEt_2)_n$ (n =1-3), according to the ^1H NMR spectroscopy. Analogous results have been obtained from the mixing of equimolar amounts of $TiCl_4$ and $Ti(O_2CNEt_2)_4$.

3.2.2 X-ray crystallography

In the course of this work fine crystals, suitable for an X-ray study, were obtained by recrystallization of $Ti(O_2CNMe_2)_4$ from a dichloromethane solution layered with pentane, at −30 °C. The crystal structure of $Ti(O_2CNMe_2)_4$ consists of discrete molecules separated by normal intermolecular contacts. Figure 1 shows a perspective ORTEP drawing of the molecule and whose bond lengths and angles are listed in Table 1. The central titanium atom is surrounded by the eight oxygen atoms of the four bidentate carbamato ligands, in a slightly distorted dodecahedral arrangement, whose short bite is mainly responsible for the distortion.

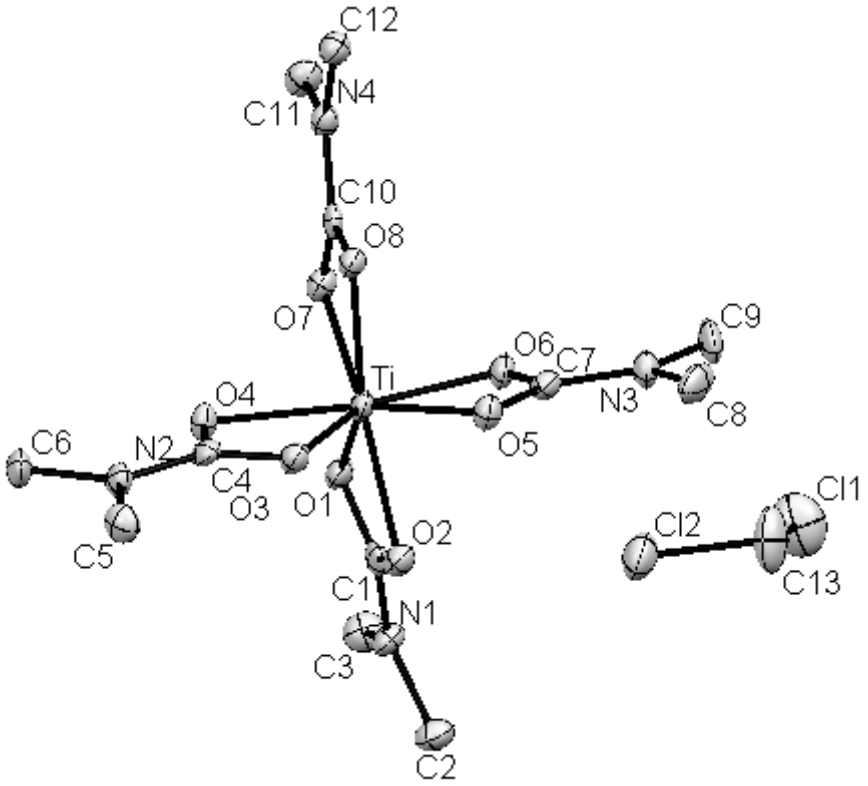

Figure 1. ORTEP diagram and numbering scheme in $Ti(O_2CNMe_2)_4.CH_2Cl_2$. The hydrogen atoms have been omitted for clarity. Thermal ellipsoids are drawn at the 50% probability level.

Table 1. Selected bond distances (Å) and angles (°) in $Ti(O_2CNMe_2)_4.CH_2Cl_2$ [estimated standard deviations (e.s.d.s) in parentheses refer to the least significant digit]

Ti—O(1)	2.098 (3)	C(1)—N(1)	1.332 (5)	C(4)—O(3)	1.277 (5)
Ti—O(2)	2.084 (3)	C(4)—N(2)	1.347 (5)	C(4)—O(4)	1.290 (5)
Ti—O(3)	2.102 (3)	C(7)—N(3)	1.338 (5)	C(7)—O(5)	1.284 (5)
Ti—O(4)	2.078 (3)	C(10)—N(4)	1.334 (5)	C(7)—O(6)	1.272 (5)
Ti—O(5)	2.108 (3)	C(1)—O(1)	1.289 (5)	C(10)—O(7)	1.275 (4)
Ti—O(6)	2.039 (3)	C(1)—O(2)	1.284 (5)	C(10)—O(8)	1.289 (5)
Ti—O(7)	2.084 (3)				
Ti—O(8)	2.062 (3)				
O(6)—Ti—O(8)	90.80 (11)	O(6)—Ti—O(1)	83.02 (11)	O(2)—Ti—O(3)	82.00 (10)
O(6)—Ti—O(4)	156.81 (11)	O(8)—Ti—O(1)	138.34 (11)	O(1)—Ti—O(3)	124.20 (11)
O(8)—Ti—O(4)	91.59 (11)	O(4)—Ti—O(1)	79.91 (11)	O(6)—Ti—O(5)	63.27 (11)
O(6)—Ti—O(7)	80.34 (11)	O(7)—Ti—O(1)	75.42 (10)	O(8)—Ti—O(5)	79.94 (10)
O(8)—Ti—O(7)	62.94 (11)	O(2)—Ti—O(1)	62.62 (10)	O(4)—Ti—O(5)	139.76 (11)
O(4)—Ti—O(7)	80.26 (11)	O(6)—Ti—O(3)	140.45 (11)	O(7)—Ti—O(5)	127.27 (11)
O(6)—Ti—O(2)	88.24 (11)	O(8)—Ti—O(3)	85.25 (10)	O(2)—Ti—O(5)	80.62 (11)
O(8)—Ti—O(2)	158.67 (11)	O(4)—Ti—O(3)	62.74 (11)	O(1)—Ti—O(5)	130.80 (11)
O(4)—Ti—O(2)	97.62 (11)	O(7)—Ti—O(3)	130.47 (10)	O(3)—Ti—O(5)	77.31 (11)
O(7)—Ti—O(2)	137.56 (11)				

This study allowed the comparison of the bonding parameters of the three titanium carbamates to be made: both the coordination geometry and the bond distances (Ti–O (mean value), 2.082(2) Å; C–N (mean value), 1.338(5) Å; C–O (mean value), 1.282(5) Å) and angles (O–Ti–O (mean value), 62.89(11)°; C–O–C (mean value), 115.77(3)°; O–C–N (mean value), 122.12(4)°) are similar to those found in $Ti(O_2CNEt_2)_4$ and $Ti(O_2CN^iPr_2)_4$.[21,22] The four carbamato ligands chelate the titanium atom in a somewhat asymmetric bidentate way, the differences between the Ti-O distances ranging from 0.02 to 0.07 Å, giving rise to planar four-membered OCOTi rings.

3.2.3 Ethylene polymerization

Blank ethylene polymerization experiments (entries 1-2, Table 2) were preliminarily performed by using either **I** without any co-catalyst or an organoaluminium compound alone, such as MAO. Under these conditions, no activity was observed, thus indicating

that the individual components of the catalytic system were not able to activate ethylene. Therefore, subsequent experiments were performed by using **I** in combination with a cocatalyst.

A preliminary experiment (entry 3; Table 3) was carried out at longer reaction time in order to gain an idea about the activity of polymerization. Because the ascertained catalytic activity was rather low, the successive reaction were carried out under different conditions, in terms of duration, MAO concentration, ethylene pressure and temperature (entries 4-11; Table 3).

Table 2. Homopolymerization of ethylene using either catalytic precursor or cocatalyst alone[a]

Entry	**I** (μmol)	Al/Ti (mol/mol)	Time (h)	Product (g)	Activity[b]	M_v (Da)	T_m (°C)	X_c (%)
1	30	-	5	0	-	-	-	-
2[c]	-	-	5	trace	-	-	-	-

[a] Reaction conditions: solvent = toluene; P_{C2H4} = 3 MPa; temperature = 25 °C; total volume = 65 mL; if not otherwise specified. [b] Activity expressed as $kg_{polymer}\ mol_{Ti}^{-1}\cdot h^{-1}$, [c] MAO = 15 mmol.

On the basis of the obtained results, the decrease of duration caused a remarkable improvement of the productivity up to 180 $kg_{polymer}\ mol_{Ti}^{-1}\cdot h^{-1}$ when duration was reduced (entry 4; Table 3). Indeed, when an Al/Ti molar ratio equal to 300 was adopted and duration was decreased to 15 min (entry 7; Table 3), a significant activity (560 $kg_{polymer}\ mol_{Ti}^{-1}\cdot h^{-1}$) was found.

Figure 2 represents the effect of polymerization time on the activity. Decreasing of activity at longer reaction times could be related to deactivation of the catalytic system during the polymerization.

Table 3. Homopolymerization of ethylene in the presence of **I**/MAO catalytic system[a]

Entry	**I** (μmol)	Al/Ti (mol/mol)	Time (h)	Product (g)	Activity[b]	M_v (Da)	T_m (°C)	X_c (%)	d (g/mL)	PDI
3	30	600	7	6.51	31	164,000	136.4	51.7	0.938	
4	30	600	1	5.40	180	372,000				
5	30	300	1	5.60	186	221,000	134.3	48.9	0.935	
6	30	300	0.5	4.69	313	246,000	134.7	47.7	0.934	
7	30	300	0.25	4.20	560	299,000	135.1	53.0	0.940	24.5[e]
8	30	150	0.25	0.32	42	311,000				
9	30	500	0.25	2.25	300	279,000	135.4	42.2	0.927	
10[c]	30	300	0.25	3.20	430	264,000	134.2	42.1	0.924	
11[d]	30	300	0.25	0.28	37	193,000				

[a] Reaction conditions: solvent = toluene; P_{C2H4} = 3 MPa; temperature = 25 °C; total volume = 65 mL; if not otherwise specified. [b] Activity expressed as $kg_{polymer}\ mol_{Ti}^{-1} \cdot h^{-1}$. [c] T= 60 °C. [d] P_{C2H4} = 0.1 MPa. [e] M_w = 408000; M_n = 16700.

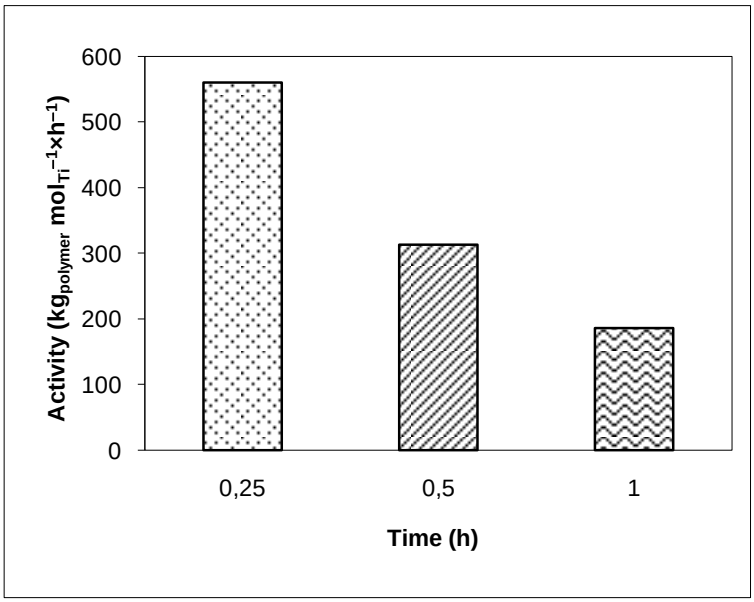

Figure 2. Catalysts' productivity in ethylene homo-polymerization as a function of the reaction time (**I**: 30 μmol, MAO/Ti: 300, P: 3 MPa, Solvent: toluene, total volume: 65 mL, T: 25 °C).

Figure 3 shows the dependence of the polymerization activity on the ratio of methyl-aluminoxane to the titanium based catalytic precursor **I**. It was observed that the polymerization activity reaches a maximum at a molar ratio of ca. 300:1. The increase

from 300 to1000 decreased the catalytic activity, suggesting that high amounts of MAO can compete with the olefin for the active site of the complex, decreasing the activity.[16,23] Another possibility could be related to the over reduction of titanium in the presence of excess of MAO which results in dropping the polymerization activity down.

Increasing the cocatalyst/catalyst ratio leads to a marked decrease of the molecular weight relatively, as shown in Figure 4. One of the main reason for this effect can be the dominant chain transfer reactions to the methyl aluminoxane.[24]

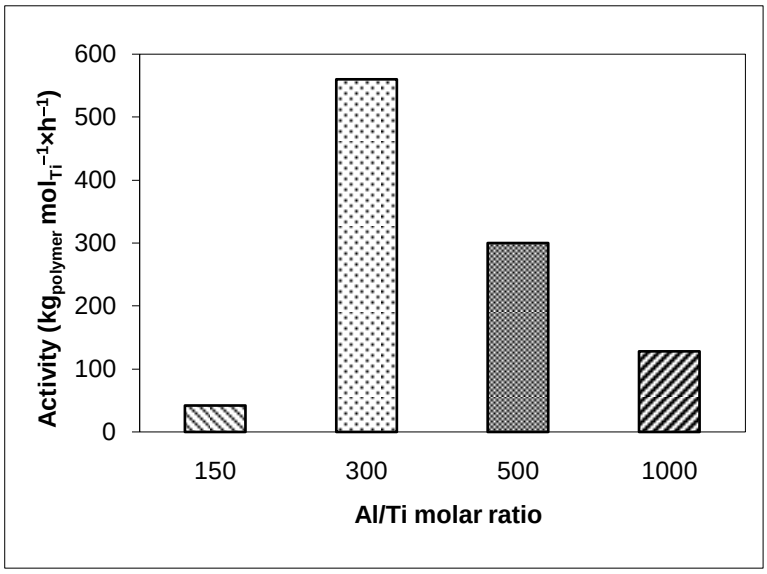

Figure 3. Productivity of the catalyst **I**/MAO versus Al/Ti molar ratio in ethylene homo-polymerization. (**I**: 30 μmol, P: 3 MPa, Solvent: toluene, total volume: 65 mL, t: 15 min, T: 25 °C).

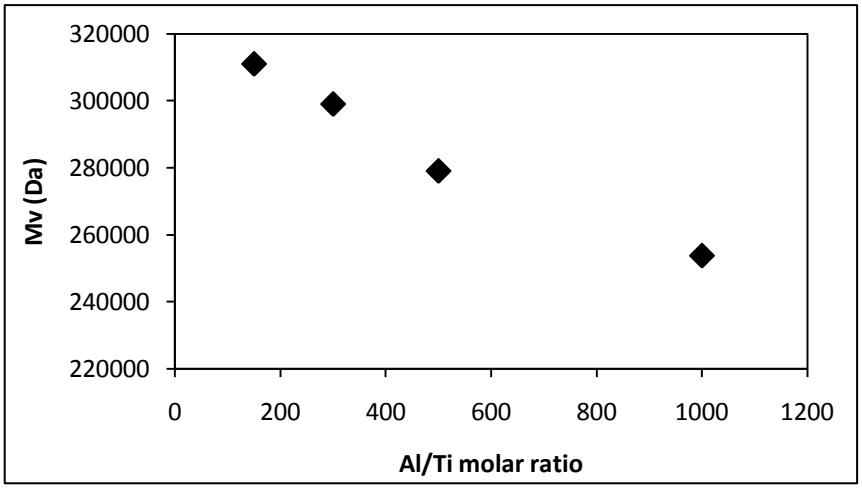

Figure 4. Influence of Al/Ti molar ratio on molecular weight.

The reaction temperature also significantly influenced the catalytic activities and the molecular weights of the resultant polymers (see entries 7 and 10). Both the catalytic activity of complex **I** and molecular weight of resultant polymer decreased with the reaction temperature from 560 $kg_{polymer}$ $mol_{Ti}^{-1}{\cdot}h^{-1}$ and 299,000 Da at 25 °C to 430 $kg_{polymer}$ $mol_{Ti}^{-1}{\cdot}h^{-1}$ and 264,000 Da, at 60 °C, respectively. This suggests that at higher temperatures the active catalytic sites are characterized by a higher rates of catalyst deactivation, generally speaking, post-metallocenes are apt to rapidly lose their polymerization activity at higher temperatures.[25] Moreover, the solubility of ethylene in toluene decreases with increasing of temperature. This causes a lowering of ethylene concentration in the polymerization system.[26]

The lower molecular weight products obtained at elevated temperatures can be reasonably ascribed to the higher chain-transfer rates.

Ethylene pressure was found to have a dramatic effect on catalyst activity. When the ethylene pressure decreases from 3 to 0.1 MPa, the productivity fell off remarkably from 560 to 37 $kg_{polymer}$ $mol_{Ti}^{-1}{\cdot}h^{-1}$.

The activity of new systems was compared with that of $TiCl_4$ (entries 12 and 13, Table 4) under the same conditions as in entries 5 and 7. $TiCl_4$ does form an active polymerization catalyst when combined with MAO, but a lower activity to give a lower crystallinity degree (37%) was observed. It was suggested that the interaction between metal centers and ligands played an important role in formation and stabilization of the active catalytic sites, thus affording the higher activity.[27,28]

Table 4. Homopolymerization of ethylene by using $TiCl_4$/MAO catalytic system[a]

Entry	$TiCl_4$ (μmol)	Al/Ti (mol/mol)	Time (h)	Product (g)	Activity[b]	M_v (Da)	T_m (°C)	X_c (%)
12	30	300	1	2.85	95	332,000	134.7	39
13	30	300	0.25	0.45	60	298,000	134.0	37

[a] Reaction conditions: solvent = toluene; P_{C2H4} = 3 MPa; temperature = 25 °C; total volume = 65 mL; if not otherwise specified. [b] Activity expressed as $kg_{polymer}$ $mol_{Ti}^{-1}{\cdot}h^{-1}$.

In order to observe how the solvent influences the activity of the new systems, we decided to increase the polarity of the reaction medium by changing the solvent from toluene ($\varepsilon = 2.38$) to chlorobenzene ($\varepsilon = 5.67$)[29] in view of the interesting results obtained

in the polymerization of olefins with niobium carbamates.[19,30] As a matter of fact, we observed a large increase of activity by working in this solvent (Table 5). A maximum polymerization activity was reached to 1443 $kg_{polymer}$ $mol_{Ti}^{-1} \cdot h^{-1}$ by using complex **I**/MAO catalytic system. This large effect on the activity may be rationalized on considering that the interactions between a ion pair and a polar solvent (such as chlorobenzene) are stronger than those with a low polarity medium such as toluene. We can suppose that in the case of chlorobenzene the interaction solvent/ion pair is sufficient to stabilize the latter but it is not too tight in order to prevent the attack of the incoming monomer to the active species.[31] Forlini *et al.*[32] reported that the dielectric constant of solvent could alter the polymerization behavior in other catalytic systems.

Table 5. Ethylene homopolymerization by **I**/MAO catalytic system in chlorobenzene[a]

Entry	**I** (μmol)	Al/Ti (mol/mol)	P_{C2H5} (MPa)	Time (h)	Product (g)	Activity[b]	M_v (Da)	PDI
14	30	300	3	0.25	5.51	735	139,000	n.d.
15	17	300	5	0.25	6.13	1443	165,000	18.9[c]

[a] Reaction conditions: T = 25 °C; total volume = 65 mL. [b] Activity expressed as $kg_{polymer}$ $mol_{Ti}^{-1} \cdot h^{-1}$. [c] M_w = 256000; M_n = 13500.

The FT-IR spectrum of polymeric samples (Figure 5) displays the typical bands corresponding to high density polyethylene at 2915 and 2848 cm^{-1}, which can be assigned to C-H stretching of the $–CH_2$ and $–CH_3$ groups. At about 1469 cm^{-1} there is a band corresponding to the $–CH_2$ group bending, and at 718 cm^{-1} another band is verified, which corresponds to the $(-CH_2-CH_2-)_n$ rocking group, with n>3.[33]

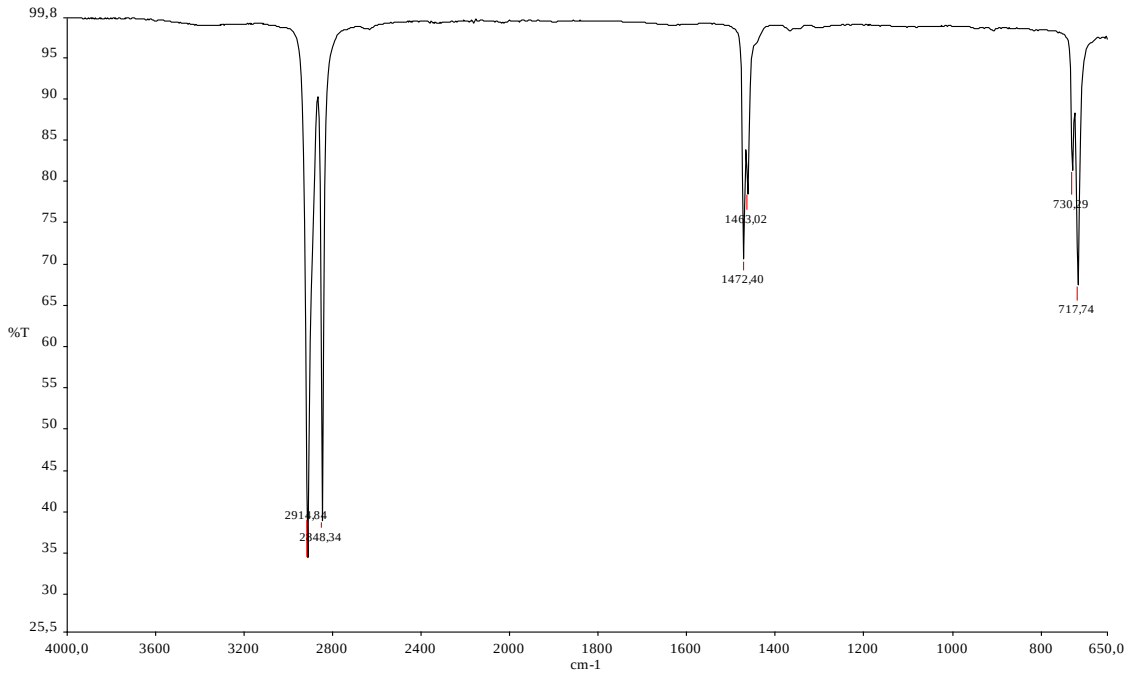

Figure 5. FTIR spectrum of polyethylene (Entry 5).

Analysis of some polymer samples by SEC (Figures 6 and 7) revealed in any case relatively high molecular weights with broad polydispersities and multimodal molecular weight distribution, an indication of a non-single site catalyst nature.

The broad polydispersity and multimodality of the polymers could be ascribed to the highly fluxional character of the precatalyst. A similar behaviour was previously observed for a zirconium complex bearing phenoxy-imine ligand, which, as a consequence of the unusual C_1 symmetric geometry was highly fluxional in solution and produced bi- and trimodal poly(ethylene)s.[34] However, it is worth mentioning that ligand redistribution could also occur during the formation of active catalytic species and/or during the polymerization process, giving rise to additional polymerization species that could cause the multimodality of molecular weight distribution as previously observed by Kempe for bis(aminopyridinato)zirconium(IV) complexes[35] and by Scott for iminophosphonamide zirconium complexes.[36]

The melting points (T_m) of the resulting poly(ethylene)s were determined by DSC analysis. The melting point ranges between 134 and 137 °C, typical of high density polyethylene (Figure 8), for different catalytic conditions. It is noteworthy that under these conditions no oligomeric products were formed.

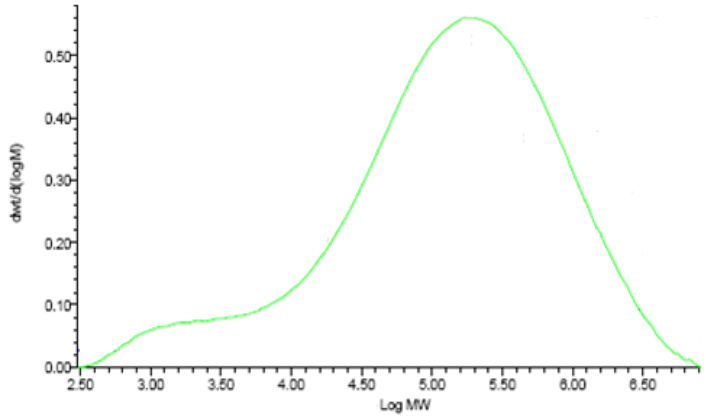

Figure 6. SEC curve of the polyethylene prepared with **I**/MAO (entry 7).

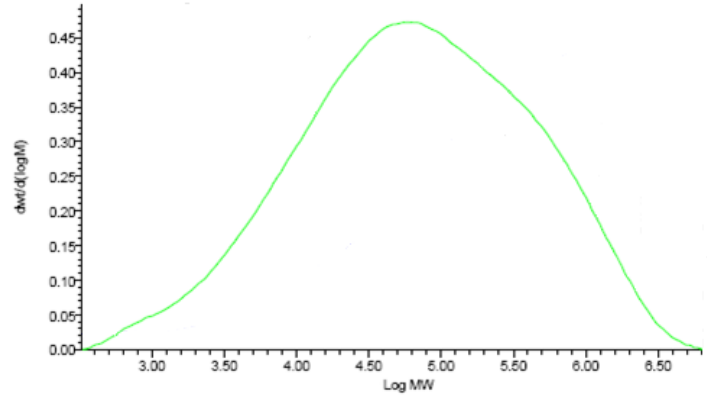

Figure 7. SEC curve of the polyethylene prepared with **I**/MAO (entry 15).

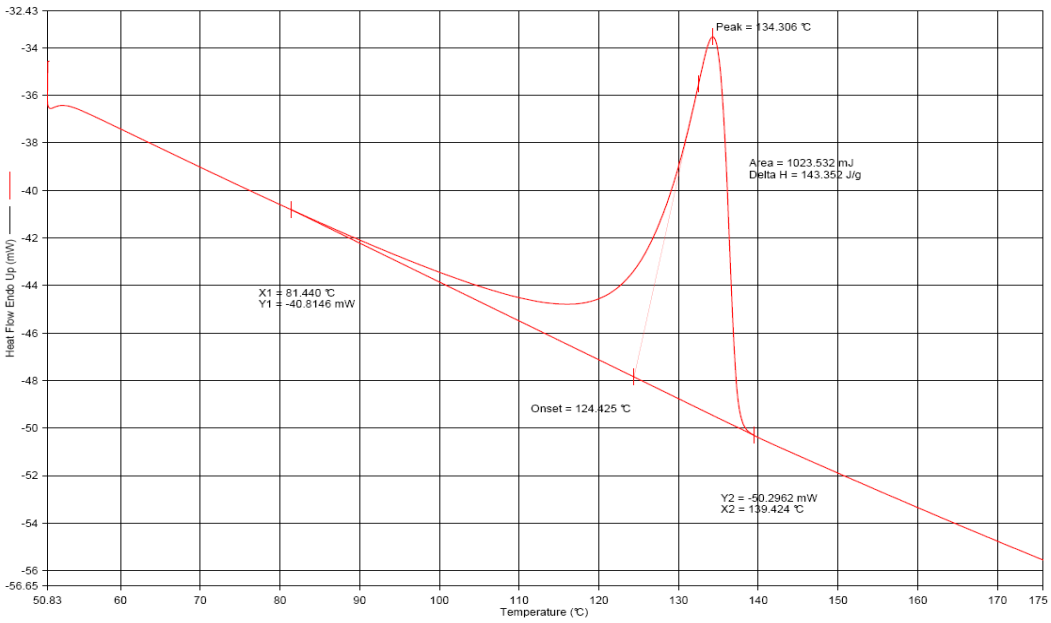

Figure 8. Typical DSC scan for the polyethylene product obtained from entry 5.

When **I** was replaced by **II** in combination with MAO (entry 16, Table 6) a moderate productivity was observed, that is significantly lower than that obtained by precursor **I** under the same condition. The activity decrease can be attributed to the lower solubility of complex **II** in toluene, subsequently decreasing the amount of complex in homogeneous phase which can be activated by MAO to form catalytic active species. Analogously to what we observed for the **I**/MAO system, the decrease of the reaction time up to 15 min caused a significant increase of the activity of 283 $kg_{polymer}\ mol_{Ti}^{-1}\cdot h^{-1}$.

Analogously to the polymerization tests using **I** as precursor, a remarkable improvement of the productivity [450 $kg_{polymer}\ mol_{Ti}^{-1}\cdot h^{-1}$] was ascertained when chlorobenzene used as a reaction medium.

Although the increase of activity may be referred to the increased solubility of catalytic precursor $Ti(O_2CNMe_2)_4$ in chlorobenzene, followed by increasing of number of active catalytic species in the reaction medium, however, the molecular weight of the resulting PE samples did not show appreciable change in the transition from toluene to chlorobenzene, suggesting that the growth mechanism of polymer chains is not affected by changing the reaction medium.

Table 6. Homopolymerization of ethylene catalyzed by titanium carbamato precursor **II** activated by MAO[a]

Entry	**II** (μmol)	Al/Ti (mol/mol)	Time (h)	Solvent	Product (g)	Activity[b]	M_v (Da)	T_m[c] (°C)
16	30	600	1	Toluene	1.98	66	252,000	n.d.
17	30	600	0.25	Toluene	2.12	283	243,000	134.7
18	30	600	0.25	CB	3.38	450	180,000	133.5

[a] Reaction conditions: P_{C2H4} = 3 MPa; temperature = 25 °C; total volume = 65 mL; if not otherwise specified. [b] Activity expressed as $kg_{polymer}\ mol_{Ti}^{-1}\cdot h^{-1}$. [c] Melting temperature determined by DSC.

The mixed chlorocarbamato species chloro-substituted chelate **III** is less efficient as promoter of the ethylene polymerization(entries 19-21, Table 7), a lower productivity was obtained in comparison with the catalyst based on **I** under similar conditions in toluene as reaction medium (compare entries 7 and 19). We believe that the reduced catalytic activity of $TiCl_2(O_2CNMe_2)_2$ is mainly due to the lower solubility of the complex **III** in toluene in contrast to **I**, which is massively soluble in that solvent.

The activity of complex **III** reaches a maximum, in toluene as reaction medium, when the Al/Ti ratio was 300 (compare entries 19 and 21). This effect is most probably enhanced by the known deactivation of catalysts in the presence of high amounts of MAO.[37] It is important to point out that high activities are reached with relatively small amounts of MAO in contrast to metallocenes or other Ziegler-Natta type systems.[38] Also the molecular weight of the polyethylene proved to be sensitive to the Al/Ti ratio and increased with the decrease of the Al/Ti ratio (entries 19 and 21), suggesting that there existed chain transfers to aluminum compounds in the olefin polymerization. Reduction of average molecular weight of the PE may be also referred to favoring the ligand exchange reactions between the titanium and the aluminium species at higher Al/Ti ratios during the polymerization, wherein the new species are not active in polymerization.[31]

Similar to what we observed in the case of precursors **I** and **II**, using polar solvents such as chlorobenzene caused a remarkable increase of the productivity of polymerization (see entries 22-24), suggesting the key role of solvent polarity in improving the catalytic performance of this class of polymerization precursors.

Table 7. Homopolymerization of ethylene catalyzed by **III**/MAO.[a]

Entry	**III** (μmol)	Al/Ti (mol/mol)	solvent	Product (g)	Activity[b]	M_v (Da)	T_m (°C)	X_c (%)	PDI
19	30	300	Toluene	2.18	291	480,000			
20	15	300	Toluene	0.27	73	590,500	133.6	45	
21	25	600	Toluene	1.09	174	350,300			
22	25	600	CB[c]	4.52	723	310,000	134.7	45	
23	15	300	CB[c]	2.98	795	330,600	135.4	49	
24[d]	15	300	CB[c]	5.21	1390	550,000	134.7	48	13.5[f]
25[e]	15	300	Toluene	0.01	3	n.d			
26[e]	15	300	CB[c]	0.18	48	n.d	134.1	55	

[a] Reaction conditions: solvent = toluene; P_{C2H4} = 3 MPa; temperature = 25 °C; total volume = 65 mL; time = 15 min. if not otherwise specified. [b] Activity expressed as $kg_{polymer}\ mol_{Ti}^{-1}\cdot h^{-1}$. [c] CB: Chlorobenzene. [d] P_{C2H4} = 5 MPa. [e] P_{C2H4} = 0.1 MPa. [f] M_w = 672000; M_n = 49700.

Lower amount of metal precursor in the system, slightly increased the productivity up to 795 $kg_{polymer}\ mol_{Ti}^{-1}\cdot h^{-1}$, assuming that an ion pair of titanium cation and MAO counterion preferably dissociates at lower concentrations, thus leading to higher activities as it is observed when going to a solvent with higher polarity.[39]

When the experiment was repeated (entry 24, Table 7) at a higher ethylene pressure (5 MPa), an enhancement in both the catalyst activity and molecular weight of the resulting PE was observed and it reached to 1390 $kg_{polymer}$ $mol_{Ti}^{-1} \cdot h^{-1}$ and 550,000 Da, respectively. As shown in Figure 9, productivity in the homopolymerization increases linearly with the pressure.

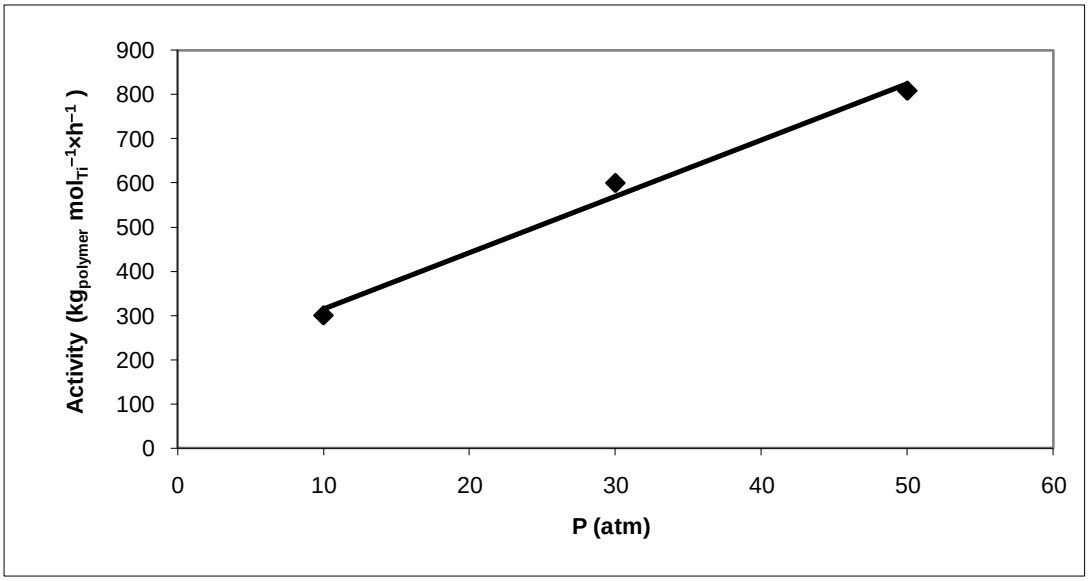

Figure 9. Activity of polymerization as a function of the total pressure in the reactor (**III** = 10 μmol; Al/Ti = 300/1; time = 15 min.; solvent = chlorobenzene; T = 50 °C; total volume = 65 mL)

As shown in Figure 10, the melting point (T_m) of the polymers obtained by complex **II** and **III** is higher than 133 °C, which is the classical T_m for HDPE (high-density polyethylene), and crystallinity degree equal to ~ 50%, as determined by DSC measurements.[7]

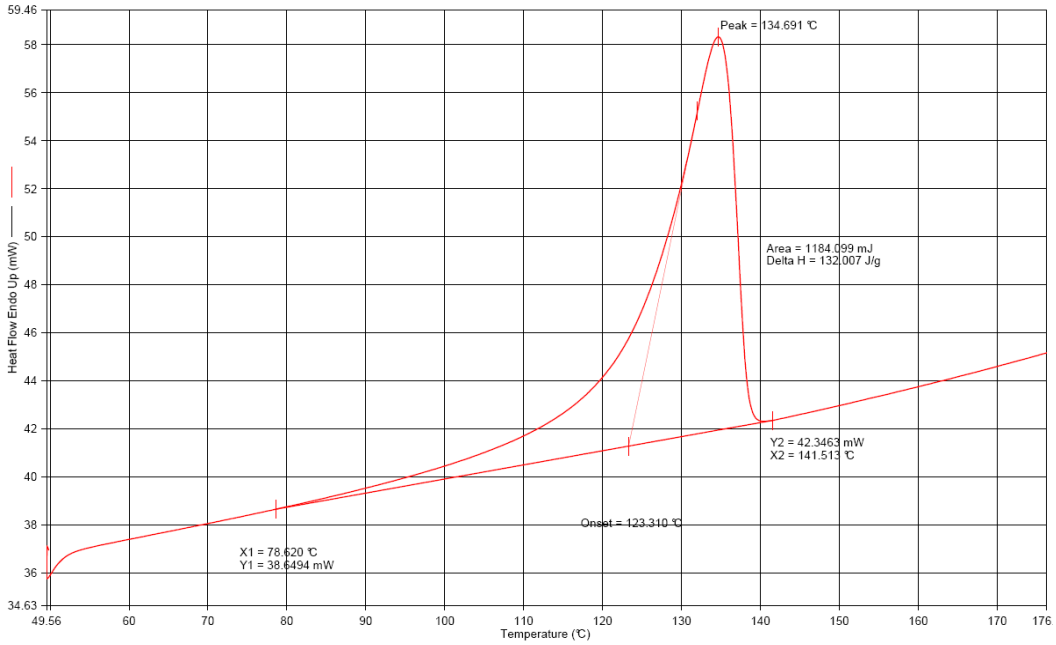

Figure 10. Typical DSC scan for the polyethylene product obtained from entry 22.

The typical bands corresponding to high density polyethylene are detectable, for PE samples obtained by the catalyst based on **II** or **III**, in FTIR spectroscopy. Figure 11 represents the FTIR spectra of PE sample obtained from entry 22.

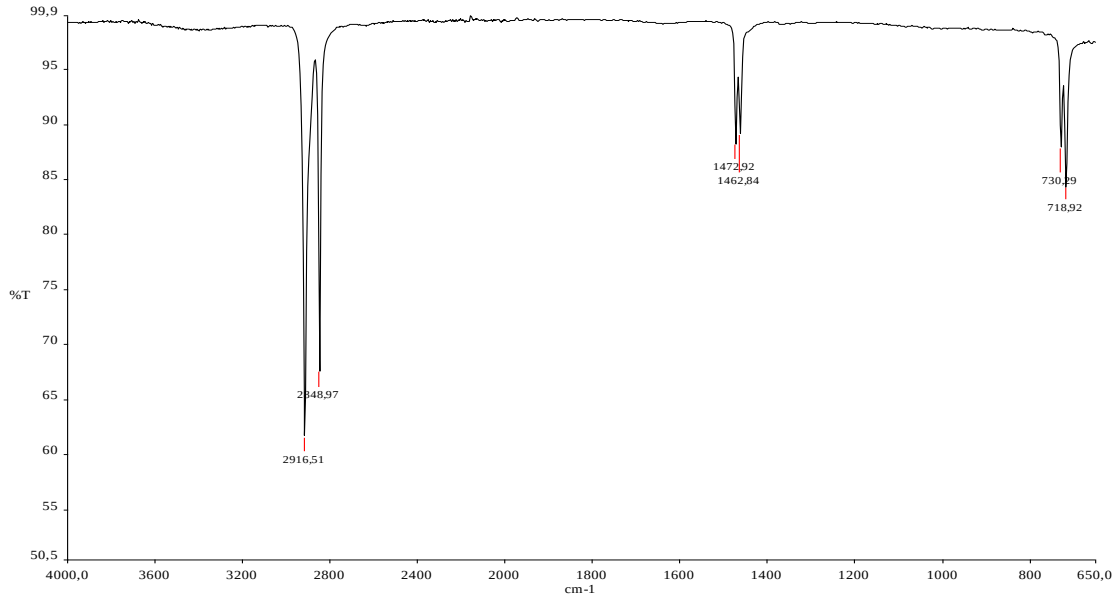

Figure 11. FTIR spectrum of polyethylene (entry 22).

Molecular weights distribution (M_w/M_n) data obtained by SEC analysis (Figure 12) showed that complex **III** afforded poly(ethylene)s with broad values and in some cases bimodal, indicating formation of more than one active species and/or the changing nature of the active species during the course of polymerization.

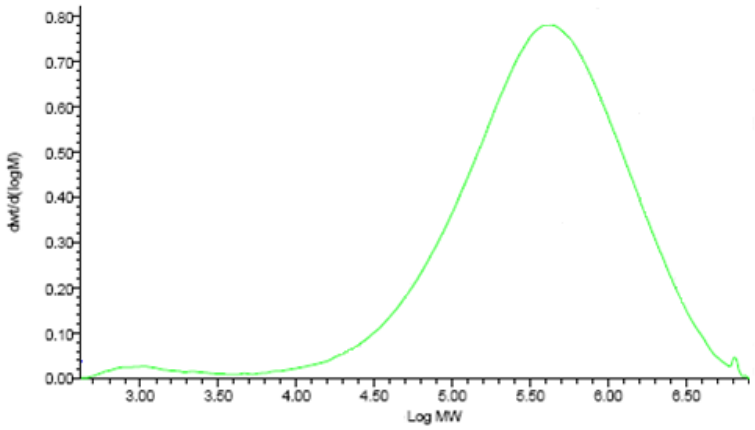

Figure 12. SEC curve of the polyethylene prepared with **III**/MAO (entry 24).

Some of the PE samples prepared by different catalytic systems were characterized by ^{13}C NMR spectroscopy in order to make clear the structure and existence of probable branches. The branch content in polyethylene was estimated from ^{13}C CPMAS NMR spectra[40] on the basis of the relative intensities of the methylene peak at 30 ppm and the peaks in the region between 8 and 20 ppm arising from all methyl carbons,[41,42] obtaining 2.5 ± 0.5 and 3.2±0.5 CH_3 every 1000 main chain carbons for the samples obtained from entries 15 and 24, respectively. As an example the ^{13}C CPMAS NMR spectra of a PE sample, obtained by the catalyst **I** (entry 15), is reported in Figure 13. This result was also consistent with the DSC and FTIR analyses.

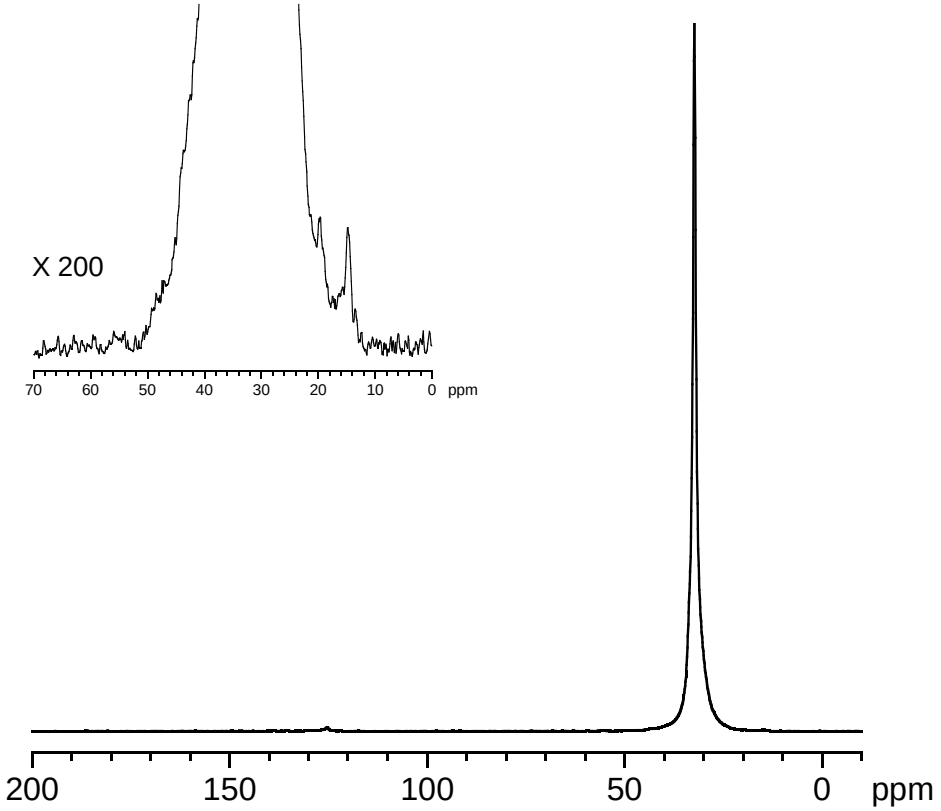

Figure 13. ^{13}C-CPMAS spectrum of polyethylene (obtained from entry 15). The insert corresponds to a 200-fold expansion which highlights the peak at ~14.4 ppm ascribable to methyl carbons of branches $C_{n\geq3}$ and the peak at ~19.5 ppm ascribable to methyl branches.

3.3 Conclusion

A series of titanium(IV) complexes based on *N*,*N*-dialkylcarbamato ligands have been synthesized and characterized. In the presence of MAO, these complexes exhibited good catalytic activity, affording high-density polyethylenes with broad molecular weight distribution. Catalyst activity and the molecular weights of polymers can be controlled over a wide range by the variation of precatalyst structure and the reaction parameters such as Al/Ti molar ratio and polymerization temperature. The branch content of selected PE samples, determined by ^{13}C NMR spectroscopy, showed 2.5-3.2 CH_3 every 1000 main chain carbons.

3.4 References

[1] Wang, C.; Ma, Z.; Sun, X. –L.; Gao, Y.; Guo, Y. –H.; Tang, Y.; Shi, L. –P. *Organometallics* **2006,** *25,* 3259.

[2] Michiue, K.; Jordan, R. F. *J. Mol. Catal. A: Chem.* **2008**, *282*, 107.

[3] Marquet, N.; Kirillov, E.; Roisnel, T.; Razavi, A.; Carpentier, J-F. *Organometallics* **2009**, *28,* 606.

[4] Elo, P.; Parssinen, A.; Nieger, M.; Leskela, M.; Repo, T. *J. Organomet. Chem.* **2009**, *694*, 2927.

[5] Hsiao, T. –J.; Tsai, J. –C. *J. Appl. Polym. Sci.* **2010**, *116*, 2040.

[6] Pärssinen, A.; Luhtanen, T.; Pakkanen, T.; Leskelä, M.; Repo, T. *Eur. J. Inorg. Chem.* **2010**, 266.

[7] Carlini, C.; D'Alessio, A.; Giaiacopi, S.; Po, R.; Pracella, M.; Raspolli Galletti, A. M.; Sbrana, G. *Polymer* **2007**, *48*, 1185.

[8] Domski, G. J.; Rose, J. M.; Coates, G. W.; Bolig, A. D.; Brookhart, M. *Prog. Polym. Sci.* **2007**, *32*, 30.

[9] Nakayama, Y.; Kawai, K.; Fujita, T. *J. Jpn. Petrol. Inst.* **2010**, *53*, 111.

[10] Bryliakov, K. P. *Russ. Chem. Rev.* **2007**, *76*, 253.

[11] Flisak, Z.; Szczegot, K. *J. Mol. Catal. A: Chem.* **2003**, *206*, 429.

[12] Linden, A.; Schaverien, C. J.; Meijboom, N.; Ganter, C.; Orpen, A. G. *J. Am. Chem. Soc.* **1995**, *117*, 3008.

[13] Gornshtein, F.; Kapon, M.; Botoshansky, M.; Eisen, M. S. *Organometallics* **2007**, *26*, 497.

[14] Sobota, P.; Przybylak, K.; Utko, J.; Jerzykiewicz, L. B.; Pombeiro, A. J. L.;; Silva, M. F. G.; Szczegot, K. *Chem. Eur. J.* **2001**, *7*, 951.

[15] Carone, C.; Lima, V.; Albuquerque, F.; Nunes, P.; Lemos, C.; Santos, J. H. Z.; Galland, G. B.; Stedile, F. C.; Einloft, S.; DE S. Basso, N. R. *J. Mol. Catal. A: Chem.* **2004**, *208,* 285.

[16] DE C. Fim, F.; Machado, T.; DE Sá, D. S.; Livotto, P. R.; DA Rocha, Z. N.; DE S. Basso, N. R.; Galland, G. B. *J. Polym. Sci. Part A: Polym. Chem.* **2008**, *46*, 3830.

[17] Elo, P.; Pärssinen, A.; Rautiainen, S.; Nieger, M.; Leskelä, M.; Repo, T. *J. Organomet. Chem.* **2010**, *695*, 11.

[18] See all references in Chapter 2.

[19] Raspolli Galletti A. M.; Pampaloni G; D'Alessio A; Patil Y; Renili F; Giaiacopi S; *Macromol. Rapid Commun.* **2009**, *30*, 1762.

[20] Belli Dell'Amico, D.; Calderazzo, F.; Labella, L.; Marchetti, F.; Pampaloni, G. *Chem. Rev.* **2003**, *103*, 3857.

[21] Straessler, N. A.; Caudle, M. T.; Groy, T. L. *Acta Cryst.* **2008**, *E64*, m48.

[22] Belli Dell'Amico, D.; Calderazzo, F.; Ianelli, S.; Labella, L.; Marchetti, F.; Pelizzi, G. *J. Chem. Soc. Dalton Trans.* **2000**, 4339.

[23] Covoet, D.; Cramail, H.; Deffieux, A.; *Macromol. Chem. Phys.* **1999**, *200*, 1208.

[24] Small, B. L.; Brookhart, M.; Bennett, A. M. A. *J. Am. Chem. Soc.* **1998**, *120*, 4049.

[25] Matsui, S.; Fujita, T. *Catalysis Today* **2001**, *66*, 63.

[26] Atigullah, M.; Hammawa, H.; Hamid, H. *Eur. Polym. J.* **1998**, *34*, 1511.

[27] Pennington, D. A.; Hughes, D. L.; Bochmann, M.; Lancaster, S. J. *Dalton Trans.* **2003**, 3480.

[28] Yi, J. J.; Zhao, W.; Jing, Z. H. *Chin. Chem. Lett.* **2005**, *16*, 1386.

[29] Landolt-Börnstein, Zahlenwerte und Funktionen aus Physik, Chemie, Astronomie, Geophysik und Technik, 6th Ed., Vol. 2, Springer Verlag / Berlin, Göttingen, Heidelberg, 1959.

[30] Marchetti, F.; Pampaloni, F.; Patil, Y.; Raspolli Galletti, A. M.; Renili, F.; Zacchini, S. *Submitted to Organometallics*.

[31].Volkis, V.; Shmulinson, M.; Averbuj, C.; Lisovskii, A.; Edelmann, F. T.; Eisen, M. S. *Organometallics* **1998**, *17*, 3155.

[32] (a) Forlini, F.; Tritto, I.; Locatelli, P.; Sacchi, M. C.; Piemontesi, F.; *Macromol. Chem. Phys.* **2000**, *201*, 401. (b) Forlini, F.; Princi, E.; Tritto, I.; Sacchi, M. C.; Piemontesi, F.; *Macromol. Chem. Phys.* **2002**, *203*, 645.

[33] Dominguez, A. M.; Zarate, A.; Quijada, R.; Lopez, T. *J. Mol. Catal. A: Chem.* **2004**, *207*, 155.

[34] Mitani, M.; Furuyama, R.; Mohri, J.; Saito, J.; Ishii, S.; Terao, H.; Kashiwa, N.; Fujita, T. *J. Am. Chem. Soc.* **2002**, *124*, 7888.

[35] Kretschmer, W. P.; Hessen, B.; Noor, A.; Scott, N. M.; Kempe, R. *J. Organomet. Chem.* **2007**, *692*, 4569.

[36] Tomaszewski, R.; Vollmerhaus, R.; Al-Humydi, A.; Wang, Q.; Taylor, N. J.; Scott, C. *Can. J. Chem.* **2006**, *84*, 214.

[37] Brinzinger, H. H.; Fischer, D.; Mülhaupt, R.; Rieger, B.; Waymouth, R. M. *Angew. Chem., Int. Ed.* **1995**, *34*, 1143.

[38] Alt, H. G.; Köppl, A. *Chem. Re*v. **2000**, *100*, *1205.*

[39] Longo, P.; Oliva, L.; Grassi, A.; Pellecchia, C. *Makromol. Chem.* **1989**, *190*, 2357.

[40] Pollard, M.; Klimke, K.; Graf, R.; Spiess, H. W.; Wilhelm, M.; Sperber, O.; Piel, C.; Kaminsky, W. *Macromolecules* **2004**, *37*, 813.

[41] Randall, J. C. *J. Polym. Sci., Polym. Phys. Ed*. **1973**, *11*, 275.

[42] Usami, T.; Takayama, S. *Macromolecules*, **1984**, *17*, 1756.

4 Homopolymerization of Propylene

4.1 Introduction

Polymers are among the most important commodity chemicals and are produced in quantities of hundreds of billions of pounds per year.[1] The last half-century has seen impressive developments in olefin polymerization catalysis (Table 1), particularly in the ability to adjust the polymer's architecture, and hence its physical properties, by controlling the structure of the catalyst.[2] It is now possible to rationally design appropriate catalysts to control polymer features such as tacticity and level of comonomer incorporation and, to a lesser extent, molecular weight. Whereas early transition metal metallocene complexes are the most important and best understood structures for olefin polymerization,[3,4] non-metallocene frameworks have recently emerged as versatile alternatives.[5,6,7]

Table 1. World production of polyolefins.[a8]

Year	LDPE	LLDPE	HDPE	PP	Total
1983	11.3	1.2	6.4	6.4	25.6
1990	14.0	4.0	11.4	12.6	42.7
1995	14.4	7.8	14.3	17.1	53.6
2001	15.8	15.2	20.9	27.7	79.6
2005	18.5	18.5	29.0	37.0	103.5
2010	19.5	19.5	37.0	50.0	126.0

[a] In million tons.

Complexes based on iron, cobalt, nickel, and palladium have been shown to polymerize and oligomerize olefins with good activities, sometimes in a living fashion.[9] In the area of early metal polymerization catalysis, frameworks displaying only one or no cyclopentadienyl ligand have been developed. Various multidentate ligands have been utilized as supporting architectures for olefin polymerization catalysts. In this context, there is increased interest in generating polymers with controlled tacticity through the use of non-metallocene catalysts.[5,7]

Promising advances have been made in both the development of single site living polymerization catalysts and the design of ancillary ligands that have the appropriate symmetry for polymer tacticity control.[7] While fundamental understanding of the factors responsible for tacticity control generally still lags behind that for metallocene systems, the area of non-metallocene olefin polymerization catalysis offers the potential for simpler catalyst synthesis and modification, improved activities, and the possibility of producing new polymer architectures.

Titanium complexes with phenoxyimine ligands **1**-**3** catalyze living polymerization of propylene.[10,11] The ligand with C_6F_5 group at the coordinating nitrogen and bulky ^{t}Bu or $SiMe_3$ substituent at the phenoxy group provide the catalyst for living syndiotactic polymerization.[12,13] Chain-end control in 2,1-insertion of the monomer, *via* smooth site-inversion, results in the syndiotactic polymer, in spite of apparent C_2-symmetric structure of the catalyst.[14] On the other hand, titanium complexes with phenoxyketimine ligand **4**,[15] which do not cause smooth site-inversion, or zirconium and hafnium complexes with phenoxyimine ligands,[16] where propylene undergoes 1,2-insertion, afford isotactic polymer as a result of the catalytic site control in the chain growth.

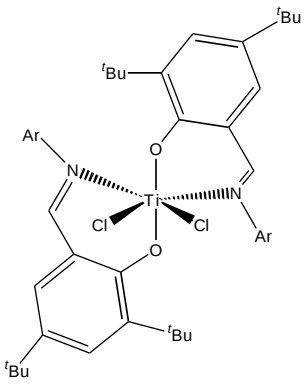

1 Ar = C_6H_5
2 Ar = C_6F_5

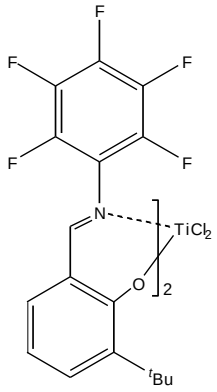

3

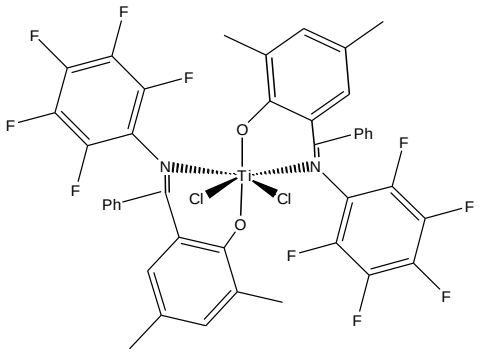

4

Bercaw reported that zirconium complexes with bisphenoxyfurane and bisphenoxypyridine ligands **5**-**7** show high catalytic activity for propylene polymerization (> 1000 $kg_{polymer}$ $mol^{-1}\cdot h^{-1}$). The bisphenoxypyridine titanium complex is *ca*. 1000 times less active but produce polypropylene with higher molecular weight.[17] Bis(phenoxy-ether) complex of titanium in the presence of appropriate cocatalyst showed moderate activity in propylene polymerization, producing stereo-irregular polypropylenes.[18] More

recently, chiral bis(phenolate) group 4 complexes **8-11** were used as active catalyst precursors for propylene polymerization. They generated high molecular weight, highly isotactic polypropylenes at elevated temperatures (50-80 °C).[19]

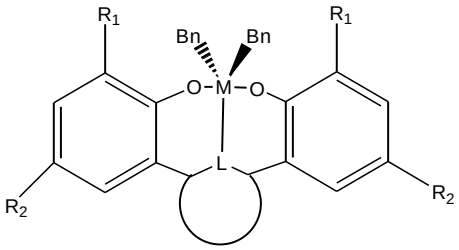

5 $R_1 = R_2 = CMe_3$, L = pyridine, M = Zr
6 $R_1 = CEt_3$, R_2 = Me, L = pyridine, M = Zr
7 $R_1 = R_2 = CMe_3$, L = furan, M = Zr

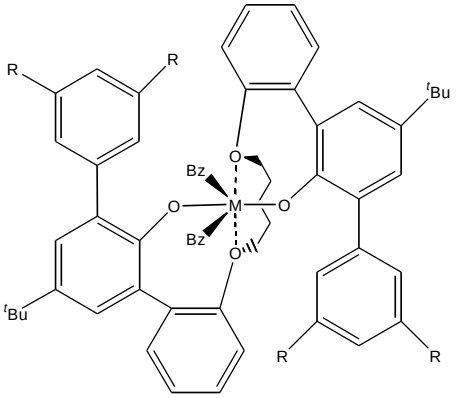

8 R = H, M = Zr
9 R = H, M = Hf
10 R = ^{t}Bu, M = Zr
11 R = ^{t}Bu, M = Hf

In the previous chapter, the *N*,*N*-dialkylcarbamato complexes of titanium (**I**, **II** and **III**) [$Ti(O_2CNR_2)_4$, R = Et (**I**), Me (**II**)] and [$Ti(O_2CNR_2)_2Cl_2$, R = Me (**III**)] (Chart 1, Chapter 3) were studied as catalyst precursors for the polymerization of ethylene. The complexes showed good catalytic activities in ethylene homopolymerization in the presence of methylaluminoxane (MAO) as cocatalyst, producing linear high density polyethylene. Consequently, there is currently great interest in using such catalytic precursors for propylene polymerization.

The subject of this chapter is a detailed study of behavior of complexes **I-III** as catalytic precursors in propylene polymerization and the analysis of polymers produced with these complexes under different reaction conditions. The effects of Al/Ti ratio, solvent, cocatalyst, reaction time and temperature in the polymerization process are presented.

4.2 Results and discussion

Complexes **I-III** were studied as pre-catalysts for propylene polymerization in combination with different cocatalyst systems and under variable conditions. When activated by MAO in chlorobenzene at 25 °C, the Complex **I** generates 1.25 g of

polypropylene within 1 h, corresponding to a productivity of 25.1 $kg_{polymer}$ $mol_{Ti}^{-1} \cdot h^{-1}$ (Table 2). When **I** was replaced by **II** in combination with MAO (entry 3, Table 2) slightly higher productivity was observed and it reached to 29 $kg_{polymer}$ $mol_{Ti}^{-1} \cdot h^{-1}$. By comparing the catalytic activity of **I** and **II**, it can be clearly seen that the ligand framework plays a significant role. The less steric hindrance around the metal center, the easier attack of oncoming monomer, thus increasing the polymerization activity.

Under the same conditions, the complex **III** yields 1.8 g of polymer (30 $kg_{polymer}$ $mol_{Ti}^{-1} \cdot h^{-1}$), indicating that the effect of precursor nature on the catalytic performances in propylene polymerization is rather different from those observed for ethylene polymerization.

Activation of both complexes **I** and **III** with "TMA-depleted" methylaluminoxane (DMAO) resulted in a significant increase of productivity and it reached to 43.5 and 98.9 $kg_{polymer}$ $mol_{Ti}^{-1} \cdot h^{-1}$, respectively (entries 2 and 5, Table 2). On the other hand, using MAO as a cocatalyst resulted in less activity than DMAO for both complexes, confirming that in the catalytic system with MAO containing less residual trimethylaluminium (TMA), titanium can remain mostly in the tetravalent state and promotes polymerization of propylene efficiently. On the other hand, a high TMA content in MAO favours the reduction of titanium to the lower valent states that do not catalyze the polymerization of propylene.[20,21] It is worth mentioning that higher activity was also achieved when **III**/DMAO catalytic system used in propylene polymerization, similar to what we found when MAO used as co-catalyst, compared to the one that **I**/DMAO applied for propylene polymerization. It reveals that less steric hindrance around the metal center causes the easiest access of propylene monomer to the active sites on the catalytic system.

In order to gain further information on the behavior of catalytic system as a result of using different cocatalyst/Ti molar ratios, we carried out some experiments with different Al/Ti molar ratio (Figure 1). The complex **III** showed the higher catalytic activity, approximately 102 $kg_{polymer}$ $mol_{Ti}^{-1} \cdot h^{-1}$, when DMAO/Ti ratio was 150. Higher cocatalyst concentration did not enhance the productivity, suggesting that high amounts of cocatalyst can compete with the olefin for the active site of the complex, decreasing the activity.[22,23] Also the diminished polymerization activity at higher Al/Ti ratio is presumably due to over-reduction of titanium from Ti(IV) to the lower valent states.[24]

Table 2. Homopolymerization of propylene catalyzed by titanium (IV) carbamates (**I-III**) activated by organoaluminium compounds[a]

Entry	Precursor (μmol)	Al/Ti (mol/mol)	Propylene (g)	Product (g)	Activity[b]	Mv (Da)
1	**I** (50)	300	50	1.25	25.1	40,000
2[c]	**I** (50)	300	50	2.14	43.5	46,000
3	**II** (50)	300	50	1.57	29.0	21,000
4	**III** (60)	300	50	1.80	30.0	27,000
5[c]	**III** (60)	300	50	4.13	98.9	33,000
6	**III** (50)	150	50	1.53	30.6	61,000
7[c]	**III** (50)	150	50	5.13	102.6	59,000
8[c]	**III** (20)	150	50	2.27	113.3	68,000
9	**III** (50)	75	50	0.28	5.5	73,000
10[c]	**III** (50)	75	50	0.62	12.3	83,000
11[c,d]	**III** (50)	300	60	1.30	25.2	41,000
12[c,e]	**III** (20)	150	40	0.35	35.4	29,000
13[c,f]	**III** (60)	150	40	3.77	62.9	41,500
14	**$TiCl_4$** (50)	300	40	0.07	1.5	n.d.
15[c]	**$TiCl_4$** (50)	300	50	trace	n.d.	n.d.

[a] Reaction conditions: Duration = 1 h; solvent = chlorobenzene (65 mL); MAO as cocatalyst; temperature = 25 °C; if not otherwise specified. [b] Activity expressed as $kg_{polymer}\ mol_{Ti}^{-1} \cdot h^{-1}$, [c] DMAO was used as cocatalyst, [d] solvent = toluene, [e] duration = 0.5 h, [f] temperature = 60 °C.

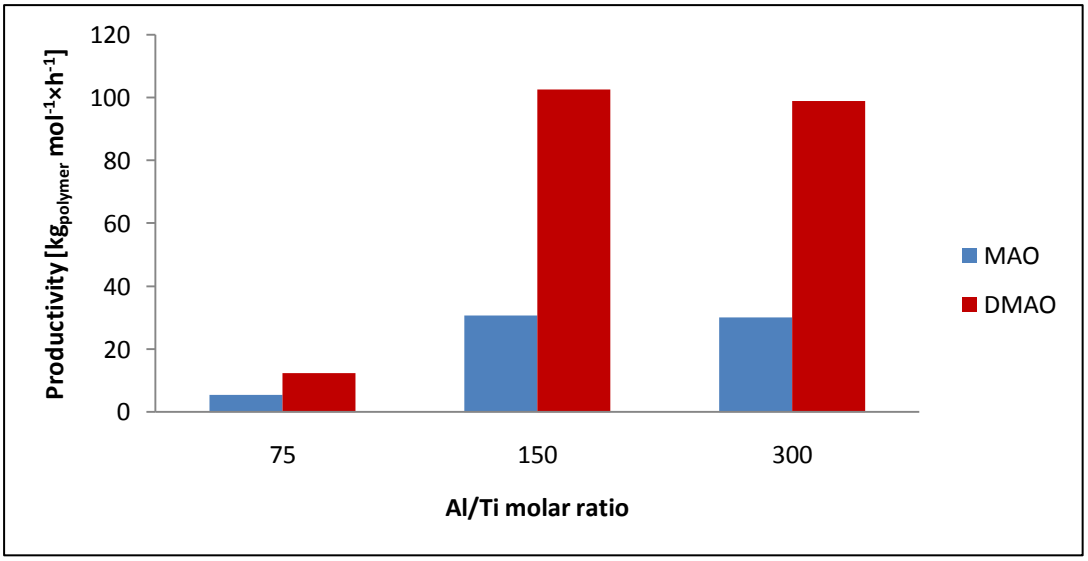

Figure 1. Productivity of the catalytic system based on pre-catalyst **III** versus Al/Ti molar ratio in propylene polymerization.

Increasing the cocatalyst/catalyst ratio resulted in a remarkable decrease of the molecular weight, as shown in Figure 2. One of the main reason for this effect can be the dominant chain transfer reactions to the methyl aluminoxane.[25]

The activity could be further increased, to 113 $kg_{polymer}$ $mol_{Ti}^{-1} \cdot h^{-1}$, by lowering the precursor amount to 20 μmol, as can be seen for entry 8. A similar finding has also been reported in the literature for supported titanium-magnesium catalysts in ethylene polymerization.[26] It can be explained by Ostwald's law for the dissociation of electrolytes assuming that an ion pair of titanocene cation and MAO counterion preferably dissociates at lower concentrations, thus leading to higher activities as it is also observed when going to a solvent with higher polarity.[27]

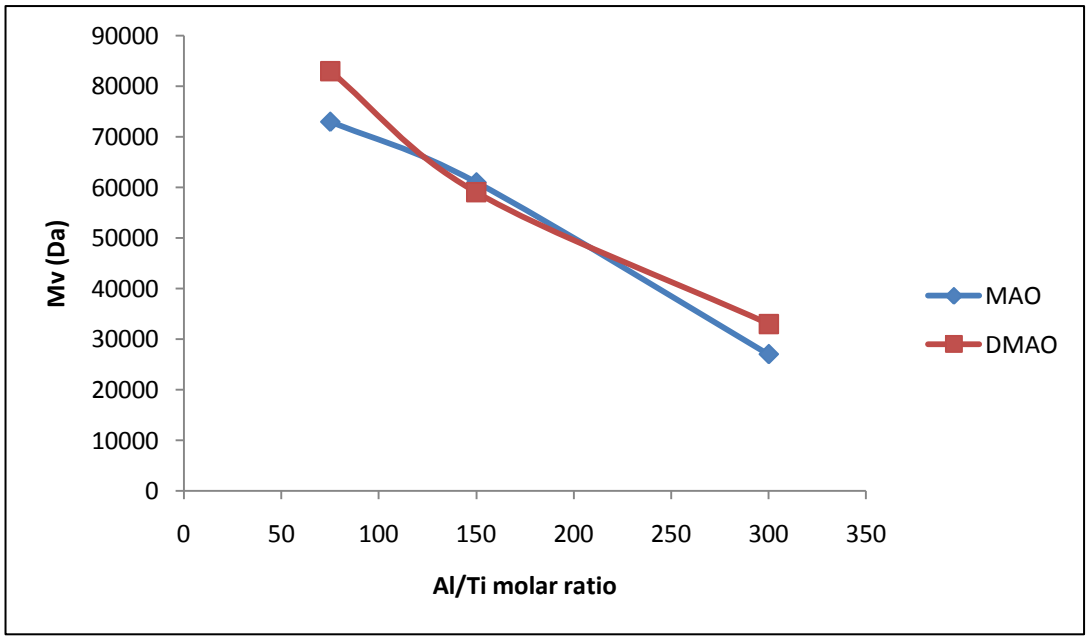

Figure 2. Influence of Al/Ti molar ratio on average viscosity molecular weight (M_v).

Experimental data also showed that the solvent has a strong effect on the catalyst activity (entries 5 and 11, Table 2). As can be seen in Table 2, the polymerization activity in the presence of toluene is approximately four times lower than that in chlorobenzene. This result is in agreement with the literature data on zirconocene compounds of general formula $[Et(Ind)_2ZrCl_2]$ which show that the polymerization activity in a polar solvent (CH_2Cl_2) is higher than that in toluene.[28,29] Scheme 1 shows the possible separation mode

of the cationic center and the MAO counterion in the presence of polar solvent that facilitate the coordination of monomer to the active polymerization center. [30]

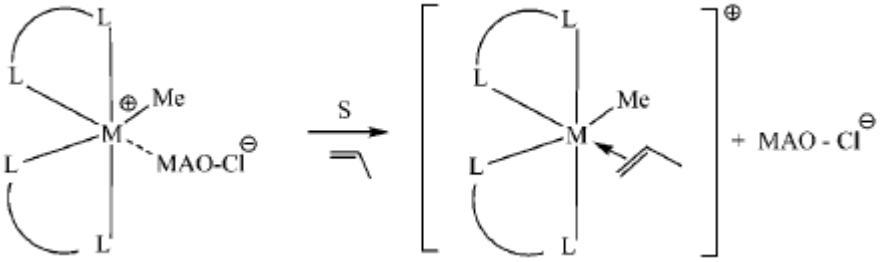

Scheme 1. Plausible separation of the cationic center and the MAO counterion by the polar solvent (M = metal; L–L = ancillary ligation; S = solvent).

The influence of polymerization temperature on activity and viscosity average molecular weight was studied, while the [Al]/[Ti] molar ratio was kept constant at [Al]/[Ti] = 150. The activity decreased at higher temperatures (60 °C) and fell to 62.9 $kg_{polymer}$ $mol_{Ti}^{-1} \cdot h^{-1}$ (entries 7 and 13, Table 2), because of the lower monomer concentration in solution. Furthermore, the reduction in catalyst activity in the polymerization performed at the upper temperature could be attributed to the catalyst deactivation. The lower viscosity average molecular weight polypropylene (M_v = 41,500 Da) was obtained at 60 °C. At lower temperatures, propagation is favored over termination and the resulting polymer has higher molecular weight. On the other hand, higher temperature supplies the activation energy requirement for chain transfer reactions which results in lower polymer molecular weight.[31]

When a reference conventional catalyst, based on $TiCl_4$, was adopted (entries 14 and 15, Table 2) under the same conditions as in entries 1 and 2, a very lower activity was ascertained

According to the DSC measurements in a temperature range of –30 to 220 °C, the glass transition temperature lies at –9 to –14 °C and no detectable melting endothermic peak was observed, which indicates that all the polypropylenes produced were atactic and amorphous.

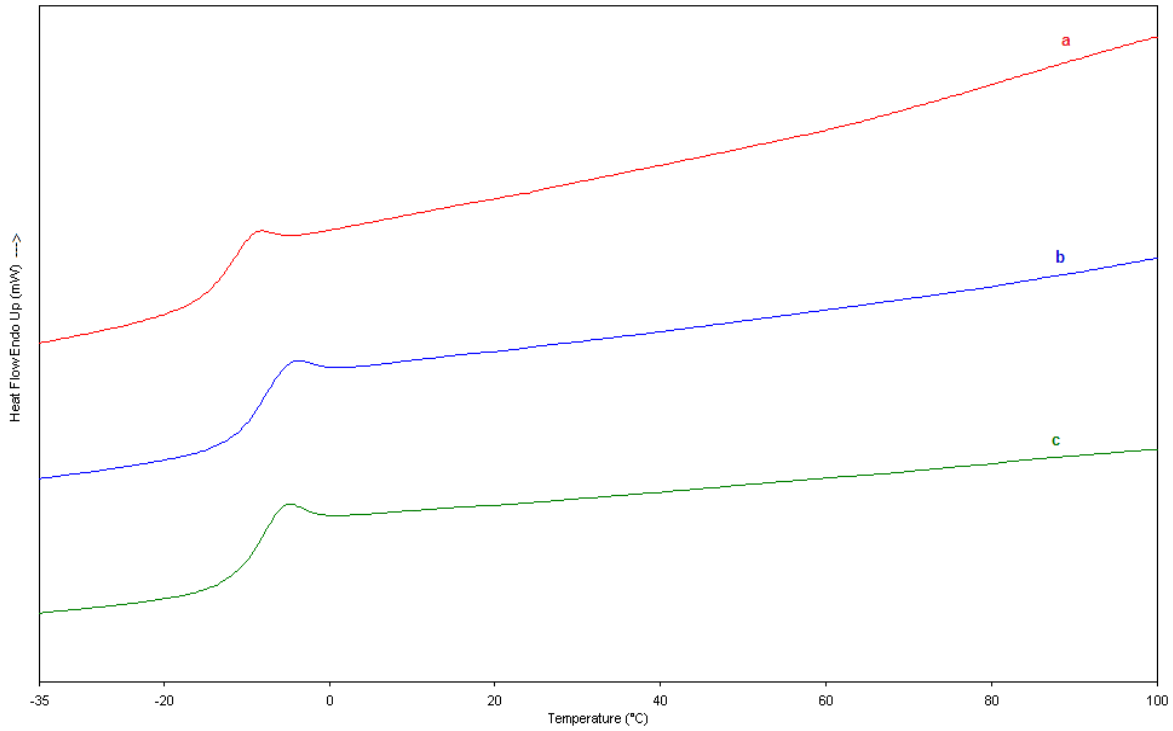

Figure 3. DSC scans of PP products obtained from (a) entry 2, (b) entry 8 and (c) entry 7.

Infrared spectroscopy has been applied to studies of the tacticity of a number of vinyl polymers.[32] There is a relationship between stereoregularity and the presence of regular chains and this leads to the appearance of infrared bands due to regular chains. The absorbance values at 970 and 1460 cm^{-1} do not depend upon the tacticity, whereas the absorbances at 840, 1000 and 1170 cm^{-1} are characteristic of isotactic PP, and the absorbance at 870 cm^{-1} is characteristic of syndiotactic PP. The FTIR spectra of the polypropylene samples obtained in entries 7 and 8 (Figure 4) indicated that the samples do not show any absorbance bands which are characteristic of isotactic or syndiotactic polypropylene, thus confirming production of atatic materials.[33]

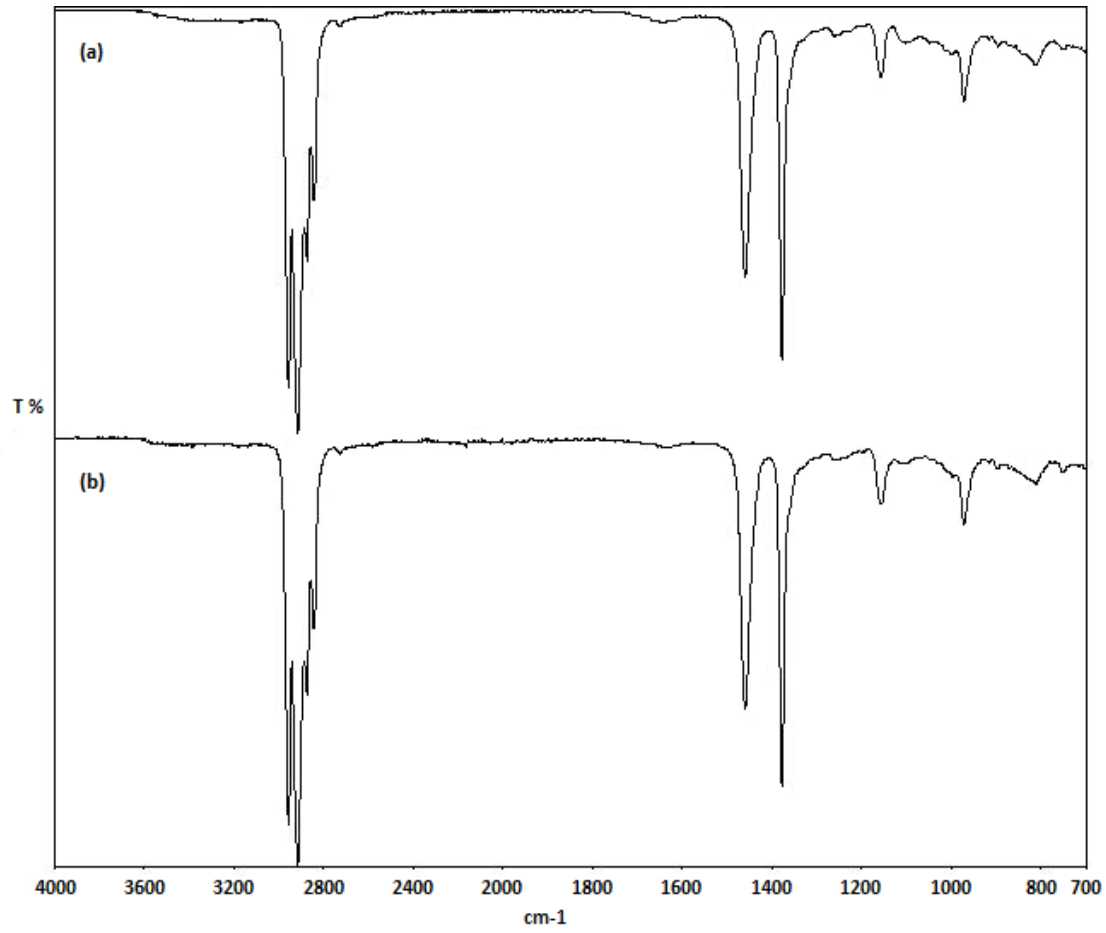

Figure 4. IR spectrum of PP samples resulting from entry 7 (**a**) and entry.8 (**b**).

^{13}C NMR analysis[34] confirms that **I**-**III**/MAO catalytic systems produce atactic polypropylene under the adopted conditions. The distributions of stereo-diad sequences of the polypropylenes prepared at entries 2 and 8 are listed in Table 3. As reported in the literature,[32] the peaks between 20.0 and 20.3 ppm were assigned to *rr* diads, those between 20.7 and 21.0 ppm to *mr* diads, whereas those between 21.3 and 21.7 ppm were assigned to *mm* diads. The diad distributions of these polypropylenes are not so different from each other. It can be observed that the polymers are stereoirregular with *rr* > *mm*.

Table 3. Stereospecificity of the polypropylenes synthesized by **I**-**III**/MAO catalysts.

Sequence	Sample 2[a]	Sample 8[a]
mm	20	26
mr	42	36
rr	38	38

[a] Sample numbers are from the entry numbers in Table 2.

The pentad distribution, determined from the peak intensities of the $P_{\beta\beta}$ methyl region (19-22 ppm),[35,36] is reported in Table 4.

Table 4. Pentad distribution of sample 12[a]

Pentad	**%**
mmmm	14.6
mmmr	10.5
rmmr	6.6
mmrr	11.6
mmrm+rmrr	15.4
mrmr	9.0
rrrr	7.2
rrrm	12.5
mrrm	12.6

[a] Sample numbers are from the entry numbers in Table 2.

Regioirregular sequences were clearly observed in the methyl and methine regions of the ^{13}C NMR spectrum (see Figures 5 and 6).[37,38] In particular, besides the intense signal at ~ 29 ppm due to $T_{\beta\beta}$ carbons, signals at ~ 31 ppm and at ~ 38 ppm, ascribable to $T_{\beta\gamma}$ and $T_{\alpha\gamma}$, respectively, are observed. The intensities of these signals were hence used to determine the concentration of the different sequences.[20] The $T_{\alpha\beta}$ signal, falling in the 34-36 ppm region, overlaps $S_{\alpha\beta}$ signals and hence its intensity cannot be determined directly.

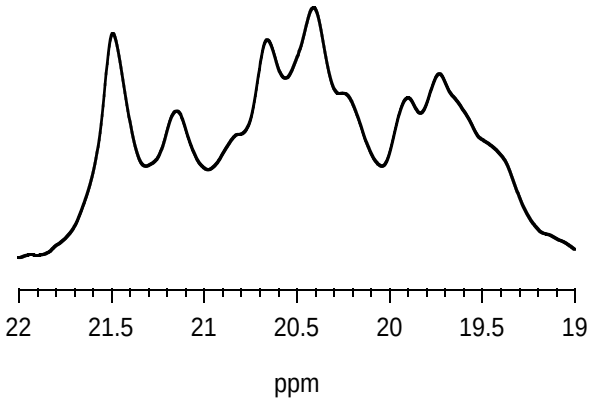

Figure 5. 19-22 ppm methyl region of the ^{13}C NMR spectrum of sample 12.

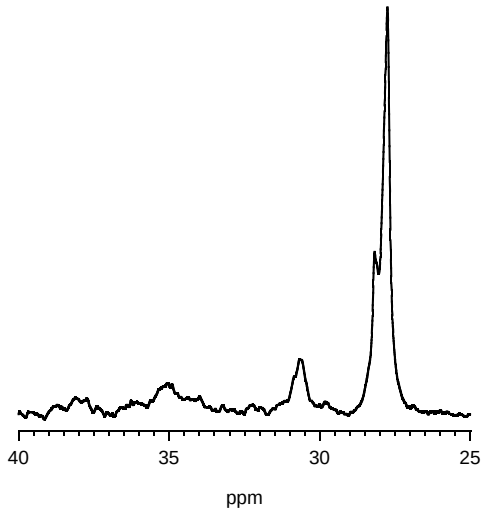

Figure 6. Methine region of the ^{13}C NMR spectrum of sample 12.

However, the H-H fraction, corresponding to both $T_{\alpha\gamma}$ and $T_{\alpha\beta}$, can be unambiguously determined from the intensity of the methyl peaks in the 14-17 ppm region with respect to the total methyl signal intensity; by combining the H-H fraction thus determined and the $T_{\beta\beta}$, $T_{\beta\gamma}$, and $T_{\alpha\gamma}$ signal intensities, it is possible to estimate the fraction of $T_{\alpha}\beta$ carbons. The results are given in Table 5.

Table 5. Regiosequence distribution of sample 12.[a]

C-Type	$T_{\beta\beta}$	$T_{\beta\gamma}$	$T_{\alpha\beta}$	$T_{\alpha\gamma}$
%	66	12	17	5

[a] Sample numbers are from the entry numbers in Table 2.

4.3 Conclusion

Titanium complexes supported by *N*,*N*-dialkylcarbamato ligands have been investigated in propylene polymerization. The complexes found to be active in polymerization of propylene upon activation with MAO, producing basically atactic polypropylenes. The nature of the solvent and TMA content of MAO appeared crucial for the catalytic performances: when toluene was replaced by chlorobenzene and DMAO was used as cocatalyst a higher activity was ascertained. In all cases, the microstructure of the polymeric products was stereoirregular and T_g lied at –9 to –14 °C. Regioirregular sequences were observed in the methyl and methane regions of ^{13}C NMR spectrum of selected sample.

4.4 References

[1] *Encyclopedia of Polymer Science and Technology*; on-line ed.; Wiley & Sons, Inc.: New York, 2006.

[2] Kissin, Y. V. In *Kirk-Othmer Encyclopedia of Chemical Technology Online*; Wiley & Sons, Inc: New York, 2005.

[3] Coates, G. W. *Chem. Rev.* **2000**, *100*, 1223.

[4] Resconi, L.; Cavallo, L.; Fait, A.; Piemontesi, F. *Chem. Rev.* **2000**, *100*, 1253.

[5] Gibson, V. C.; Spitzmesser, S. K. *Chem. Rev.* **2003**, *103*, 283.

[6] Britovsek, G. J. P.; Gibson, V. C.; Wass, D. F. *Angew. Chem., Int. Ed.* **1999**, *38*, 428.

[7] Coates, G. W.; Hustad, P. D.; Reinartz, S. *Angew. Chem., Int. Ed.* **2002**, *41*, 2236.

[8] Kaminsky, W. *Macromol. Chem. Phys.* **2008**, *209*, 459.

[9] Ittel, S. D.; Johnson, L. K.; Brookhart, M. *Chem. Rev.* **2000**, *100*, 1169.

[10] Tian, J.; Hustad, P. D.; Coates, G. W. *J. Am. Chem. Soc.* **2001**, *123*, 5134.

[11] Saito, J.; Mitani, M.; Mohri, J. -I.; Ishii, S. -I.; Yoshida, Y.; Matsugi, T.; Kojoh, S. -I.; Kashiwa, N.; Fujita, T. *Chem. Lett.* **2001**, 576.

[12] Mitani, M.; Furuyama, R.; Mohri, J. -I.; Saito, J.; Ishii, S.; Terao, H.; Kashiwa, N.; Fujita, T. J. Am. Chem. Soc. 2002, 124, 7888.

[13] Mitani, M.; Furuyama, R.; Mohri, J. -I.; Saito, J.; Ishii, S.; Terao, H.; Nakano, T.; Tanaka, H.; Fujita, T. J. Am. Chem. Soc. 2003, 125, 4293.

[14] (a) Saito, J.; Mitani, M.; Onda, M.; Mohri, J. -I.; Ishii, S. -I.; Yoshida, Y.; Nakano, T.; Tanaka, H.; Matsugi, T.; Kojoh, S. -I.; Kashiwa, N.; Fujita, T. *Macromol. Rapid Commun.* **2001**, *22*, 1072. (b) Hustad, P. D.; Tian, J.; Coates, G. W. *J. Am. Chem. Soc.* **2002**, *124*, 3614.

[15] (a) Mason, A. F.; Coates, G. W. *J. Am. Chem. Soc.* **2004**, *126*, 16326. (b) Edson, J. B.; Wang, Z.; Kramer, E. J.; Coates, G. W. *J. Am. Chem. Soc.* **2008**, *130*, 4968.

[16] (a) Saito, J.; Onda, M.; Matsui, S.; Mitani, M.; Furuyama, R.; Tanaka, H.; Fujita, T. *Macromol. Rapid Commun.* **2002**, *23*, 1118. (b) Prasad, A. V.; Makio, H.; Saito, J.; Onda, M.; Fujita, T. *Chem. Lett.* **2004**, *33*, 250.

[17] Agapie, T.; Henling, L. M.; DiPasquale, A. G.; Rheingold, A. L.; Bercaw, J. E. *Organometallics* **2008**, *27*, 6245.

[18] Lamberti, M.; Mazzeo, M.; Pellecchia, C. *Dalton Trans.* **2009**, 8831.

[19] Kiesewetter, E. T.; Randoll, S.; Radlauer, M.; Waymouth, R. M. *J. Am. Chem. Soc.* **2010**, *132*, 5566.

[20] Wu, Q.; Ye, Z.; Gao, Q.; Lin, S. *J. Polym. Sci. Part A: Polym. Chem.* **1998**, *36*, 2051.

[21] Makio, H.; Fujita, T. *Bull. Chem. Soc. Jpn.* **2005**, *78*, 52.

[22] He, L. –P.; Liu, J. –Y.; Pan, L.; Li, Y. –S.; *J. Polym. Sci. Part A: Polym. Chem.* **2008**, *46*, 7062.

[23] Fim, F. C.; Machado, T.; Sa, D. S.; Livotto, P. R.; Rocha, Z. N.; Basso, N. R. S.; Galland, G. B.; *J. Polym. Sci. Part A: Polym. Chem.* **2008**, *46*, 3830.

[24] Yu, E.-Y.; Choi, B.-R. *J. Ind. Eng. Chem.* **1996**, *2*, 7.

[25] Small, B. L.; Brookhart, M.; Bennett, A. M. A. *J. Am. Chem. Soc.* **1998**, *120*, 4049.

[26] Echevskaya, L. G.; Matsko, M. A.; Mikenas, T. B.; Nikitin, V. E.; Zakharov, V. A. *J. Appl. Polym. Sci.* **2006**, *102*, 5436.

[27] Longo, P.; Oliva, L.; Grassi, A.; Pellecchia, C. *Makromol. Chem.* **1989**, *190*, 2357.

[28] Forlini, F.; Tritto, I.; Locatelli, P.; Sacchi, M. C.; Piemontesi, F. *Macromol. Chem. Phys.* **2000**, *201*, 401.

[29] Forlini ,F.; Princi, E.; Tritto, I.; Sacchi, M. C.; Piemontesi, F. *Macromol. Chem. Phys.* **2002**, *203*, 645.

[30] Volkis, V.; Shmulinson, M.; Averbuj, C.; Lisovskii, A.; Edelmann, F. T.; Eisen, M. S. O*rganometallics* **1998**, *17*, 3155.

[31] Busico, V.; Talarico, G.; Cipullo, R. *Macromol. Symp*. **2005**, *226*, 1.

[32] Chalmers, J. M., Hannah, R. W. and Mayo, D. W., 'Spectra–Structure Correlations: Polymer Spectra', in *Handbook of Vibrational Spectroscopy*, Vol. 3, Chalmers, J. M. and Griffiths, P. R. (Eds), Wiley, Chichester, UK, 2002, pp. 1893–1918.

[33] Luongo, J. P. *J. Appl. Polym. Sci.* **1960**, *3*, 302.

[34] Randall, J. C. *J. Polym. Sci., Polym. Phys. Ed*. **1974**, *12*, 703.

[35] Asakura, T.; Doi, Y. *Macromolecules* **1983**, *16*, 786.

[36] Chen, R.; Xie, M.; Wu, Q.; Lin, S. *J. Polym. Sci., Part A: Polym. Chem*. **2000**, *38*, 411.

[37] Asakura, T.; Nishiyama, Y.; Doi, Y. *Macromolecules* **1987**, *20*, 616.

[38] Asakura, T.; Nakayama, N.; Demura, M.; Asano, A. *Macromolecules* 1992, **25**, 4876.

5 Ethylene/1-Hexene Copolymerization in the Presence of Titanium Precursors and Organoaluminium Cocatalysts

5.1 Introduction

Ethylene-based copolymers are industrially important materials and have been the most widely used thermoplastic materials for decades now,[1] with linear low-density polyethylene (LLDPE) playing an important role,[2] because of the diversity of materials that can be produced. The copolymerization of ethylene with α-olefins introduces short-chain branching (SCB) into the chain backbone, thus the physical properties of LLDPE can be tuned by manipulating the amount of SCB and the short-chain branch distribution (SCBD)[3,4] as well as by controlling the mode of polymerization, catalyst type, pressure and temperature.

Of course, the identity of comonomer, which inserts the short chain branch into the main chain, is important. Commonly, 1-butene is chosen because of its low cost, but the use of 1-hexene or 1-octene has shown to improve the mechanical properties of final material.[5] It has also been observed that the properties of LLDPE are affected by interactions between the polymer chains.[6,7,8]

LLDPE is most commonly produced by chain-growth polymerization using classical Ziegler–Natta or single-site metallocene catalysts.[9,10] In contrast to multisite Ziegler-Natta systems, the metallocene ones offer the advantage of structurally homogeneous polyolefins in terms of narrow distributions of molecular weight and of a random insertion of the comonomers in the backbone.[11,12,13]

Recently, non-metallocene catalytic systems have also gained much attention in α-olefin copolymerization. Several studies comparing different group 4 non-metallocene structures in ethylene/α-olefin copolymerization have been reported in the literature,[14,15] and in 2004, Dow launched VERSIFY™ plastomers and elastomers as family of propylene/ethylene-based copolymers made with group 4 complexes bearing pyridyl amine ligand systems (Figure 1).[16] More recently, ethylene-octene block copolymers were also developed in Dow employing a new chain shuttling technology.[17] This technology (Figure 2) employs two catalysts, one forming high-density PE with higher melting points and the second forming an elastomer with high incorporation of octene in the ethylene chain. A chain shuttling agent (diethyl zinc) forces an exchange of catalysts

as the polymer chain grows leading to blocky polymers that combine the attributes of high-density PE and the olefin elastomer.

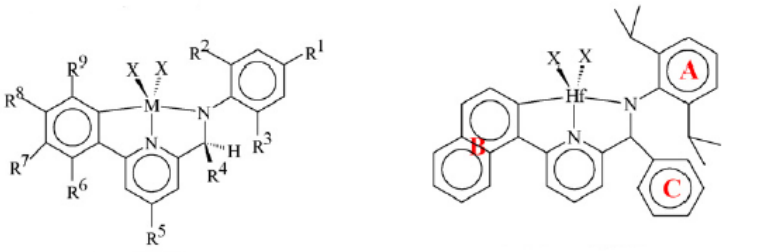

Figure 1. Pyridyl amine-based catalyst: a post-metallocene catalyst.

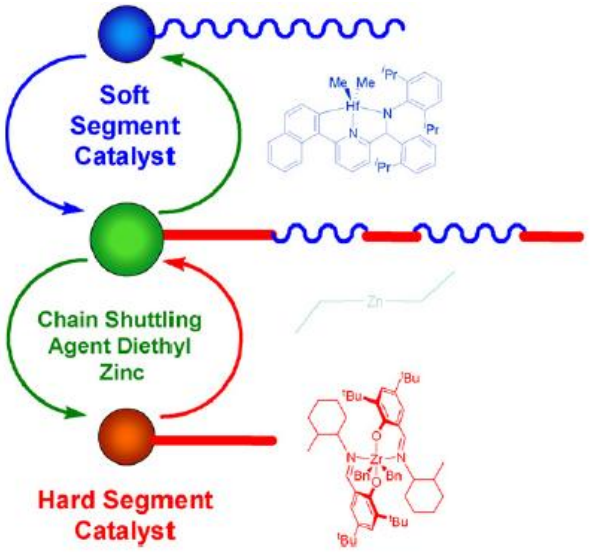

Figure 2. Chain shuttling technology for olefin block copolymers.

The main objective of this new study is to further investigate the behaviour of *N*,*N*-dialkylcarbamato complexes of titanium (**I**, **II** and **III**) [$Ti(O_2CNR_2)_4$, R = Et (**I**), Me (**II**)] and [$Ti(O_2CNR_2)_2Cl_2$, R = Me (**III**)] (Chart 1, Chapter 3) in α-olefin polymerization, in particular, in the copolymerization of ethylene with higher α-olefins such as 1-hexene. These precatalysts exhibit moderate activity for copolymerization of ethylene with 1-hexene featured broad MWD and high comonomer incorporation. The effects of

performing conditions, such as polymerization temperature, ratio of Al/Ti and monomer pressure on the polymerization behaviours are investigated as well.

5.2 Results and discussion

In order to study the influence of the titanium complexes bearing *N*,*N*-dialkylcarbamato ligands on the copolymerization of ethylene with 1-hexene, we have investigated two different activation process: in the first process, pre-catalysts are activated by combination of $Et_3Al_2Cl_3$ and Al-$^{i}Bu_3$, and in the second one, MAO is used as unique cocatalyst.

Employing the first process allowed us to have a comparison between the catalytic behaviour of these precursors (**I-III**) with titanium complexes based on the known bis-carboxylate and chloro-substituted bis-carboxylate ligands (Figure 3)[18] in the copolymerization of ethylene with 1-hexene. The precursors **I-III** exhibited greater activity and higher comonomer insertion ability than the previous carboxylato complexes of titanium[18] tested in analogous conditions.

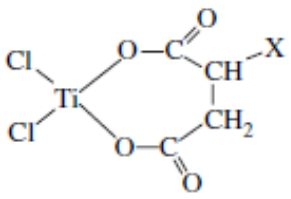

X = H, Cl

Figure 3. Schematic structure of bis-carboxylato complexes of titanium.

5.2.1 Ethylene/1-hexene copolymerization using titanium precursors activated by $Et_3Al_2Cl_3$/Al-$^{i}Bu_3$

Preliminarily ethylene and 1-hexene homopolymerization experiments (entries 1 and 2, Table 1) were carried out by using **III** as catalytic precursor and adopting the best conditions claimed for ethylene/1-hexene copolymerization, in which carboxylato complexes of titanium were used as pre-catalysts,[18] afforded only low activity of 1.68

$kg_{polymer}$ $mol^{-1}\cdot h^{-1}$ for 1-hexene homopolymerization, even prolonging the reaction time up to 24 h, while the productivity reached to 10.3 $kg_{polymer}$ $mol^{-1}\cdot h^{-1}$ when the catalyst was used for ethylene polymerization, working at 0.1 MPa.

Table 1. Homopolymerization of ethylene and 1-hexene using **III**/$Et_3Al_2Cl_3$/Al-$^iBu_3$ catalytic system[a]

Entry	**III** (μmol)	Feed		Time (h)	Crude Polymer (g)	Activity[b]
		P_{C2H4} (MPa)	1-hexene (mL)			
1	20	-	30	5	0.168	1.68
2	20	0.1	-	0.5	0.103	10.3

[a] Reaction conditions: $Et_3Al_2Cl_3$/Ti = 3 mol/mol; Al-$^iBu_3$/Ti = 50 mol/mol; T = 30 °C; solvent = chlorobenzene (10mL). [b] Activity expressed as $kg_{polymer}$ $mol_{Ti}^{-1}\cdot h^{-1}$.

When the chloro-substituted chelate **III** was employed for the ethylene/1-hexene copolymerization under similar condition (entry 3, Table 2), as that adopted for 1-hexene homopolymerization (entry 1, Table 1) but in the presence of ethylene (0.1 MPa), productivity increased up to 11.75 $kg_{polymer}$ $mol_{Ti}^{-1}\cdot h^{-1}$ and polymeric product with a significant incorporation of 1-hexene co-units of 28 mol% and melting temperature of 119.1 °C was obtained. A further decrease of relative amount of 1-hexene (entry 4, Table 2) reduced the productivity to 7.8 $kg_{polymer}$ $mol_{Ti}^{-1}\cdot h^{-1}$, with a remarkable diminishing of 1-hexene co-units content in the product (6 mol%).

It is commonly observed that the addition of a comonomer increases the polymerization rate significantly. Several explanations for this comonomer effect have been proposed, including an activation of dormant sites, an enhancement of the ethylene insertion rate in the presence of the comonomer, and an increase in the solubility of the copolymer followed by reduced diffusion limitations.[19,20,21] This phenomenon is very much catalyst and comonomer specific. For ethylene/propylene copolymerizations in solution, it was furthermore found that the comonomer effect is also lowered with higher ethylene concentration in feed.[22]

Comparison between the percentage of the comonomer incorporated in the copolymer and the comonomer content in the feed indicates that the content of the former increases with the increase of its concentration in the feed.

By increasing the ethylene pressure up to 1 MPa, the productivity enhanced almost two times, but 1-hexene content decreased to 2 mol% and an even relatively linear polymeric product with higher T_m (126 °C) was obtained (entries 5 and 6, Table 2). The incorporation of the comonomer is favored at low ethylene concentrations in the solution, and this means a higher 1-hexene/ethylene ratio in the reactor. Furthermore, it follows that the melting point and the crystallinity of the copolymers increase with increasing ethylene concentration.

Quijada et al.[23] also reported a linear decrease in the 1-hexene incorporation with increasing ethylene pressure when the initial 1-hexene concentration was constant. They used $Et(Ind)_2ZrCl_2$/MAO as a catalytic system. Shan et al.[24] studied the effects of polymerization parameters on the catalyst activity and polymer microstructure in ethylene/1-octene copolymerization. The catalyst was *in situ* supported Me_2Si(2-Me-4,5-BenzInd)$_2ZrCl_2$ (Figure 4) activated with triethylaluminum, and the support material was MAO-treated silica. They reported a decrease in the 1-octene incorporation as the ethylene pressure was increased, even though the 1-octene/ethylene feed ratio was kept constant at different ethylene pressures. At a constant 1-octene/ethylene ratio, the total 1-octene incorporation should have remained constant, regardless of the ethylene pressure.

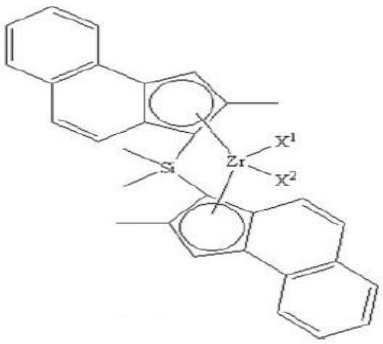

Figure 4. Schematic structure of zirconium complex.

Shan et al. indicated that even though the bulk 1-octene/ethylene ratio was constant, at the active sites it was not. The observed effect was proposed to be related to other factors, such as mass-transfer resistance during polymerization.

The activity of complex **III** for ethylene/1-hexene copolymerization also strongly depends on the polymerization temperature. An obvious decrease of more than 4-fold in

activity was observed as the polymerization temperature increased from 30 to 70 °C, the productivity being reduced from 11.8 to 2.7 $kg_{polymer}$ $mol_{Ti}^{-1} \cdot h^{-1}$ (entries 7 and 8, Table 2), thus suggesting that the active titanium species responsible for the polymerization are rather thermolabile. Although, a decrease in the melting temperature of polymer samples indicated that insertion of 1-hexene co-units into the backbone of polymer increases at the higher temperatures.

Table 2. Ethylene/1-hexene copolymerization using titanium carbamato precursor **III** activated by $Et_3Al_2Cl_3$ and Al-$^{i}Bu_3$[a]

Entry	Ti precursor type (μmol)	Feed		Time (h)	Temperature (°C)	Crude polymer					
		P_{C2H4} (MPa)	1-hexene (mL)			(g)	Activity[b]	1-Hexene (mol %)		Melting point (°C)	PDI
								IR	NMR		
3	**III** (20)	0.1	30	5	30	1.18	11.8	28.2	28	119.1	7[d]
4	**III** (20)	0.1	5	5	30	0.75	7.5	6.8	6	121.2	
5	**III** (21)	1	5	5	30	1.29	12.3	0	0	131.6	
6	**III** (25)	1	30	5	30	3.06	24.5	2.0		126.1	
7	**III** (14)	0.1	30	5	50	0.54	7.7	24.5	25	119.9	
8	**III** (12)	0.1	30	5	70	0.16	2.7			116.5	
9[c]	**III** (14)	0.1	30	5	30	0.26	3.7	20.6		120.7	
10	**III** (17)	0.1	5	2.5	30	0.47	11.1	7.0	6	121.0	

[a] Reaction conditions: $Et_3Al_2Cl_3$/Ti = 3 mol/mol; Al-$^{i}Bu_3$/Ti = 50 mol/mol; T = 30 °C; solvent = chlorobenzene, total volume = 65 mL. [b] Activity expressed as $kg_{polymer}\ mol_{Ti}^{-1}\cdot h^{-1}$. [c] Solvent = toluene. [d] M_w = 371000, M_n = 53300.

The polarity of solvent greatly affects the polymerization activity. When toluene was employed as solvent (entry 9, Table 2), the productivity was greatly decreased (3.7 $kg_{polymer}\ mol_{Ti}^{-1}\cdot h^{-1}$), confirming that the solvent has a key role in the polymerization. It also showed that insertion of 1-hexene was higher with chlorobenzene (28 mol%) compared to its value with toluene (20.6 mol%). Therefore, it was suggested that the higher dielectric constant of solvent clearly resulted in the higher degree of 1-hexene insertion.[25]

A reduction of reaction time to 2.5 h led to a slightly increase in productivity (11.1 $kg_{polymer}\ mol_{Ti}^{-1}\cdot h^{-1}$) without a great change in 1-hexene incorporation degree (entry 10, Table 2).

When **I** was replaced by **III**, either a much higher catalytic activity up to 20.9 $kg_{polymer}\ mol_{Ti}^{-1}\cdot h^{-1}$ and a higher content of 1-hexene co-units (26 mol%) in the polymer were obtained (Table 3).

Table 3. Ethylene/1-hexene copolymerization using titanium carbamato precursors **I** and **II** activated by $Et_3Al_2Cl_3$ and Al-$^{i}Bu_3$[a]

Entry	Ti precursor type (μmol)	Crude polymer					
		(g)	Activity[b]	1-hexene (mol%)		Melting point (°C)	PDI
				IR	NMR		
11	**I** (20)	2.09	20.9	27.8	26	118.9	24.5[c]
12	**II** (20)	1.63	16.3	23.8		120.3	

[a] Reaction conditions: $Et_3Al_2Cl_3$/Ti = 3 mol/mol; Al-$^{i}Bu_3$/Ti = 50 mol/mol; T = 30 °C; P_{C2H4} = 0.1 MPa; 1-hexene = 30 mL; t = 5 h; solvent = chlorobenzene, total volume = 65 mL. [b] Activity expressed as $kg_{polymer}\ mol_{Ti}^{-1}\cdot h^{-1}$. [c] M_w = 350000, M_n = 14300.

When **II** was adopted as catalyst precursor (entry 12, Table 3), under analogous reaction conditions as those used in entry 11, a slightly decrease in productivity was observed (16.3 $kg_{polymer}\ mol_{Ti}^{-1}\cdot h^{-1}$), the resulting crude polymeric product showed melting temperature of 120.29 °C.

However, when the experiment was repeated for comparison, employing a conventional catalyst based on $TiCl_4$ (entry 13, Table 4), a completely different behavior was ascertained and both the productivity and 1-hexene incorporation were lower than those obtained by titanium carbamato precursors at the same reaction conditions.

Table 4. Ethylene/1-hexene copolymerization employing $TiCl_4/Et_3Al_2Cl_3/Al\text{-}^iBu_3$ as catalyst [a]

Entry	Ti precursor type (μmol)	Crude polymer			
		(g)	Activity[b]	1-hexene (mol%)	Melting point (°C)
13	**$TiCl_4$** (20)	1.04	10.4	22.8	121.1

[a] Reaction conditions: $Et_3Al_2Cl_3/Ti$ = 3 mol/mol; $Al\text{-}^iBu_3/Ti$ = 50 mol/mol; T = 30 °C; P_{C2H4} = 0.1 MPa; 1-hexene = 30 mL; t = 5 h; solvent = chlorobenzene, total volume = 65 mL. [b] Activity expressed as $kg_{polymer}\ mol_{Ti}^{-1}\cdot h^{-1}$.

Analysis of polymer samples by SEC (Figures 5 and 6) revealed in any case relatively high molecular weights with broad polydispersities, an indication of a multisite catalyst nature. The distribution of molecular weight for the polymer obtained with the precursor **III** appears as a unimodal broad peak, centered at 371,000 (MW), and the other, obtained with the precursor **I,** as a broad one with shoulder with 350,000 (MW).

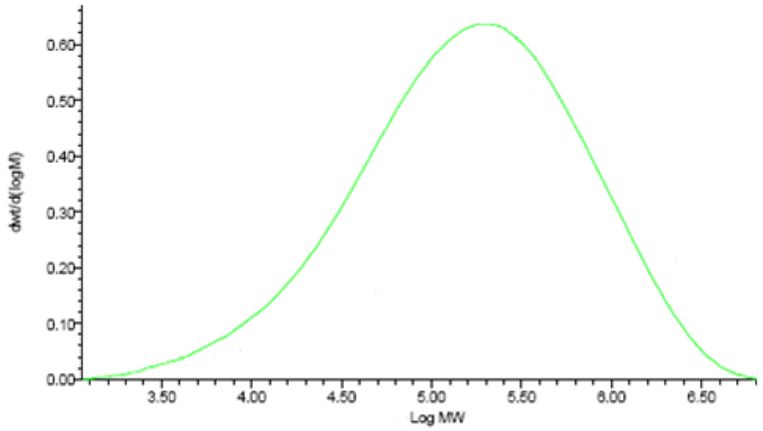

Figure 5. GPC curve of ethylene/1-hexene copolymer obtained from entry 3.

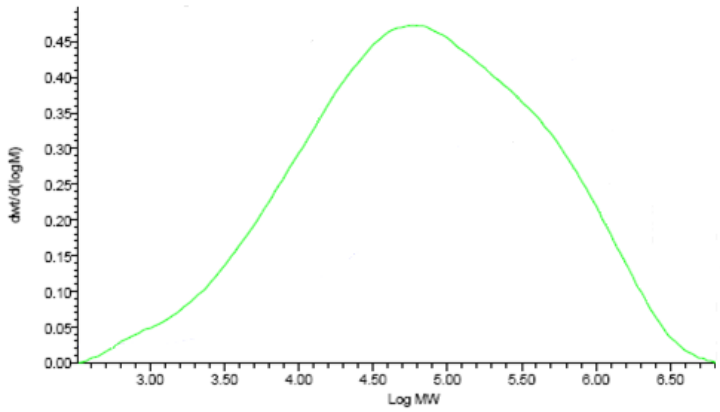

Figure 6. GPC curve of ethylene/1-hexene copolymer obtained from entry 11.

There is a strong dependence of the melting temperature on the molar ratio of the α-olefin in the copolymer (Figure 7). The melting temperature decreases up to 119.1 °C for a copolymer containing 28 mol % of 1-hexene. Moreover, the crystallization temperature of the copolymer samples, as determined by thermal measurements, substantially showed a monotonic decrease with increasing the comonomer content (Figure 8). Similar melting point depressions have been observed in the case of random copolymers of ethylene and 1-hexene synthesized using metallocene catalyst.[26]

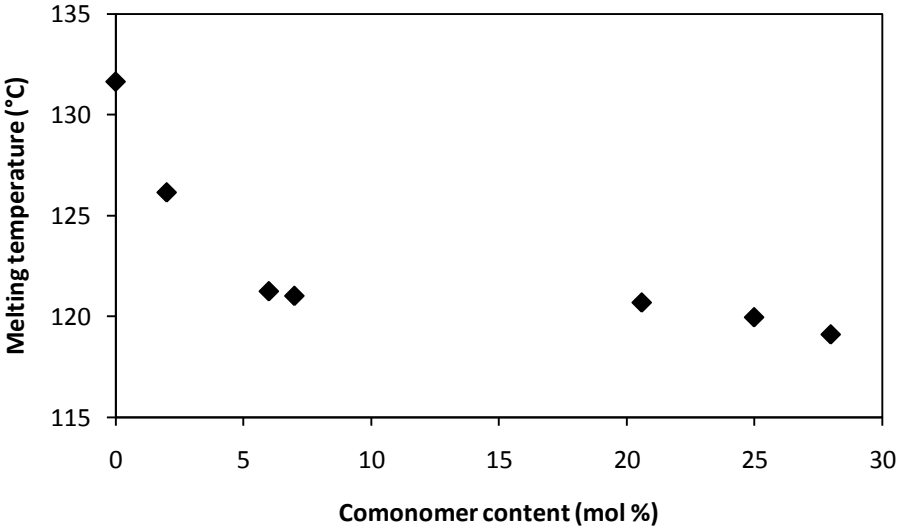

Figure 7. Effect of 1-hexene incorporation on the melting temperature of ethylene/1-hexene copolymers obtained with **III**/ $Et_3Al_2Cl_3$/Al-$^{i}Bu_3$ as catalyst.

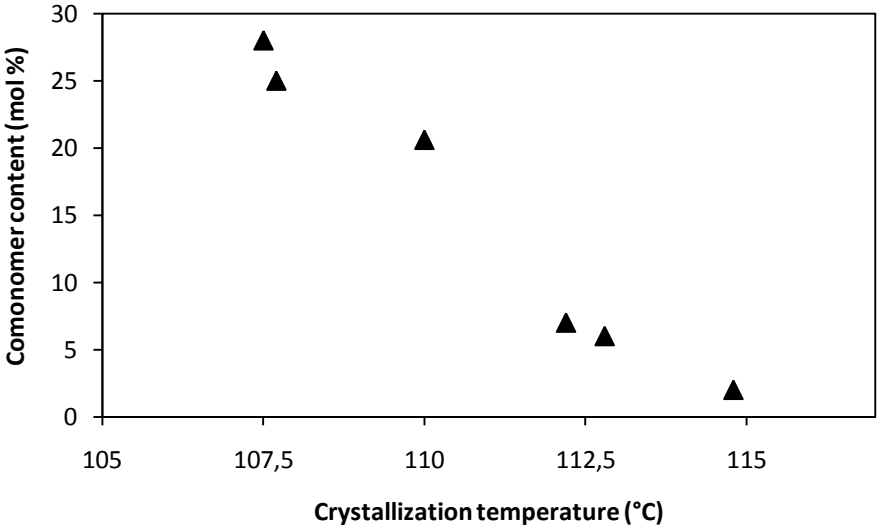

Figure 8. Effect of comonomer content on the crystallization temperature of copolymers.

5.2.2 Copolymerization of ethylene with 1-hexene in the presence of titanium precursors (I-III)/MAO as catalytic system

The homopolymer of ethylene was synthesized for reference purpose. When the catalytic system based on **III** precursor was employed (entry 14, Table 5) a moderate productivity was observed, giving polyethylene with melting point of 133 °C.

Table 5. Homopolymerization of ethylene using **III**/MAO catalytic system [a]

Entry	Ti precursor (μmol)	P_{C2H4} (MPa)	Time (h)	Crude Polymer (g)	Activity[b]	Melting point (°C)
14	**III** (20)	0.1	0.5	0.41	41	133.3

[a] Reaction conditions: T = 25 °C; Al/Ti = 300 mol/mol; solvent = chlorobenzene, total volume = 65 mL. [b] Activity expressed as $kg_{polymer}\ mol_{Ti}^{-1} \cdot h^{-1}$.

When $Et_3Al_2Cl_3$/Al-$^{i}Bu_3$ was replaced by MAO as cocatalyst for the copolymerization of ethylene with 1-hexene, a great improvement of productivity was ascertained, even at short reaction times (entries 15-25, Table 6). A preliminary experiment (entry 15, Table 6) was carried out by using **III** as catalytic precursor in the presence of MAO and the positive effect of the comonomer was observed; for example, the catalytic activity at 0.1 MPa pressure of ethylene and 20 mL of 1-hexene in the feed was higher than that of the homopolymerization of ethylene at 0.1 MPa (entry 14 in Table 5 *vs*. Entry 15 in Table 6) and it reached to 86 $kg_{polymer}\ mol_{Ti}^{-1} \cdot h^{-1}$.

A further decrease of relative amount of 1-hexene (entries 16 and 17, Table 6) reduced the productivity, suggesting positive effect of high comonomer concentration on the enhancement of productivity in the adopted conditions.[27]

Table 6. Ethylene/1-hexene copolymerization using titanium carbamato precursor **III** activated by MAO[a]

Entry	Ti precursor type (μmol)	Feed		Al/Ti (mol/mol)	Crude polymer				
		P_{C2H4} (MPa)	1-hexene (mL)		(g)	Activity[b]	1-hexene (mol %)		Melting point (°C)
							IR	NMR	
15	**III** (20)	0.1	20	300	0.86	86	17.8	17.0	85.0
16	**III** (20)	0.1	10	300	0.69	69	16.9	16.0	105.6
17	**III** (20)	0.1	5	300	0.51	51	14.2		111.9
18	**III** (20)	0.1	20	150	0.48	48	21.5		83.2
19	**III** (20)	0.1	20	600	0.74	74	21.0		88.0
20	**III** (20)	1	20	300	4.23	423	10.9	11.0	116.5
21[c]	**III** (20)	1	20	300	3.73	373	12.9		115.6
22[d]	**III** (12)	1	20	300	2.10	1093	8.7	8.5	117.0
23[e]	**III** (20)	0.1	20	300	0.08	8	9.4	10.5	116.6
24[f]	**III** (20)	0.1	20	300	0.02	2	n.d.		
25[g]	**III** (29)	0.1	20	300	4.49	309	>30		No T_m

[a] Reaction conditions: T = 25 °C; t = 0.5 h; solvent = chlorobenzene, total volume = 65 mL, if not otherwise specified. [b] Activity expressed as $kg_{polymer}\ mol_{Ti}^{-1} \cdot h^{-1}$.

[c] T = 50 °C. [d] t = 10 min. [e] Solvent = toluene. [f] Solvent = n-heptane. [g] Cocatalyst = DMAO.

The activities by **III** were dependent upon the Al/Ti molar ratios employed (Figure 9). Complex **III** displayed the highest catalytic activity of 86 kg $kg_{polymer}$ $mol_{Ti}^{-1} \cdot h^{-1}$ with Al/Ti molar ratio of 300/1 at room temperature under adopted condition. Even if the Al/Ti molar ratio was as low as 150, the activity of **III** was still moderate (48 $kg_{polymer}$ $mol_{Ti}^{-1} \cdot h^{-1}$). Further increase in Al/Ti ratio from 300 to 600 led to a reduction in the catalytic activity up to 74 $kg_{polymer}$ $mol_{Ti}^{-1} \cdot h^{-1}$.

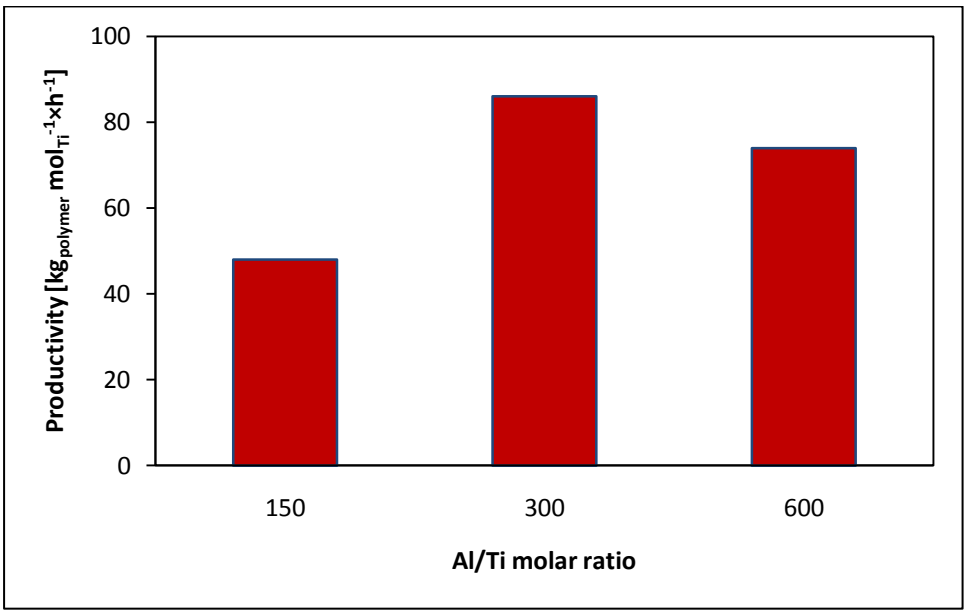

Figure 9. Productivity of the catalytic system based on pre-catalyst **III** *versus* Al/Ti molar ratio in ethylene/1-hexene copolymerization.

On the basis of obtained results, the increase of ethylene pressure caused a remarkable improvement of the productivity up to 423 $kg_{polymer}$ $mol_{Ti}^{-1} \cdot h^{-1}$. Obviously, The T_m values of copolymers increase gradually along with ethylene pressure (entries 20 and 22, Table 6).

The reaction temperature significantly affected the catalytic activities; the higher the reaction temperature the lower the catalytic activity obtained (entry 21, Table 6). This is in agreement with the trends observed in propylene homopolymerizations, where the highest activity was observed at 25 °C and might be due to the occurrence of catalyst deactivation processes at higher temperatures.

When the reaction time decreased to 10 min together with a lower concentration of the pre-catalyst (12 μmol), significant improvement was obtained in terms of activity (1093 $kg_{polymer}$ $mol_{Ti}^{-1} \cdot h^{-1}$) which was approximately two-times more than that obtained at long reaction time (compare entry 20 with 22, Table 6), indicating that prolonging the reaction time may proceed deactivation of active catalytic species in reaction medium. However, comonomer incorporation was reduced with shortening the reaction time.

In the case of solution and slurry polymerization, the nature of the solvent is one of the most important factors, which can affect the catalytic polymerization behaviors. It was found that using chlorobenzene as the polymerization medium, activity was the highest followed by that in toluene and heptane (Figure 10). This indicated that once again (see chapters 5 and 6) the higher polarity of solvent resulted in a high activity.

Furthermore, 1-hexene insertion is decreasing from 17 to 9 mol % by passing from chlorobenzene to toluene. The lower 1-hexene reactivity observed in toluene can be reasonably correlated to the formation of stable complexes between the cation and the coordinating solvent, i.e. toluene, on which the 1-hexene insertion is disfavored with respect to less bulkier comonomers.[28,29]

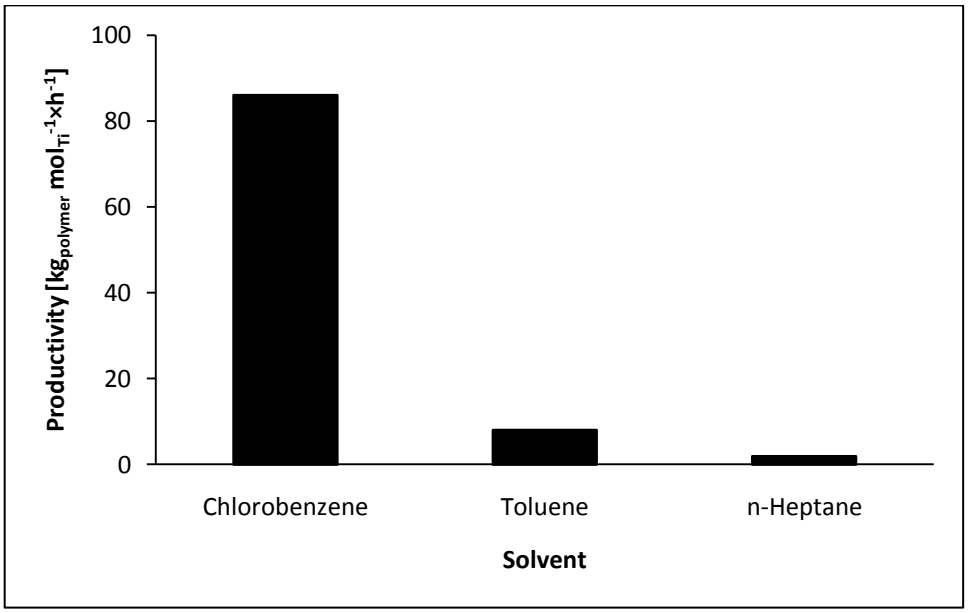

Figure 10. Effect of solvent on the catalytic activity of **III**/MAO system.

When MAO was replaced by DMAO as cocatalyst (entry 25, Table 6), under analogous reaction conditions as those used in entry 15, a rubbery amorphous product without detected melting point in DSC was obtained, together with a much higher productivity, suggesting that a high TMA content in MAO favors the reduction of titanium to the lower valent states that do not catalyze the polymerization reaction.

When **I** was employed for ethylene/1-hexene copolymerization under similar conditions, as previously performed with **III** (entry 15 in Table 6 *vs*. entry 26, Table 7), a decrease in catalytic activity was ascertained together with an improvement in 1-hexene insertion up to approximately 21 mol%.

An increase in ethylene pressure at shorter reaction time led to slightly improvement in the productivity (90 $kg_{polymer}$ $mol_{Ti}^{-1} \cdot h^{-1}$) with reduction of comonomer incorporation and hence, increase of melting point. When heptane was used as solvent, only traces of product was obtained (entry 28, Table 7).

Table 7. Ethylene/1-hexene copolymerization using titanium carbamato precursors **I and II** activated by MAO[a]

Entry	Ti precursor (μmol)	Feed		Crude polymer			
		P_{C2H4} (MPa)	1-hexene (mL)	(g)	Activity[b]	1-hexene[c] (mol%)	Melting point (°C)
26	**I** (20)	0.1	20	0.70	70	21.4	83.7
27[d]	**I** (12)	1	20	0.18	90	5.5	118.3
28[e]	**I** (20)	0.1	20	trace	-		
29	**II** (20)	0.1	20	0.08	8		116.8
30[d]	**II** (12)	1	20	0.09	43.5	7.9	122.2

[a] Reaction conditions: T = 25 °C; t = 0.5 h; Al/Ti = 300 mol/mol; solvent = chlorobenzene, total volume = 65 mL, if not otherwise specified. [b] Activity expressed as $kg_{polymer}$ $mol_{Ti}^{-1} \cdot h^{-1}$. [c] Content of 1-hexene co-units in the copolymer, as determined by FTIR microscopy. [d] t = 10 min. [e] Solvent = n-heptane.

Finally, when **II** was employed as catalytic precursor (entry 29, Table 7) a very low productivity was obtained in comparison with the catalysts based on **I** and **III** under similar reaction conditions (Figure 11). The increase of relative ethylene pressure in the feed at short reaction time allowed to remarkable improve, more than five-times, the productivity (43.5 $kg_{polymer}$ $mol_{Ti}^{-1} \cdot h^{-1}$). However, the increase of ethylene pressure in the

feed caused a drop of comonomer incorporation and a raise of melting temperature of the resulting polymeric material.

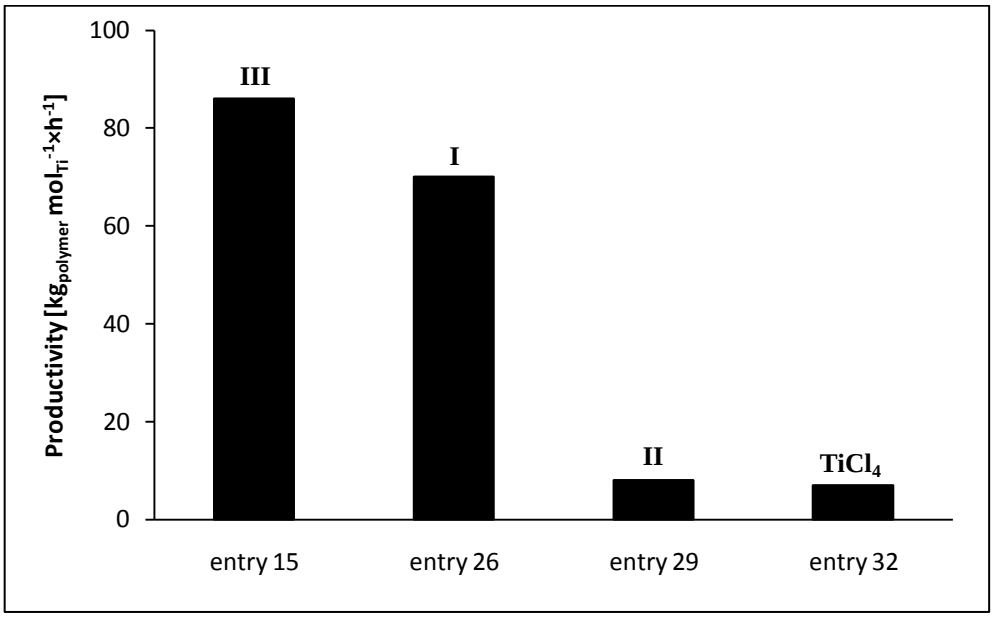

Figure 11. Catalysts' productivity in ethylene/1-hexene copolymerization as a function of the type of titanium precursor.

When a reference conventional catalyst , based on $TiCl_4$, was adopted (entry 32, Table 8) under the same conditions as in entries 15, 26 and 29 lower activity was ascertained.

Table 8. Ethylene/1-hexene copolymerization employing $TiCl_4$/MAO as catalyst [a]

Entry	$TiCl_4$ (μmol)	Feed		Crude polymer	
		P_{C2H4} (MPa)	1-hexene (mL)	(g)	Activity[b]
31	20	0.1	-	0.17	17
32	20	0.1	20	0.07	7

[a] Reaction conditions: T = 25 °C; t = 0.5 h; Al/Ti = 300 mol/mol; solvent = chlorobenzene, total volume = 65 mL. [b] Activity expressed as kg$_{polymer}$ mol$_{Ti}^{-1}$·h^{-1}.

Copolymer compositions could be determined by ^{13}C NMR spectroscopy. The ^{13}C NMR spectra of ethylene-1-hexene copolymers with 1-hexene content up to 17.3 mol % have been already reported in the literature.[30-33] A typical ^{13}C NMR spectra on our sample is presented in Figure 12.

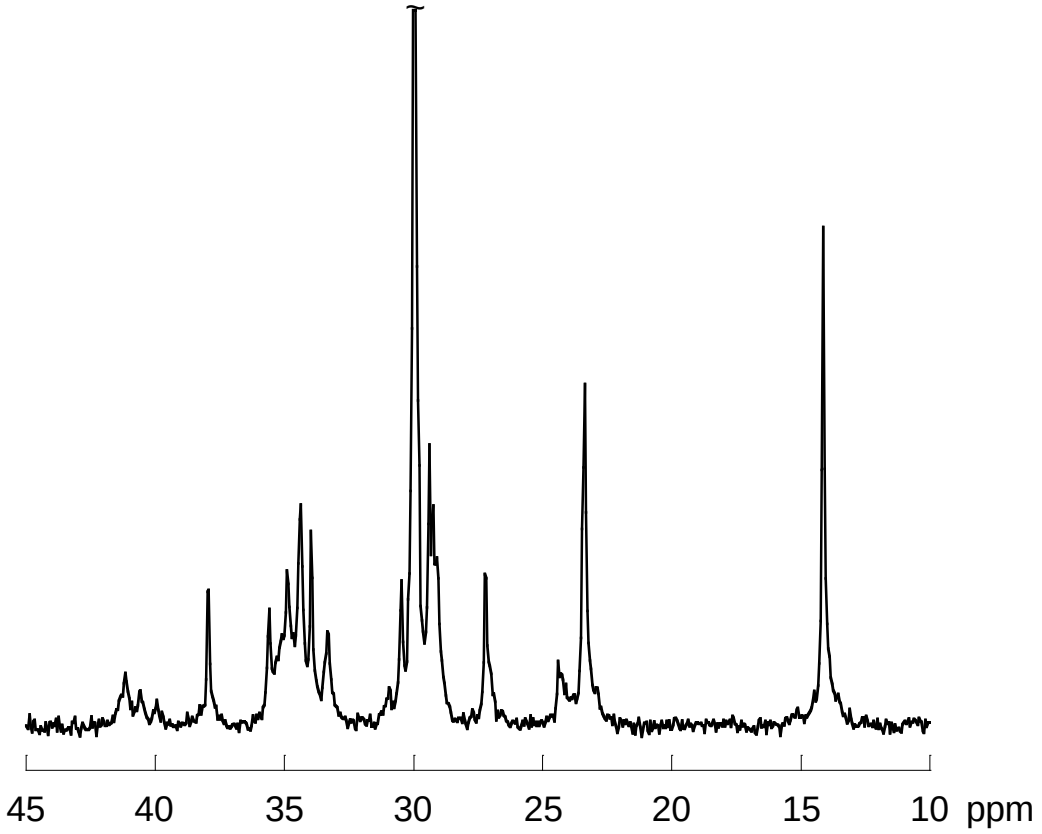

Figure 12. ^{13}C NMR spectrum of the sample obtained from entry 11, containing 26 mol% 1-hexene content.

A quantitative determination of triad sequences was made for some samples following Hsieh et al.[30] by integration of the regions of interest, and verified by using the individual peak areas determined by spectral deconvolution. From the triad sequence composition the average sequence lengths for the ethylene ($\bar{n}_E$) and 1-hexene ($\bar{n}_H$) monomers, given by the ratio of monomer mole fraction and 1-hexene runs per average molecule, N, ([N]=1/2 [HE]) [30], were obtained.

It is interesting to underline that the composition of the examined copolymers, as determined by NMR analysis, is in substantial agreement with that obtained by FTIR and DSC analysis.

Table 9. Observed 1-hexene mole fractions, average sequence lengths and triad distribution.[a]

Entry				Triad distribution					
	[H]	$\overline{n}_H$	$\overline{n}_E$	[EHE]	[EHH]	[HHH]	[HEH]	[HEE]	[EEE]
3	0.28	1.8	4.5	0.07	0.18	0.03	0.08	0.16	0.48
4	0.06	1.0	15.7	0.06	0.00	0.00	0.00	0.12	0.82
11	0.26	2.1	5.9	0.10	0.05	0.11	0.08	0.09	0.57
15	0.17	1.3	6.4	0.11	0.04	0.02	0.03	0.20	0.60
16	0.16	1.3	6.7	0.12	0.04	0.00	0.04	0.17	0.63

[a] H = 1-hexene, E = ethylene

5.3 Conclusion

In this chapter we have reported the use of titanium(IV) precursors **I-III**, based on bidentate carbamato ligands, in the copolymerization of ethylene with 1-hexene, in the presence of organoaluminium cocatalysts. All the pre-catalysts were active in the copolymerization, afforded copolymers with high 1-hexene incorporation within the copolymer chain, under adopted conditions. Upon activation with DMAO, higher activity was obtained compared to the MAO and $Et_3Al_2Cl_3$/Al-$^{i}Bu_3$ cocatalyst systems. Precursor **III** based catalytic systems are much more active than those derived from **I** and **II** to afford copolymeric materials with modulable composition(8-22 mol% of H co-units) as a function of adopted reaction conditions. Polymerization conditions, such as temperature, solvent, pressure of ethylene and Al/Ti ratio show considerable effects on the catalytic activity and comonomer insertion. The main characteristics of the E/H copolymers are dependent on the functionalization extent. The GPC results confirm that the obtained polymers feature relatively high molecular weight and broad M_w/M_n ratio. The ^{13}C NMR analysis of selected polymeric products has allowed to conclude that these materials are really copolymers where isolated H units are inserted in ethylene sequences.

5.4 References

[1] Univation Technologies – Market Information, http://www.univation.com.

[2] McKnight, A. L.; Waymouth, R. M. *Chem. Rev.* **1998**, *98*, 2587.

[3] Müller, A. J.; Hernandez, Z. H.; Arnal, M. L.; Sanchez, J. J. *Polym. Bull.* **1997**, *39*, 465.

[4] Czaja, K.; Sacher, B.; Bialek, M. *J. Therm. Anal. Calorim.* **2002**, *67*, 547.

[5] James, D. E. *Encyclopedia of Polymer Science and Engineering*; Mark, H. F.; Bikales, N. M.; Overberger, C. G.; Menges, G., Eds.; Wiley-Interscience: New York, 1985; Vol. 6, p 429.

[6] Wright, K. J.; Lesser, A. J. *Macromolecules* **2001**, *34*, 3626.

[7] Bracco, S.; Comotti, A.; Simonutti, R.; Camurati, I.; Sozzani, P. *Macromolecules* **2002**, *35*, 1677.

[8] Gupta, P.; Wilkes, G. L.; Sukhadia, A. M.; Krishnaswamy, R. K.; Lamborn, M. J.; Wharry, S. M.; Tso, C. C.; DesLauriers, P. J.; Mansfield, T.; Beyer, F. L. *Polymer* **2005**, *46*, 8819.

[9] Peacock, A. J. *Handbook of Polyethylene: Structures, Properties, and Applications*; Marcel Dekker: New York, 2000; p 123.

[10] Shan, C. L. P.; Soares, J. B. P.; Penlidis, A. *J. Polym. Sci. Part A: Polym. Chem.* **2002**, *40*, 4426.

[11] Madkour, T. M.; Goderis, B.; Mathot, V. B. F.; Reynaers, H. *Polymer* **2002**, *43*, 2897.

[12] Suhm, J.; Schneider, M. J.; Mülhaupt, R. *J. Polym. Sci. Part A: Polym. Chem.* **1997**, *35*, 735.

[13] Suhm, J.; Schneider, M. J.; Mülhaupt, R. *J. Mol. Catal. A: Chem.* **1998**, *128*, 215.

[14] Oakes, D. C. H.; Gibson, V. C.; White, A. J. P.; Williams, D. J. *Inorg. Chem.* **2006**, *45*, 3476.

[15] Park, S.; Han, Y.; Kim, S. K.; Lee, J.; Kim, H. K.; Do, Y. *J. Organomet. Chem.* **2004**, *689*, 4263.

[16] Chum, P. S.; Swogger, K. W. *Prog. Polym. Sci.* **2008**, *33*, 797.

[17] Arriola, D. J.; Carnahan, E. M.; Hustad, P. D.; Kuhlman, R. L.; Wenzel, T. T. *Science* **2006**, *312*, 714.

[18] Carlini, C.; D'Alessio, A.; Giaiacopi, S.; Po, R.; Pracella, M.; Raspolli Galletti, A. M.; Sbrana, G: *Polymer* **2007**, *48*, 1185.

[19] Herfert, N.; Montag, P.; Fink, G. *Makromol. Chem.* **1993**, *194*, 3167.

[20] Lehmus, P.; Härkki, O.; Leino, R.; Luttikhedde, H. J. G.; Näsman, J. H.; Seppälä, J. V. *Macromol. Chem. Phys.* **1998**, *199*, 1965.

[21] Camurati, I.; Cavicchi, B.; Dall'Occo, T.; Piemontesi, F. *Macromol. Chem. Phys.* **2001**, *202*, 701.

[22] Villar, M. A.; Ferreira, M. L. *J. Polym. Sci. Part A: Polym. Chem.* **2001**, *39*, 1136.

[23] Quijada, R.; Rojas, R.; Mauler, R. S.; Galland, G. B.; Scipioni, R. B. *J. Appl. Polym. Sci.* **1997**, *64*, 2567.

[24] Shan, C. L. P.; Soares, J. B. P.; Penlidis, A. *J. Polym. Sci. Part A: Polym. Chem.* **2002**, *40*, 4426.

[25] (a) Intaragamjon, N.; Shiono, T.; Jongsomjit, B.; Praserthdam, P. *Catal. Commun.* **2006**, *7*, 721. (b) Chapters 5 and 6 in this thesis.

[26] Zhang, P.; Li, Y.; Chai, Y. *e-Polymers* **2008**, no. 009.

[27] Awudza, J. A. M.; Tait, P. J. T. *J. Polym. Sci. Part A: Polym. Chem.* **2008**, *46*, 267.

[28] Forlini, F.; Tritto, I.; Locatelli, P.; Sacchi, M. C.; Piemontesi, F. *Macromol. Chem. Phys.* **2000**, *201*, 401.

[29] Forlini, F.; Princi, E.; Tritto, I.; Locatelli, P.; Sacchi, M. C.; Piemontesi, F. *Macromol. Chem. Phys.* **2002**, *203*, 645.

[30] Hsieh, E. T.; Randall, J. C. *Macromolecules* **1982**, *15*, 1402.

[31] Dorman, D. E.; Otocka, E. P.; Bovey, F. A. *Macromolecules* **1972**, *5*, 574.

[32] Randall, J. C. *J. Polym. Sci. Polym. Phys. Ed.* **1973**, *11*, 275.

[33] Assumption, H. J.; Vermeulen, J. P.; Jarrett, W. L.; Mathias, L. J.; van Reenen, A. J. *Polymer* **2006**, *47*, 67.

6 Structural and Thermal Investigation of Ethylene/1-Hexene Random Copolymers Having high Comonomer Content: Insights into the Isothermal Crystallization Behavior

6.1 Introduction

Linear low-density polyethylene (LLDPE), generally produced by the copolymerization of ethylene with various comonomers such as 1-butene, 1-hexene and 1-octene, is an important class of commercial polymers because of their specific properties making them applicable in a variety of sectors in our daily life such as plastic bags and sheets, toys, pipes and cables.

The properties of these materials are strongly related not only to the type and amount of the α-olefin comonomer in the polymer but also to its distribution along the polymer chain. Differences in comonomer content and distribution can cause significant changes in the polymer properties, such as differences in melting and glass transition temperatures, melt viscosity, mechanical and optical properties, all of them determine the type and range of application of these materials. The control of the properties can be obtained by using appropriate catalytic systems which offer the opportunity of tailoring the polymer micro-structure.

Extensive studies have been directed to the use of homogeneous metallocene[1,2,3,4] and non-metallocene[5,6,7] catalysts in the synthesis of ethylene copolymers with different types and amounts of branching, producing narrow distributions of molecular weight and a random insertion of the comonomer units in the backbone, as compared to conventional Ziegler-Natta catalysts. However, more recently the research has been devoted to the study of new copolymerization catalysts, which may offer a higher versatility and lower costs with respect to the other catalytic systems.[8]

In this regard, the homo- and copolymerization of ethylene with 1-hexene in the presence of titanium precursors bearing bidentate *N*,*N*-dialkylcarbamato ligands or chloro substituted *N*,*N*-dialkylcarbamate ones as catalytic precursors were already described in the previous chapters. In the present chapter, we report on the characterization of the above ethylene-1-hexene (E/H) copolymers by means of spectroscopic and calorimetric methods.

Fourier transform infrared spectroscopy (FTIR) has become one of the more often used spectroscopic techniques for the analysis of structure, composition, stereoregularity and

crystallinity of polymers.[9] The combination of a microscope with the FTIR spectrometer, the so called FTIR-microspectroscopy (FTIR-M)[10,11], represents a powerful tool which make it possible to analyse different microareas of a sample, allowing correlation of the molecular structure with morphology and a better resolution as compared to the overall infrared spectrum of the same polymer. Polyethylene and its copolymers with 1-alkenes have been deeply investigated, in terms of crystallinity, conformational changes and chain branching, with spectroscopic tools.[12,13,14] To estimate the chain branching in ethylene copolymers several FTIR methods have been applied, however, these methods requires polymeric films with a uniform thickness and can be applied to macroareas with size on the scale of 10^3 μm, while FTIR-M permits to examine areas of 10^2-10^1 μm in diameter, giving the opportunity of selecting different zones of the same sample, even with non-uniform thickness. On the other hand, the α-olefin incorporation into polymer chain influences the crystalline structure and the thermodynamic properties, with consequent changes of crystalline morphology and phase transition processes as well as of the dynamic-mechanical behavior. The thermal behavior of various ethylene copolymers has been extensively studied as a function of type, content and distribution of comonomer. Although Pracella et al.[15] reported the structural characterization and isothermal crystallization behavior of E/H copolymers with 1-5 mol% comonomer content, however, the crystallization behavior of E/H copolymers with higher 1-hexene co-units has not yet been examined. In this chapter, we first analyzed the structural aspects of the copolymers applying a FTIR-M calibration method for the evaluation of comonomer content and studied the effect of thermal treatments on the crystallinity of the samples. Then we have considered the isothermal crystallization processes and melting behavior of E/H copolymers to get insights into the effect of 1-hexene content on the thermodynamic and kinetic parameters which control the nucleation and growth of polymer crystals.

6.2 Results and discussion

The comonomer content of the examined E/H copolymers is listed in Table 1, together with the values of DSC phase transition parameters.

Table 1. Composition and thermal properties of E/H copolymers.

Sample	1-Hexene content[a] (mol%)	1-Hexene content[b] (mol%)	$T_{c\ onset}$ °C	T_c °C	ΔH_c J.g^{-1}	T_m °C	ΔH_m J.g^{-1}
PE	-	-	121.6	118.8	-131.7	133.1	133.9
E/H1	1.8	2.0	118.0	115.4	-92.3	126.1	117.5
E/H2	6.0	6.8	112.1	110.2	-32.0	121.1	63.8
E/H3	24.0	24.5	111.6	108.5	-9.5	119.9	15.3
E/H4	28.0	28.2	110.1	107.4	-8.9	118.9	6.8

[a] ^{13}C NMR data; [b] FTIR data

6.2.1 FT-IR analysis

According to Pracella's[15] finding, we have concentrated on three main frequency regions for the FTIR-M analysis of E/H copolymers: 1500-1400, 1400-1320 and 750-690 cm^{-1}. The region from 1400 to 1320 cm^{-1} is mostly useful for the compositional analysis of ethylene/α-olefin copolymers. In this region, Figure 1 shows the spectra of the E/H standard copolymers, as well as of PE and PH homopolymers. There is only little difference of absorbance among the various examined microdomains as shown by FTIR-M spectra recorded for each sample.

The absorbance bands at 1378 and 1369 cm^{-1} have been considered: the former is related to the symmetric deformation of the methyl end-group of 1-hexene units, while the latter is ascribed to the methylene units wagging.[16,17,18] It can be seen that the intensity of the methyl band at 1378 cm^{-1} continuously increases with incorporation of 1-hexene along the PE backbone: it is very weak for E/H copolymer with 1.8 mol% of comonomer, due to the low 1-hexene content, but materials with higher comonomer contents present more intense absorptions with areas proportional to the branching content. Therefore, from the absorption ratio of these bands it is possible to estimate the total methyl branching amount, i.e. the comonomer content in each copolymer.

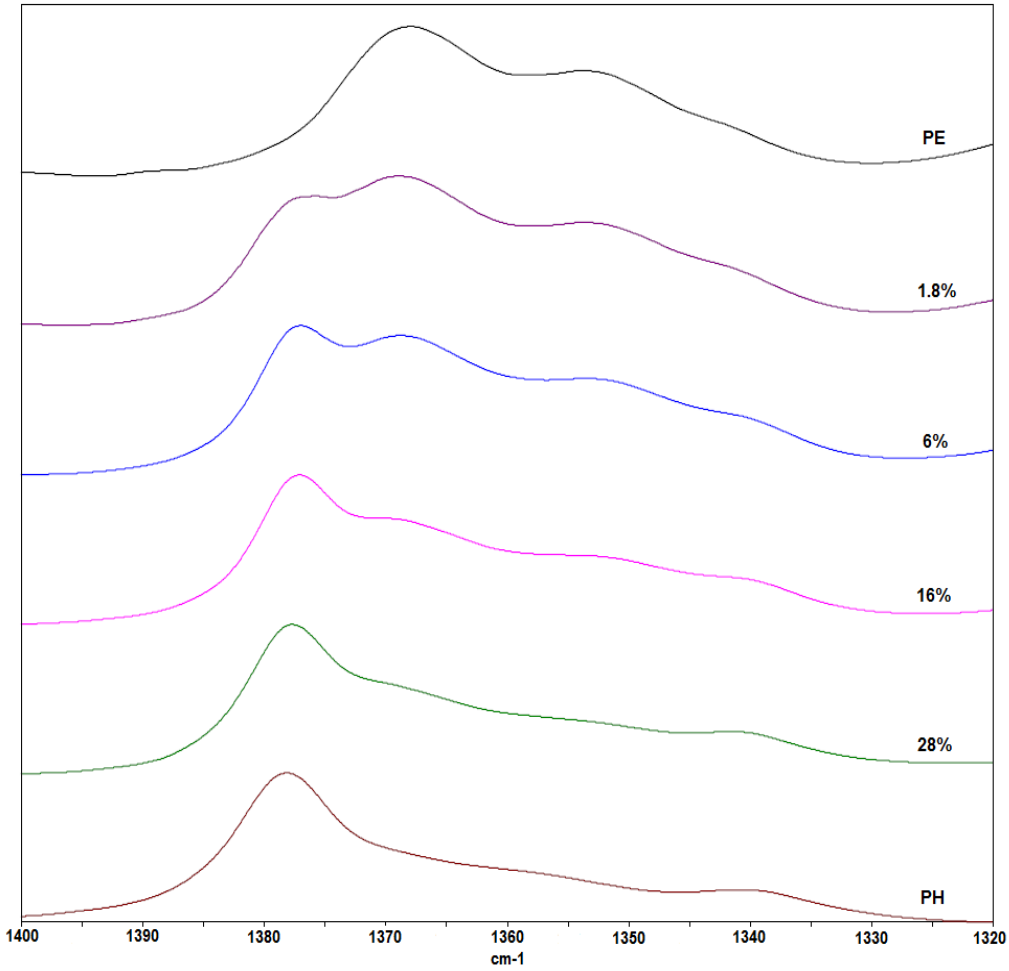

Figure 1. FTIR-M spectra of PE, PH and E/H copolymers (with known 1-hexene content in mol %) recorded in the region of 1400-1320 cm^{-1}.

For all the examined microareas the average normalized integrated areas in the ranges of 1385–1373 cm^{-1} (A_1) and 1373-1360 cm^{-1} (A_2) have been determined, then the ratio $R = A_1/A_2$, which is independent of the film thickness, has been related to the molar content of 1-hexene in the reference standard samples, as shown in Figure 2.

The linear plot in Figure 2 has been used to determine the comonomer content in the E/H copolymers obtained with the new titanium-based catalyst systems. The values of 1-hexene concentration obtained by FTIR-M, as reported in Table 1, show a very satisfactory agreement with those determined by ^{13}C NMR analysis.

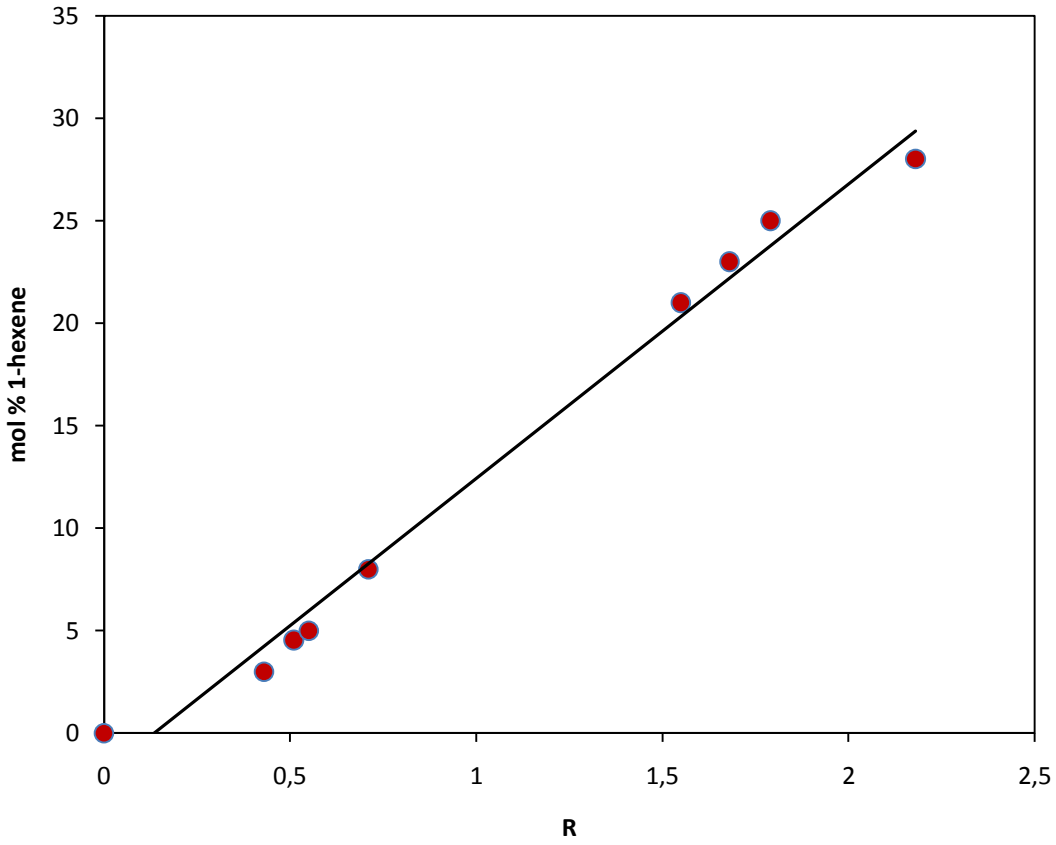

Figure 2. Calibration plot of 1-hexene mol percent versus the integrated areas ratio, $R = A_1/A_2$, in standard samples.

The regions 1500–1400 and 750–690 cm^{-1} were analyzed to evaluate the effect of comonomer content on the phase transitions of the samples. The former region consists of the absorption bands at 1473 and 1463 cm^{-1} due respectively to the bending of CH_2 sequences in the crystalline and amorphous phases of PE, respectively.[19,20]

As shown in Figure 3, linear PE shows two bands at 1473 and 1463 cm^{-1}, thus suggesting the presence of a well-organized crystalline structure. However, gradual insertion of 1-hexene units in the PE chains leads to a progressive change of intensity of the band at 1473 cm^{-1} [Figure 3(a)] as compared with the homopolymer: in fact, the absorbance of the crystalline bands decreases according to the comonomer content. This effect corresponds to the reduction of crystallinity degree due to the major disorder induced by the 1-hexene units.

The band at 720 cm^{-1} [Figure 3(b)], which is associated with the rocking vibration of methylene sequences, splits for PE into two components at 729 and 719 cm^{-1}

corresponding to in-phase and out-of-phase vibrations, respectively, in the case of an orthorhombic lattice.[21] Chain branching reduces the possibility for regular order in the chains, and thus reduces the crystalline content. This will therefore influence the relative intensities of the two bands; in linear PE these generally appear sharper than LLDPE, and the relative intensity of the 719 cm^{-1} band is somewhat stronger.

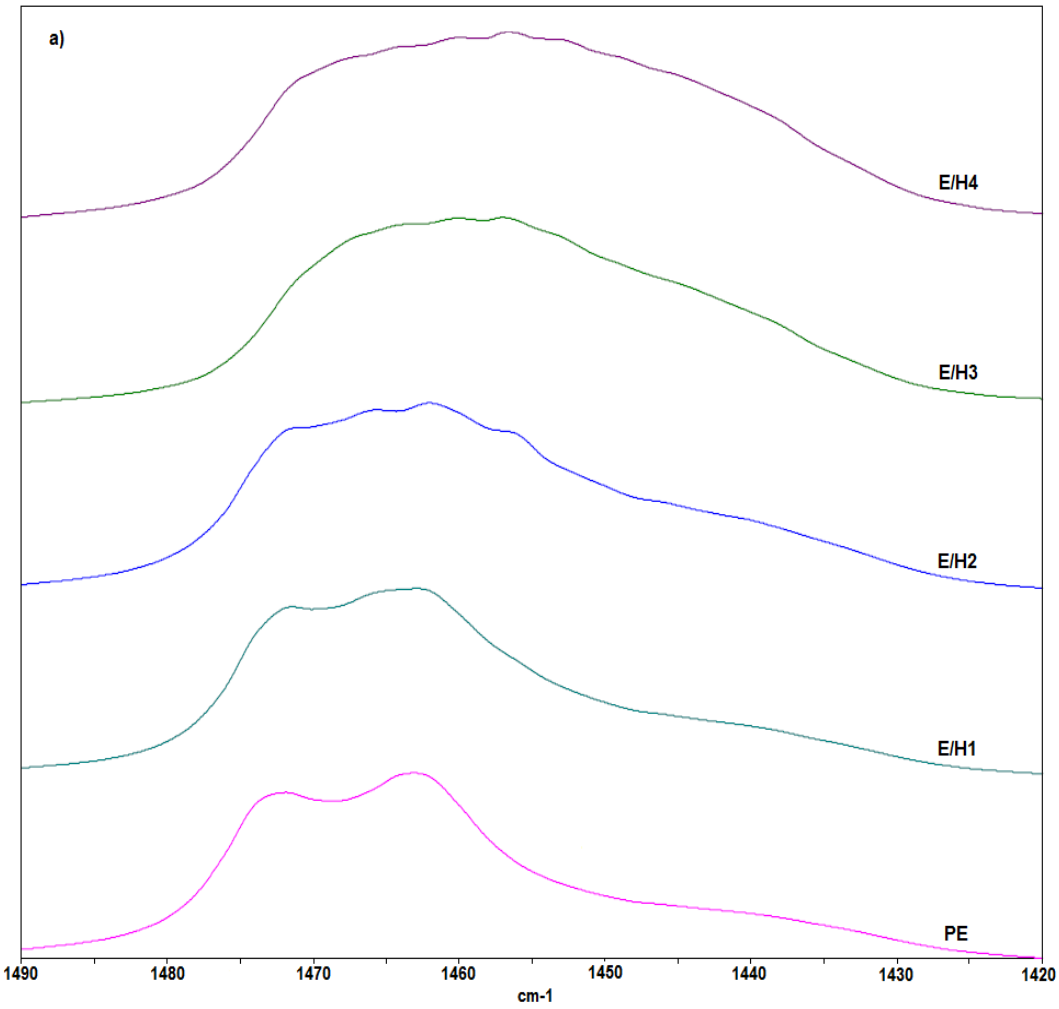

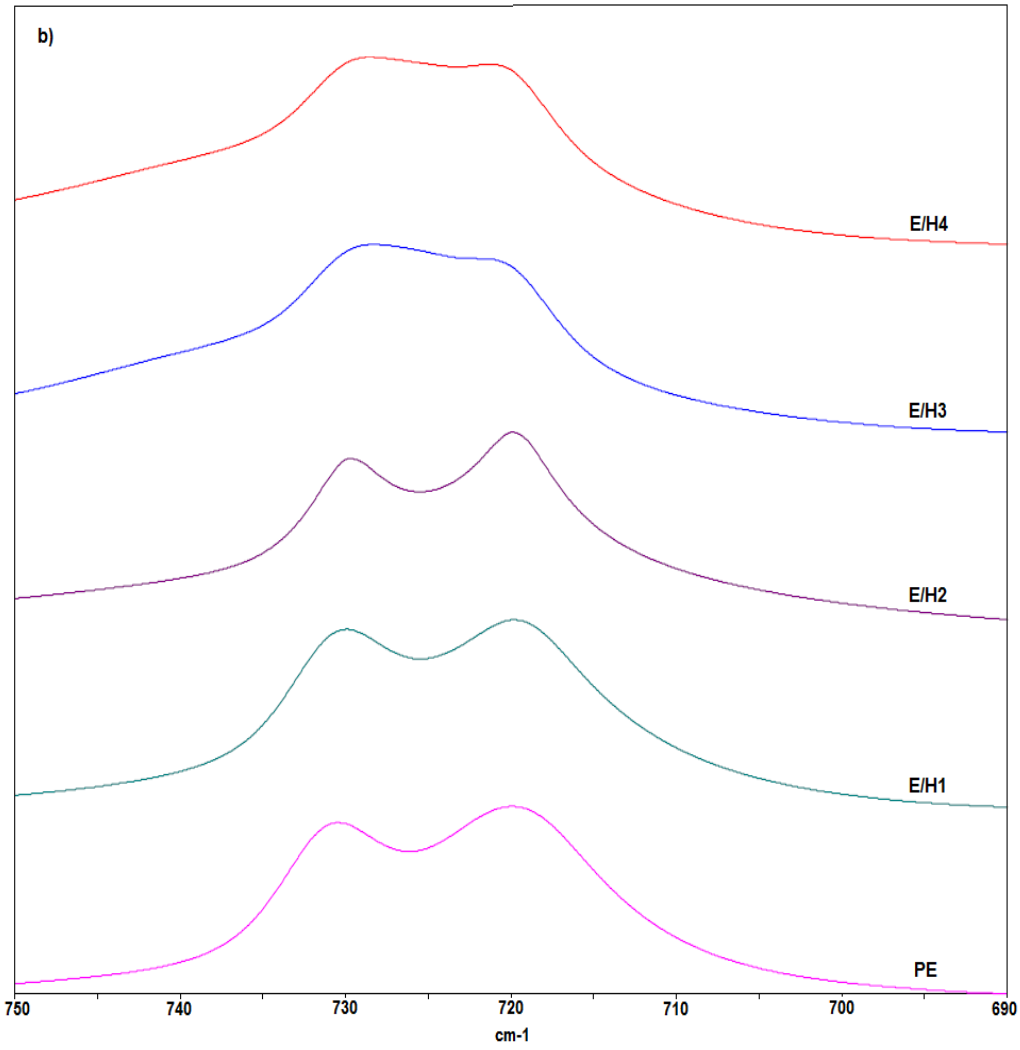

Figure 3. FTIR spectra of PE and E/H copolymers in the methylene bending (a) and rocking (b) absorbance regions.

The same behavior was reported by Wagener et al.[22] for irregularly sequenced E/H model copolymers, synthesized by step-growth acyclic diene metathesis (ADMET), while precisely sequenced ones showed no signs of orthorhombic crystal behavior.

6.2.2 Thermal behavior

The DSC cooling and melting (second run) thermograms of E/H copolymers and PE homopolymer are shown in Figure 4. The values of the crystallization (T_c) and melting

(T_m) temperatures as well as of the corresponding enthalpies (ΔH_c, ΔH_m) are summarized in Table 1.

On cooling from the melt [Figure 4(a)], all samples displayed a crystallization peak at a temperature close to that characteristic of linear PE. The values of T_c decreased with increase in the 1-hexene content from about 118 °C of PE to about 107 °C of E/H4, while the corresponding crystallization enthalpy underwent a drastic reduction from 131 to about 8 J g^{-1}. In the second heating run [Figure 4(b)], a single melting peak was found at temperatures below 135 °C. The peak became progressively broader and less intense as the comonomer content increased. The observed T_m values decreased from 133.1 °C for the homopolymer to 118.9 °C for the copolymer with the highest 1-hexene content (E/H4, 1-hexene content: 28 mol%), and the corresponding ΔH_m changed from about 133.9 to 6.8 J g^{-1}.

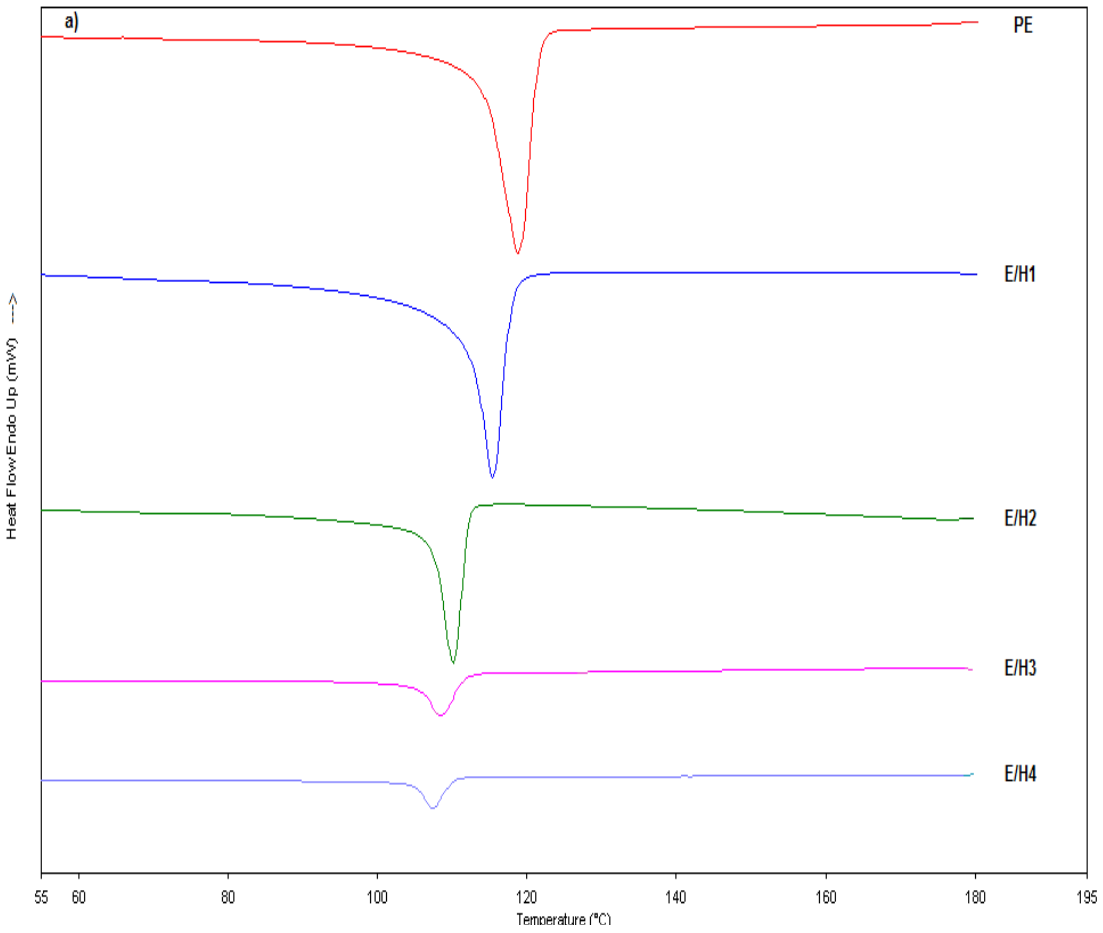

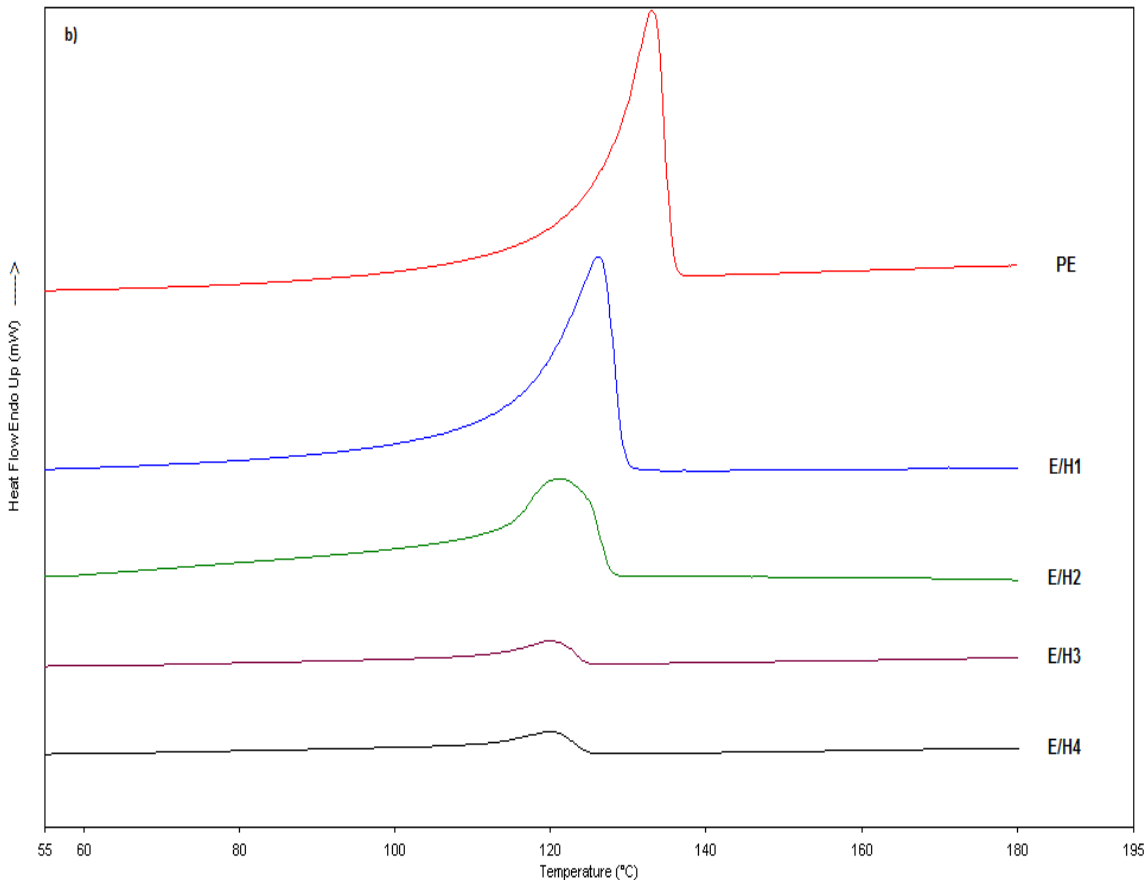

Figure 4. DSC cooling (a) and melting (b) thermograms of E/H copolymers and PE recorded at cooling/heating rate of 10 °C min^{-1}.

The values of the enthalpy of fusion (ΔH_m) of the copolymers examined on the second run versus the 1-hexene content are plotted in Figure 5. It shows that the ΔH_m decreases by increasing of comonomer content in the copolymers, where the number of chain irregularities also increases.[23]

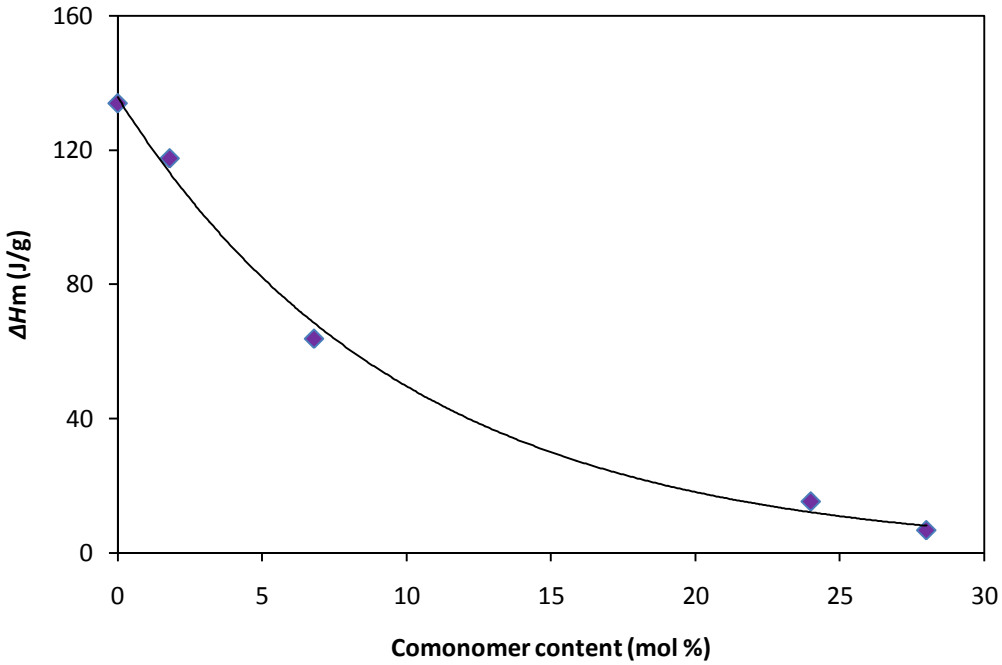

Figure 5. Plot of enthalpy of fusion ΔH_m versus comonomer content.

According to Burfield's analysis[23,24], the value of ΔH_m for a random copolymer should be related to polyethylene sequence length by eqn. (1), independently of the copolymer unit type.

$$\log_{10} \Delta H_m = \log_{10} k + n \log_{10} x_E \quad (1)$$

where k is a constant referring to the enthalpy of fusion of the parent homopolymer and x_E^n represents the probability of forming consecutive polyethylene sequences of n units (n being the critical sequence length below which chains will not crystallize). It follows that a plot of $\log_{10} \Delta H_m$ versus $\log_{10} x_E$ should give a straight line, whose slope is determined by the critical sequence length n:

In Figure 6, the values of $\log_{10} \Delta H_m$ of the copolymers examined are plotted as a function of logarithm of ethylene content (mol %); linear relationship is found with slope n = 8.5 (in the composition range from 2 to 28 mol% 1-hexene). Extrapolation to x_E = 100 mol% of ethylene content, gives a value of 131.2 J g^{-1} which found to be in good agreement with melting enthalpy of PE homopolymer, ΔH_m = 133.9 J g^{-1}, reported in Table 1.

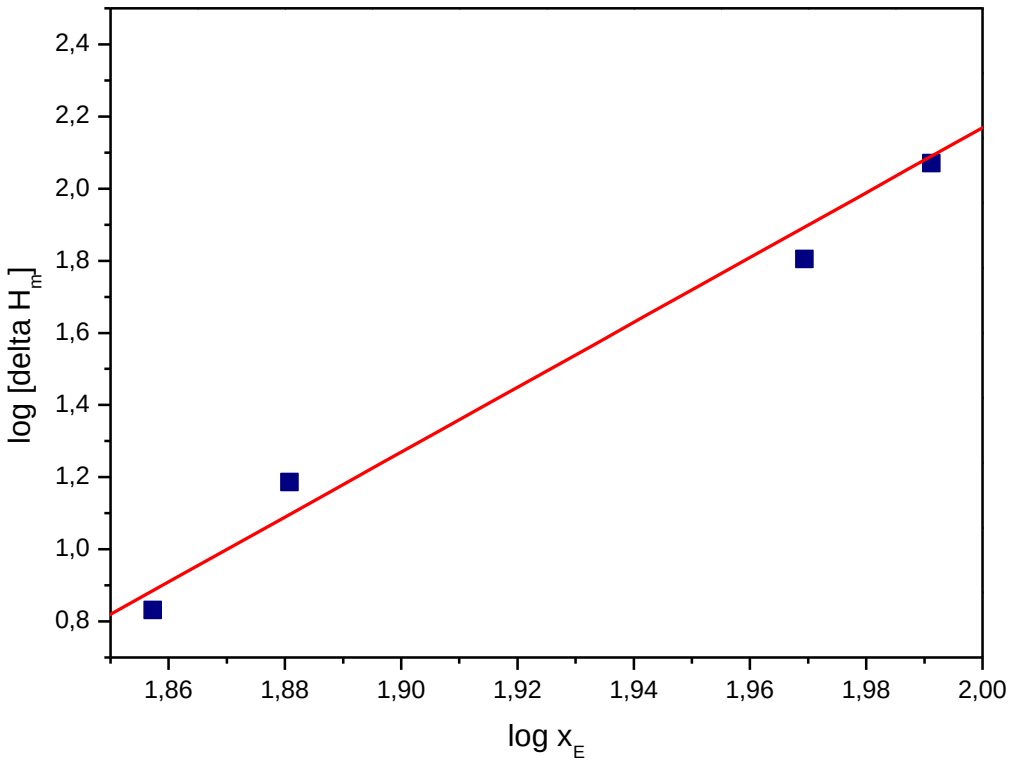

Figure 6. Logarithmic plot of ΔH_m versus mol% of ethylene (x_E) for the examined ethylene/1-hexene copolymers

6.2.3 Crystallization kinetics

The isothermal crystallization behavior of the polymer samples was examined by DSC in the range from 111 to 121 °C. In particular, the isothermal crystallization of E/H copolymers with high comonomer content was carried out at T_c lower than 116 °C, while E/H1 was crystallized at T_c higher than 115 °C. For T_c<115 °C the crystallization of the E/H1 was completed in a very short time, lower than that necessary to reach the thermal equilibrium of DSC cells; on the other hand, the crystallization of the copolymers with high comonomer content at T_c>115 °C generally required too long times for completion.

A plot of the relative amount of crystallinity X_t , calculated as the integral of crystallization heat at the time t over the integral of the total heat up to the completion of the isothermal crystallization, as a function of crystallization time t is reported in Figure 7 for E/H copolymers isothermally crystallized at T_c = 115 °C. For all samples the relative crystallinity, developed at a definite time t, was found to depend on the comonomer

content and the crystallization temperature. From the comparison among the crystallization isotherms at the same T_c, it was pointed out that the crystallization rate of copolymers with higher comonomer content was markedly lower than that of copolymers with low 1-hexene units and decreased as the comonomer content increased. Similar findings have been reported for various random copolymers of ethylene or propylene with a-olefins.[25,26]

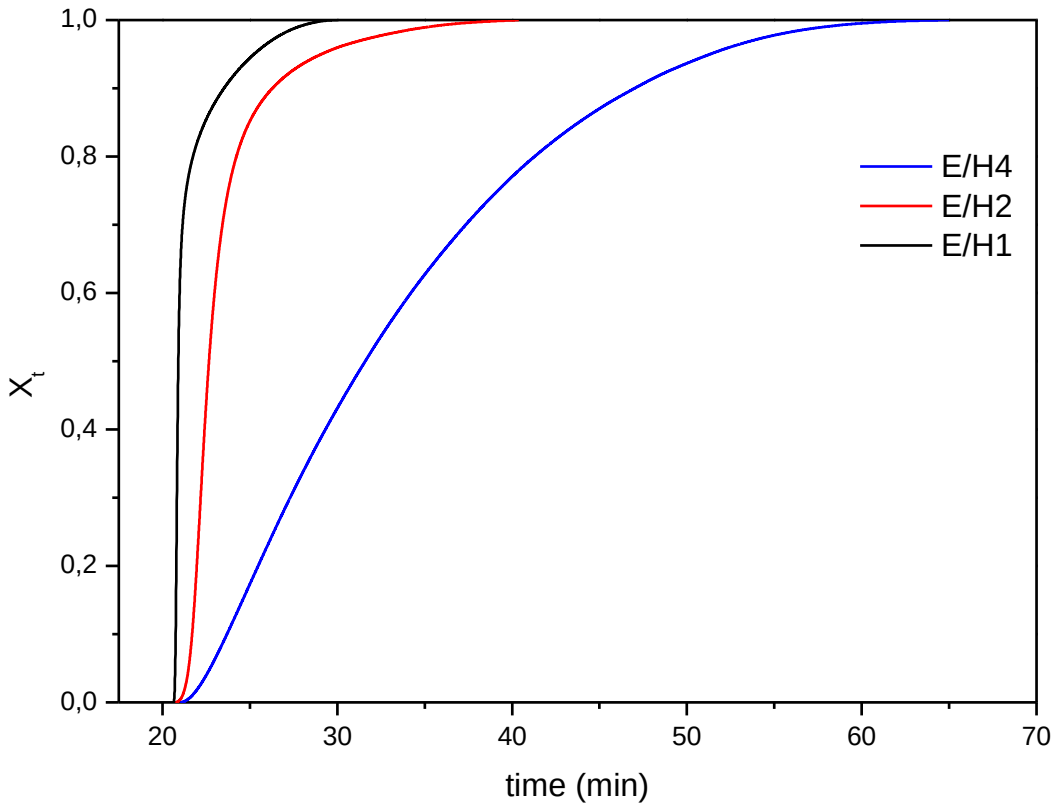

Figure 7. Crystallization isotherms of E/H copolymers at T_c = 115 °C. X_t is the relative weight fraction of the polymer crystallized after time t.

The bulk crystallization rate of the various copolymers, expressed as the reciprocal of the crystallization half-time ($1/t_{0.5}$), is reported in Figure 8 as a function of the 1-hexene content, at T_c = 115 °C. It may be noticed that for comonomer contents higher than 6 mol%, the crystallization rate of copolymers decreases to more than one order of magnitude with respect to the E/H1 at the same T_c.

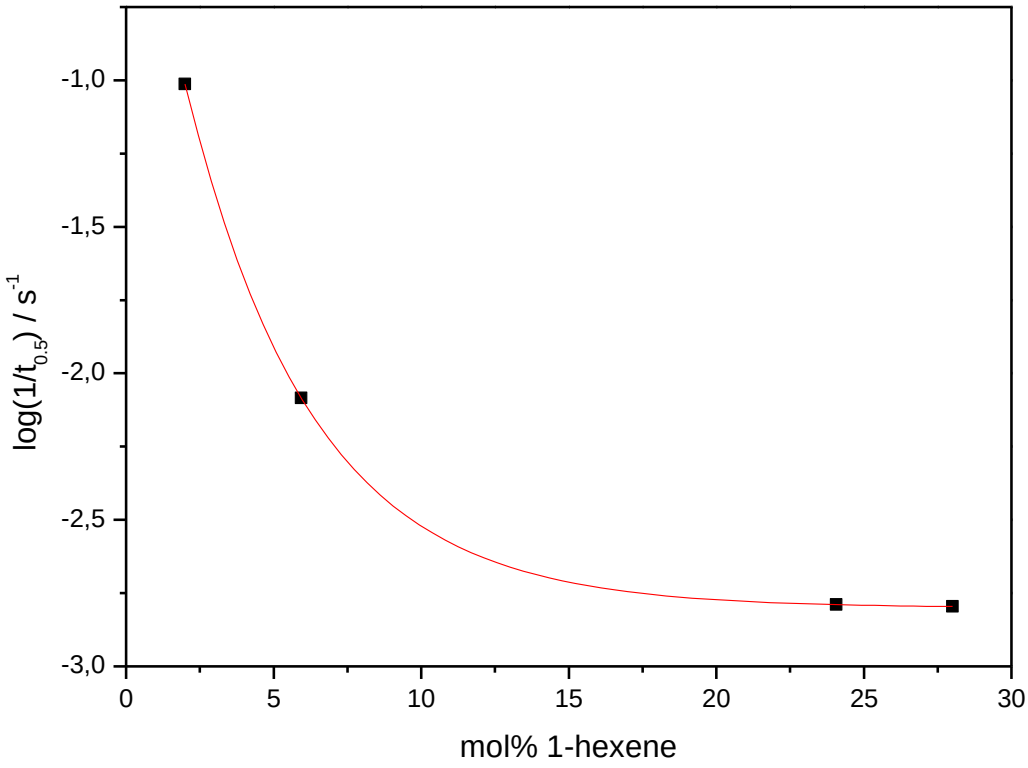

Figure 8. Isothermal crystallization rate (s^{-1}) of E/H copolymers at T_c = 115 °C as a function of 1-hexene molar percent.

The temperature dependence of the crystallization rate is shown for all examined samples in Figure 9 as a function of T_c. In all cases the crystallization rate decreased exponentially with increase in T_c, as expected for a crystallization process controlled by nucleation. Moreover, with an increase in the 1-hexene content the curves shifted to lower temperature values with a significant decrease in the crystallization.

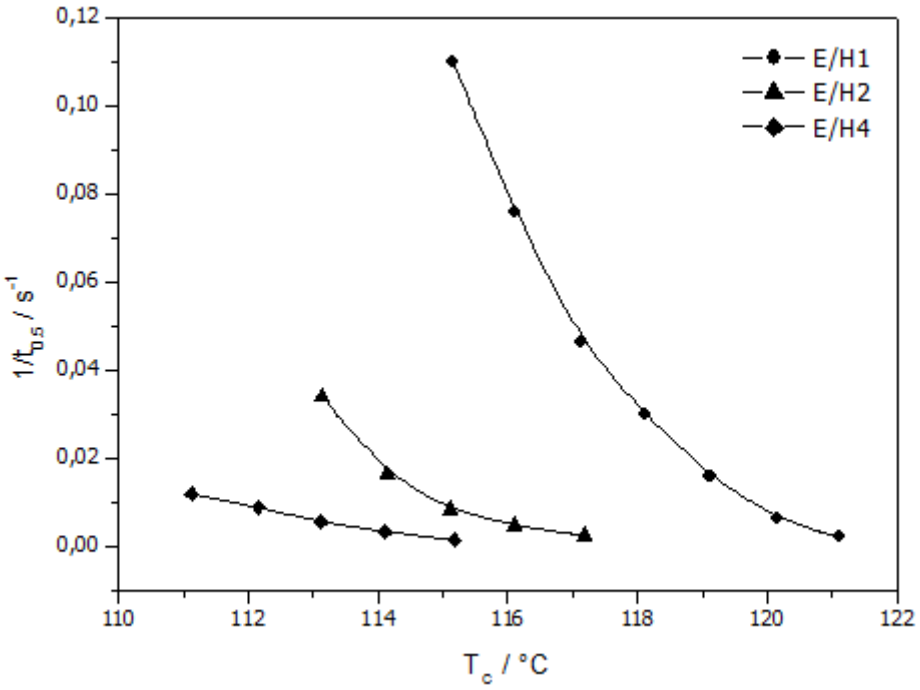

Figure 9. Temperature dependence of isothermal crystallization rate of E/H copolymers.

The application of the Avrami expression[27,28,29] is generally effective in describing the overall crystallization kinetics. However, because it does not take into consideration secondary crystallization effects, it is useful only in the initial stages of crystallization The Avrami equation has the following form:

$$X_t = 1 - \exp(-k_n t^n) \quad (2)$$

where X_t is the relative weight fraction of the polymer crystallized at time t, k_n is the kinetic constant related to the nucleation and growth rates of the crystals and n is the Avrami exponent, depending on the growth geometry and nucleation type. Values of k_n and n were obtained from the intercepts and slopes, respectively, of the linear regression of $\log(-\ln(1-X_t))$ versus log(t). Examples of these plots are shown in Figure 10 for E/H copolymers crystallized at various T_c. In the case of lower 1-hexene content copolymer samples, almost linear trends were obtained for a conversion degree X_t of the crystallizing polymer up to 15–20% (corresponding to a $\log(-\ln(1-X_t))$ value of about –0.65 to –0.79), while linearity changes very fast using the copolymers with higher 1-hexene content. At higher values of X_t marked changes of slope were observed especially at higher

comonomer content, because of the increasing effect of secondary crystallization phenomena.[30]

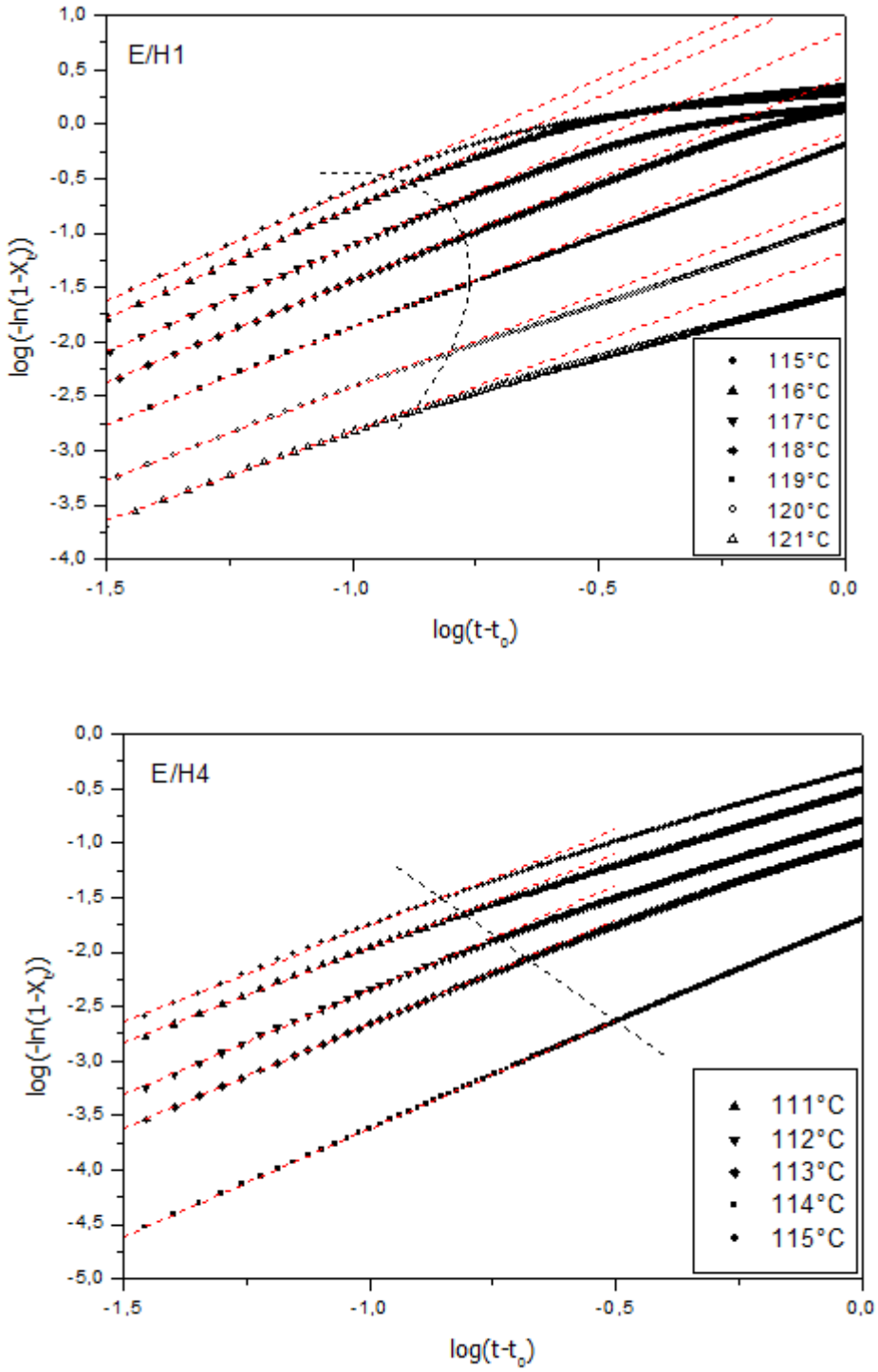

Figure 10. Avrami plots of E/H1 and E/H4 copolymers crystallized at various T_c [see Equation (2)].

The Avrami exponent varied from an average value of 1.96 for E/H1 to average values of 2.35 for the copolymer E/H2 and of 2.51 for E/H4. The values of the kinetic constant k_n (= $\ln 2/t_{0.5}^{n}$) decrease with increase in the crystallization temperature, in agreement with the decrease in spherulite growth rate, while they show minor differences by varying the 1-hexene content.

6.2.4 Melting behavior

The DSC thermograms of isothermally crystallized samples showed a relatively sharp melting peak with shoulder for E/H1 near to 130 °C while a broad less intense multiple peak was recorded at lower melting temperatures for the copolymers with high comonomer content, in the range of 120–124 °C, as indicated in Figure 11. The temperature of the higher melting peak decreased with increase in the comonomer amount, according to a reduction of lamellar thickness in the crystals of copolymers.[31] Likewise, at same T_c = 115 °C, the melting enthalpy ΔH_m decreases with an increase in the 1-hexene content from 78.6 J·g^{-1} for E/H1 to 5.3 J·g^{-1} for E/H4.

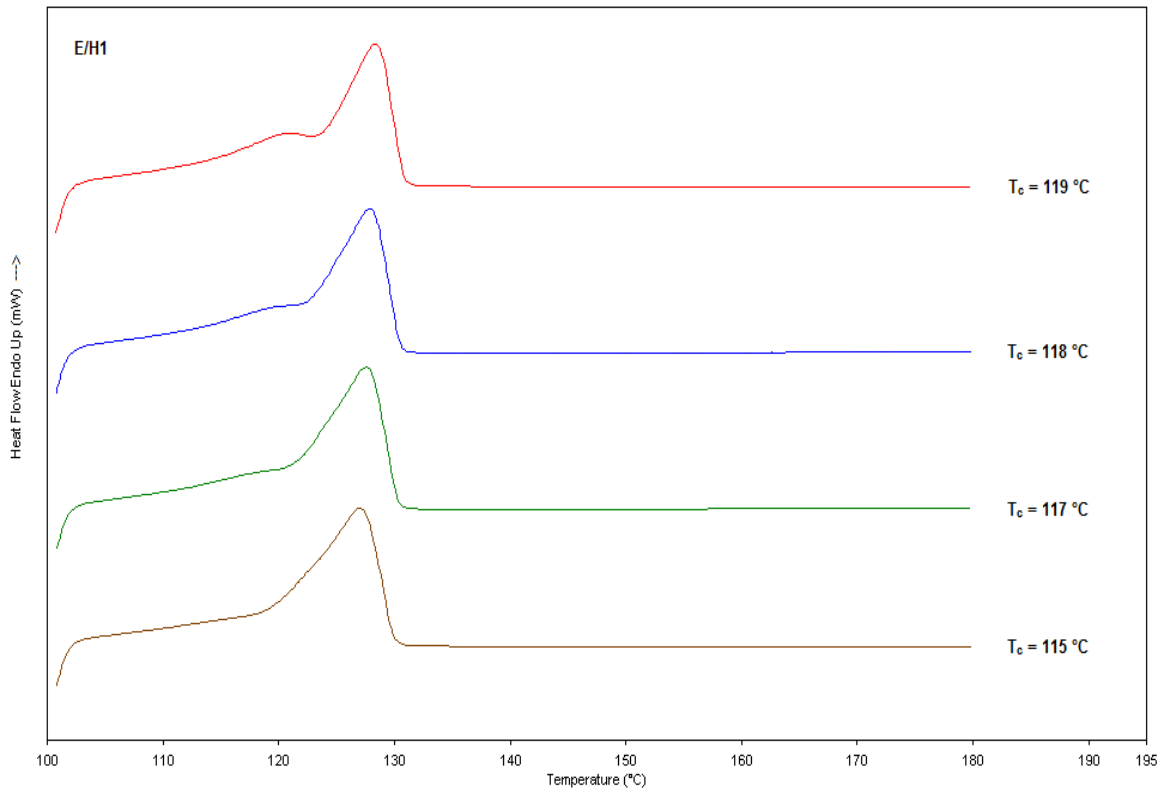

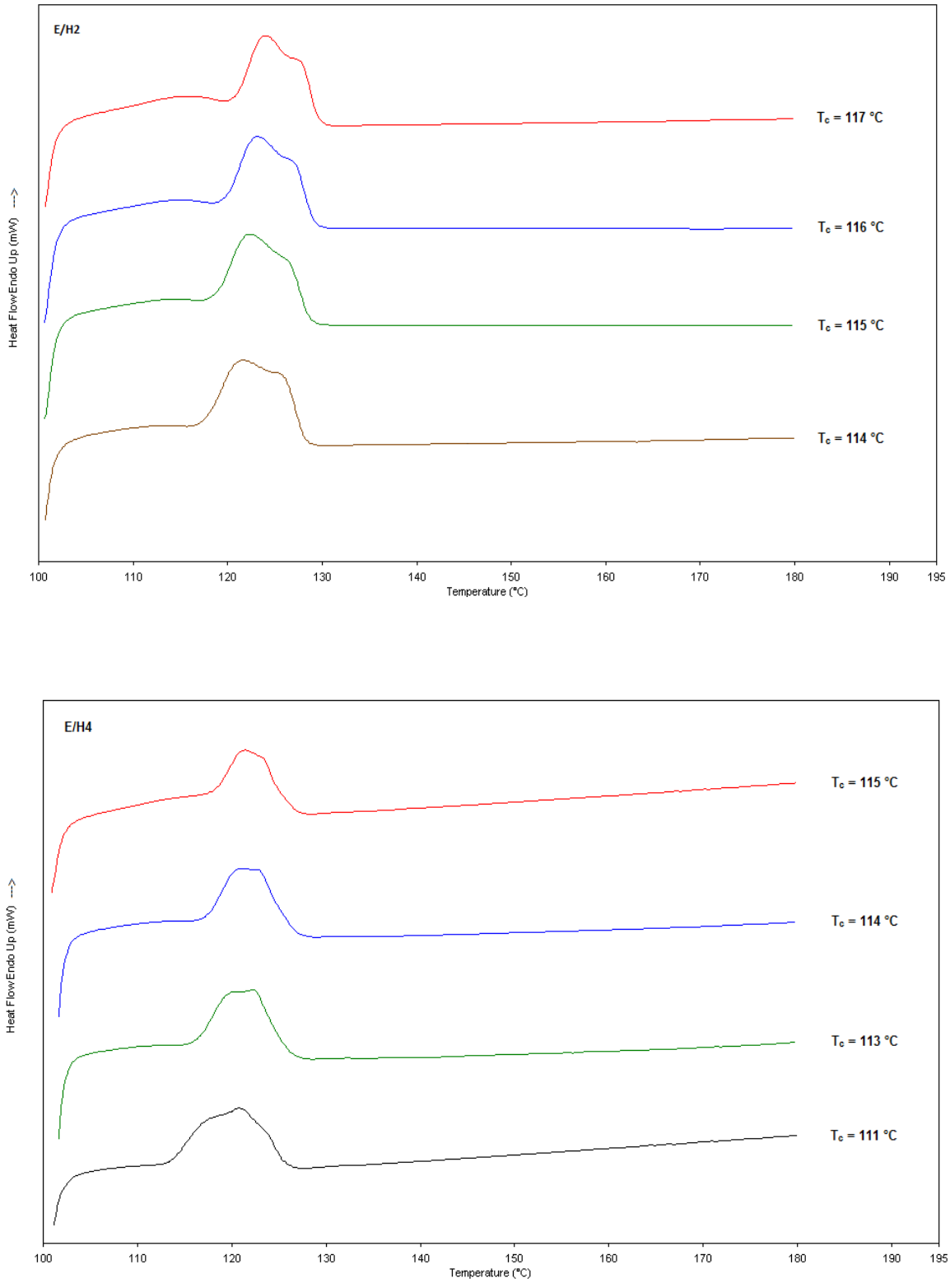

Figure 11. DSC melting thermograms of E/H copolymers after isothermal crystallization at various T_c (heating rate: 10 °C.min^{-1}).

The equilibrium melting point, T_m°, was determined using Hoffman-Weeks method[32,33] in which the polymer was crystallized at different temperatures, T_c, and then the melting points, T_m, relative to each corresponding temperature was obtained. According to Hoffman-Weeks equation a plot of T_m against T_c gives a linear relationship as:

$$T_m = T_m^\circ(1-\frac{1}{\beta}) + (\frac{1}{\beta})T_c \quad (3)$$

where β is a parameter relating the mean lamellar thickness of the crystals to the initial thickness of the growth nuclei at T_c. Figure 12 shows the relationship between T_m and T_c for E/H copolymers. The intersection of the straight line with the diagonal $T_m = T_c$ gives values of T_m° which decrease from 136 °C for E/H1 to about 122 °C for the copolymer E/H4 with a higher content of 1-hexene. The decrease in T_m° recorded for the polymers confirms that the thermodynamic stability of the PE crystals is strictly influenced by the content of side branches, i.e. by the length of crystallizable sequences in the copolymer chain.

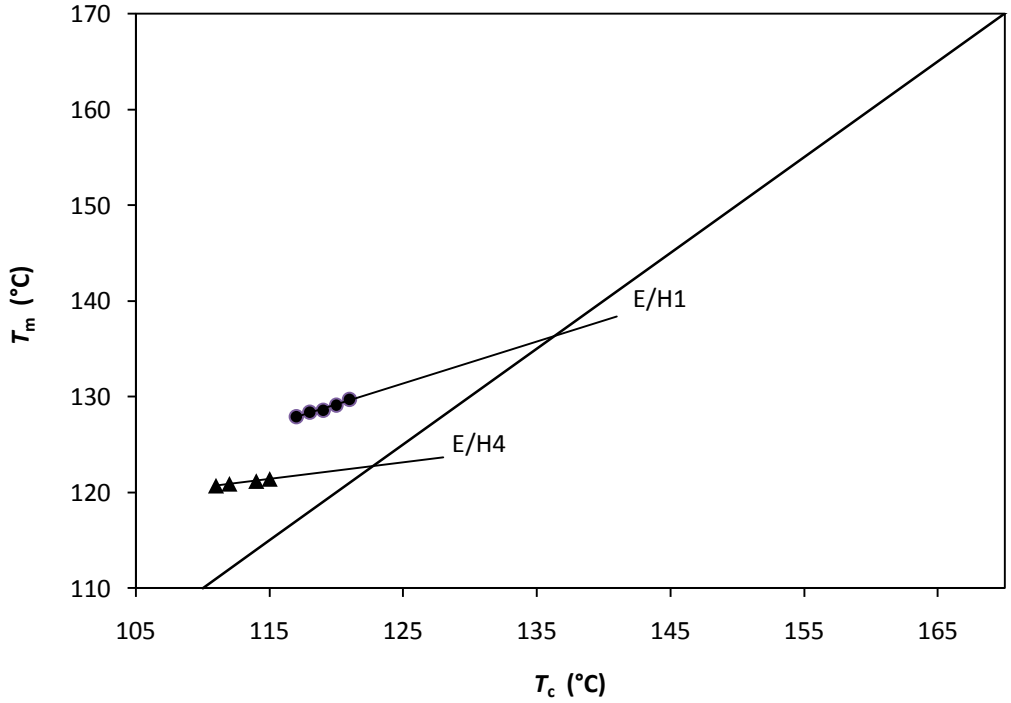

Figure 12. The plot of T_m against T_c according to Hoffman-Weeks method. (broken line: $T_m = T_c$).

6.3 Conclusion

The FTIR-M approach has been employed for the structural characterization of E/H copolymers with comonomer content in the range of 2–28 mol%. The bands of methyl deformation and methylene wagging in the region of 1400–1330 cm^{-1} were used for determining the comonomer content: the values of 1-hexene concentration obtained by FTIR were in full agreement with those determined by ^{13}C NMR analysis. The regions 1500–1400 and 750–690 cm^{-1} were analyzed to study the effect
of comonomer content on the phase transitions of the samples. Linear variations of the absorbance ratio of methylene bending and rocking vibrations have been observed by varying the comonomer content.

The crystallization behavior of the copolymers has been studied by DSC both in dynamic and isothermal conditions. The analysis of the isothermal crystallization kinetics evidenced a marked decrease in the bulk crystallization rate with an increase in the comonomer content, which according to the Avrami model, was attributed to changes in the type and density of nucleation sites as well as in the crystal growth geometry. The temperature dependence of crystallization rate was examined on the basis of polymer nucleation rate theory.

The analysis of the melting behavior of isothermally crystallized samples has shown a linear dependence of T_m on T_c for all examined samples.

6.4 References

[1] Piel, C.; Starck, P.; Seppälä, J. V.; Kaminsky, W. *J. Polym. Sci. Part A: Polym. Chem.* **2006**, *44*, 600.

[2] Schweier, G.; Brintzinger, H.-H. *Macromol. Symp.* **2001**, *173*, 89.

[3] Alt, G. H.; Köppl, A. *Chem. Rev.* **2000**, *100*, 1205.

[4] Feng, L.; Kamal, M. R. *Polym. Eng. Sci.* **2005**, *45*, 1140.

[5] Coates, G. W.; Hustad, P. D.; Reinartz, S. *Angew. Chem. Int. Ed.* **2002**, *41*, 2236.

[6] Gibson, V. C.; Spitzmesser, S. K. *Chem. Rev.* **2003**, *103*, 283.

[7] Tang, L.-M.; Li, Y.-G.; Ye, W.-P.; Li, Y.-S. *J. Polym. Sci. Part A: Polym. Chem.* **2006**, *44*, 5846.

[8] Carlini, C.; D'Alessio, A.; Giaiacopi, S.; Po, R.; Pracella, M.; Raspolli Galletti, A. M.; Sbrana, G. *Polymer* **2007**, *48*, 1185.

[9] Rao, C. N. R. *''Chemical Applications of Infrared Spectroscopy''*, Academic Press Inc., New York 1963, Chapter 10.

[10] Bhargava, R.; Wang, S. -Q.; Koenig, J. L. *Adv. Polym. Sci.* **2003**, *163*, 137.

[11] Chalmers, J. M.; Everall, N. J.; Hewitson, K.; Chesters, M. A.; Pearson, M.; Grady, A.; Ruzicka, B. *Analyst* **1998**, *123*, 579.

[12] Dominik, A.; Chapman, W. G.; Swindoll, R. D.; Eversdyk, D.; Jog, P. K.; Srivastava, R. *Ind. Eng. Chem. Res.* **2009**, *48*, 4127.

[13] Chelazzi, D.; Ceppatelli, M.; Santoro, M.; Bini, R.; Schettino, V.; *J. Phys. Chem. B* **2005**, *109*, 21658.

[14] Zhang, M.; Lynch, D. T.; Wanke, S. E. *J. Appl. Polym. Sci.* **1998**, *70*, 1893.

[15] Pracella, M.; D'Alessio, A.; Giaiacopi, S.; Raspolli Galletti, A. M.; Carlini, C.; Sbrana, G. *Macromol. Chem. Phys.* **2007**, *208*, 1560.

[16] Krimm, S. *Fortschr. Hochpolym-Forsch*. 1960, 2, S 51.

[17] Boerio, F. J. In *Handbook of Vibrational Spectroscopy*, Vol. 4, Chalmers, J. M.; Griffiths, P. R. (Eds), Wiley, Chichester, UK, 2002, pp. 2419–2536.

[18] Koenig, J. L., *Spectroscopy of Polymers*, 2nd Edn, Elsevier, Amsterdam, The Netherlands, 1999.

[19] Xiao, A. Y.; Zhu, X.; Yan, L.; Yan, D. *Polym. Prepr.* **2003**, *44*, 1206.

[20] Zerbi, G. *''Modern Polymer Spectroscopy''*, Wiley-VCH, New York 1999.

[21] Rueda, D. R.; Baltá-Calleja, F. J.; Hidalgo, A. *J. Polym. Sci., Polym. Phys. Ed.* **1977**, *15*, 2027.

[22] Rojas, G.; Wagener, K. B. *Macromolecules* **2009**, *42*, 1934.

[23] Burfield, D. R.; Kashiwa, N. *Makromol. Chem.* **1985**, *186*, 2657.

[24] Burfield, D. R. *Macromolecules* **1987**, *20*, 3020.

[25] Bartczak, Z.; Chiono, M.; Pracella, M. *Polymer* **2004**, *45*, 7549.

[26] Feng, L.; Kamal, M. R. *Polym. Eng. Sci.* **2005**, *45*, 1140.

[27] Avrami, M. *J. Chem. Phys*. **1939**, *7*, 1103.

[28] Avrami, M. *J. Chem. Phys.* **1940**, *8*, 212.

[29] Avrami, M. *J. Chem. Phys*. **1941**, *9*, 177.

[30] Wunderlich, B. "*Macromolecular Physics*", Academic Press, New York 1976, Vol. 2, Chapter VI.

[31] Clas, S. D.; Heiding, R. D.; McFaddin, D. C.; Russell, K. E.; Scammell-Bullock, M. V. *J. Polym. Sci. Part B: Polym. Phys.* **1988**, *26*, 1271.

[32] Young, R. J.; Lovell, P. A. "*Introduction to Polymers",* 2nd ed., Chapman and Hall, London, 1991, Ch. 4, 286.

[33] Hatakeyama, T.; Liu, Z. "*Handbook of Thermal Analysis",* John Wiley, Chichester, 1998, Ch. 4, 74.

7 Synthesis of New Aminoacid-Containing Group 4 Tetracarbamato Complexes to be Employed as Catalytic Precursors

7.1 Introduction

Transition-metal *N,N*-dialkylcarbamato complexes represent an interesting class of compounds that may be conveniently used as precursors for olefin polymerization, for the controlled formation of inorganic surfaces (e.g. oxides) as well as for the synthesis of inorganic-organic hybrid materials.[1] In this context, the reactivity and catalytic properties of the group 4 metal carbamates[2] have been almost unexplored so far, in spite of the fact that these compounds are rather cheap, easy to synthesize and scarcely toxic.

Recently, Pampaloni et al.[3] have found that homoleptic *N,N*-dialkylcarbamato complexes of Group 4 metals are active in the polymerization of *rac*-lactide, *via* a pathway including loss of one carbamato unit per active species to let the polymerization process to go on.

On the other hand, the use of transition-metal reagents in stoichiometric and catalytic reactions aimed to organic synthesis represented one of the great challenges of the second half of the 20th century.[4] One of the most delicate task in this field has been the use of chiral metal compounds to obtain organic products in pure enantiomeric form, as well as stereo-regular polymers. Since the preparation and efficiency of chiral-on-the-metal complexes display considerable difficulties, it has been recognized soon that pure enantiomers of asymmetric ligands can be used successfully to the purpose.[5] Thus organophosphorous derivatives have revealed to be very efficient ligands,[6,7] however they are accessible only by very laborious synthetic processes and, consequently, are very expensive[8] and also environmentally problematic.[9] Reports on induction of chirality by inexpensive organic ligands were fairly rare and those existent have became very popular, as is the case of Sharpless catalysts, based on tartaric acid derivatives.[10] In principle, enantiomers of natural proteinogenic aminoacids are a further class of enantiomeric substrates which may be used as chiral ligands.

On account of the fact that natural aminoacids are soluble in water or highly-polar solvents, [11,12] aminoacid-containing metal complexes are often non soluble in common organic solvents, as is the case of natural-aminoacidic derivatives of $TiCl_4$.[13] This feature may be consequence of the establishment of hydrogen bonds between [NH] units, and

makes the same complexes not useable for catalytic purposes. The solubility problem may be circumvented by using ancillary ligands able to confer solubility, and/or by introducing two alkyl substituents at the aminoacidic nitrogen; for instance, the titanium compound $[Ti(Cp)_2(OOCCH_2NMe_2)]$ has been reported to be well soluble in benzene.[14]

In this chapter, we report the synthesis and the characterization of natural aminoacid derivatives of *N*,*N*-dialkylcarbamato complexes of titanium and zirconium. Interestingly these products are well soluble in common low-polarity solvents, in spite of the presence of $[NH_2]$ amino groups. Moreover, the introduction of the chiral ligand may hopefully impart characteristics of stereo-selective catalyst.

7.2 Results and discussion

Homoleptic *N*,*N*-dialkylcarbamato complexes of Group 4 metals of formula $[M(O_2CNR_2)_4]$ (M = Ti, R = Me, Et, ^{i}Pr; M = Zr, R = Et, ^{i}Pr) react with chiral aminoacids (L-leucine and L-phenylalanine, Figure 1) in CH_3CN in 1:1 molar ratio, to afford new coordination compounds of formula $[M(O_2CNR_2)_4(aa)]$ (aa = aminoacid) in 20-45% yield.

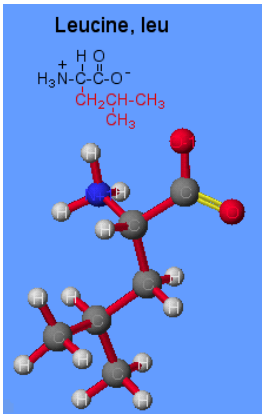

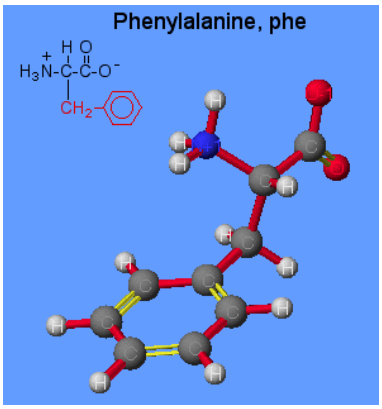

Figure 1. General structure of leucine and phenylalanine.

$M(O_2CNR_2)_4] + aa \rightarrow [M(O_2CNR_2)_4(aa)]$

1	M = Ti, R = Me, aa = L-leucine, **2a**	M = Ti, R = Me, aa = L-phenylalanine, **2d**
	M = Ti, R = Et, aa = L-leucine, **2b**	M = Ti, R = Et, aa = L-phenylalanine, **2e**
	M = Ti, R = ^{i}Pr, aa = L-leucine, **2c**	M = Ti, R = ^{i}Pr, aa = L-phenylalanine, **2f**
	M = Zr, R = Et, aa = L-leucine, **3a**	M = Zr, R = Et, aa = L-phenylalanine, **3c**
	M = Zr, R = ^{i}Pr, aa = L-leucine, **3b**	M = Zr, R = ^{i}Pr, aa = L-phenylalanine, **3d**

Scheme 1. Reactions of homoleptic carbamato complexes with aminoacids.

As stated above, the new compounds exhibit quite enhanced solubility in organic solvents, even though the corresponding non coordinated aminoacids are sparingly soluble in water and insoluble in common organic solvents (CH_2Cl_2, $CHCl_3$). The complexes containing phenylalanine show good solubility even in toluene.

In principle, the *N*,*N*-dialkylcarbamato ligand is a good leaving group and may reacts promptly with protic reagents giving release of carbon dioxide and dialkylamine.[15] It should be noted here that preliminary studies on the coordination chemistry of group 4 carbamato complexes with alcohols have indicated that no amine release occurs with ROH (R = Me and Et); instead, phenol has sufficient acidity (pK_a = 9.95) to determine proton transfer (see Scheme 2).

$M(O_2CNR_2)_4] + L \rightarrow [M(O_2CNR_2)_4L]$

1

M = Ti, R = Me, L = MeOH, **4a**
M = Ti, R = Et, L = MeOH, **4b**
M = Ti, R = Me, L = EtOH **4c**
M = Ti, R = Et, L = EtOH, **4d**

M = Zr, R = Et, L = MeOH, **5a**
M = Zr, R = ^{i}Pr, L = MeOH, **5b**
M = Zr, R = Et, L = EtOH, **5c**
M = Zr, R = ^{i}Pr, L = EtOH, **5d**

Scheme 2. Reactions of alcohols with carbamato complexes.

On account of the reactivity shown by **1** with alcohols, it may be expected that the reactions of the carbamato complexes with aminoacids (see Scheme 1) could proceed with proton transfer and, thus, amine release. In order to investigate the point, we performed the reactions in sealed NMR tubes and monitored them by NMR spectroscopy. Surprisingly, the NMR analyses did not evidence loss of the amine NHR_2 in every cases, neither at high temperature (50 °C).

This observation indicates that no carbamato degradation takes place in the course of the synthesis of the complexes **2**, coherently with the general formula attributed to the products (see Scheme 1).

The reaction of $Ti(O_2CNEt_2)_4$ with L-phenylalanine in CH_3CN afforded compound **2e**. This has been characterized by IR and NMR spectroscopies. The IR spectrum shows the absorptions related to the aminoacidic carbonyl group and the O_2CNEt_2 fragment at 1634 and 1589 cm^{-1}, respectively. The ^{13}C NMR spectra of **2e**, obtained in $CDCl_3$ at –90 °C, shows two resonances at δ = 179.8 and 174.0 ppm attributed to the carbonyl groups of the aminoacid ligand and the monodentate carbamates, respectively. Otherwise the

resonances due to the bidentate carbamato ligands have been found at δ = 163.1, 162.7 and 162.2 ppm. The resonances at δ = 134.4, 129.9, 128.6, 127.0 ppm have been assigned to the phenyl carbons. The presence of three resonances for the carboxylic carbon atoms of the bidentate carbamato ligands suggests the non-equivalence of such ligands, as consequence of the loss of symmetry determined by the introduction of the aminoacid moiety (Scheme 3). However, on the basis of the spectroscopic data, we have not been able to establish with certainty whether the coordination of the aminoacid to the metal center occurs through the carboxylic unit or the amino one.

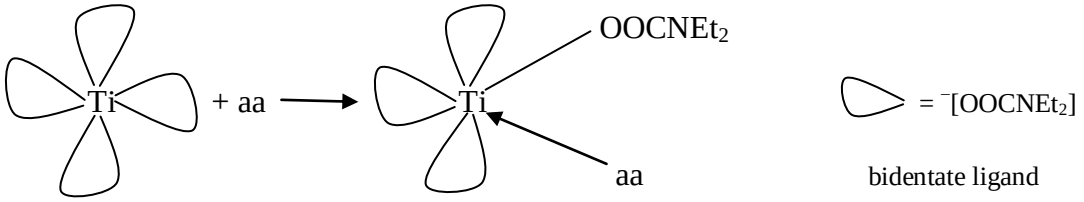

Scheme 3. Schematic representation of reaction of carbamato complex of titanium with aminoacid (L-phenylalanine).

The NMR spectra of the compounds **3a**-**3d**, display broad signals at low temperature (–90 °C) and also the IR spectra appeared difficult to interpret. Nevertheless, NMR experiments have ruled out the formation of amine in the course of the reactions. This evidence supports the hypothesis of aminoacid coordination to the metal atom, leading to change in the coordination fashion of one carbamato ligand from bi- to monodentate (see Scheme 3). No degradation of the carbamato ligands occurs even at 50 °C.

The ethylene polymerization behaviors of the new compounds **2a**-**2f** and **3a**-**3d** were studied in the presence of MAO as cocatalyst. If on one hand the titanium complexes afforded only trace amount of polyethylene, instead the zirconium ones revealed completely inactive in the polymerization. These outcomes indicate that the addition of an aminoacid unit determines significant drop off of the catalytic activity with respect to the parent homoleptic carbamato complexes.

7.3 Conclusion

A series of natural aminoacid-containing carbamato complexes of titanium and zirconium have been prepared under mild conditions. In spite of the low solubility exhibited by [NH_2] containing aminoacids in organic solvents, the new complexes present remarkable solubility in $CHCl_3$, CH_2Cl_2 and, in some cases, in toluene. (IR, NMR) characterization of the new compounds indicates clearly the coordination of the aminoacid to the metal center, made possible presumably by change in the coordination mode of one carbamato ligand from bidentate to monodentate.

Investigations are in progress in order to study the catalytic behavior of the new metal species in a variety of reactions. Unfortunately, preliminary results regarding ethylene polymerization have revealed that the new complexes are not effective in the polymerization, by contrast with what observed for the homoleptic carbamato precursors.

7.4 References

[1] Albinati, A.; Carraro, M. L.; Gross, S.; Rancan, M.; Rizzato, S.; Tondello, E.; Venzo, A. *Eur. J. Inorg. Chem.* **2009**, 5346.

[2] Belli Dell'Amico, D.; Calderazzo, F.; Labella, L.; Marchetti, F.; Pampaloni, G. *Chem. Rev.* **2003**, *103*, 3857.

[3] Marchetti, F.; Pampaloni, G.; Pinzino, C.; Renili, F.; Repo, T.; Vuorinen, S. *Manuscript under preparation*.

[4] "Encyclopedia of Catalysis", Ed. Horváth, I. T.; Wiley-Interscience, Hoboken, 2003.

[5] Knowles, W. S. *Angew. Chem., Int. Ed.* **2002**, *41*, 1998.

[6] Noyori, R. *Angew. Chem., Int. Ed.* **2002**, *41*, 2008.

[7] (a) "Catalytic Asymmetric Synthesis", 2nd edn., Ed. Ojima, I. Wiley-VCH, Weinheim, 2000; (b) "Applied Homogeneous Catalysis with Organometallic Compounds", 2nd edn., Eds. Cornils, B.; Herrmann, W. A. VCH-Wiley,Weinheim, 2002.

[8] (a) "Chiral Compounds Chemistry", Fluka, Buchs, 1994; (b) "Chiral Non-Racemic Compounds", Sigma-Aldrich, Milwaukee, 1998.

[9] (a) Bartha, K.; Csékei, M.; Csihony, S.; Mehdi, H.; Horváth, I. T.; Pusztai, Z.; Vlád, G.; *Magyar Kém. Lapja* **2000**, *55*, 173; (b) Lindstrém, U. M. *Chem. Rev.* **2002**, *102*, 2751; (c) Horváth, I. T. *Acc. Chem. Res.* **2002**, *35*, 685.

[10] Sharpless, K. B. *Angew. Chem., Int. Ed.* **2002**, *41*, 2024.

[11] Micskei, K.; Patonaya, T.; Caglioti, L.; Pályi, G. *Chemistry & Biodiversity* **2010**, *7*, 1660.

[12] Klapötke, T. M.; Köpf, H.; Tornieporth-Oetting, I. C. *Organometallics* **1994**, *13*, 3628.

[13] Neelam Jalil, N. S.; Hameed, L. T. *Synth. React. Inorg. Met. Org. Chem.* **1995**, *25*, 1633.

[14] Krüger, T.; Wagner, C.; Lis, T.; Kluge, R.; Mörke, W. Steinborn, D. *Inorg. Chim. Acta* **2006**, *359*, 2489.

[15] Belli Dell'Amico, D.; Boschi, D.; Calderazzo, F.; Ianelli, S.; Labella, L.; Marchetti, F.; Pelizzi, G.; Frieda Quadrelli, E. G. *Inorg. Chim. Acta* **2000**, *300-302*, 882.

8 Experimental Section

8.1 Introduction

All reagents and solvents were carefully purified and dried prior to use. All manipulations of air- and/or moisture-sensitive compounds were performed under inert atmosphere (N_2 or Ar); thus the Schlenk technique was used for the reactions, and the products isolated were stored in sealed vials. The purification, synthesis and characterization procedures will be described in the following.

8.2 Materials

Table 1. List of chemicals used.

Name of chemical	**Formula/ Abbreviation**	**Grade/ Purity**	**Source**
Acetone	C_3H_6O	AR	Carlo Erba
Acetonitrile	CH_3CN	99.8%	Aldrich
Benzene (d_6)	C_6D_6	99.6%	Aldrich
Calcium hydride	CaH_2	99%	Aldrich
Carbon dioxide	CO_2	≥99.99%	Air Liquide
Chlorobenzene	C_6H_5Cl	99%	Aldrich
Chloroform	$CHCl_3$	AR	Normapur
Chloroform (d_1)	$CDCl_3$	99.8%	Aldrich
Decahydronaphthalene	$C_{10}H_{16}$	98%	Aldrich
1,2-Dichlorobenzene	$C_6H_4Cl_2$	99%	Aldrich
Dichloromethane	CH_2Cl_2 (DCM)	Reagent	Fluka
Dichloromethane (d_2)	CD_2Cl_2 (DCM)	99%	Aldrich
Diethylaluminiumchloride	$(C_2H_5)_2AlCl$ (DEAC)	25 wt% soln	Aldrich
Diethylamine	$NHEt_2$	≥99.5%	Aldrich
Diisopropylamine	NH^iPr_2	≥99.5%	Aldrich
Ethylaluminiumsesquichloride	$(C_2H_5)_2AlCl{\cdot}Cl_2AlC_2H_5$	97%	Aldrich
Ethylene	C_2H_4	≥99%	Rivoira
Heptane	$H_3C(CH_2)_5CH_3$	99%	Panreac
1-Hexene	$CH_3(CH_2)_4{=}CH_2$	95%	J.T. Baker

Hydrochloric acid	HCl	37%	Panreac
L-leucine	$(CH_3)_2CHCH_2CH(NH_2)CO_2H$	Reagent Gr.	Aldrich
L-phenylalanine	$C_6H_5CH_2CH(NH_2)CO_2H$	Reagent Gr.	Aldrich
Methanol	CH_3OH	HPLC	Carlo Erba
Methylaluminoxane	$(Al(CH_3)O)_n$ (MAO)	25 wt% soln	Aldrich
Phosphorus pentaoxide	P_2O_5	Reagent Gr.	Aldrich
Potassium hydroxide	KOH	Reagent Gr.	Aldrich
Propylene	$CH_3CH_2=CH_2$	>99%	Union Carbide
Sodium metal	Na	99%	Merck
Tetrakis(dimethylamido)titanium	$Ti(NMe_2)_4$	99.999%	Aldrich
Titanium(IV) chloride	$TiCl_4$	98%	Fluka
Toluene	$C_6H_5CH_3$	98%	J.T. Baker
Trichlorobenzene	$C_6H_3Cl_3$	99%	Aldrich
Triisobutylaluminium	$[(CH_3)_2CHCH_2]_3Al$(TIBAL)	25 wt% soln	Aldrich
Zirconium(IV) chloride	$ZrCl_4$	99.9%	Aldrich

8.3 Purification and drying

All solvents and reagents were purified and dried under dry nitrogen atmosphere by standard procedures.[1] Toluene, n-hexane, diethyl ether and tetrahydrofuran were distilled after refluxing 8 h on sodium/potassium alloy. Chlorobenzene, 1,2-dichlorobenzene, 1-hexene were dried and distilled after refluxing 8 h over Na. Dichloromethane, dichloromethane (d_2), chloroform (d_1), were distilled before use under argon atmosphere from P_4O_{10}, while pentane was distilled from $LiAlH_4$. 1-Hexene was refluxed over Na, distilled under argon and stored in the refrigerator. $TiCl_4$ was distilled under reduced pressure before use. "TMA-depleted" MAO (DMAO) was prepared by removing toluene and free TMA from the commercial solution of MAO in vacuo at room temperature for 6 h, followed by repeated slurring in heptane.[2] Ethylaluminiumsesquichloride, DEAC, MAO, decahydronaphthalene, hydrochloric acid, methanol, potassium hydroxide, sodium metal were used as received without further purification. Ethylene, propylene and carbon dioxide were used as received.

8.4 Synthesis of complexes

8.4.1 Synthesis of $[M(O_2CNR_2)_4]$ (M = Ti or Zr; R = Et or ^{i}Pr)

Only the synthesis of $Ti(O_2CNEt_2)_4$ is described in detail, the other compounds being prepared in a similar way. The preparation of $Ti(O_2CNEt_2)_4$ (**I**) was performed by modification of the published literature.[3] $TiCl_4$ (5.31 g; 0.020 mmol) was dissolved in toluene (200 mL) and treated at room temperature with Et_2NH (13.0 mL, 0.102 mol). Then a large excess of carbon dioxide was introduced into the system, thus an exothermic reaction with precipitation of a colorless solid was noticed. After 4 h stirring at room temperature, the suspension was filtered and the solution was concentrated to about 10 mL and added of heptane (80 mL). The pale-yellow solid was recovered by filtration, washed with heptane (4-5 mL), dried *in vacuo* at room temperature and identified as $Ti(O_2CNEt_2)_4$ (7.73 g, 73% yield) on the basis of elemental analysis and IR and NMR (^{1}H and ^{13}C) spectra.

^{1}H NMR (200 MHz in $CDCl_3$) δ (ppm): 3,32 [quartet, **H**(CH_2)]; 1,06 [triplet, **H**(CH_3)]

^{13}C NMR (50 MHz in $CDCl_3$) δ (ppm): 169,16 [**C**OO]; 38,66 [**C**H_2]; 13, 01 [**C**H_3]

FTIR: 2970m, 2930m, 2870mw, 1550vs, 1500vs, 1430vs, 1380ms, 1310vs, 1210ms, 1100w, 1075ms, 975m, 940w, 835ms, 790s cm^{-1}.

Elemental analysis: Calculated: C, 46.9%; H, 7.9%; CO_2, 34.3%; N, 10.9%; Ti, 9.3 %. Found: C, 46.7%; H, 7.4%; CO_2, 34.2%; N, 10.6%; Ti, 8.8 %.

[Ti(O$_2$CN^{i}Pr$_2$)$_4$]. Color: pale green; yield: 72%.

^{1}H NMR (200 MHz in toluene-d_8) δ (ppm): 3,78 [heptet, **H**(CH)]; 1,11 [doublet, **H**(CH_3)].

^{13}C NMR (50 MHz in toluene-d_8) δ (ppm): 170,1 [**C**OO]; 46,1 [**C**H$(CH_3)_2$]; 21,5 [**C**H_3].

FTIR: 2970ms, 2940m, 2880mw, 1550vs, 1500s, 1460m, 1320vs, 1200m, 1160m, 1140m, 1060m, 1030mw, 900w, 815s, 790s cm^{-1}.

Elemental analysis: Calculated: C, 53.9%; H, 9.0%; CO_2, 28.2%; N, 9.0%; Ti, 7.7 %. Found: C, 52.7%; H, 8.4%; CO_2, 29.1%; N, 8.5%; Ti, 8.0 %.

[Zr(O_2CNEt_2)$_4$]. Color: colorless; yield: 76%.

^{1}H NMR (200 MHz in toluene-d_8) δ (ppm): 3,00 [quartet, **H**(CH_2)]; 0,84 [triplet, **H**(CH_3)].

^{13}C NMR (50 MHz in toluene-d_8) δ (ppm): 169,8 [**C**OO]; 39,6 [**C**H_2]; 13,6 [**C**H_3].

FTIR: 2990m, 2980m, 2940mw, 1565vs, 1505vs, 1450vs, 1380m, 1325vs, 1220m, 1100m, 1080m, 1070m, 975m, 940w, 835ms, 795ms cm^{-1}.

Elemental analysis: Calculated: C, 43.2%; H, 7.2%; CO_2, 31.7%; N, 10.1%; Zr, 16.4 %. Found: C, 42.2%; H, 6.8%; CO_2, 31.2%; N, 9.5%; Zr, 15.9 %.

[Zr($O_2CN^iPr_2$)$_4$]. Color: colorless; yield: 73%.

^{1}H NMR (200 MHz in benzene-d_6) δ (ppm): 3,75 [heptet, **H**(CH)]; 1,01 [doublet, **H**(CH_3)].

^{13}C NMR (50 MHz in toluene-d_8) δ (ppm): 170,1 [**C**OO]; 45,3 [**C**H(CH_3)$_2$]; 21,2 [**C**H_3].

FTIR: 2970ms, 2940m, 2880w, 1535vs, 1500vs, 1380s, 1360s, 1200m, 1160ms, 1140m, 1060ms, 810s, 795ms cm^{-1}.

Elemental analysis: Calculated: C, 50.3%; H, 8.4%; CO_2, 26.3%; N, 8.4%; Zr, 13.6 %. Found: C, 50.3%; H, 8.3%; CO_2, 26.9%; N, 8.2%; Zr, 13.3 %.

8.4.2 Synthesis of Ti(O_2CNMe_2)$_4$

Ti(O_2CNMe_2)$_4$ (**II**) was prepared according to the literature.[4] In a typical procedure, CO_2 was bubbled in excess into a solution of Ti(NMe_2)$_4$ (0.5 g, 22.30 mmol) in toluene (250 mL) at room temperature under vigorous stirring. After 4 h the yellow precipitate was filtered off, washed out with 2×5 mL of toluene and dried *in vacuo* (Yield = 95%).

^{1}H NMR (200 MHz in $CDCl_3$) δ (ppm): 2,89 [singlet, **H**(CH_3)]

^{13}C NMR (50 MHz in $CDCl_3$) δ (ppm): 169,23 [**C**OO]; 34,23 [**C**H_3].

FTIR: 2935w, 1580s, 1505s, 1455ms, 1401s, 1265s, 1040ms, 865m, 842m, 787s cm^{-1}.

8.4.3 Synthesis of $TiCl_2$(O_2CNMe_2)$_2$

The preparation of $TiCl_2$(O_2CNMe_2)$_2$ (**III**) was performed for the first time. A suspension of Ti(O_2CNMe_2)$_4$ (1.67 g, 4.16 mmol) in toluene (100 mL) was treated with $TiCl_4$ (0.45 mL, 4.19 mmol) and left to stir at room temperature for 24 h. The resulting

bright-yellow solid was filtered and washed with toluene (3x3 mL) and dried *in vacuo* (10^{-2} mmHg). Yield: 2.29 g, 93%.

^{13}C CP-MAS NMR: δ = 161.1 [**C**OO]; 38,2 and 36,1 [**C**H_3].

FTIR: 2965w, 2936w, 1575s, 1479s, 1455s, 1400s, 1260s cm^{-1}.

Elemental analysis: Calculated: Ti, 16.2%; Cl, 24.1%; CO2, 29.8%. Found: Ti, 16.0%; Cl, 24.0%; CO2, 29.5%.

8.4.4 Synthesis of [M(O_2CNR_2)$_4$(aa)] (M = Ti, R = Me, aa = L-leucine, **2a**; M = Ti, R = Et, aa = L-leucine, **2b**; M = Ti, R = ^{i}Pr, aa = L-leucine, **2c**; M = Ti, R = Me, aa = L-phenylalanine, **2d**; M = Ti, R = Et, aa = L-phenylalanine, **2e**; M = Ti, R = ^{i}Pr, aa = L-phenylalanine, **2f**; M = Zr, R = Et, aa = L-leucine, **3a**; M = Zr, R = ^{i}Pr, aa = L-leucine, **3b**; M = Zr, R = Et, aa = L-phenylalanine, **3c**; M = Zr, R = ^{i}Pr, aa = L-phenylalanine, **3d**.

L-phenylalanine (0.107 g, 0.65 mmol) was added to a solution of Ti(O_2CNEt_2)$_4$ (0.332 g, 0.65 mmol) in CH_3CN (10 mL), in a Schlenk tube. The suspension was stirred at room temperature for 48 h, and the solvent was removed *in vacuo* from the final solution. The pale-yellow solid product **2e** dried *in vacuo* (10^{-2} mmHg) and stored under argon in sealed vials (Yield: 53%). When L-leucine was used for the preparation of **2a**–**c** and **3a**–**b** the reaction time prolonged to 72 h.

Compounds **2a**-**d**, **2f** and **3a**-**d** were prepared by analogous procedure, by allowing the *N*,*N*-dialkylcarbamato complexes of titanium and zirconium to react with the appropriate aminoacid.

2a: yellow; 42% yield.

FT-IR: 3261m, 2956m, 2932w, 2870w-m, 1677m, 1661w, 1586vs, 1499m, 1468m, 1411s, 1269vs, 1143s, 1049m, 996w, 931w, 834m, 785s, 761m cm^{-1}.

2b:pale-yellow, 32% yield.

FT-IR: 2959m, 2932m, 2870w, 1738m-sh, 1608w, 1579m, 1490vs, 1428s, 1375s, 1304vs, 1216s, 1096w, 1073m, 977m, 939m, 847w, 790m, 769w, 702w cm^{-1}.

2c: yellow, 30% yield.

FT-IR: 2967w-m, 2933w, 2873w, 2720w, 1715w, 1613m, 1486s, 1470vs, 1452s, 1353vs, 1205m, 1154m, 1068m-s, 899 m, 870w, 787w-m cm^{-1}.

3a: white, 37% yield.

FT-IR: 2963m, 2933w, 2870w, 1664m, 1493vs, 1458w, 1431s, 1376m, 1311vs, 1259vs, 1217s, 1093w, 1073m-s, 1016 m, 980w, 938w, 790vs cm^{-1}.

3b: white, 27% yield.

FT-IR: 3420w, 2968m, 2935w, 2247w, 1677m, 1533vs, 1496s, 1463m, 1354vs, 1261w, 1159m, 1057s, 814vs, 796vs cm^{-1}.

2d: pale-yellow, 45% yield.

FT-IR: 3326w, 3275w, 3026 w, 2971w-sh, 2927w-m, 2875w, 1653w-sh, 1589s, 1494m, 1455w, 1402m, 1377m, 1261vs, 1090w, 1043w, 950w-sh, 785s, 700s cm^{-1}.

2e: pale-yellow, 42% yield.

FT-IR: 2971w, 2932w, 2873w, 1740w, 1634m, 1589w-sh, 1479vs, 1455w, 1431s, 1376m, 1308vs, 1216s, 1073m, 977m, 785s, 696vs cm^{-1}.

^{13}C-NMR (50 MHz in $CDCl_3$) δ (ppm): 179,8 [**C**O, aminoacid]; 174,0 [**C**OO, monodentate]; 163,1; 162,7; 162,2 [**C**OO, bidentate]; 134,4; 129,9; 128.6; 127,0 [$\mathbf{C}_6H_5$]; 54,7 [**C**H]; 41,6 [broad, $\mathbf{C}H_2$]; 13,9 [$\mathbf{C}H_3$].

2f: orange, 28% yield.

FT-IR: 2967m, 2933w, 2873w, 2720w, 1715w, 1631w, 1486s, 1470vs, 1452s, 1382w, 1353vs, 1205s, 1154s, 1104w, 1068s, 899 m, 870w, 787w, 749w, 699s cm^{-1}.

3c: creamy, 38% yield.

FT-IR: 2975m, 2931w, 2875w, 1638m, 1589w, 1492vs, 1455w, 1432s, 1378m-s, 1312vs, 1217s, 1137w, 1096w, 1074m, 977m, 938 w-m, 786m, 695vs cm^{-1}.

3d: white, 22% yield.

FT-IR: 3336w, 3030vw, 2969m, 2934w, 1740w, 1660m, 1538s, 1495m, 1454w, 1384m, 1353vs, 1254m, 1198m-s, 1159m, 1057s, 901w, 814vs, 796vs, 751m, 701s cm^{-1}.

8.5 Polymerization techniques

8.5.1 Ethylene polymerization

Ethylene polymerization was carried out in a 250-mL stainless steel reactor (Figure 1) under magnetic stirring. In a typical procedure, the titanium precursor was dissolved in the proper solvent (10 mL) in a Schlenk-type vessel under nitrogen. The solution was added into a flask containing a solution of MAO in toluene. When this catalytic system was used in polymerization of ethylene under pressure, it was transferred with a cannula into the reactor under ethylene atmosphere. The reactor was then closed, pressurized with ethylene up to the chosen pressure. Then, under magnetic stirring, the polymerization reaction was performed at room temperature or at the desired temperature. After the prescribed time the polymerization mixture was poured into an excess of acidified methanol. The precipitated polymer was recovered by filtration, dried *in vacuo*, weighed and finally characterized.

Figure 1. Stainless autoclave for polymerization of ethylene at higher pressure.

In the case of polymerization at 0.1 MPa pressure of ethylene, the experiments were performed, with the assembly described in Figure 2, into a 250 mL round-bottomed flask where the catalytic system was directly prepared with the same procedure as previously described. The recovery of the crude polymer and its purification were performed according to the experiment approach above mentioned.

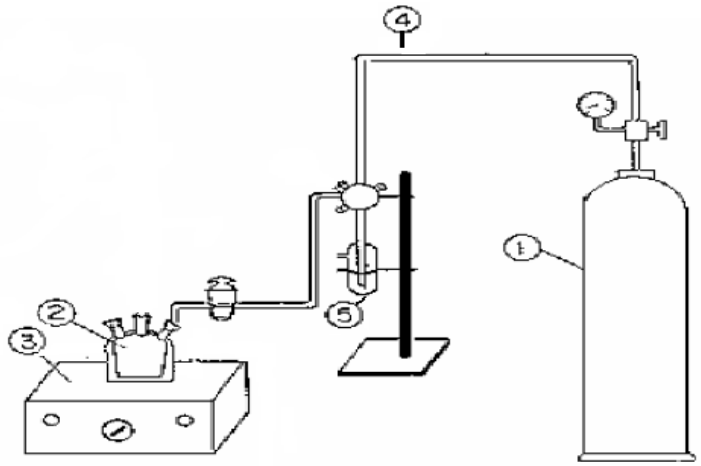

1.ETHYLENE GAS CYLINDER **2.**GLASS FLASK
3.MAGNETIC STIRRER **4.**PRESSURE TUBING
5.MERCURY

Figure 2. Set up for polymerization of ethylene at one bar pressure.

8.5.2 Propylene polymerization

Polymerizations were conducted in a 250-mL stainless steel reactor equipped with a magnetic stirrer (see Figure 1). The titanium precursor and cocatalyst were dissolved in the solvent (total volume: 65 mL) in a Schlenk-type vessel under dry nitrogen. The catalytic solution was transferred into the reactor under propylene atmosphere. The reactor was then closed and charged with the desired amount of propylene to initiate the polymerization. After the desired period of time, the reactor was vented. The polymer was precipitated from methanol/HCl, filtered washed with methanol, and dried to constant weight.

8.5.3 Copolymerization of ethylene with 1-hexene

Polymerization was conducted using a three-necked 250mL round-bottom flask with an ethylene inlet and a magnetic stirring. Solvent (chlorobenzene, toluene) was introduced into the flask and was saturated with 0.1 MPa ethylene at the required temperature. Calculated amounts of 1-hexene, cocatalyst and precursor solution in solvent were added in this order. The total volume of reaction mixture was 65 mL. After desired reaction time, polymerization was terminated by acidified methanol and the reaction mixture was poured into an excess amount of methanol. The precipitated polymer was filtrated, washed and dried under vacuum.

In the case of copolymerization in higher pressures, the catalytic system was transferred into a 250 mL stainless-steel reactor under ethylene atmosphere. After the eventual addition of the proper amount of the comonomer, the reactor was closed and pressurized with ethylene up to the chosen pressure.

8.6 Characterization techniques

8.6.1 Gel permeation chromatography (GPC)

In a limited number of PE samples the molecular weight and its distribution were determined by SEC analysis at 135 °C performed in trichlorobenzene, with a Waters 150C chromatograph equipped with a refractive index detector. The universal calibration method was applied to evaluate molecular weights, by using narrow distribution poly(styrene) standards.

8.6.2 Differential scanning calorimetry (DSC)

The thermal behavior of PE and copolymers was examined with a Perkin-Elmer Pyris Diamond DSC at a standard heating/cooling rate of 10 °C/min, under dry nitrogen flow. The samples were first melted to 180 °C (first run) and kept at this temperature for 3 min, then cooled down to 50 °C and again heated up to the melting (second run). Temperatures and heats of phase transitions were determined, respectively, from the maxima and the areas of crystallization and melting peaks. The degree of crystallinity X_c of PE was calculated from the ratio between the values of melting enthalpy, ΔH_m (as calculated from

the second heating run) and the heat of fusion of 100% crystalline PE, taken as $\Delta H°_m$ = 293 J g^{-1}.[5] The DSC temperature scale was calibrated by using standard materials (indium, tin, zinc) at various heating rates; indium was used to calibrate the transition heats.

The isothermal crystallization kinetics were analyzed in the temperature range of 114-126 °C. The samples (5-10 mg) were heated from 50 to 190 °C at 10 °C/min, kept at this temperature 5 min in order to erase any previous thermal history and then rapidly cooled (at a nominal rate of 100 °C/min) to various prefixed T_c, recording the heat of crystallization as a function of time. The starting time for the crystallization was taken as the time at which the sample temperature reached the programmed value of T_c. The weight fraction X_t of the material crystallized after time t was evaluated by the ratio of the integral of crystallization heat at the time t over the integral of the total heat up to the completion of the isothermal crystallization. The half-time of crystallization at each T_c was determined from the plots of X_t *versus* t, as the time corresponding to $X_t = 0.5$.

The melting behavior of the isothermally crystallized samples was examined by heating them in the DSC directly from T_c up to 180 °C at 10 °C/min. Temperatures and heats of melting were thus recorded as a function of T_c.

For PP samples, thermal behavior was recorded at the scanning rate of 10 °C/min, from –30 to 180 °C. The reported T_g values are referred to the second heating scan.

8.6.3 Intrinsic viscosity

Intrinsic viscosity ([η]) measurements on polymeric samples were performed by using a Desreaux-Bischoff dilution viscometer in decalin solution at 135 °C. The viscometric average molecular weight (M_v) was then determined according to the equations $[\eta] = 2.3\times10^{-5} M_v^{0.82}$ and $[\eta] = 1.066\times10^{-4} M_v^{0.804}$ valid for PE and atactic PP, respectively.[6,7]

8.6.4 Infrared spectroscopy

FTIR spectra were carried out on a Perkin-Elmer Spectrum One spectrometer equipped with an attenuated-total-reflectance apparatus. Data elaboration was performed by a Spectrum V 3.2 Perkin-Elmer program.

The FTIR-M spectra of films of E/H copolymers, obtained by compression molding at 150 °C, were recorded by means of an Autoimage microscope connected with a Perkin-Elmer 2000 spectrophotometer in the 4000-600 cm^{-1} region with a 2 cm^{-1} resolution. The composition of copolymers was evaluated by FTIR-M analysis of several microareas of compression-molded films in the 1400-1265 cm^{-1} region, typical for the absorbance of methyl groups and methylene sequences. The average absorbance ratio of the methyl-to-methylene bands, which is independent of the film thickness, was calculated from measurements on five different microareas for each sample.[8]

8.6.5 NMR spectroscopy

^{1}H and ^{13}C NMR spectra were performed on a FT Varian Gemini 200 spectrometer at 200 and 50 MHz, respectively, by using tetramethylsilane (TMS) as an internal standard, unless otherwise specified.

The ^{13}C Cross Polarization/Magic Angle Spinning (CP-MAS) NMR spectra of complex $[TiCl_2(O_2CNMe_2)_2]$ were recorded on a Bruker AMX300WB spectrometer working at 75.47 MHz, using 4 mm zirconia rotors at a spinning rate of 5 kHz, with high power ^{1}H decoupling. The 90° pulse was 4 μs, the contact pulse was 5 ms and the recycle delay 4 s; 1200 scans were acquired.

The branch content in polyethylene was estimated from ^{13}C CPMAS NMR spectra.[9] The spectra were recorded at room temperature under proton decoupling conditions on samples of polyethylene using a 4 mm CP/MAS probe head for solid state measurements. The 90° pulse length was 4 μs, a contact time of 2 ms was used and the recycle delay was 4 s acquiring 20000 scans. The MAS frequency was 7 kHz. Peak integrals were determined after deconvolution using the SPORT-NMR software.[10]

NMR experiments were carried out on a Bruker AMX-300 WB spectrometer working at 300.13 MHz for proton and at 75.47 MHz for carbon-13. ^{13}C NMR spectra were recorded under inverse gated proton decoupling on selected samples of 10 w/v % solutions of polypropylene in a o-dichlorobenzene-deuteriobenzene (9:1 v/v) mixture. A recycle delay of 6 s was used, and 20000 scans were acquired. The spectra were recorded at 90 °C; the temperature was controlled within 0.1 °C. Peak intensities were determined from integration of the peaks obtained from spectral deconvolution.[10]

The ethylene/1-hexene copolymer samples for NMR experiments were prepared directly in the NMR tube by adding *o*-dichlorobenzene (Aldrich, ≥ 99%) to weighed amounts of the dry polymers, obtaining approximately 5 % by weight solutions. The samples were heated above 80 ^{o}C in a water bath for at least one hour in order to obtain complete dissolution. The NMR experiments were carried out on a Bruker AMX-300 WB spectrometer working at 75.13 MHz for carbon, using a 10 mm probehead. ^{13}C spectra were recorded using a 20° pulse of 2 μs and a recycle delay of 6 s in order to obtain quantitative spectra, acquiring 5000 scans. The spectra were recorded at 90 ^{o}C; the temperature was controlled within 0.1°C. Chemical shifts were referenced to an external tetramethylsilane standard. Relative peak intensities within each spectrum were obtained by spectral deconvolution using the SPORT-NMR software.[9] Hsieh et al. [11] were followed for the spectral assignment and the determination of monomer sequence distribution.

8.6.6 Single crystal X-ray crystallography

The diffraction experiments were carried out on a Bruker APEX II diffractometer equipped with a CCD detector and using Mo-Kα radiation. Data were corrected for Lorentz polarization and absorption effects (empirical absorption correction SADABS).[12] Structures were solved by direct methods and refined by full-matrix least-squares based on all data using F^2. All non-hydrogen atoms were refined with anisotropic displacement parameters. H-atoms were placed in calculated positions and treated isotropically using the 1.2 fold U_{iso} value of the parent atom except methyl protons, which were assigned the 1.5 fold U_{iso} value of the parent C-atom.

8.7 References

[1] Armarego, L. F.; Perrin, D. D. "*Purification of laboratory chemicals*" W. Eds., 4th Edn., Butterworth Heinemann 1996.

[2] Pedeutour, J. -N.; Radhakrishnan, K.; Cramail, H.; Deffieux, A. J. Mol. Catal. A: Chem. **2002**, *185*, 119.

[3] Calderazzo, F.; Ianelli, S.; Pampaloni, G.; Pelizzi, G.; Sperrle, M. *J. Chem. Soc., Dalton Trans.* **1991**, 693.

[4] (a) Chisholm, M. H.; Extin, M. W. *J. Am. Chem. Soc.* **1977**, *99*, 782.; (b) Chisholm, M. H.; Extin, M. W. *J. Am. Chem. Soc.* **1977**, *99*, 792.

[5] Wunderlich, B. "Macromolecular Physics, Vol. 3 Crystal Melting", Plenum Press, New York 1980.

[6] Chien, J. C. W.; Wang, B. P. *J. Polym. Sci. Part A: Polym. Chem.* **1990**, *28*, 15.

[7] Zirkel, A.; Urban, V.; Richter, D.; Fetters, L. J.; Huang, J. S.; Kampmann, R.; Hadjichristidis, N. *Macromolecules* **1992**; *25*, 6148.

[8] Pracella, M.; D'Alessio, A.; Giaiacopi, S.; Raspolli Galletti, A. M. Carlini, C.; Sbrana, G. Macromol. Chem. Phys. 2007, 208, 1560.

[9] Pollard, M.; Klimke, K.; Graf, R.; Spiess, H. W.; Wilhelm, M.; Sperber, O.; Piel, C.; Kaminsky, W. Macromolecules **2004**, *37*, 813.

[10] Geppi, M.; Forte, C. *J. Magn. Reson.* **1999**, *137*, 177.

[11] Hsieh, E. T.; Randall, J. C. *Macromolecules* **1982**, *15*, 1402.

[12] Sheldrick, G. M. SHELX97-Program for the refinement of Crystal Structure, University of Göttingen, Göttingen, Germany, 1997.

9 Concluding Remarks

There have been significant advances during the past decade in the area of non-metallocene olefin polymerization catalysts, based on early transition metals. A variety of new ligands and complexes has been designed and studied in olefin polymerization.
This thesis describes the catalytic behavior of Group 4 metals-based complexes in homo and copolymerization of olefins as well as the reaction of these complexes with some natural aminoacides.

Titanium and zirconium complexes bearing *N*,*N*-dialkylcarbamato ligands and mixed chloro-substituted derivative have been prepared and characterized by elemental analysis, FTIR and NMR spectroscopy. The titanium precursors exhibited moderate to high activities in ethylene polymerization upon activation with MAO under adopted conditions. High density polyethylenes with broad molecular weight distributions were produced using these catalysts. The nature of solvent was found to be crucial for the catalytic performances: a higher productivity was ascertained when the polar solvent was used.

The results showed that these titanium(IV) carbamato precursors were active for propylene polymerization in the presence of organoaluminium-based cocatalysts, giving rise to the formation of atactic polypropylenes. The T_g of polypropylene samples lied at –9 to –14 °C. A notable increase in the catalytic activity for propylene polymerization could be attained by using DMAO as cocatalyst.

Polymerization studies revealed that titanium complexes bearing *N*,*N*-dialkylcarbamato ligands were useful precursors for the copolymerization of ethylene and 1-hexene at room temperature. ^{13}C NMR results confirmed that the copolymers have high content of 1-hexene incorporation within the copolymer chain. The DSC showed that the melting points of the obtained polymer are dependent on the content of 1-hexene insertion, obviously decreased with increasing of the comonomer incorporation. The SEC results confirmed that the obtained polymers feature relatively high molecular weight and broad molecular weight distribution. The composition of the examined copolymers, as determined by NMR analysis, represented a substantial agreement with that obtained by FTIR and DSC analyzes.

The structural characterization of the selected E/H copolymers has been investigated by FTIR-M in the range of 2–28 mol% 1-hexene content. The bands of methyl

deformation and methylene wagging in the region of 1400–1330 cm^{-1} were used for determining the comonomer content. The study of isothermal crystallization behavior of copolymers by DSC revealed a marked decrease in the bulk crystallization rate with an increase in the comonomer content.

A series of aminoacid-containing carbamato complexes of titanium and zirconium have been prepared under mild conditions. The new complexes showed good solubility in organic solvents, however, they were not effective in the ethylene polymerization wherein there were employed as catalytic precursors.

Appendix

Tetrakis(*N*,*N*-dimethylcarbamato)titanium(IV).CH_2Cl_2

Crystal data

$[Ti(C_3H_6NO_2)_4].CH_2Cl_2$	$F000 = 504$
$M_r = 485.18$	$D_x = 1.521$ Mg m^{-3}
Triclinic, $P1$	Mo $K\alpha$ radiation, $\lambda = 0.71073$ Å
$a = 8.602$ (2) Å	$\mu = 0.\ 7$ mm^{-1}
$b = 10.576$ (3) Å	$T = 100$ K
$c = 12.609$ (3) Å	Prism, colorless
$\alpha = 101.563$ (3)º	0.18 × 0.13 × 0.11 mm
$\beta = 104.924$ (3)º	
$\gamma = 98.996$ (3)º	
$V = 1059.4$ (4) Å^3	
$Z = 2$	

Data collection

Bruker SMART APEX CCD diffractometer	3718 independent reflections
Radiation source: fine-focus sealed tube	2604 reflections with $I > 2\sigma(I)$
Monochromator: graphite	$R_{int} = 0.051$
Absorption correction: empirical	$\theta_{max} = 25.0$º
$T_{min} = 0.884$, $T_{max} = 0.927$	$\theta_{min} = 1.7$º
7626 measured reflections	$h = -10 \rightarrow 10$
	$k = -12 \rightarrow 12$
	$l = -14 \rightarrow 14$

Refinement

Refinement on F^2	Secondary atom site location: difference Fourier map
Least-squares matrix: full	Hydrogen site location: inferred from neighbouring sites
$R[F^2 > 2\sigma(F^2)] = 0.055$	H-atom parameters constrained
$wR(F^2) = 0.144$	$w = 1/[\sigma^2(F_o^2) + (0.062P)^2]$ where $P = (F_o^2 + 2F_c^2)/3$
$S = 0.99$	$(\Delta/\sigma)_{max} < 0.001$
3718 reflections	$\Delta\rho_{max} = 0.86$ e Å^{-3}
253 parameters	$\Delta\rho_{min} = -0.44$ e Å^{-3}
0 restraints	Extinction correction: none

Primary atom site location: structure-invariant direct methods

Refinement of F^2 against ALL reflections. The weighted R-factor wR and goodness of fit S are based on F^2, conventional R-factors R are based on F, with F set to zero for negative F^2. The threshold expression of $F^2 > 2$sigma(F^2) is used only for calculating R-factors(gt) etc. and is not relevant to the choice of reflections for refinement. R-factors based on F^2 are statistically about twice as large as those based on F, and R- factors based on ALL data will be even larger.

Fractional atomic coordinates and isotropic or equivalent isotropic displacement parameters (Å^2)

	x	*y*	*z*	U_{iso}*/U_{eq}
C1	0.2792 (5)	0.7519 (4)	0.3810 (3)	0.0174 (9)
C2	0.4841 (5)	0.7782 (4)	0.5476 (3)	0.0254 (10)
H2A	0.5156	0.8725	0.5431	0.038*
H2B	0.5751	0.7404	0.5377	0.038*
H2C	0.4595	0.7741	0.6204	0.038*
C3	0.2671 (6)	0.5578 (4)	0.4577 (4)	0.0272 (10)
H3A	0.1706	0.5171	0.3960	0.041*
H3B	0.2337	0.5509	0.5277	0.041*
H3C	0.3493	0.5099	0.4475	0.041*
C4	0.0217 (5)	0.9784 (4)	0.3230 (3)	0.0179 (9)

C5	0.0008 (5)	1.1935 (4)	0.4233 (3)	0.0239 (10)
H5A	0.1109	12.256	0.4087	0.036*
H5B	0.0081	12.145	0.5036	0.036*
H5C	−0.0722	12.384	0.3888	0.036*
C6	−0.2272 (5)	0.9821 (4)	0.3934 (3)	0.0243 (10)
H6A	−0.2570	0.8847	0.3598	0.036*
H6B	−0.3088	10.193	0.3581	0.036*
H6C	−0.2249	0.9976	0.4729	0.036*
C7	0.4257 (5)	0.8746 (4)	0.1535 (3)	0.0185 (9)
C8	0.6668 (5)	1.0179 (5)	0.1104 (4)	0.0313 (12)
H8A	0.6135	10.878	0.1315	0.047*
H8B	0.6899	10.172	0.0367	0.047*
H8C	0.7703	10.373	0.1645	0.047*
C9	0.6016 (5)	0.7668 (5)	0.0590 (4)	0.0317 (11)
H9A	0.5167	0.6853	0.0601	0.048*
H9B	0.7081	0.7689	0.1018	0.048*
H9C	0.6095	0.7660	−0.0178	0.048*
C10	−0.0077 (5)	0.7546 (4)	0.0428 (3)	0.0158 (9)
C11	−0.1889 (5)	0.5615 (4)	−0.1002 (3)	0.0248 (10)
H11A	−0.1634	0.5147	−0.0430	0.037*
H11B	−0.1565	0.5229	−0.1677	0.037*
H11C	−0.3075	0.5502	−0.1168	0.037*
C12	−0.1133 (5)	0.7896 (4)	−0.1368 (3)	0.0208 (9)
H12A	−0.0574	0.8845	−0.0976	0.031*
H12B	−0.2300	0.7781	−0.1655	0.031*
H12C	−0.0621	0.7637	−0.1986	0.031*
C13	0.7690 (6)	0.5438 (5)	0.2445 (5)	0.0450 (14)
H13A	0.7684	0.5718	0.1741	0.054*
H13B	0.8747	0.5979	0.2967	0.054*
Cl1	0.75792 (19)	0.37315 (13)	0.21927 (12)	0.0535 (4)
Cl2	0.60539 (14)	0.57948 (13)	0.30031 (10)	0.0384 (3)
N1	0.3383 (4)	0.7001 (3)	0.4607 (3)	0.0185 (8)
N2	−0.0650 (4)	1.0483 (3)	0.3773 (3)	0.0189 (8)
N3	0.5577 (4)	0.8865 (4)	0.1082 (3)	0.0223 (8)
N4	−0.0988 (4)	0.7042 (3)	−0.0604 (3)	0.0171 (8)
O1	0.1541 (3)	0.6810 (3)	0.3020 (2)	0.0181 (6)
O2	0.3396 (3)	0.8751 (3)	0.3777 (2)	0.0187 (6)
O3	0.1614 (3)	1.0340 (3)	0.3040 (2)	0.0178 (6)
O4	−0.0317 (3)	0.8482 (3)	0.2898 (2)	0.0183 (6)
O5	0.3867 (3)	0.9767 (3)	0.2002 (2)	0.0192 (6)
O6	0.3298 (3)	0.7578 (3)	0.1499 (2)	0.0191 (6)
O7	0.0021 (3)	0.6807 (3)	0.1106 (2)	0.0189 (6)
O8	0.0755 (3)	0.8804 (3)	0.0816 (2)	0.0166 (6)
Ti1	0.17687 (8)	0.84320 (7)	0.22724 (6)	0.0155 (2)

Atomic displacement parameters (Å^2)

	U^{11}	U^{22}	U^{33}	U^{12}	U^{13}	U^{23}
C1	0.016 (2)	0.020 (2)	0.019 (2)	0.0097 (18)	0.0091 (18)	0.0014 (18)
C2	0.023 (2)	0.029 (3)	0.023 (2)	0.0087 (19)	−0.0019 (19)	0.006 (2)
C3	0.031 (3)	0.021 (3)	0.030 (3)	0.009 (2)	0.004 (2)	0.008 (2)
C4	0.015 (2)	0.025 (3)	0.015 (2)	0.0113 (18)	−0.0006 (17)	0.0029 (18)
C5	0.028 (2)	0.021 (2)	0.026 (2)	0.013 (2)	0.008 (2)	0.004 (2)
C6	0.015 (2)	0.033 (3)	0.026 (2)	0.0099 (19)	0.0079 (18)	0.003 (2)
C7	0.014 (2)	0.022 (2)	0.018 (2)	0.0056 (18)	0.0004 (17)	0.0053 (18)
C8	0.014 (2)	0.043 (3)	0.034 (3)	−0.002 (2)	0.003 (2)	0.017 (2)
C9	0.025 (2)	0.049 (3)	0.033 (3)	0.022 (2)	0.019 (2)	0.013 (2)
C10	0.012 (2)	0.019 (2)	0.021 (2)	0.0087 (17)	0.0087 (17)	0.0051 (19)
C11	0.023 (2)	0.020 (2)	0.027 (2)	0.0070 (19)	0.0008 (19)	−0.0018 (19)
C12	0.018 (2)	0.023 (2)	0.021 (2)	0.0075 (18)	0.0028 (18)	0.0046 (19)
C13	0.032 (3)	0.035 (3)	0.076 (4)	0.009 (2)	0.030 (3)	0.020 (3)
Cl1	0.0647 (10)	0.0306 (8)	0.0677 (10)	0.0150 (7)	0.0227 (8)	0.0104 (7)
Cl2	0.0224 (6)	0.0510 (8)	0.0462 (8)	0.0135 (6)	0.0099 (5)	0.0169 (6)
N1	0.0137 (17)	0.020 (2)	0.0210 (19)	0.0052 (14)	−0.0001 (14)	0.0059 (15)
N2	0.0150 (18)	0.021 (2)	0.0213 (18)	0.0096 (15)	0.0045 (15)	0.0019 (16)
N3	0.0160 (18)	0.028 (2)	0.026 (2)	0.0092 (15)	0.0094 (15)	0.0074 (17)
N4	0.0148 (17)	0.0162 (19)	0.0187 (18)	0.0045 (14)	0.0032 (14)	0.0011 (15)
O1	0.0123 (14)	0.0202 (16)	0.0201 (15)	0.0051 (12)	0.0011 (12)	0.0027 (12)
O2	0.0152 (14)	0.0175 (17)	0.0210 (15)	0.0056 (12)	0.0002 (12)	0.0016 (12)
O3	0.0146 (15)	0.0180 (16)	0.0192 (15)	0.0055 (12)	0.0020 (12)	0.0015 (12)
O4	0.0141 (14)	0.0168 (17)	0.0250 (15)	0.0057 (12)	0.0073 (12)	0.0038 (13)
O5	0.0151 (15)	0.0190 (16)	0.0236 (15)	0.0057 (12)	0.0053 (12)	0.0039 (13)
O6	0.0131 (14)	0.0220 (17)	0.0233 (15)	0.0071 (12)	0.0057 (12)	0.0047 (13)
O7	0.0139 (14)	0.0195 (16)	0.0222 (15)	0.0045 (12)	0.0023 (12)	0.0049 (13)
O8	0.0128 (14)	0.0179 (16)	0.0184 (15)	0.0048 (12)	0.0023 (11)	0.0038 (12)
Ti1	0.0103 (4)	0.0178 (4)	0.0186 (4)	0.0059 (3)	0.0030 (3)	0.0029 (3)

Geometric parameters (Å, °)

C1—O2	1.284 (5)	C8—H8B	0.9800
C1—O1	1.289 (5)	C8—H8C	0.9800
C1—N1	1.332 (5)	C9—N3	1.461 (5)
C1—Ti1	2.473 (4)	C9—H9A	0.9800
C2—N1	1.459 (5)	C9—H9B	0.9800
C2—H2A	0.9800	C9—H9C	0.9800
C2—H2B	0.9800	C10—O7	1.275 (4)
C2—H2C	0.9800	C10—O8	1.289 (5)
C3—N1	1.462 (5)	C10—N4	1.334 (5)
C3—H3A	0.9800	C10—Ti1	2.452 (4)
C3—H3B	0.9800	C11—N4	1.450 (5)
C3—H3C	0.9800	C11—H11A	0.9800

C4—O3	1.277 (5)	C11—H11B	0.9800
C4—O4	1.290 (5)	C11—H11C	0.9800
C4—N2	1.347 (5)	C12—N4	1.459 (5)
C4—Ti1	2.465 (4)	C12—H12A	0.9800
C5—N2	1.451 (5)	C12—H12B	0.9800
C5—H5A	0.9800	C12—H12C	0.9800
C5—H5B	0.9800	C13—Cl1	1.743 (5)
C5—H5C	0.9800	C13—Cl2	1.760 (5)
C6—N2	1.456 (5)	C13—H13A	0.9900
C6—H6A	0.9800	C13—H13B	0.9900
C6—H6B	0.9800	O1—Ti1	2.098 (3)
C6—H6C	0.9800	O2—Ti1	2.084 (3)
C7—O5	1.272 (5)	O3—Ti1	2.102 (3)
C7—O6	1.284 (5)	O4—Ti1	2.078 (3)
C7—N3	1.338 (5)	O5—Ti1	2.108 (3)
C7—Ti1	2.436 (4)	O6—Ti1	2.039 (3)
C8—N3	1.455 (5)	O7—Ti1	2.084 (3)
C8—H8A	0.9800	O8—Ti1	2.062 (3)
O2—C1—O1	115.3 (3)	C4—N2—C6	121.7 (3)
O2—C1—N1	123.1 (4)	C5—N2—C6	117.2 (3)
O1—C1—N1	121.6 (4)	C7—N3—C8	121.8 (4)
O2—C1—Ti1	57.39 (19)	C7—N3—C9	120.6 (4)
O1—C1—Ti1	58.03 (19)	C8—N3—C9	117.5 (4)
N1—C1—Ti1	177.3 (3)	C10—N4—C11	120.7 (3)
N1—C2—H2A	109.5	C10—N4—C12	121.8 (3)
N1—C2—H2B	109.5	C11—N4—C12	117.6 (3)
H2A—C2—H2B	109.5	C1—O1—Ti1	90.5 (2)
N1—C2—H2C	109.5	C1—O2—Ti1	91.3 (2)
H2A—C2—H2C	109.5	C4—O3—Ti1	90.3 (2)
H2B—C2—H2C	109.5	C4—O4—Ti1	91.0 (2)
N1—C3—H3A	109.5	C7—O5—Ti1	88.7 (2)
N1—C3—H3B	109.5	C7—O6—Ti1	91.4 (2)
H3A—C3—H3B	109.5	C10—O7—Ti1	90.5 (2)
N1—C3—H3C	109.5	C10—O8—Ti1	91.1 (2)
H3A—C3—H3C	109.5	O6—Ti1—O8	90.80 (11)
H3B—C3—H3C	109.5	O6—Ti1—O4	156.81 (11)
O3—C4—O4	115.9 (3)	O8—Ti1—O4	91.59 (11)
O3—C4—N2	123.3 (4)	O6—Ti1—O7	80.34 (11)
O4—C4—N2	120.8 (4)	O8—Ti1—O7	62.94 (11)
O3—C4—Ti1	58.51 (19)	O4—Ti1—O7	80.26 (11)
O4—C4—Ti1	57.44 (19)	O6—Ti1—O2	88.24 (11)
N2—C4—Ti1	177.8 (3)	O8—Ti1—O2	158.67 (11)
N2—C5—H5A	109.5	O4—Ti1—O2	97.62 (11)
N2—C5—H5B	109.5	O7—Ti1—O2	137.56 (11)
H5A—C5—H5B	109.5	O6—Ti1—O1	83.02 (11)
N2—C5—H5C	109.5	O8—Ti1—O1	138.34 (11)

H5A—C5—H5C	109.5	O4—Ti1—O1	79.91 (11)
H5B—C5—H5C	109.5	O7—Ti1—O1	75.42 (10)
N2—C6—H6A	109.5	O2—Ti1—O1	62.62 (10)
N2—C6—H6B	109.5	O6—Ti1—O3	140.45 (11)
H6A—C6—H6B	109.5	O8—Ti1—O3	85.25 (10)
N2—C6—H6C	109.5	O4—Ti1—O3	62.74 (11)
H6A—C6—H6C	109.5	O7—Ti1—O3	130.47 (10)
H6B—C6—H6C	109.5	O2—Ti1—O3	82.00 (10)
O5—C7—O6	116.7 (4)	O1—Ti1—O3	124.20 (11)
O5—C7—N3	122.4 (4)	O6—Ti1—O5	63.27 (11)
O6—C7—N3	121.0 (4)	O8—Ti1—O5	79.94 (10)
O5—C7—Ti1	59.9 (2)	O4—Ti1—O5	139.76 (11)
O6—C7—Ti1	56.8 (2)	O7—Ti1—O5	127.27 (11)
N3—C7—Ti1	176.9 (3)	O2—Ti1—O5	80.62 (11)
N3—C8—H8A	109.5	O1—Ti1—O5	130.80 (11)
N3—C8—H8B	109.5	O3—Ti1—O5	77.31 (11)
H8A—C8—H8B	109.5	O6—Ti1—C7	31.80 (12)
N3—C8—H8C	109.5	O8—Ti1—C7	84.15 (12)
H8A—C8—H8C	109.5	O4—Ti1—C7	170.89 (13)
H8B—C8—H8C	109.5	O7—Ti1—C7	104.75 (12)
N3—C9—H9A	109.5	O2—Ti1—C7	83.85 (12)
N3—C9—H9B	109.5	O1—Ti1—C7	108.58 (12)
H9A—C9—H9B	109.5	O3—Ti1—C7	108.76 (13)
N3—C9—H9C	109.5	O5—Ti1—C7	31.47 (12)
H9A—C9—H9C	109.5	O6—Ti1—C10	83.04 (12)
H9B—C9—H9C	109.5	O8—Ti1—C10	31.70 (11)
O7—C10—O8	115.2 (3)	O4—Ti1—C10	86.96 (12)
O7—C10—N4	121.9 (4)	O7—Ti1—C10	31.33 (11)
O8—C10—N4	122.9 (4)	O2—Ti1—C10	167.12 (12)
O7—C10—Ti1	58.20 (19)	O1—Ti1—C10	106.72 (12)
O8—C10—Ti1	57.22 (19)	O3—Ti1—C10	110.71 (12)
N4—C10—Ti1	175.7 (3)	O5—Ti1—C10	103.64 (12)
N4—C11—H11A	109.5	C7—Ti1—C10	93.53 (13)
N4—C11—H11B	109.5	O6—Ti1—C4	171.64 (13)
H11A—C11—H11B	109.5	O8—Ti1—C4	87.99 (12)
N4—C11—H11C	109.5	O4—Ti1—C4	31.55 (12)
H11A—C11—H11C	109.5	O7—Ti1—C4	106.38 (12)
H11B—C11—H11C	109.5	O2—Ti1—C4	89.88 (11)
N4—C12—H12A	109.5	O1—Ti1—C4	103.32 (12)
N4—C12—H12B	109.5	O3—Ti1—C4	31.19 (12)
H12A—C12—H12B	109.5	O5—Ti1—C4	108.38 (13)
N4—C12—H12C	109.5	C7—Ti1—C4	139.85 (15)
H12A—C12—H12C	109.5	C10—Ti1—C4	100.07 (12)
H12B—C12—H12C	109.5	O6—Ti1—C1	83.51 (12)
Cl1—C13—Cl2	112.9 (3)	O8—Ti1—C1	168.80 (12)
Cl1—C13—H13A	109.0	O4—Ti1—C1	89.92 (12)

Cl2—C13—H13A	109.0	O7—Ti1—C1	106.44 (12)
Cl1—C13—H13B	109.0	O2—Ti1—C1	31.26 (11)
Cl2—C13—H13B	109.0	O1—Ti1—C1	31.42 (12)
H13A—C13—H13B	107.8	O3—Ti1—C1	105.27 (12)
C1—N1—C2	121.8 (3)	O5—Ti1—C1	105.81 (12)
C1—N1—C3	120.4 (3)	C7—Ti1—C1	95.82 (13)
C2—N1—C3	117.6 (3)	C10—Ti1—C1	137.43 (14)
C4—N2—C5	121.1 (4)	C4—Ti1—C1	99.01 (13)
O2—C1—N1—C2	−3.9 (6)	O5—C7—Ti1—O8	80.3 (2)
O1—C1—N1—C2	177.4 (4)	O6—C7—Ti1—O8	−101.1 (2)
Ti1—C1—N1—C2	96 (7)	N3—C7—Ti1—O8	−57 (6)
O2—C1—N1—C3	−178.1 (4)	O5—C7—Ti1—O4	17.8 (9)
O1—C1—N1—C3	3.1 (6)	O6—C7—Ti1—O4	−163.6 (7)
Ti1—C1—N1—C3	−78 (7)	N3—C7—Ti1—O4	−120 (6)
O3—C4—N2—C5	−3.3 (6)	O5—C7—Ti1—O7	140.3 (2)
O4—C4—N2—C5	174.6 (3)	O6—C7—Ti1—O7	−41.1 (2)
Ti1—C4—N2—C5	139 (7)	N3—C7—Ti1—O7	3 (6)
O3—C4—N2—C6	177.4 (3)	O5—C7—Ti1—O2	−82.1 (2)
O4—C4—N2—C6	−4.8 (6)	O6—C7—Ti1—O2	96.6 (2)
Ti1—C4—N2—C6	−41 (8)	N3—C7—Ti1—O2	140 (6)
O5—C7—N3—C8	0.6 (6)	O5—C7—Ti1—O1	−140.4 (2)
O6—C7—N3—C8	179.3 (3)	O6—C7—Ti1—O1	38.2 (2)
Ti1—C7—N3—C8	137 (6)	N3—C7—Ti1—O1	82 (6)
O5—C7—N3—C9	177.7 (3)	O5—C7—Ti1—O3	−2.7 (2)
O6—C7—N3—C9	−3.5 (6)	O6—C7—Ti1—O3	176.0 (2)
Ti1—C7—N3—C9	−46 (6)	N3—C7—Ti1—O3	−140 (6)
O7—C10—N4—C11	−1.0 (6)	O6—C7—Ti1—O5	178.7 (3)
O8—C10—N4—C11	179.4 (3)	N3—C7—Ti1—O5	−138 (6)
Ti1—C10—N4—C11	89 (4)	O5—C7—Ti1—C10	110.6 (2)
O7—C10—N4—C12	178.4 (3)	O6—C7—Ti1—C10	−70.7 (2)
O8—C10—N4—C12	−1.2 (6)	N3—C7—Ti1—C10	−27 (6)
Ti1—C10—N4—C12	−92 (4)	O5—C7—Ti1—C4	0.4 (3)
O2—C1—O1—Ti1	4.2 (3)	O6—C7—Ti1—C4	179.1 (2)
N1—C1—O1—Ti1	−176.9 (3)	N3—C7—Ti1—C4	−137 (6)
O1—C1—O2—Ti1	−4.3 (3)	O5—C7—Ti1—C1	−111.0 (2)
N1—C1—O2—Ti1	176.9 (3)	O6—C7—Ti1—C1	67.7 (2)
O4—C4—O3—Ti1	0.5 (3)	N3—C7—Ti1—C1	111 (6)
N2—C4—O3—Ti1	178.4 (3)	O7—C10—Ti1—O6	82.8 (2)
O3—C4—O4—Ti1	−0.5 (3)	O8—C10—Ti1—O6	−103.0 (2)
N2—C4—O4—Ti1	−178.4 (3)	N4—C10—Ti1—O6	−10 (4)
O6—C7—O5—Ti1	−1.2 (3)	O7—C10—Ti1—O8	−174.2 (3)
N3—C7—O5—Ti1	177.6 (3)	N4—C10—Ti1—O8	93 (4)
O5—C7—O6—Ti1	1.3 (3)	O7—C10—Ti1—O4	−76.2 (2)
N3—C7—O6—Ti1	−177.5 (3)	O8—C10—Ti1—O4	98.0 (2)
O8—C10—O7—Ti1	−5.4 (3)	N4—C10—Ti1—O4	−169 (4)
N4—C10—O7—Ti1	175.0 (3)	O8—C10—Ti1—O7	174.2 (3)

O7—C10—O8—Ti1	5.4 (3)	N4—C10—Ti1—O7	−92 (4)
N4—C10—O8—Ti1	−174.9 (3)	O7—C10—Ti1—O2	35.1 (6)
C7—O6—Ti1—O8	77.5 (2)	O8—C10—Ti1—O2	−150.7 (5)
C7—O6—Ti1—O4	173.5 (3)	N4—C10—Ti1—O2	−57 (4)
C7—O6—Ti1—O7	139.9 (2)	O7—C10—Ti1—O1	2.3 (2)
C7—O6—Ti1—O2	−81.2 (2)	O8—C10—Ti1—O1	176.5 (2)
C7—O6—Ti1—O1	−143.8 (2)	N4—C10—Ti1—O1	−90 (4)
C7—O6—Ti1—O3	−6.0 (3)	O7—C10—Ti1—O3	−135.5 (2)
C7—O6—Ti1—O5	−0.8 (2)	O8—C10—Ti1—O3	38.7 (2)
C7—O6—Ti1—C10	108.3 (2)	N4—C10—Ti1—O3	132 (4)
C7—O6—Ti1—C4	−4.1 (9)	O7—C10—Ti1—O5	143.1 (2)
C7—O6—Ti1—C1	−112.1 (2)	O8—C10—Ti1—O5	−42.7 (2)
C10—O8—Ti1—O6	75.3 (2)	N4—C10—Ti1—O5	51 (4)
C10—O8—Ti1—O4	−81.6 (2)	O7—C10—Ti1—C7	112.9 (2)
C10—O8—Ti1—O7	−3.4 (2)	O8—C10—Ti1—C7	−72.9 (2)
C10—O8—Ti1—O2	162.5 (3)	N4—C10—Ti1—C7	21 (4)
C10—O8—Ti1—O1	−5.0 (3)	O7—C10—Ti1—C4	−105.0 (2)
C10—O8—Ti1—O3	−144.1 (2)	O8—C10—Ti1—C4	69.2 (2)
C10—O8—Ti1—O5	138.0 (2)	N4—C10—Ti1—C4	163 (4)
C10—O8—Ti1—C7	106.5 (2)	O7—C10—Ti1—C1	10.4 (3)
C10—O8—Ti1—C4	−112.9 (2)	O8—C10—Ti1—C1	−175.4 (2)
C10—O8—Ti1—C1	16.0 (7)	N4—C10—Ti1—C1	−82 (4)
C4—O4—Ti1—O6	−179.3 (3)	O3—C4—Ti1—O6	−2.4 (9)
C4—O4—Ti1—O8	−83.5 (2)	O4—C4—Ti1—O6	178.1 (7)
C4—O4—Ti1—O7	−145.7 (2)	N2—C4—Ti1—O6	−145 (7)
C4—O4—Ti1—O2	77.2 (2)	O3—C4—Ti1—O8	−84.2 (2)
C4—O4—Ti1—O1	137.5 (2)	O4—C4—Ti1—O8	96.3 (2)
C4—O4—Ti1—O3	0.3 (2)	N2—C4—Ti1—O8	133 (8)
C4—O4—Ti1—O5	−7.3 (3)	O3—C4—Ti1—O4	179.5 (3)
C4—O4—Ti1—C7	−21.6 (8)	N2—C4—Ti1—O4	37 (7)
C4—O4—Ti1—C10	−114.9 (2)	O3—C4—Ti1—O7	−145.2 (2)
C4—O4—Ti1—C1	107.6 (2)	O4—C4—Ti1—O7	35.3 (2)
C10—O7—Ti1—O6	−92.5 (2)	N2—C4—Ti1—O7	72 (8)
C10—O7—Ti1—O8	3.4 (2)	O3—C4—Ti1—O2	74.6 (2)
C10—O7—Ti1—O4	100.3 (2)	O4—C4—Ti1—O2	−104.9 (2)
C10—O7—Ti1—O2	−169.1 (2)	N2—C4—Ti1—O2	−68 (8)
C10—O7—Ti1—O1	−177.7 (2)	O3—C4—Ti1—O1	136.4 (2)
C10—O7—Ti1—O3	59.5 (3)	O4—C4—Ti1—O1	−43.1 (2)
C10—O7—Ti1—O5	−47.2 (3)	N2—C4—Ti1—O1	−6 (8)
C10—O7—Ti1—C7	−71.9 (2)	O4—C4—Ti1—O3	−179.5 (3)
C10—O7—Ti1—C4	82.4 (2)	N2—C4—Ti1—O3	−143 (8)
C10—O7—Ti1—C1	−172.7 (2)	O3—C4—Ti1—O5	−5.4 (2)
C1—O2—Ti1—O6	−80.4 (2)	O4—C4—Ti1—O5	175.0 (2)
C1—O2—Ti1—O8	−168.1 (3)	N2—C4—Ti1—O5	−148 (8)
C1—O2—Ti1—O4	77.1 (2)	O3—C4—Ti1—C7	−5.7 (3)
C1—O2—Ti1—O7	−6.8 (3)	O4—C4—Ti1—C7	174.8 (2)

C1—O2—Ti1—O1	2.7 (2)	N2—C4—Ti1—C7	−148 (7)
C1—O2—Ti1—O3	138.1 (2)	O3—C4—Ti1—C10	−113.6 (2)
C1—O2—Ti1—O5	−143.6 (2)	O4—C4—Ti1—C10	66.9 (2)
C1—O2—Ti1—C7	−112.0 (2)	N2—C4—Ti1—C10	104 (8)
C1—O2—Ti1—C10	−33.1 (6)	O3—C4—Ti1—C1	104.6 (2)
C1—O2—Ti1—C4	107.8 (2)	O4—C4—Ti1—C1	−74.9 (2)
C1—O1—Ti1—O6	89.0 (2)	N2—C4—Ti1—C1	−38 (8)
C1—O1—Ti1—O8	172.3 (2)	O2—C1—Ti1—O6	97.3 (2)
C1—O1—Ti1—O4	−106.8 (2)	O1—C1—Ti1—O6	−87.2 (2)
C1—O1—Ti1—O7	170.8 (2)	N1—C1—Ti1—O6	−4 (7)
C1—O1—Ti1—O2	−2.7 (2)	O2—C1—Ti1—O8	157.2 (5)
C1—O1—Ti1—O3	−59.9 (2)	O1—C1—Ti1—O8	−27.3 (7)
C1—O1—Ti1—O5	43.8 (3)	N1—C1—Ti1—O8	56 (7)
C1—O1—Ti1—C7	69.8 (2)	O2—C1—Ti1—O4	−105.0 (2)
C1—O1—Ti1—C10	169.5 (2)	O1—C1—Ti1—O4	70.5 (2)
C1—O1—Ti1—C4	−85.5 (2)	N1—C1—Ti1—O4	154 (7)
C4—O3—Ti1—O6	179.5 (2)	O2—C1—Ti1—O7	175.2 (2)
C4—O3—Ti1—O8	94.0 (2)	O1—C1—Ti1—O7	−9.3 (2)
C4—O3—Ti1—O4	−0.3 (2)	N1—C1—Ti1—O7	74 (7)
C4—O3—Ti1—O7	46.1 (3)	O1—C1—Ti1—O2	175.4 (4)
C4—O3—Ti1—O2	−103.2 (2)	N1—C1—Ti1—O2	−101 (7)
C4—O3—Ti1—O1	−54.2 (2)	O2—C1—Ti1—O1	−175.4 (4)
C4—O3—Ti1—O5	174.7 (2)	N1—C1—Ti1—O1	83 (7)
C4—O3—Ti1—C7	176.1 (2)	O2—C1—Ti1—O3	−43.3 (2)
C4—O3—Ti1—C10	74.7 (2)	O1—C1—Ti1—O3	132.1 (2)
C4—O3—Ti1—C1	−82.1 (2)	N1—C1—Ti1—O3	−145 (7)
C7—O5—Ti1—O6	0.8 (2)	O2—C1—Ti1—O5	37.5 (2)
C7—O5—Ti1—O8	−95.3 (2)	O1—C1—Ti1—O5	−147.0 (2)
C7—O5—Ti1—O4	−175.7 (2)	N1—C1—Ti1—O5	−64 (7)
C7—O5—Ti1—O7	−50.9 (2)	O2—C1—Ti1—C7	68.0 (2)
C7—O5—Ti1—O2	93.6 (2)	O1—C1—Ti1—C7	−116.6 (2)
C7—O5—Ti1—O1	52.9 (3)	N1—C1—Ti1—C7	−33 (7)
C7—O5—Ti1—O3	177.4 (2)	O2—C1—Ti1—C10	169.6 (2)
C7—O5—Ti1—C10	−74.0 (2)	O1—C1—Ti1—C10	−14.9 (3)
C7—O5—Ti1—C4	−179.7 (2)	N1—C1—Ti1—C10	68 (7)
C7—O5—Ti1—C1	74.9 (2)	O2—C1—Ti1—C4	−74.6 (2)
O5—C7—Ti1—O6	−178.7 (3)	O1—C1—Ti1—C4	100.8 (2)
N3—C7—Ti1—O6	44 (6)	N1—C1—Ti1—C4	−176 (7)

All esds (except the esd in the dihedral angle between two l.s. planes) are estimated using the full covariance matrix. The cell esds are taken into account individually in the estimation of esds in distances, angles and torsion angles; correlations between esds in cell parameters are only used when they are defined by crystal symmetry. An

approximate (isotropic) treatment of cell esds is used for estimating esds involving l.s. planes.